TABLE OF CONTENTS

CELLULAR STUDIES

PHYSICS, BIOPHYSICS, AND MODELING

Rutherford, the Curies, and Radon

David J. Brenner

As a postscript to the two recent articles in *Medical Physics* on the Curies' discovery of radium, and its application to medicine (*1-2*), it is interesting to note that the Curies were also responsible for the discovery of radon-222, the naturally occurring radioactive gas which is of much current interest in terms of background radiation exposure to the general population (*3-4*).

Their discovery followed closely on the insights of Rutherford and Owens in 1899 who, studying the "emanations" from thorium, made the key observation that " *the radiation from thorium oxide was not constant, but varied in a most capricious manner*" whereas "*all the compounds of uranium give out a radiation which is remarkably constant*" (*5*). For example, if a door was opened, the amount of thorium emanation decreased, and if fresh air was blown across the detector, the thorium emanations decreased. Based on these observations Rutherford concluded that "*the emanation … acts like an ordinary gas*", and "*the intensity of the radiation has fallen to one half its value after an interval of about one minute"* (*6*). In modern terminology, Rutherford and Owens had discovered radon in the form of the short-lived isotope radon-220 (half life 51 seconds).

Later in 1899, Pierre and Marie Curie, studying the emanations from radium, concluded that "*elle reste radioactive pendant plusieurs jours"* [*it stayed radioactive for several days*] (*7*). The Curies had detected the isotope radon-222 (half life 3.8 days), which is primarily responsible for domestic radon-progeny exposure, though they remained equivocal as to whether this emanation was, in fact, a gas: in 1901 Pierre Curie and Debierne discussed "*la formation continue de gaz radio-actifs"* [*the continual formation of radioactive gas"*] from radium (*8*), but in Marie Curie's 1903 doctoral thesis she suggested that "*we think, M. Curie and I, that the supposition that radium emits a gas is not yet justified"* (*9*). In fact that the emanations emitted by radium are a radioactive gas was clearly demonstrated by Rutherford and Brooks in 1901 (*10*), though they were careful to give credit to the prior observations of the Curies.

It is interesting to note that most standard sources (*11*) on the chemical elements list Ernst Dorn as the discoverer of radon, in 1900. In fact Dorn had merely repeated the Curies' experiment with more active radium compounds (*12*).

References

1. E. L. Saenger and G. D. Adamek, "Marie Curie and nuclear medicine: closure of a circle," Med. Phys. **26**, 1761-1765 (1999).
2. R. F. Mould, "Marie and Pierre Curie and radium: history, mystery, and discovery," Med. Phys. **26**, 1766-1772 (1999).
3. Committee on Health Risks of Exposure to Radon. Health risks of exposure to radon: BEIR VI. (National Academy Press, Washington, D.C., 1999).

4. D. J. Brenner, "Radon: current challenges in cellular radiobiology," Int. J. Radiat. Biol. **61**, 3-13 (1992).
5. E. Rutherford and R. B. Owens, "Thorium and uranium radiation," Trans. R. Soc. Can. **2**, 9-12 (1899).
6. E. Rutherford, "A radioactive substance emitted from thorium compounds," Phil. Mag. **5/49**, 1-14 (1900).
7. P. Curie and M.-P. Curie, "Sur la radioactivité provoquée par les rayons de Becquerel," Compt. Rend. **129**, 714-716 (1899).
8. P. Curie and A. Debierne, "Sur la radio-activité induite et les gaz activés par le radium," Compt. Rend. **132**, 768-770 (1901).
9. M. Curie, "Recherches sur les substances radioactives," Chem. News **88**, (1903).
10. E. Rutherford and H. T. Brooks, "The new gas from radium," Trans. R. Soc. Can. **7**, 21-25 (1901).
11. *Handbook of Chemistry and Physics,* 79th Edition, edited by D. R. Lide, Jr., (CRC, Ohio, 1998).
12. E. Dorn, "Versuche über sekundästrahlen und radiumstrahlen," Abh. Naturf. Ges. Halle **22**, 37-43 (1900).

The Potential Impact of the Bystander Effect on Radiation Risks on a Mars Mission

David J. Brenner and Carl D. Elliston

Radiation risks in free space are dominated by densely ionizing (high-LET) galactic cosmic rays (GCR). As can be seen in Figure 1, over a period of a few months -- sufficient perhaps for the initial stages of radio- carcinogenesis to occur -- a significant proportion of cell nuclei will not be traversed.

There is quite convincing evidence, at least *in vitro*, that irradiated cells can send out signals which can result in damage to nearby unirradiated cells. This observation can hold even when the unirradiated cells have been exposed to low doses of low-LET radiation. We have used a quantitative model, based on a BaD approach incorporating radiobiological damage both from a Bystander response to signals emitted by irradiated cells, and also from Direct traversal of high-LET radiations through cell nuclei (*1*). The model produces results consistent with a series of studies of the bystander phenomenon using a high-LET microbeam, with the endpoint of *in-vitro* oncogenic transformation (*1*).

As illustrated in Figure 2, for exposure to high-LET particles such as GCR, according to this picture, the bystander effect is significant primarily at low fluences, i.e., where there are significant numbers of untraversed cells. If the mechanisms postulated here were applicable *in vivo*, a linear extrapolation of risks derived from studies using intermediate doses of high-LET doses radiation (where the bystander contribution might be negligible), to estimate risks at very low doses (where the bystander effect may dominate), could significantly underestimate the true risk from low doses of high-LET radiation. It would be highly premature to simply abandon current high-LET low dose risk projections; however these considerations would suggest caution in applying results derived from high-LET experiments at fluences above ~1 particle per nucleus to risk estimation for a Mars mission.

Reference

1. Brenner DJ, Little JB, Sachs RK, *The Bystander Effect in Radiation Oncogenesis: II. A Quantitative Model*. Radiat. Res. (Accepted for publication, 2001).

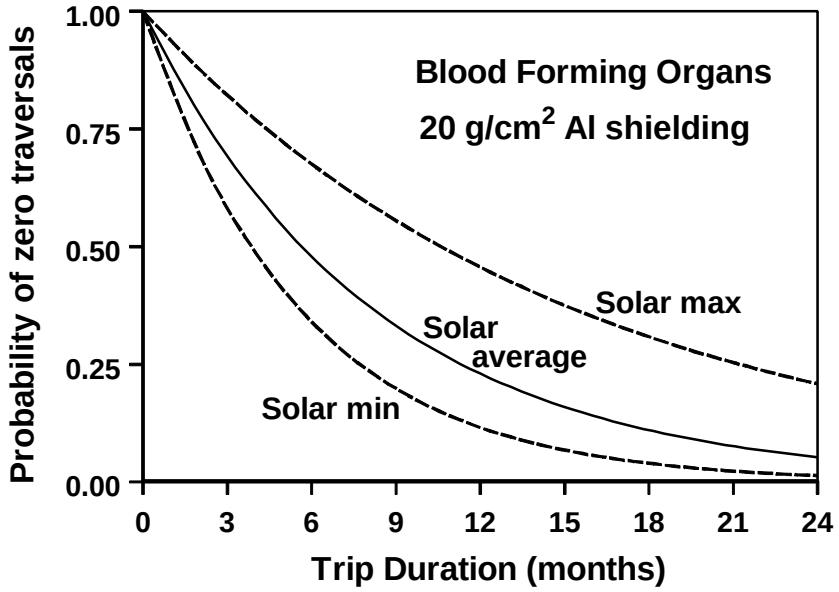

FIG. 1. Estimated probability that a nucleus in a blood-forming organ will not be traversed by the track core of a galactic cosmic ray, as a function of solar cycle position and duration in free space. Results derived for 20 g/cm^2 of aluminum shielding.

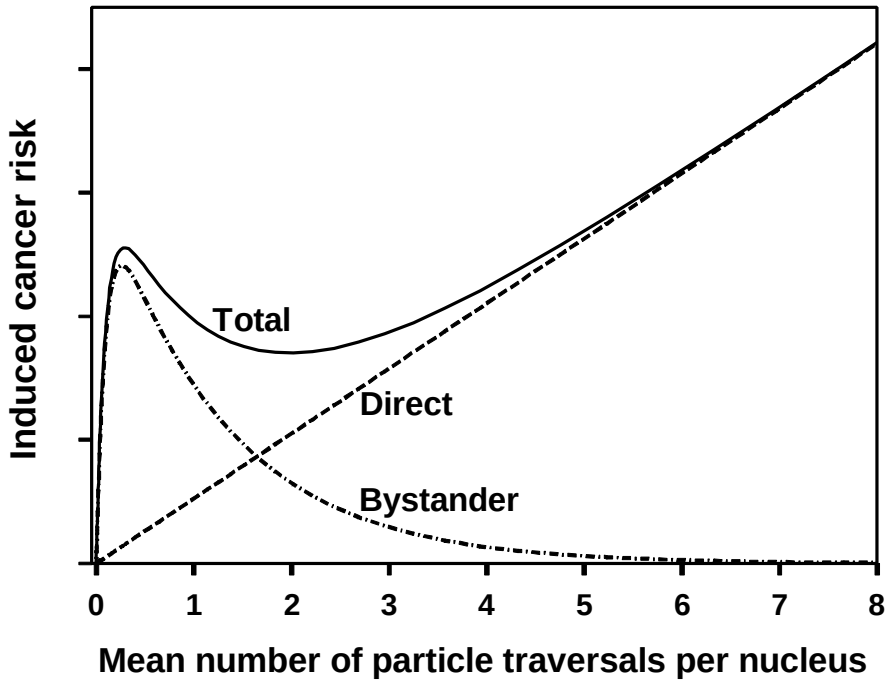

FIG. 2. Schematic of the potential relative contributions of the direct and bystander effects to the total cancer risk produced by radiation exposure on a Mars mission.

A Quantitative Model of the Bystander Effect in Radiation Oncogenesis

D. J. Brenner, J. B. Little (Department of Cancer Cell Biology, Harvard School of Public Health, Boston, MA), and R. K. Sachs (Department of Mathematics, University of California, Berkeley)

There is strong evidence that biological response to ionizing radiation has a contribution from unirradiated "bystander" cells which respond to signals emitted by irradiated cells. We have developed an approach (denoted "BaD") incorporating a radiobiological Bystander response, superimposed on a Direct response due to direct energy deposition in cell nuclei (*1*).

A quantitative model, based on the BaD approach, incorporaties radiobiological damage both from a bystander response to signals emitted by irradiated cells, and also from direct traversal of ionizing radiations through cell nuclei (*1*). In the current model, no detailed signaling mechanisms were hypothesized, so the approach could, in principle, apply to the situation where cells are in direct contact with one other, as well as the situation where the cells are further apart.

In essence we have assumed, at least for high-LET radiation, that the oncogenic bystander phenomenon is a binary "all or nothing" response to the bystander signal in a small sensitive subpopulation of cells; we assume that cells from this sensitive subpopulation are also very sensitive to direct hits from alpha particles, generally resulting in a directly-hit sensitive cell being inactivated.

The model has been applied to a series of experiments on alpha-particle-induced in-vitro oncogenic transformation with a single-cell/single-particle microbeam, as well as with broad-beam irradiation. It was able to reproduce the main features of the data, both for single and larger numbers of alpha particles (*1*).

We have referred to the minority of bystander cells that are sensitive to signal-mediated transformation as a sensitive "subpopulation". It is possible that their sensitivity could be by virtue of their geometric location (i.e., unusually near a hit cell), rather than by virtue of their biological status. In other words, a cell which is very close to a hit cell would receive an extremely large bystander signal. Although for endpoints other than oncogenic transformation, the type of data that would argue against this interpretation is the apparently very long range of the bystander signal (hundreds of microns) in microbeam studies of micronuclei and of apoptotic response. Again though for other endpoints, the type of data that would argue for a geometric interpretation of the sensitive subpopulation comes from low-dose broad-beam alpha-particle studies of gene expression in confluent cells, where bystander-mediated changes in gene expression seem to occur in geometric clusters. To help elucidate this issue for oncogenic transformation, we plan experiments with very low doses of alpha particles irradiating exponentially-growing cells at differing densities.

While some of the details of the model could change, some of its essential features currently seem quite constrained by the available data. Various different experiments on the bystander effect do seem to suggest a rapid rise to a plateau at low doses with little further dose dependence. Sensitive subpopulations characteristically produce such a plateau, though other phenomena, such as indirect, multistage pathways or radiation-induced adaptive response can also produce similar dose-response relations. The existence of an inverse dose-rate effect in other experiments is also suggestive of a cell-subpopulation which is hyper-responsive to a bystander signal: typically, if such a subpopulation has a saturated response for acute irradiation but is restored by endogenous processes during prolonged irradiation, inverse dose-rate effects can result, which are indeed observed at low doses of high-LET radiation.

According to the picture presented above, the bystander effect is important primarily at low doses, at least for high-LET-induced *in-vitro* oncogenic transformation. Based on fits to the *in-vitro* oncogenic transformation data, the bystander component contributes only 6% of the total transformation rate for a broad-beam irradiation with a mean of 4 alpha particles (corresponding to a mean dose 0.3 Gy), increasing to 38% for a mean of 2 alpha particles (mean dose 0.15 Gy), and to 73% for a mean of 1 alpha particle (mean dose 0.074 Gy).

If the mechanisms postulated here were applicable *in vivo*, the consequences for low-dose risk estimation might be major. A linear extrapolation of risks from intermediate doses (where the bystander effect might be negligible) to very low doses (where the bystander effect may dominate) could underestimate the risk at very low doses -- an issue of considerable relevance in domestic radon risk estimation.

The BaD approach, here applied to *in-vitro* oncogenic transformation by acute doses of alpha particles (*1*), may be applicable to a more general model describing different endpoints, radiation qualities, and dose rates. In the current work, we have used some of the specific features of high-LET alpha-particle radiation to generate a fairly simple, preliminary model, in order to explore the fundamental trends without excessive parameterization.

Our understanding of the bystander phenomenon is prelim inary in nature, and the applicability of conclusions derived from *in-vitro* studies to the *in-vivo* situation is quite uncertain. It seems clear that as additional experimental evidence becomes available, modifications to models describing the effect will become possible and necessary. It is our hope that this quantitative approach will facilitate these developments.

Reference

1. Brenner DJ, Little JB, Sachs RK, *The Bystander Effect in Radiation Oncogenesis: II. A Quantitative Model*. Radiat. Res. (Accepted for publication, 2001).

MICROBEAM STUDIES

The Bystander Effect in Radiation Oncogenesis: Oncogenic Transformation Can Be Initiated in the Unirradiated Neighbors of Irradiated Cells

Satin G. Sawant, Gerhard Randers-Perhson, Charles R. Geard, David J. Brenner, and Eric J. Hall

Purpose

It has been accepted dogma for over half a century that radiation-induced heritable damage required interaction of the radiation with DNA (*1*,*2*), either by direct ionization or by the production of hydroxyl radicals in water molecules close to the DNA. However, over the past decade, a number of reports have appeared describing alpha-particle irradiations in which a larger proportion of cells showed biological damage than was estimated to have been hit by the alpha particles. The endpoints observed include cell killing, micronucleus induction, mutation induction, changes in gene expression, increases in intracellular oxygen species, and increases in cell growth (*3*-*7*). The goal of this study was to compare induced oncogenic frequencies in populations of cells, sparsely plated on dishes, in which a) all cell nuclei were hit with precisely defined numbers of alpha particles, and b) only a small proportion of the population was hit with the same numbers of alpha particles, the rest receiving no direct radiation exposure.

Materials and Methods

Before irradiation, C3H10T½ mouse fibroblast cells from passages 8-14 were grown in Eagle's basal medium supplemented with fetal bovine serum with added iron and gentamycin. 24 h before exposure, about 1000 exponentially growing cells were attached to the thin bases (3.8 μm polypropylene) of 6.3-mm diameter mini-wells. The attached cells were stained for 0.5 h with an extremely low concentration (50 nM) of the vital nuclear dye, Hoechst 33342, enabling individual nuclei to be identified and located with the optical image analysis system. The average stopping power of the alpha particles traversing the cells was 90 keV/ μm. Either 10% or 100% of the cells were exposed to defined numbers of alpha particles through the nucleus. Following irradiation, the cells were trypsinized from the irradiation container and replated at a low density of about 300 viable cells per dish into 100-mm culture dishes. The cells were incubated for 7 weeks with fresh culture medium every 12 days, before being fixed and stained to identify morphologically transformed types II and III foci. In parallel, dishes were plated with about 30 viable cells that had been subject to exactly the same conditions, and incubated for 2 weeks, after which the cells were stained to determine plating efficiencies and surviving fractions of the control and irradiated cells.

Results

The results are shown in Table 1 and Figures 1 and 2. With regard to clonogenic survival, irradiation of 10% of the cells with large numbers of alpha particles (8 or more) results in a clonogenic survival of slightly, though significantly, less than 90%, using a chi-square test. In other words, some cells were inactivated whose nuclei had not been traversed by alpha particles. With regard to oncogenic transformation, when only 10% of the cells were exposed to exactly 2 or more alpha particles, the resulting induced oncogenic transformation frequencies were

statistically indistinguishable from the those induced when *all* of the cells were irradiated with the same number of alpha particles. By contrast, and quite surprisingly, when 10% of the population was exposed to exactly one alpha particle, the induced oncogenic transformation rate was significantly larger than when all the cells were exposed to one alpha particle ($p = 0.047$).

Discussion

The three observations discussed here are that a) more cells can be inactivated by alpha particles than were actually traversed, b) when 10% of the cells on a dish are exposed to two or more alpha particles, the resulting induced oncogenic transformation frequency is indistinguishable from that when all the cells on the dish are exposed to the same number of alpha particles, and c) when 10% of the cells on a dish are exposed to exactly one alpha particle, the resulting induced oncogenic transformation frequency is significantly greater than when all the cells on the dish are exposed to one alpha particle. Each of these observations is evidence for a "bystander" effect, i.e., that unirradiated cells are responding to damage induced in irradiated cells. Taken together, the observations discussed here provide quite a stringent framework to guide the quantitative modeling of bystander effects. For example, the increased frequency of transformation when 10% of cells are irradiated with a single alpha particle, relative to when all are irradiated, points strongly to a low-dose mechanism dominated by bystander effects in unirradiated cells.

References

1. R. E. Zirkle and W. Bloom. *Science* **117**, 487-493 (1953).
2. T. R. Munro. *Radiat. Res.* **42**, 451-470 (1970).
3. C. Mothersill and C. B. Seymour. *Radiat. Res.* **149**, 256-262 (1998).
4. E. I. Azzam, S. M. de Toledo, T. Gooding and J. B. Little. *Radiat. Res.* **150**, 497-504 (1998).
5. H. Nagasawa and J. B. Little. *Radiat. Res.* **152**, 552-557 (1999).
6. H. Zhou, G. Randers-Pehrson, C. A. Waldren, D. Vannais, E. J. Hall and T. K. Hei. *Proc. Natl. Acad. Sci. USA* **97**, 2099-2104 (2000).
7. R. Iyer and B. E. Lehnert. *Cancer Res.* **60**:1290-1298 (2000).

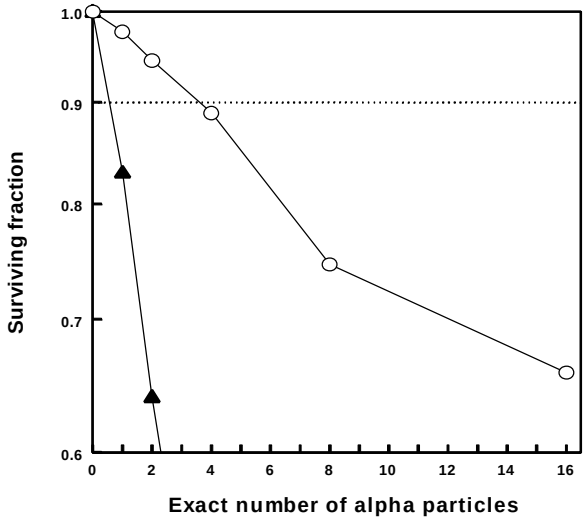

FIG. 1. Surviving fraction of cells resulting from by nuclear traversals by 5.3-MeV alpha particles. *Triangles* refer to exposure of all cell nuclei on each dish to exact numbers of alpha particle traversals using the microbeam system. *Circles* refer to exposure of 1 in 10 cell nuclei on each dish to exact numbers of alpha particle traversals; the dashed line indicates the 90% survival level -- results of experiments using the 1 in 10 irradiation protocol that exhibit surviving fractions below this level reflect direct evidence of a bystander effect.

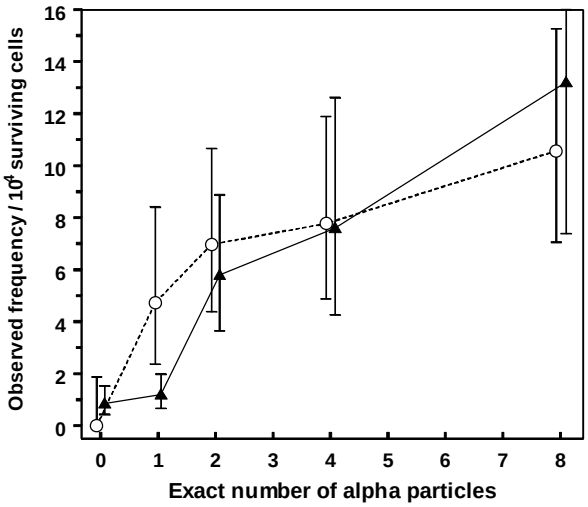

FIG. 2. Yield, per surviving C3H10T½ cell, of oncogenically transformed cells, produced by nuclear traversals by 5.3-MeV alpha particles. *Triangles* refer to exposure of all cell nuclei on each dish to exact numbers of alpha particle traversals using the microbeam system. *Circles* refer to exposure of 1 in 10 cell nuclei on each dish to exact numbers of alpha-particle traversals. Standard errors (±1 SD) were estimated assuming an underlying Poisson distributed number of transformed cells.

TABLE 1. Results from Microbeam Bystander Studies

% of cells irradiated	# of α particles through each irradiated cell	Clonogenic surviving fraction	# of dishes exposed	# of surviving cells exposed*	# of transformed clones produced**	Transformation frequency / 10^4 surviving cells
0	0		26	9,600	0	0
10	1	0.98	23	8,500	4	4.7
10	2	0.95	27	10,000	7	7.0
10	4	0.89	25	9,000	7	7.8
10	8	0.75	18	8,500	9	10.6
0	0		143	46,200	4	0.86
100	1	0.83	105	42,700	5	1.2
100	2	0.64	69	12,200	7	5.8
100	4	0.41	18	6,600	5	7.6
100	8	0.16	13	3,800	5	13.2

* Estimated, accounting for measured plating efficiency and clonogenic survival.

** No more than one transformed clone per dish was observed.

† Two sided comparisons made using Fisher's exact test. *S:* difference is statistically significant. *NS*: not significantl 5% significance level.

Adaptive Response and The Bystander Effect

Satin G. Sawant, Gerhard Randers-Pehrson, and Eric J. Hall,
in collaboration with Noelle F. Metting (Pacific Northwest National Laboratory)

Introduction

Cancer risk estimates for low-LET radiation are available from the epidemiological study of the A-bomb survivors, covering the dose range from 0.2 to 2.5 Sv. For lower doses of importance in radiation protection, risks must be inferred by an extrapolation from high doses. Both ICRP and NCRP recommend a linear, no-threshold extrapolation, but this generates great controversy. Two conflicting phenomena appear to be of importance at low doses and have the potential to impact on the shape of the dose-response relationship.

First, there is the *bystander effect*, the term used to describe the biological effects observed in cells that are not themselves traversed by a charged particle, but are neighbors of cells that are. Second, there is the *adaptive response*, whereby exposure to a low level of DNA stress resulting, for example, from a low dose of radiation, renders cells resistant to a subsequent exposure.

These two low-dose phenomena are conflicting in the sense that they operate in opposite directions. The bystander effect tends to exaggerate the effect of low doses by communicating damage from hit to non-hit cells, while the adaptive response confers resistance to a subsequent dose by a low initial priming dose.

Radiation-induced adaptive response has been observed for several endpoints, including gene mutations, chromosome and chromatid aberrations, DNA strand breaks, and micronuclei formation. Several recent studies have also shown evidence for the bystander effect of radiation using end points, such as the accumulation of p53 protein, frequencies of sister chromatid exchange and micronuclei formation. Utilizing the charged-particle microbeam as a mean of localized energy delivery system, we have observed a bystander effect on clonogenic cell survival and oncogenic transformation in mouse C3H10T½ cells. The present study was undertaken to determine the relative importance of the adaptive response and the bystander effect in mouse C3H10T½ fibroblast cells.

Materials and Methods

Mouse C3H10T½ fibroblast cells from passage 9 were grown in Eagle's basal medium supplemented with 10% heat-inactivated fetal bovine serum and gentamycin. Cells were irradiated at the Radiological Research Accelerator Facility of Columbia University. Cells were plated in 75-cm^2 flasks or microbeam dishes (800-1000 cells per dish) and were exposed to 0 or 2 cGy of 250 kVp X-rays from a Westinghouse Coronado machine at 5 mA with 0.2-mm copper and 1-mm aluminum external filters. The absorbed dose rate was calculated at 5.5 cGy min^{-1}. Six hours after the initial exposure cells were irradiated with either 4-Gy X-rays at 15 mA, with absorbed dose rate of 1.2 Gy min^{-1} or nuclei of 10% cells were exposed to 8 alpha particles accelerated by a 4-MV Van de Graaff accelerator to energy of 5.3 MeV (stopping power 90 keV/μm). Cells from the microbeam

experiment were replated in 100-mm cell culture dishes at cell density of 100 cells per dish to determine plating efficiencies and surviving fractions in control and X-ray-irradiated cells. Cells irradiated with X-rays were used to estimate the effect of low-dose radiation on clonogenic survival and oncogenic transformation induced by 4 Gy of X-rays. For the assay of neoplastic transformation, culture medium was changed at 12-day intervals during the 7-week incubation. Cells plated for clonogenic survival determinations were incubated for 2 weeks without medium change. At the end of either 2- or 7-week incubation, cells were fixed in formalin and stained with Giemsa. Cell survival was determined by the colony assay method while neoplastically transformed foci types II and III were identified according to the criteria of Reznikoff et al. (*1*).

Results

Cells exposed to the adaptive low radiation dose of 2 cGy followed by the 4-Gy X-ray dose showed higher clonogenic survival (49% vs. 32 % compared to control) compared to cells receiving only the higher radiation dose of 4 Gy (Figure 1, lower panel). Neoplastic transformation, expressed as number of transformed foci per dish, was lower in cells receiving the adaptive dose (4.30 vs. 5.40 per 10^4 surviving cells) compared to cells exposed to 4 Gy of X-rays alone (Figure 1, upper panel). With regard to microbeam irradiation, exposure of 10% of the cells with 4 or more alpha particles resulted in less than 90% clonogenic survival, indicating the presence of bystander effect. Prior exposure of cells to low-dose radiation showed higher clonogenic survival compared to the corresponding populations treated with same number of alpha particles through their nuclei (Figure 2).

Conclusion

These findings indicate that a small dose of 2 cGy of X-rays can result in an adaptive response that cancels out about half of the bystander effect induced by nuclear irradiation of α-particles.

Reference

1. Reznikoff CA, Brankow DW and Heidelberger C. Cancer Res. **33**:3231-3238 (1973).

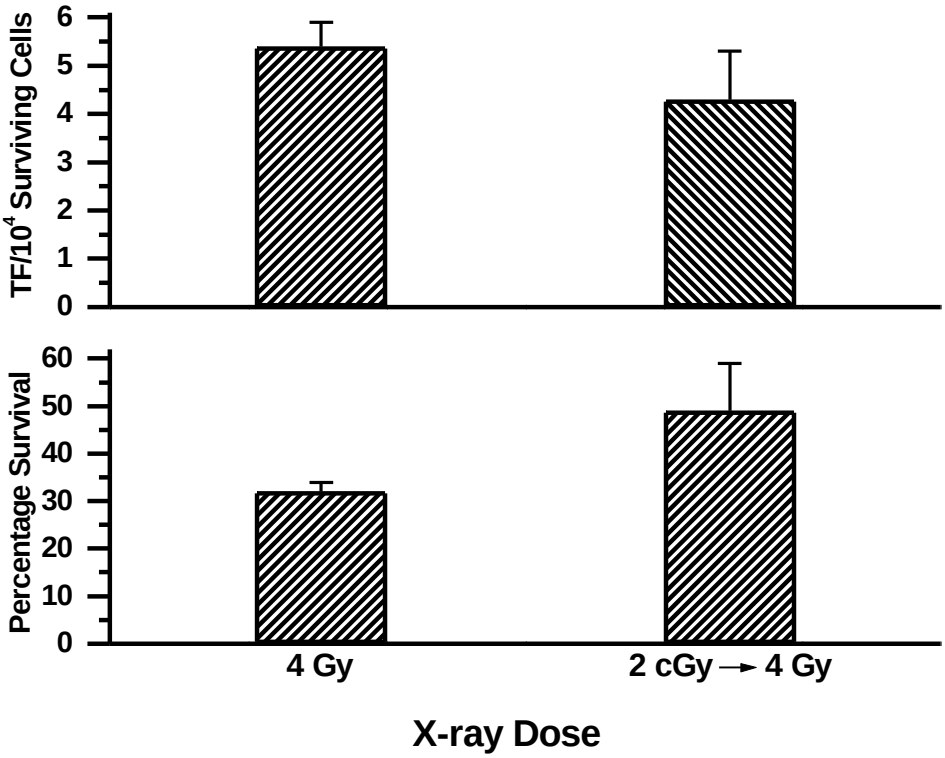

FIG. 1. Radiation-induced adaptive response in C3H10T½ cells. **Upper panel**. Cells exposed to 2 cGy adaptive dose followed by 4 Gy of X-rays show lower number of transformed foci compared to cells exposed to 4 Gy of X-rays alone. **Lower panel**. More colonies were observed in cells pretreated with 2 cGy followed by high X-ray dose compared to cells receiving only 4 Gy of X-rays.

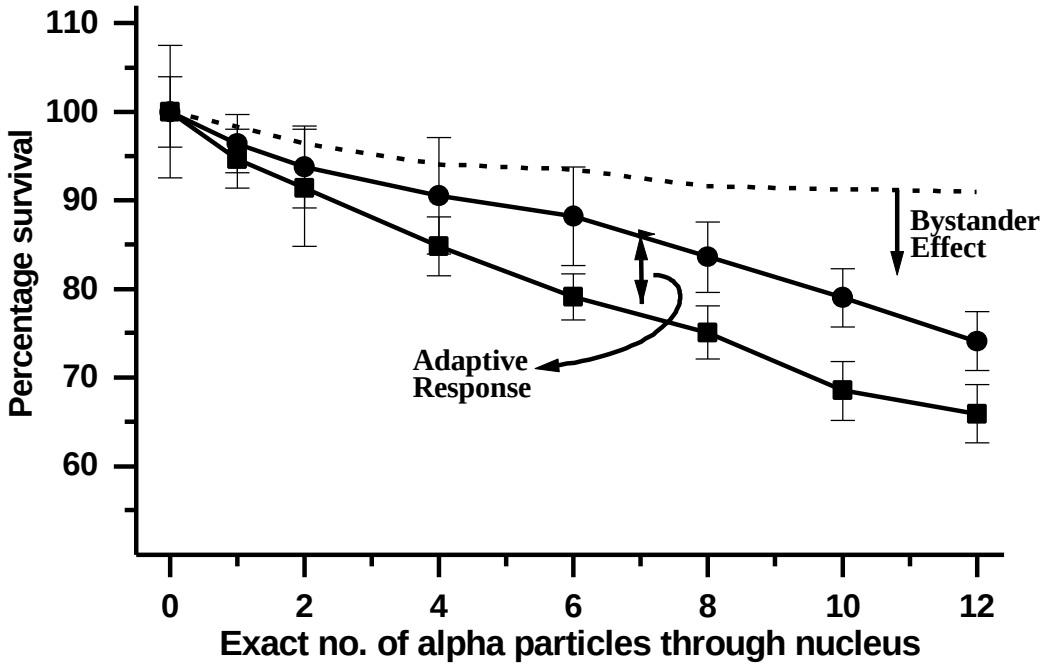

FIG. 2. Adaptive response and the bystander effect (Cell lethality): *Squares* refer to exposure of 1 in 10 cell nuclei on each dish to exact numbers of alpha-particle traversals; the dashed line indicates the expected survival level -- results of experiments using the 1 in 10 irradiation protocol that exhibit surviving fractions below this level reflect direct evidence of a bystander effect. *Circles* refer to cell survival from groups pretreated with 2 cGy of X-rays followed by exposure of 1 in 10 cell nuclei on each dish to exact numbers of alpha particle traversals using the microbeam system. Higher percentage of survival in groups pretreated with 2-cGy X-ray dose compared to corresponding untreated groups indicate presence of adaptive response on bystander effect of radiation.

Studies of a Bystander Mutagenic Effect in Mammalian Cells Using a Charged-Particle Microbeam

Hongning Zhou, Gerhard Randers-Pehrson, Charles A. Waldren (Department of Radiological Health Sciences, Colorado State University, Ft. Collins, CO), James E. Trosko (Department of Pediatrics, University of Michigan Medical School, East Lansing, MI), Eric J. Hall, and Tom K. Hei

Radon, a well-documented cause of lung cancer in underground miners, is a colorless, odorless gas present in indoor environments including homes and schools. Two of its progeny, Polonium-218 and Polonium-214, emit alpha particles during decay. When these emissions take place in the lung as the inhaled and deposited progeny undergo decay, the epithelial cells living in the airways can be damaged in such a way that lung cancer may eventually develop (*1*). Underground miners exposed to radon and its progeny have been shown to be at increased risk of lung cancer. Except for those at the highest levels of exposure, the lung cancer risk in these miners is related roughly linearly to exposure (*2-5*). Due to a lack of direct epidemiological evidence linking indoor radon and lung cancer, risk models for exposures received by the general population have been based on extrapolation from higher exposures in studies of underground miners. The most recent report from the U.S. National Academy of Sciences on the health effects of environmental exposure to radon gas estimated that 10-14% of all lung cancer deaths (~15,400 to 21,800) per year in the United States are linked to radon gas exposure from the environment (*1*). At high exposure levels, the cells at risk in the bronchial epithelium of miners may be traversed by several alpha particles, whereas for individuals exposed in homes at normal domestic radon level, it is unlikely that any cells at risk will be traversed by more than one alpha particle in a lifetime.

Over the past several years, there have been many reports on alpha-particle-induced bystander effects in mammalian cells (*6-13*). When only a fraction of the cell population is irradiated by alpha particles, biological effects such as SCE (*6-7*), induction of micronuclei (*8*), gene mutation (*9-10*), and expression of certain stress-related genes (*11-12*), have been observed at a significantly higher proportion of cells than those that are actually estimated to be traversed by an alpha particle. Although the mechanisms of the bystander effects are not yet clear, these investigations surely raise one important issue: how to assess the risk of exposure to radon? What is the modulation of bystander effects in evaluating such a risk, especially in normal domestic radon exposure?

It has been difficult to measure the induction of genetic changes in cell populations where only a small fraction of the cells are traversed by an exact, single alpha particle, particularly in the case of mutations, where the frequencies observed are low and are more correlative with cancer incidence. Although several studies were carried out using traditional track-segment alpha-particle irradiation, a precision charged-particle microbeam can solve this problem easily since, under the control of the image analysis system, a randomly selected small fraction of cells or a part of cells

can be traversed by an exact number of alpha particles, including a single alpha particle. Using the Columbia University microbeam together with human-hamster hybrid A_L cells, we found that irradiation through the nuclei of 5-20% of randomly selected cells with 2 alpha particles each result in mutant fractions that are significantly higher than expected, assuming no bystander modulation effect (Fig. 1). Furthermore, analysis by multiplex PCR shows that the types of mutants induced are significantly different from those of spontaneous origin. Pre-treatment of cells with the radical scavenger DMSO only had limited effect on the mutagenic incidence, however, pretreatment with 40 μM lindane, which inhibits gap junction cell-cell communication, significantly decreased the mutant yield. The doses of DMSO and lindane used in these experiments were non-toxic and non-mutagenic. To further determine whether release of labile mediators from irradiated cells was necessary for the bystander mutagenic effect, we incorporated a mixing experiment. After each cell was hit by 2 alpha particles in nucleus, the cells were detached by trypsination and mixed in with 4 times the number of non-irradiated cells to achieve a 20% ratio of irradiated population. No enhancement in bystander mutagenic effect was detected in these mixing studies, suggesting that cell-cell contact was required and that the contribution of a labile mediator(s) to a bystander mutagenic response was, at best, limited.

After that, we extended these finding to cells that are traversed by an exact single alpha particle. We show here that irradiation through the nuclei of 5 to 20% of randomly selected cells with a single alpha particle each results in mutant fractions that are significantly higher than expected assuming no bystander modulation effect. Pre-treatment of cells with the intracellular radical scavenger 10-mM N-acetyl cysteine (NAC) resulted in only a modest reduction in the mutagenic incidence. In contrast, cells pretreated with a 1-mM dose of Octanol, which inhibits gap-junction-mediated intercellular communication, significantly decreased the mutant yield. The dose of NAC and Octanol used in these experiments are non-toxic and non-mutagenic. To further investigate the role of cell-cell communication in bystander effects, we transfected AH1-9 cells (A_L cells plus a hygromycin resistance vector in chromosome 11) with either a dominant negative connexin 43 vector which shut down gap junctional communication or with connexin 43 expressing vector and repeated the bystander mutagenic studies. The data indicated that A_L cells containing the connexin 43 vector expressed a higher bystander mutagenic yield than that of vector control. In contrast, there was no significant mutagenic effect observed among A_L cells containing the dominant negative connexin 43 vector (Fig. 2). Our studies provide clear evidence that cells irradiated with alpha particles can induce a bystander mutagenic response in non-irradiated neighboring cells, and that gap-junction cell-cell communication plays a critical role in mediating such a bystander mutagenesis. The results are of considerable importance in reassessing the potential carcinogenic effect of domestic radon exposure and understanding the possible mechanisms involved.

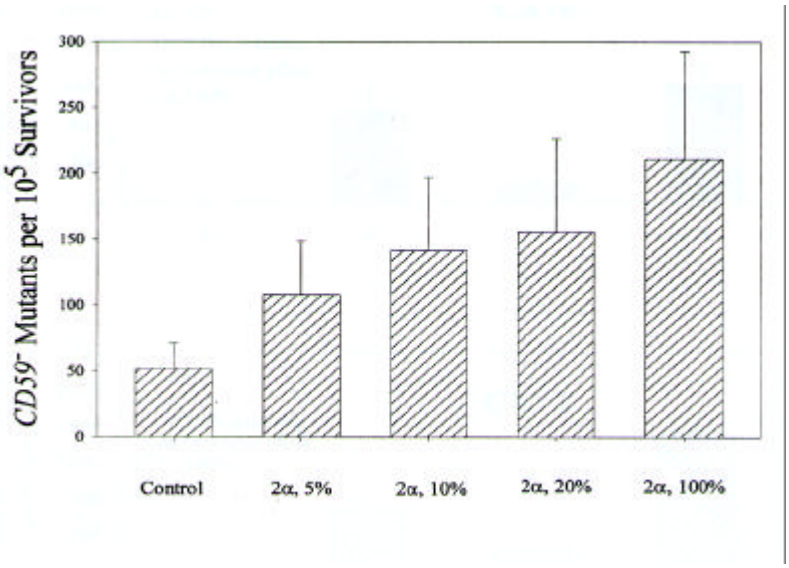

FIG. 1. Mutation fraction obtained from a population of A_L cells in which a fixed proportion of whose nuclei were traversed by 2 alpha particles. Data were pooled from 5 to 17 independent experiments. Bars represent ± SD.

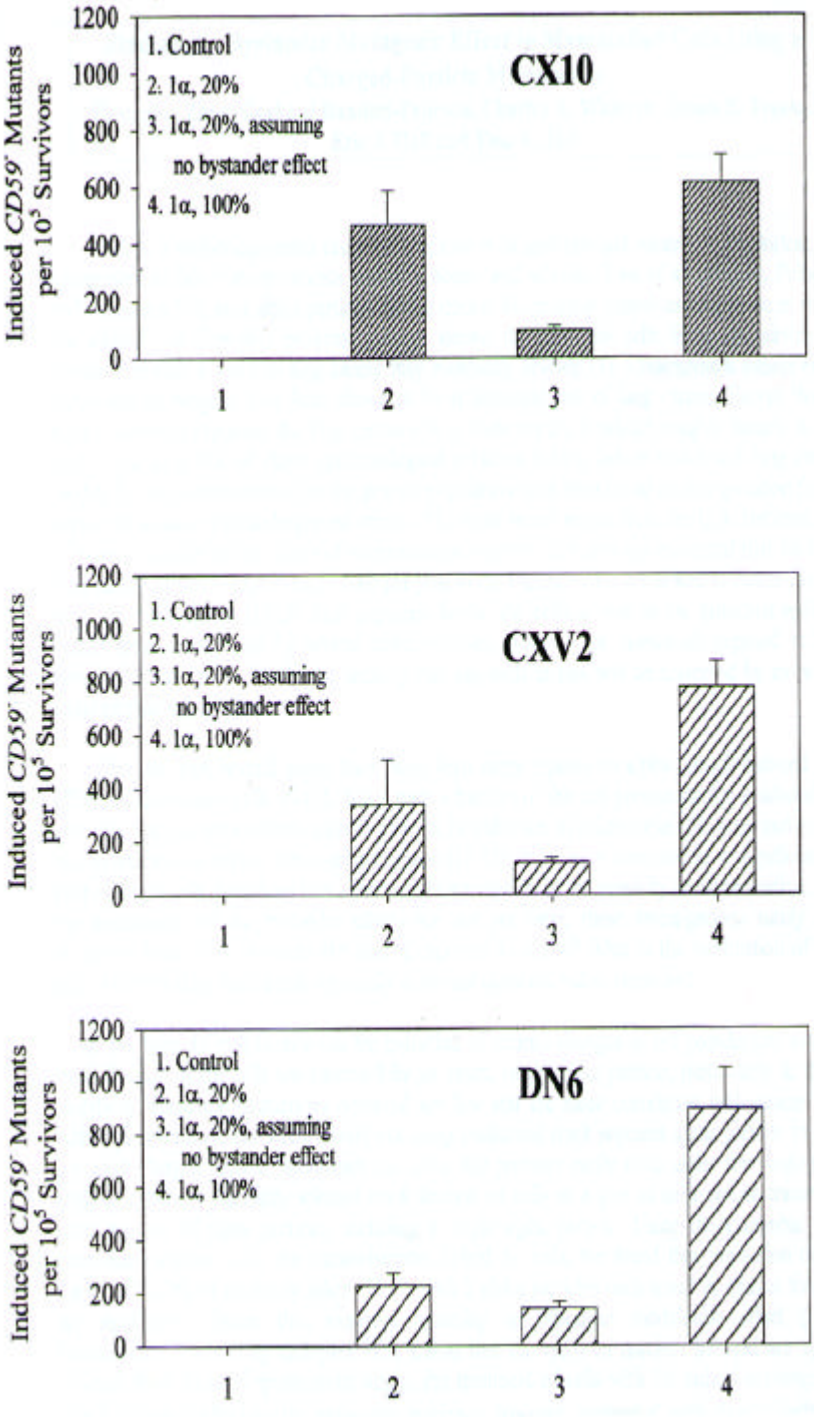

FIG. 2. Mutation fraction obtained from a population of AH1-9 cells transfected with conexin 43 expressing vector (CX10), a dominant negative conexin 43 vector (DN6), or vector alone (CXV2). Data were pooled from 2 to 4 independent experiments. Bars represent ± SD.

References

1. National Research Council Committee on Health Risks of Exposure to Radon (BEIV), Health Effects of Exposure to Radon: Time for Reassessment?, National Academy Press, Washington DC, 1994.
2. Samet, J.M. Radon and lung cancer. J. Natl. Cancer Inst. (Bethesda), 81:745-757, 1989.
3. Lubin, J. H., and Boice, J. D. Lung-cancer risk from residential radon: metaanalysis of 8 epidemiologic studies. J. Natl. Cancer Inst. (Bethesda), 89:49-57, 1997.
4. Lubin, J. H., Boice, J. D., Jr., and Edling, C. Radon and Lung Cancer Risk: A Joint analysis of 11 Underground Miner Studies. Bethesda: NIH, 1994.
5. Puskin, J.S., and Boice, J.D., Jr. EPA's perspective on risks from residential radon exposure. J. Air Pollut. Control Assoc., 39:915-920,1989.
6. Nagasawa, H. and Little, J. Induction of sister chromatid exchanges by extremely low doses of α-particles. Cancer Res., 52: 6394-6396, 1992.
7. Deshpande, A., Goodwin, E.H., Bailey, S.M., Marrone, B.L., and Lehnert, B.E. Alpha-particle-induced sister chromatid exchange in normal human lung fibroblasts: evidence for an extranuclear target. Radiat. Res., 145: 260-267, 1996.
8. Prise, K.M., Belyakov, O.V., Folkard, M., and Michael, B.D. Studies of bystander effects in human fibroblasts using a charged particle microbeam. Int. J. Radiat. Biol., 74: 793-798, 1998.
9. Nagasawa, H., and Little, J. Unexpected sensitivity to the induction of mutations by very low doses of alpha-particle radiation: evidence for a bystander effect. Radiat. Res., 152: 552-557, 1999.
10. Zhou, H., Randers-Pehrson, G., Waldren, C.A., Vannais, D., Hall, E.J., and Hei, T.K. Induction of a bystander mutagenic effect of alpha particles in mammalian cells. Proc. Natl. Acad. Sci. USA, 97:2099-2104, 2000.
11. Hickman, A.W., Jaramillo, R.J., Lechner, J.F., and Johnson, N.F. α-Particle-induced p53 protein expression in a rat lung epithelial cell strain. Cancer Res., 54: 5797-5800, 1994.
12. Azzam, E.I., de Toledo, S.M., Gooding, T., and Little, J.B. Intercellular communication is involved in the bystander regulation of gene expression in human cells exposed to very low fluencies of alpha particles. Radiat, Res., 150: 497-504, 1998.
13. Mothersill, C., and Seymour, C.B. Cell-cell contact during gamma irradiation is not required to induce a bystander effect in normal human karatinocytes: evidence for release during irradiation of a signal controlling survival into the medium. Radiat. Res., 149: 256-262, 1998.

Mutagenicity of Cytoplasmic Irradiation in Mammalian Cells: Role of Peroxynitrite Anions

An Xu, Gerhard Randers-Pehrson, and Tom K. Hei

Evidence derived from uranium mine workers and animal studies has demonstrated that radon is a risk factor in the development of lung cancer (*1*). Alpha particles emitted from radon and its progeny have been shown to cause cell transformation, damage in chromosomes, and gene mutations containing a wide range of deletions as well as base changes (*2-3*). Although alpha-particle traversals of the nuclei of target cells were of primary concern for the induction of lung cancer in earlier studies, recent evidence suggests that extranuclear or extracellular targets may also be important in mediating these effects (*4-5*). Using a precision charged-particle microbeam and dual fluorochrome dyes to locate nucleus and cellular cytoplasm, respectively, thereby avoiding inadvertent traversal of nuclei, we showed previously that cytoplasmic irradiation was, in fact, mutagenic at *CD59* locus of human-hamster hybrid (A_L) cells while inflicting minimal cytotoxicity (*6*). Furthermore, preliminary evidence suggests that reactive oxygen species mediate this process.

Nitric oxide (NO) is an important bioregulatory molecule with a range of physiological functions, including controlling of blood pressure and nerve transmission (*7*). In biological systems, NO is generated through the conversation of L-arginine to citralline, which is catalyzed by nitric oxide synthases (NOS) (*8*). NOS produce sustained high concentrations of NO in various mammalian cells after exposure to cytokines, hypoxia, heavy metals, and asbestos (*9-11*). *In vivo* and *in vitro* studies have suggested that high concentrations of NO and its metabolites, such as N_2O_3 and peroxynitrite ($ONOO^-$), can damage DNA which include deaminated bases, DNA cross-links, oxidized bases, and single-strand breaks, and lead to mutations (*10-11*).

To evaluate the role of NO in mediating the mutagenicity of cytoplasmic irradiation, individual human-hamster hybrid (A_L) cells were targeted and irradiated with 8 alpha particles through cytoplasm by using the microbeam in the presence or absence of N^G-methyl-L-arginine (L-NMMA). L-NMMA has been shown to competitively inhibit NOS activity in various cells (*12*). It is shown in Figure 1 that pretreatment of A_L cells with L-NMMA significantly suppressed mutation induction by ~3-fold to near background level ($p<0.05$). Furthermore, pretreatment of A_L cells with D-NMMA, the enantiomer of L-NMMA, which does not inhibit the activity of NOS (*13*), has less effect on the yield of mutants at equal doses. The doses of both L-NMMA and D-NMMA used here have been shown to be nontoxic and nonmutagenic in mammalian cells. These results strongly implicate free radicals, particularly NO, as being the mediator of the mutagenic response of cytoplasmic irradiation. In contrast, we found that L-NMMA treatment had no effect on the mutagenic yield in A_L cells irradiated by 2 alpha particles through the nuclei. Our studies provide direct evidence that peroxynitrite anions are involved in the induction of the mutants as a result of cytoplasmic irradiation.

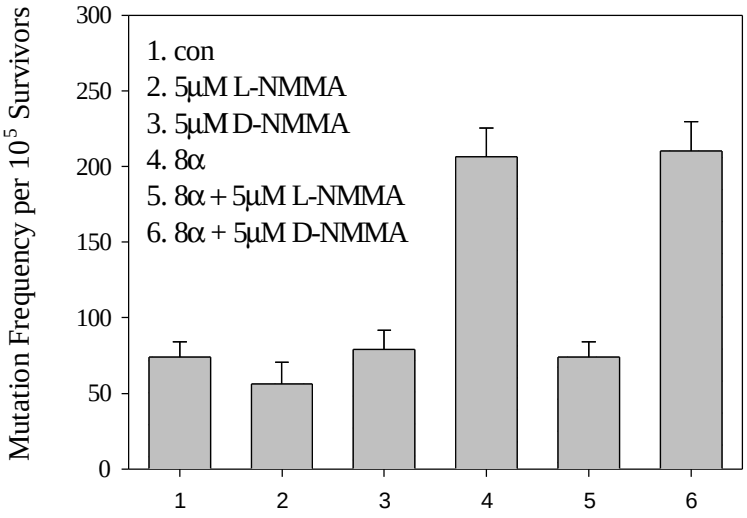

FIG. 1. Effects of L-NMMA or D-NMMA on the mutation yields in A_L cells irradiated with 8α through cytoplasma. Error bars represent ± SEM.

References

1. Jostes, R. F. Genetic, Cytogenetic, and carcinogenic effects of radon: a review. Mutation Res., *340*: 125-139, 1996;
2. Evans, H. H. Cellular and molecular effects of radon and other alpha particle emitters. Adu. Mutagen.Res., *3*: 28-52, 1991;
3. Evans, H. H., Hencl, J., Hui, T. E., Ricanati, M., Hong, M. F., DiDalvo, C., Bakale, G., and Rao, P. S. Cytotoxic and mutagenic effects of radon and radon daughters on murine L5178Y lines differing in DNA repair. Radiat. Res. *136*: 57-64, 1993;
4. Nagasawa, H., and Little, J. B. Induction of sister chromatid exchanges by extremely low doses of alpha-particles. Cancer Res. *52*: 6394-6396, 1992;
5. Hickman, A. W., Jaramillo, R. J., Lechner, J. F., Johnson, N. F. Alpha-particle-induced p53 protein expression in a rat lung epithelial cell strain. Cancer Res. *54*: 5797-5800, 1994;
6. Wu, L. J., Randers-Pehrson, G., Xu, A., Waldren, C. A., Geard, C. R., Yu, Z. L., and Hei, T. K. Targeted cytoplasmic irradiation with alpha particles induces mutations in mammalian cells. Proc. Natl. Acad. USA *96*: 4959-4964, 1999;
7. Moncada, S., Palmer, R. M., and Higgs, E. A. Nitric oxide: physiology, pathophysiology, and pharmacology. Pharmacol. Rev., *43*: 109-142, 1991;
8. Nathan, C. Nitric oxide as a secretory product of mammalian cells. FASEF J., *6*: 3051-3064, 1992;
9. Liu, F., and Jan, K. Y. DNA damage in arsenite- and cadmium-treated bovine aortic endothelial cells. Free Radical. Biology. & Medicine, *28*: 55-63, 2000;
10. Chao, C. C., Park, S. H., and Aust, A. E. Participation of nitric oxide and iron in the oxidation of DNA in asbestos-treated human lung epithelial cells. Archives. Biochem. & Biophys., *326*: 152-157, 1996;
11. Zhuang, J. C., Lin, C., Lin, D., and Wogan, G. N. Mutagenesis associated with nitric oxide production in macrophages. Proc. Natl. Acad. USA. *95*: 8286-8291, 1998;
12. Olken, N. M., Osawa, Y., and Marletta, M. A. Charaterization of the inactivation of nitric oxide synthase by N^G-methyl-L-arginine: evidence for heme loss. Biochem., *33*: 14784-14791, 1994;
13. Rees, D. D., Palmer, R. M., Schulz, R., Hodson, H. F., Moncada, S. Characterization of three inhibitors of endothelial nitric oxide synthase in vitro and in vivo. Br. J. Pharmacol., *101*: 746-52, 1990.

Investigation of the Bystander Effect in Known Irradiated and Non-Irradiated Normal Human Fibroblasts

Brian Ponnaiya, Gloria Jenkins-Baker, Gerhard Randers-Pehrson, and Charles R. Geard

Here we compare the response of known human fibroblast bystander cells to that of microbeam-irradiated cells using a modified vital staining protocol that allows direct identification and discrimination between hit and bystander cells. This approach takes full advantage of the ability of the microbeam to target specific cells in a population, and these are the first studies that directly visualize and assay known hit and bystander cells in the same population and compare the biological responses.

Normal human fibroblasts in plateau phase (≅95% G1 phase) were stained with the vital nuclear dye Hoechst 33342 (blue fluorescence) or the vital cytoplasmic dye Cell Tracker Orange (orange fluorescence) and plated at a ratio of 1:1 (Table 1).

Table 1. Cell numbers and BrdU labeling index of Hoechst 33342 and CTO stained cells at 2 hours post irradiation.

Dose	Number of Cells Counted (number of dishes)		Ratio of	% Cells Labeled	
	Hoechst Stained	CTO Stained	Hoechst: CTO cells	Hoechst Stained	CTO Stained
0 α-particles	2114 (9)	2120 (9)	0.997	2.78 ± 0.42	3.17 ± 3.06
1 α-particle	2138 (9)	2366 (9)	0.904	5.5 ± 2.60	4.81 ±1.92
2 α-particles	765 (3)	668 (3)	1.145	3.35 ± 2.47	4.43 ± 2.80
5 α-particles	1338 (6)	1574 (6)	0.850	3.52 ± 1.70	1.75 ± 0.82
25 α-particles	1607 (7)	1884 (7)	0.853	6.95 ± 2.05	4.10 ± 1.84

Only the blue fluorescing nuclei were microbeam irradiated with a defined number of 90-keV/μm alpha particles. The orange fluorescing cells were then bystanders. At specific times following irradiation, cells were either fixed *in situ* or isolated individually, and the responses of the bystander cells were compared to that of the irradiated cells. Hit cells showed a fluence-dependent induction of micronuclei as well as delays in progression from G1 to S phase. Known bystander cells also showed enhanced frequencies of micronuclei and transient cell delays (Figure 1, Table 2, Figure 2). Yields of micronuclei (Table 2) are expressed as totals for 24, 32, and 48 hrs. Increases in bystander cells ranged from 1.2- to 1.8-fold higher than controls, with no clear increase with alpha-particle number. In hit cells one alpha particle raised the incidence 2.8 times that of control, with 5 and 25 particles being 4.6- and 2.6-fold higher, respectively. Even 25 alpha particles do not hold cells in G1 permanently, but G2/M delay may apply, hence fewer micronuclei.

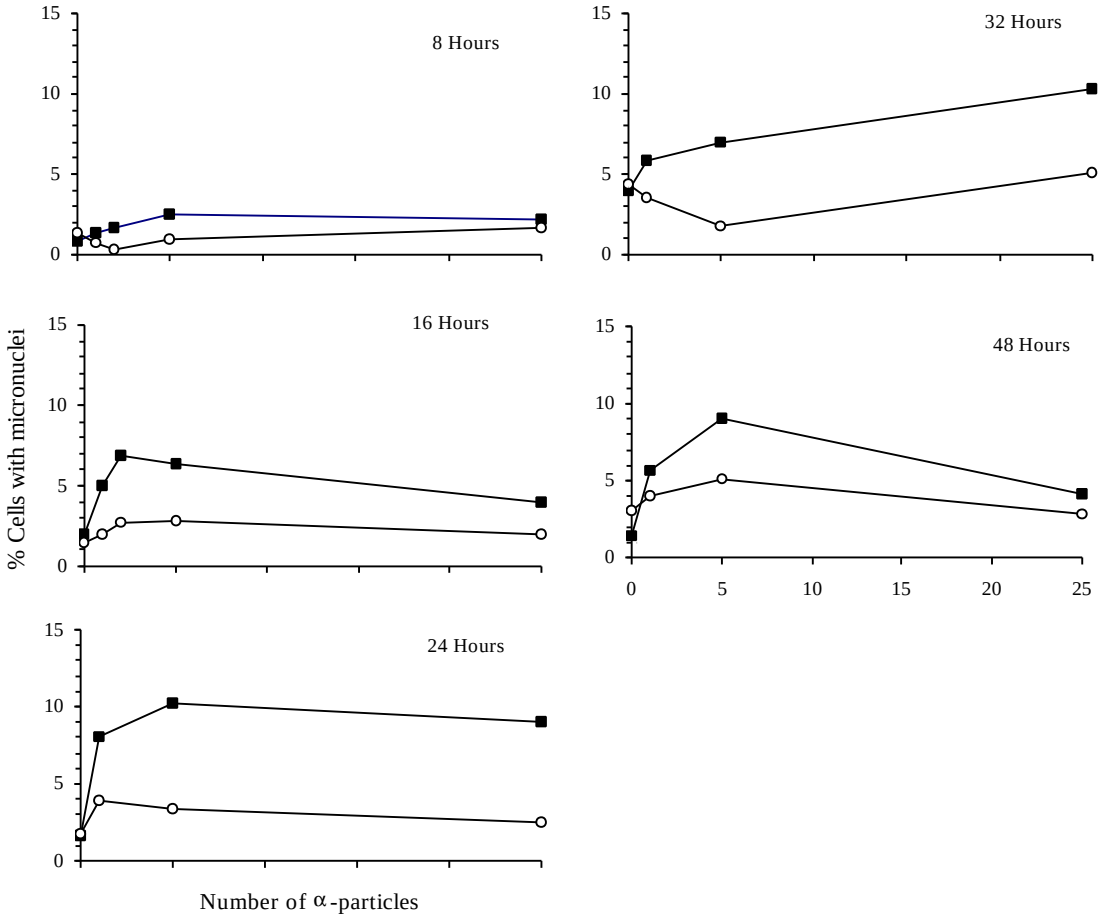

FIG. 2. Frequencies of microbeam-irradiated (■) and bystander (○) cells expressing micronuclei at various times following irradiation with α particles.

Table 2. Frequencies of micronuclei observed in hit and bystander cells following microbeam irradiation.

# of Particles	# of Cells Counted	Expected # of Micronuclei[a]	# of Micronuclei Scored
Control – Hoechst Stained	4898	-	81
Control – CTO Stained	5633		113
Control – total	10,531		194
1 α-particle -- Hoechst Stained	8221		436
1 α-particle -- CTO Stained	9205	184	256*
2 α-particles -- Hoechst Stained	2306		114
2 α-particles -- CTO Stained	1916	38	39
5 α-particles -- Hoechst Stained	6883		547
5 α-particles -- CTO Stained	8309	166	276*
25 α-particles -- Hoechst Stained	4760		313
25 α-particles -- CTO Stained	6745	135	180*

[a]Expected frequencies of micronuclei for bystander cells based on corresponding control values in the absence of a bystander effect. * Indicates observed frequencies are significantly different from expected values as determined by the χ^2 test ($p<0.001$).

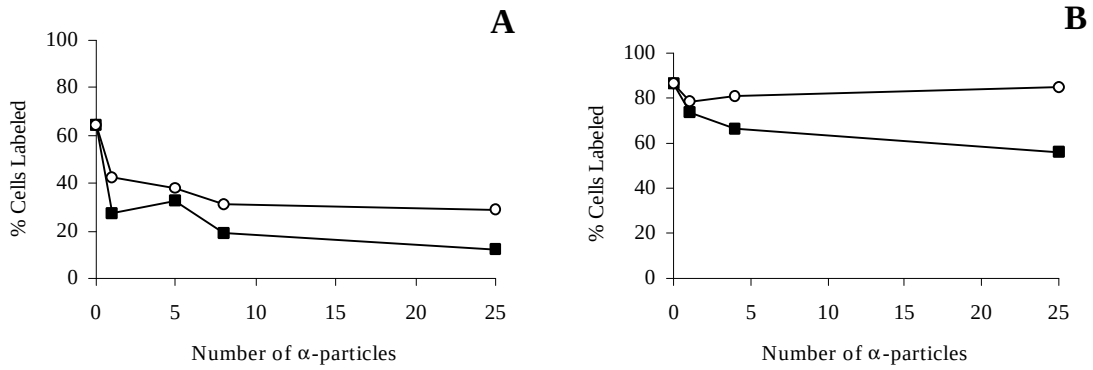

FIG. 2. Percentage of BrdU positive cells in irradiated (■) and bystander (○) populations at 24 hours (A) and 48 hours (B) post irradiation.

However, the induction of micronuclei in bystander cells did not appear to be dependent on the fluence of particles delivered to neighboring hit cells (see Figure 1). The cell-cycle delay correlated with the induction of p21/WAF1 in irradiated and some bystander cells (as seen by immunofluorescence). Single-cell RT-PCR of the p21/WAF1 message demonstrated that the hit cells showed a 4- to 10-fold increase in p21/WAF1 1 hour after microbeam irradiation with 10 α particles (Figure 3).

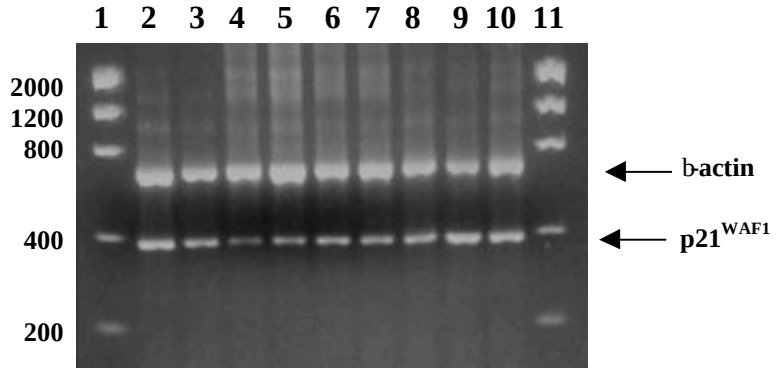

FIG. 3. Semi-quantitative RT-PCR of β-actin and p21/WAF1 mRNA from individual control (lane 2), irradiated (lanes 3,4,7 and 8) and bystander cells (lanes 5,6,9 and 10) one hour after microbeam irradiation with 10 α articles. Lanes 1 and 11 are molecular weight markers.

The response in individual bystander cells was more variable, with some cells showing little or no increase over control cells, while other cells showed induction of p21/WAF1 intermediate between that observed in known hit cells and control non-irradiated cells (Figure 4).

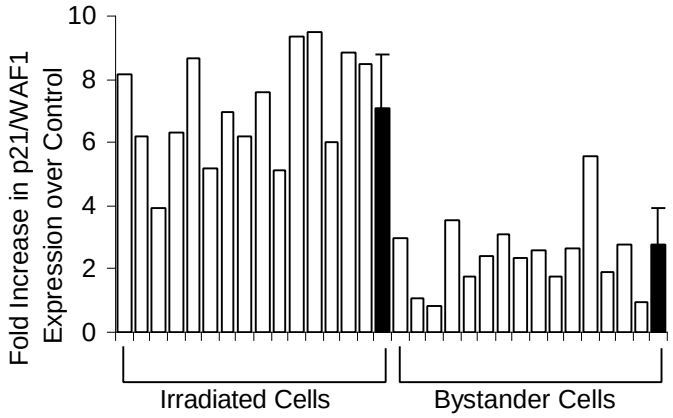

FIG. 4. Relative induction of p21/ WAF1 in single cells over controls, one hour following exposure to 10 α particles. Clear bars represent single cells; black bars represent the mean of 10 irradiated or bystander cells (error bars are SD).

These are the first studies wherein the bystander effect has been directly visualized rather than inferred. Relative to all other endpoints examined in bystander studies, enhanced gene expression, as seen for p21/WAF1, is the most common indication of a bystander effect. This is reflected both by immunofluorescence and complementary single-cell RT-PCR detection. The majority of bystander cells show a response, indicating that the signal from hit cells is widespread, although its nature remains to be determined. These data obtained with normal human fibroblasts, where the majority of cells were not in contact, indicate that the bystander phenomenon has a quantitative basis and strongly imply that the target for radiation effects cannot be considered to be the individual cell.

Bystander Cell Responses in Normal Human Fibroblasts as a Function of Hit-Cell Fraction

Charles R. Geard, Brian Ponnaiya, Gloria Jenkins-Baker,
and Gerhard Randers-Pehrson

The experiments described previously established definitive responses in known bystander cells when 50% of cells in a population were irradiated. Here a comparison is made between 2 approaches aimed at determining whether bystander cells show a hit-cell fraction responsiveness. Cells were prepared as 2 distinguishable populations where 2, 10 or 20% of cells were Hoechst stained and the remaining bystander cells cyto-orange stained. Only the Hoechst-stained cells were microbeam irradiated. Alternatively, all cells were stained with Hoechst, and 2, 10, or 20% of cells chosen at random and irradiated. This is the approach adopted in the mutation and transformation bystander studies and by others. After 17 experiments it was determined that both approaches produced similar results with the known hit-cell responses in agreement with expectation. Some results for cell cycle progression and % of cells with micronuclei are shown in Figures 1 and 2.

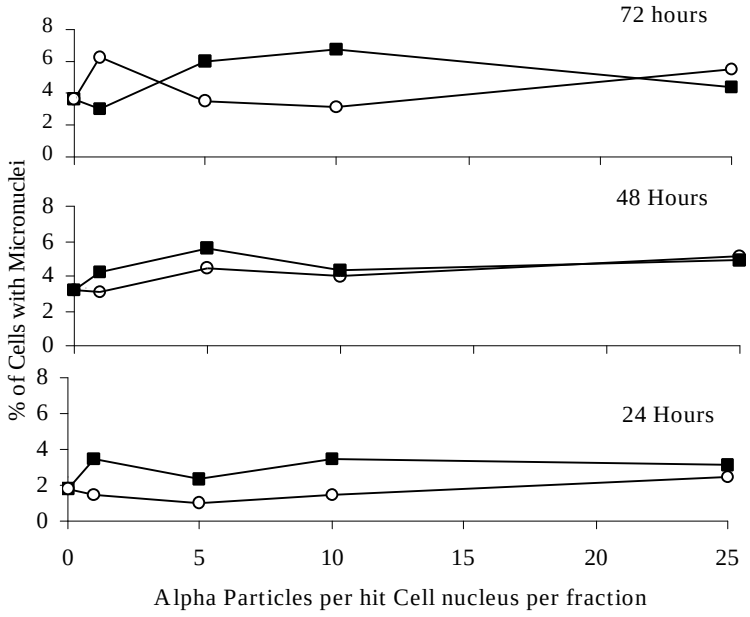

FIG. 1. Incidence of micronuclei in normal human fibroblasts after microbeam irradiation of nuclei of 2 (○) or 10 (■) % of G0/G1 phase cells.

The % of labeled cells was little different for 2 or 10% hit cells, with small changes from control levels. However, levels of micronuclei were greater than expected, and this effect was enhanced for 10 over 2 % of hit cells. That is, these results confirm the previous conclusion that there is a quantitative basis to the bystander effect, with

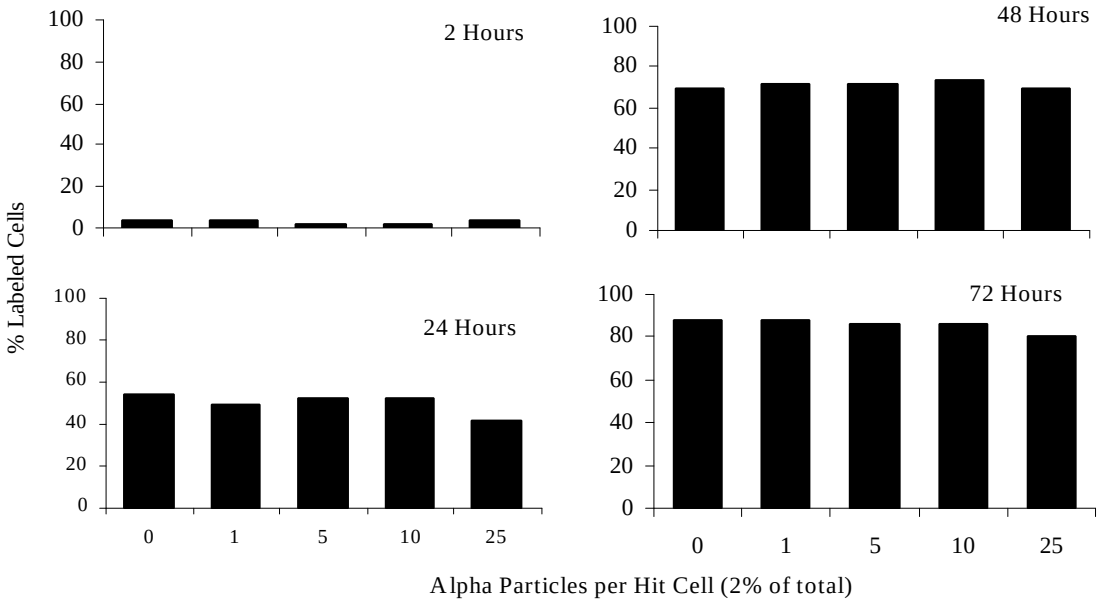

FIG. 2. Microbeam irradiation of 2% of cells in populations of G0/G1phase normal human fibroblasts. BrdU uptake (% labeled cells) as a function of time post irradiation.

responsiveness being dependent on the fraction of cells hit in a population [50>20>10>2 % of hit cells]. However, this response does not change as particle number per hit cell increases. One alpha particle per cell nucleus, the lowest dose it can receive, is as effective as 5,10 or 25 particles. These results clearly impact in the low-dose region and provide for strong rationale for this systematic evaluation of the bystander effect.

Evaluation of single-cell responsiveness in hit versus bystander cells (for 10% of known hit cells) is ongoing.

Cytoplasmic Irradiation of Normal Human Fibroblasts

Charles R. Geard, Brian Ponnaiya, Gloria Jenkins-Baker, and Gerhard Randers-Pehrson

It has recently been reported that targeted irradiation of the cytoplasm of hamster-human hybrid A_L cells resulted in enhanced mutation yields. The mutant spectrum differed from that for nuclear irradiation, and the effect was reduced by free-radical scavengers, also in contrast to nuclear irradiation. As pointed out by Grosovsky in 1999, these findings have a significant potential impact, clearly indicating that the radiation target extends to non-nuclear regions of the cell. Since in any trans-nuclear microbeam irradiation cytoplasmic regions are transgressed (along with extra-cellular medium), it is desirable to define the contribution of each cellular component. The cytoplasmic regions of normal human fibroblasts were defined and alpha particles fired through cytoplasmic regions on both sides of the cell nucleus. That is, 0+0, 1+1, 2+2, 5+5, or 10+10 particles per cell. Care is taken to ensure that nuclei are not hit. Both G0/G1 cells released from plateau phase and cycling cells were irradiated in 3 and 2 experiments, respectively. Results for % of labeled cells and % of cells with micronuclei as a function of time post irradiation are shown in Figures 1 and 2.

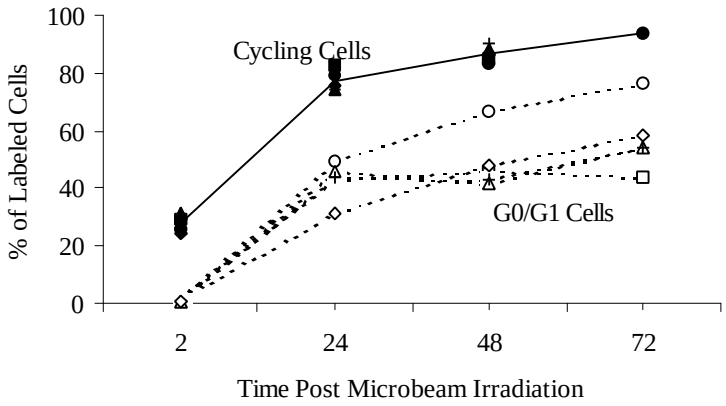

FIG. 1. Targeted cytoplasmic irradiation of cycling or G0/G1-phase normal human fibroblasts. BrdU uptake (% labeled cells) determined. Irradiated G0/G1 cells only are significantly different from control at 48 and 72 hours, with no difference as a function of alpha particles (2, 4, 10, or 20) per cell. Symbol distinctions not given.

The response for % labeled cells differed significantly between the cycling (about 28% cells showing BrdU uptake after 2 hrs) and G0/G1 cells (~2%). Cytoplasmic irradiation had no effect on the cell cycle progression of cycling, but for the G0/G1 cells there were only minor differences from control at 24 hrs, with relatively little progression thereafter. It appears that a significant fraction of cells suffer no effect but the remainder fail to enter S phase for 48 hrs or more. This differential response is interesting and has not been noted previously. With regard to micronucleus induction there are no consistent differences throughout. That is, though cytoplasmic irradiation is mutagenic, with mainly base changes and small deletions in A_L cells, it is not clastogenic in normal human fibroblasts. It was predicted that cycling cells "will be most sensitive to the effects of

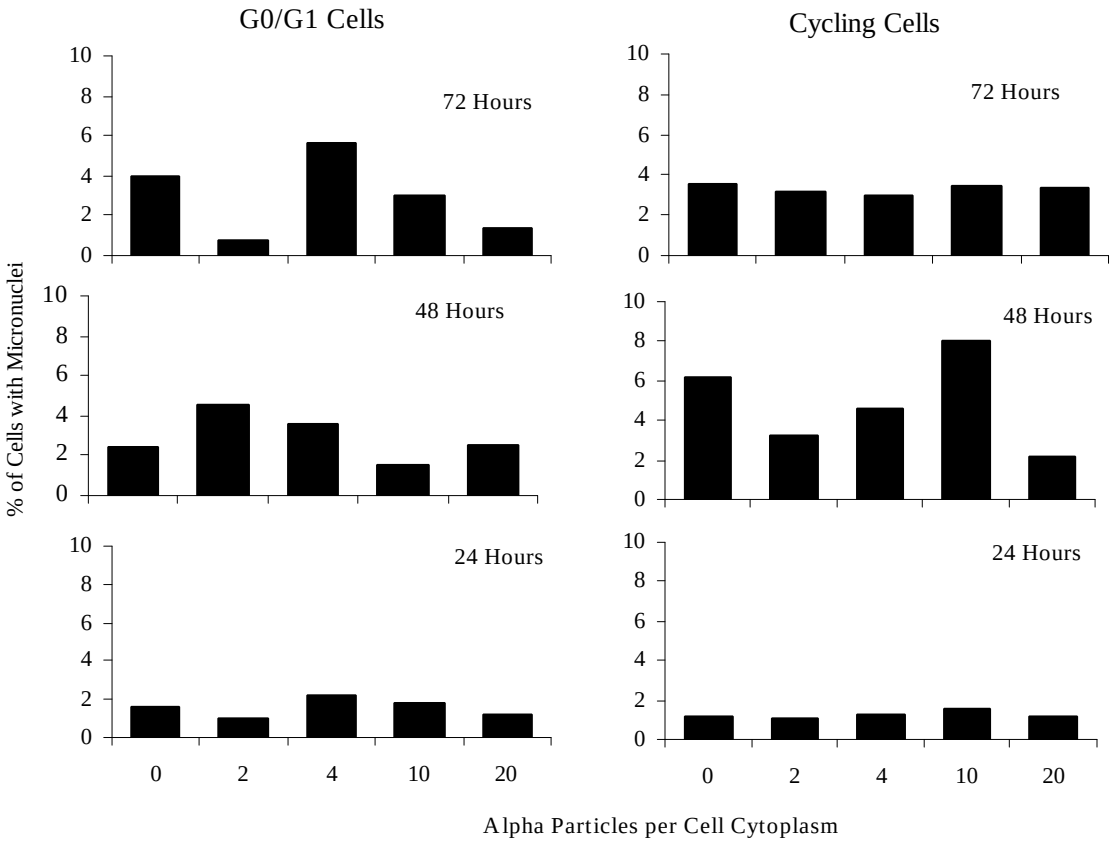

FIG. 2. Cytoplasmic irradiation with 0, 2, 4, 10, and 20 particles per cell (from left to right in each panel). There are no consistent differences for incidences of micronuclei for irradiated G0/G1 (left) or cycling cells (right).

cytoplasmic irradiations". Clearly, this prediction was wrong, but this helps to reinforce the value of precisely targeted irradiations to assess scientific predictions. The principal contribution to the clastogenic effect of alpha particles therefore resides in the nucleus, with a possible variable contribution from cytoplasmic hits for cytostatic effects.

Microbeam Irradiation of Intercellular Medium Between Normal Human Fibroblasts

Charles R. Geard, Brian Ponnaiya, Gloria Jenkins-Baker, and Gerhard Randers-Pehrson

Since it has been suggested that irradiation of medium alone can contribute to cellular changes, and, since some energy from alpha-particle traversals has to be deposited in medium, a protocol was devised to irradiate intercellular space. The largely ellipsoidal cell nuclei are recognized and 150 micrometers is set on either side of the short axis of these cells whose cytoplasm mainly elongates in the directions of the long axis. Irradiation does not take place if any nucleus is within these bounds. For each cell on a given dish, 0+0, 1+1, 5+5, 10+10, or 50+50 alpha particles were delivered to medium alone. These experiments require cells to be plated at low density (~150 per microbeam dish) in order to ensure wide separation, hence it is difficult to generate a substantial body of data.

The combined results from 4 experiments involving 72 dishes showed that microbeam irradiation of the thin layer of medium adjacent to cells, with up to 100 particles per cell, results in no consistent differences from controls, neither for cell cycle progression, nor for incidence of micronuclei. These results encourage the conclusion that effects on medium alone are of no concern in these microbeam studies.

p53 Modulation and Microbeam Responses: Studies with MCF-7 and MCF-7/E6 Cells

Charles R. Geard, Gloria Jenkins-Baker, Gerhard Randers-Pehrson,
with David Boothman (Case Western Reserve University)

It is clear that cell responses to ionizing radiation significantly involve p53. Cells transfected with an E6 construct have an abrogated p53 response since p53 catabolism is enhanced. Breast carcinoma MCF-7 cells and MCF-7/E6 cells were microbeam irradiated through nuclear centroids, and cell cycle progression and the incidence of micronuclei assessed. These studies were undertaken as a preliminary to evaluating the hypothesis that wild-type p53 function is required for bystander responsiveness. Mixed cell cultures will be irradiated with one known cell type being the bystanders and vice versa. Results are shown in Figure 1.

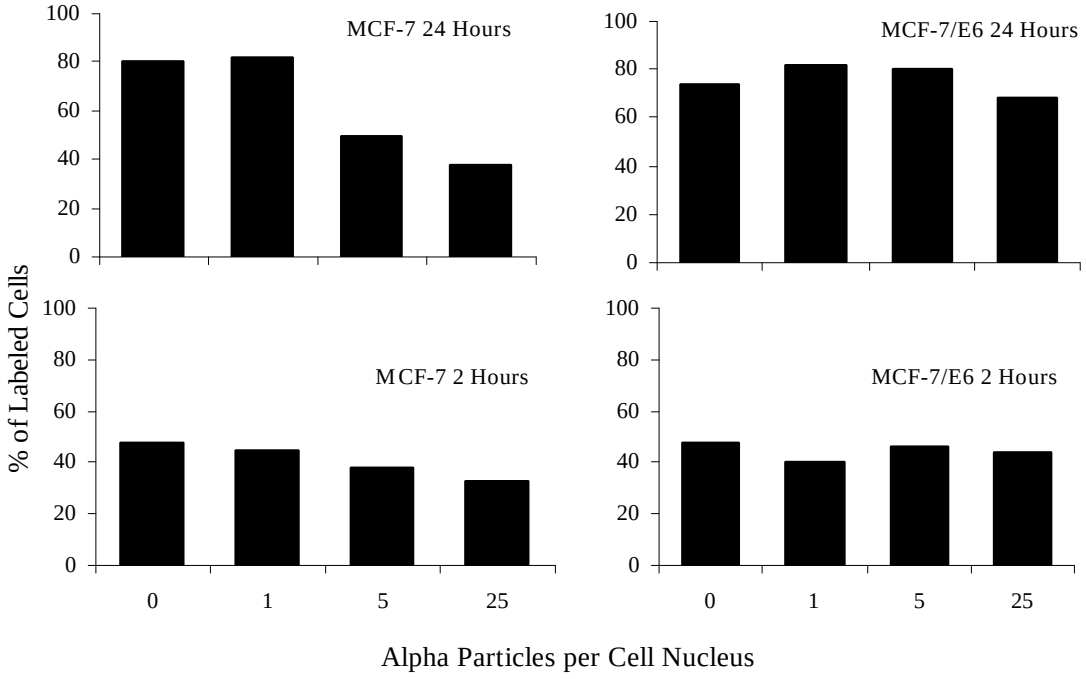

FIG. 1. BrdU uptake (% labeled cells) at 2 and 24 hrs post microbeam irradiation. There is particle-dependent reduction for MCF-7 (p53 wild-type), but no effect for MCF-7/E6 (p53 abrogated) cells.

The MCF-7 cells show profound differences from the MCF-7/E6 cells for % of labeled cells, with particle-number-dependent delays, reflecting the functioning p53-p21/WAF1 pathway. This difference allows for a determination of whether irradiated MCF-7/E6 cells can initiate a delay in bystander MCF-7 cells. Also, whereas micronuclei frequencies are similar, the incidence of apoptotic cells is distinct (data not shown), providing another assay for bystander responsiveness.

Microbeam Studies with Lifespan-Extended Human Retinal Pigmented Epithelial Cells

Charles R. Geard, Brian Ponnaiya, Gloria Jenkins-Baker,
and Gerhard Randers-Pehrson

The broad range of studies undertaken over many years with normal human fibroblasts, has at times proved frustrating because of response variation as passage number increases towards senescence. This applies to cell progression parameters and background incidence of micronuclei. Lifespan-extended cell lines expressing human telomerase have been developed from normal human cells, and show long term consistent growth parameters. Preliminary microbeam studies have been undertaken with retinal pigmented epithelial cells, RPE-htert. The combined results from three experiments involving trans-nuclear irradiations are shown in Figure 1.

These cells show similar responses to human fibroblasts for micronuclei induction and cell cycle delay, and are very good for imunofluorescent localization of p53 and p21/WAF1. Interestingly, and supporting the contention for evaluations on single cells, there is a broad range of responses between cells and often a lack of concordance between single cell levels of p53 and p21/WAF1.

In other studies, broad-beam alpha particles in track-segment mode are being used to examine aspects of media transfer of bystander signals. Special dishes were devised to allow for two populations of cells to be cultured but only one irradiated. Stainless steel rings with 35-mm internal diameter and 10 mm high have mylar epoxied to both sides. One cell type can be plated on one or both inner surfaces via sealable ports in the side. RPE-htert cells and human fibroblast BJ/1-htert cells have been used in these studies, where the dish is filled with medium, nurturing both cell surfaces. Cells on one side are irradiated with alpha particles which stop in the medium, the other cells are then bystanders.

The question being asked is: Do irradiated cells release a factor/s into the medium which can initiate a bystander response in recipient cells? This has been done on a same-cell-type and a mixed-cell-type basis. Other dishes were also devised which enabled the distance between the two cell populations, and hence the volume of medium to be controlled. These studies are ongoing but have provided significant experience with the two cell types proposed for usage in this proposal. Bystander responses have been observed in these very clearly non-contacting cells, confirming the results with the microbeam bystander studies.

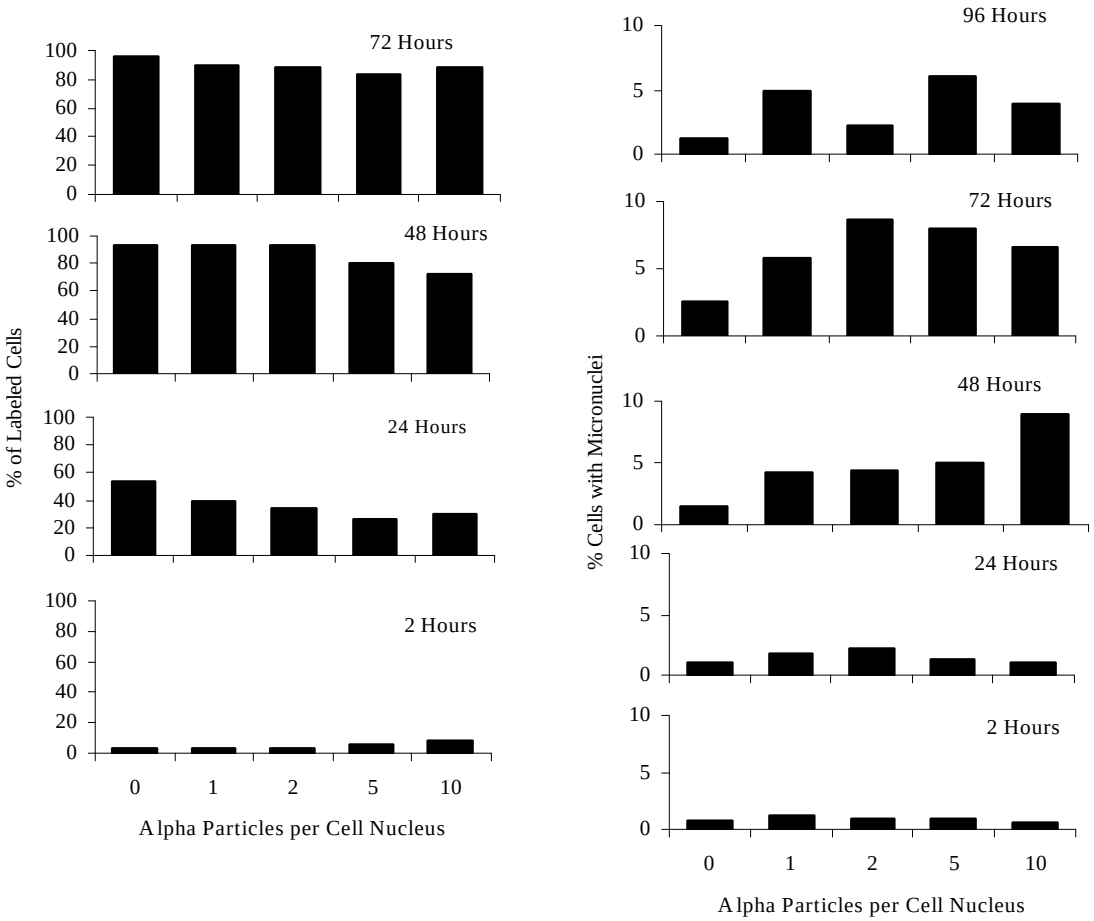

FIG. 1. Human epithelial cells (RPE-htert) were released from plateau phase, plated as single cells, and microbeam irradiated through nuclear centroids, then analyzed in situ up to 96 hrs.

As is clear from previous data, the single-cell RT-PCR approach is working well. This procedure was developed using a serial dilution of cell numbers over a significant period of time as experience was gained. The first studies, where known single cells were collected by micromanipulation, resulted in about a 40% success rate. This has now doubled, and the success rate (that is when products are obtained) for known single cells is now routinely 80%. Loss of a cell by, for example, attachment to surfaces can not be circumvented completely. An example of single-cell RT-PCR for some early-response genes which may play a role in bystander cell responsiveness, is shown in Figure 1.

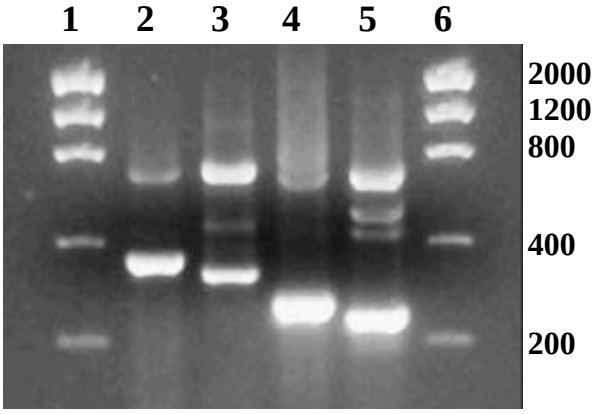

Figure 13: Single-cell RT-PCR using β-actin primers (lanes 2-5) in combination with primers for *c-fos* (lane 2), *c-jun* (lane 3), *junB* (lane 4) and *H-ras* (lane 5). Lanes 1 and 6 are molecular weight markers.

This clearly shows the power of single-cell analyses.

SCGE Detection of DNA Damage in Human Nuclei Induced by Microbeam Irradiation Using Alpha Particles

Adayabalam S. Balajee, Brian Ponnaiya, M. Prakash Hande, T.S. Kumaravel and Althaf Lohani (Laboratory of Molecular Genetics, NIH Gerontology Research Center), Gerhard Randers-Pehrson, Stephen A. Marino, and Charles R. Geard

Double-strand breaks (DSBs) are considered to be one of the most important lesions induced by ionizing radiation. DSBs, if unrepaired or misrepaired, lead to cell mortality and stable genetic alterations. Recent studies have shown that the spatial distribution of DSBs within the interphase nuclei upon irradiation largely depends on the track structure of radiation. DSBs generated by high-LET radiations are found to be non-random and the distribution pattern of DSB is dependent on higher order chromatin structure (*1*). In order to determine the lesion induction and distribution in interphase nuclei, precise targeted irradiation with a defined number of charged particles is an absolute requirement. This would enable us to understand the impact of chromatin structure on lesion induction and repair in different sub-cellular components. Using such a facility developed at RARAF for microbeam α-particle irradiation, Wu, et al. (*2*) have shown that targeted cytoplasmic irradiation has the potential to induce mutations in mammalian cells. Induction of "bystander" mutagenic effects has also been noticed in unirradiated cells (*3*). Elucidation of the molecular cause for the mutagenicity and bystander effects require the characterization of the DNA lesions induced by α-particle irradiation. Determination of the types of DNA lesions and their repair kinetics induced by targeted nuclear and cytoplasmic α-particle irradiation may provide insights towards understanding the mechanistic basis for mutagenicity/bystander effects caused by microbeam irradiation.

Attempts are made to measure the induction and repair of DNA strand breaks and oxidative DNA lesions by single-cell gel electrophoresis (SCGE) assay in primary fibroblast cells of Normal (NHDF, WI38), and radiosensitive Ataxia telangiectasia (GM2052C, GM5823C). The layout and microbeam irradiation procedure have been previously described (*4*). Briefly, plateau-phase cells were trypsinized and 500-1000 cells were seeded in dishes specially designed for microbeam irradiation. The cells were stained with a 50-nM solution of Hoechst 33342 for 30 min prior to irradiation. In the initial experiments, we have irradiated the nuclei of normal diploid fibroblasts (WI38) with 1, 2, 4 and 8 α-particle irradiation and analyzed the induction and repair of all types of DNA lesions by alkaline SCGE under two pH conditions (12 and 13.1). The initial induction of DNA damage after 8-alpha-particle irradiation of human nuclei is shown in Figure 1. The damaged DNA migrates out of the nuclei and appears as tail of the comet. The tail length was measured using a COMET software program and expressed as Olive Tail Movement (OTM). OTM gives an indication of the initial DNA damage and repair after radiation treatment.

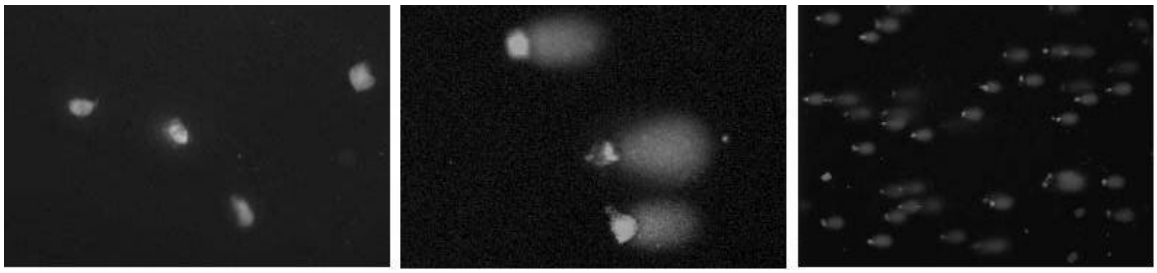

Control **8 a-particles, 0 min** **8 a-particles, 0 min**

FIG. 1. SCGE detection of initial DNA damage by nuclear irradiation of 8 α particles in WI38 cells.

Using this assay, we found that more than 90% of the lesions induced by 8 α particles are efficiently repaired by 3 hrs after treatment (Fig. 2). Dose-response experiments done at two different pH conditions indicated that the lesions induced by 4 α particles and above are detectable using this assay (Fig. 2).

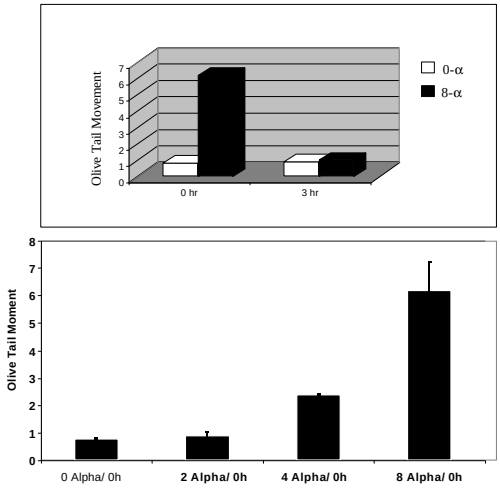

FIG. 2. Histogram showing the induction and repair of DNA damage in human fibroblast cells detected by SCGE assay.

Experiments comparing repair kinetics of DNA lesions induced by microbeam irradiation in Normal and AT cells are in progress. Initial experiments revealed that the initial induction of lesions by 8 alpha particles is similar in primary as well as SV-40-transformed Normal and AT fibroblast cells.

In addition to DNA strand breaks, efforts are being made to determine the oxidative base lesions such as thymine glycol and 8-Oxoguanine by a modified SCGE assay. This assay involves the enzymatic digestion of nucleoids with endonuclease III (Endo III) and Formamido pyrimidine glycosylase (FPG) prior to gel electrophoresis. This modified SCGE assay may improve the overall sensitivity of DNA damage detection if combined with the analysis of DNA strand breaks. Our future goal is to increase the sensitivity of this assay to detect the damage induced by a single α particle. We are planning to use this assay to determine the effect of cytoplasmic irradiation on nuclear DNA damage and also the impact of cytoplasmic vs. nuclear irradiation on bystander effects. We wish to investigate bystander effects in p53 mutant cell lines as well as in human, mouse, and hamster cell lines that are defective in DSB repair proteins. Additionally, we would like to determine the DNA damage and repair in defined genomic sequences by a combination of SCGE and fluorescence in situ hybridization (FISH) techniques.

References

1. Newman, H.C. et al. (2000) Int. J. Radiat. Biol. 76, 1085-1093.
2. Wu, Li-Jun et al. (1999) Proc. Natl. Acad. Sci. (USA) 96, 4959-4964.
3. Zhou, H. et al. (2000) Proc. Natl. Acad. Sci. (USA) 97, 2099-2104.
4. Hei, T.K. et al. (1997) Proc. Natl. Acad. Sci. (USA) 94, 3765-3770.

CELLULAR STUDIES

Routine Mammographic Screening and Breast Cancer Induction

Satin G. Sawant, Stephen A. Marino, Charles R. Geard, and David J. Brenner,
in collaboration with Zugen Fu (SUNY/Stony Brook)

There is a good deal of evidence, both experimental and theoretical, that X rays below 40 keV are biologically more effective per unit dose than higher-energy gamma rays. Screening mammography with X rays results in tissue doses being delivered primarily by photons with an energy of less than 20 keV. Such photons interact with tissue predominantly through the photoelectric effect, producing low-energy electrons that have different patterns of energy deposition at the cellular level compared with those from higher-energy X rays. Given the increasing emphasis on breast cancer detection using mammographic screening and in keeping with a recent ACS recommendation that "the stated risk" from mammography should be further quantified, it is very important to provide realistic risk estimates for breast cancer induction from mammographic X rays . The aim of the present work is to assess the relative biological effectiveness of low-energy X rays for an endpoint pertinent to carcinogenesis: *in vitro* oncogenic transformation.

Mouse C3H10T½ fibroblast cells from passage 9 were grown in Eagle's basal medium supplemented with 10% heat-inactivated fetal bovine serum and gentamycin. Cell dishes made from Kynar (less than 80 μm thick) were coated with a thin layer of CellTak. Approximately 40 hours prior to irradiation cells were plated at a density of 8×10^3 cells per dish, such that the cells would be in exponential phase of growth at the time of irradiation. Since the X-ray beam is horizontal, the cell dishes were vertical and the side on each dish opposite to the Kynar surface was sealed with 6-μm-thick Mylar held in place with help of a metal ring. In order to prevent cells from drying, the dishes were filled with fresh medium through one of the ports on the edge of the dish. The dishes, completely filled with medium, were transported to Brookhaven National Laboratory in Upton, NY in portable incubators set to maintain a 37 ^{o}C environment. The Kynar dishes containing exponentially growing C3H10T½ cells in monolayer were placed in a radiation wheel capable of holding up to 20 dishes and the cells were irradiated with 0, 1, 2 or 4 Gy of 15.2-keV X rays at room temperature. Upon completion of the irradiations with soft X rays, dishes were returned to the incubators and transported back to the Radiological Research Accelerator Facility (RARAF). Between 12 to 22 hours post irradiation cells were trypsinized and used for determination of cell survival and induction of transformation.

For determination of relative biological effectiveness (RBE), cells were exposed to 250-kVp X rays and gamma rays at RARAF and the Center for Radiological Research (CRR) of Columbia University, respectively. Cells irradiated at RARAF were plated in 75-cm^2 flasks, whereas cells irradiated at CRR were plated in Kynar dishes and transported to CRR in portable incubators. Cells were exposed to 4 Gy of 250-kVp X rays from a Westinghouse Coronado machine at 15 mA with 0.25-mm copper and 1-mm aluminum external filters. Simultaneously, c ells carried to CRR were irradiated at room temperature with 0, 1, 2 or 4 Gy of gamma rays at a dose rate of 1.1 Gy/min using a ^{137}Cesium source.

Following irradiation, the cells were trypsinized from the irradiation container and replated at a low density of about 300 viable cells per dish into 100-mm culture dishes. The cells were incubated for 7 weeks with fresh culture medium every 12 days, before being fixed and stained to identify morphologically transformed types II and III foci. In parallel, dishes were plated with about 30 viable cells that had been subject to exactly the same conditions, and incubated for 2 weeks, after which the cells were stained to determine plating efficiencies and surviving fractions of the control and irradiated cells.

Oncogenic transformation induction frequencies were determined for C3H10T½ fibroblasts exposed to low-energy X rays, and the results were compared with those for higher-energy X rays. At a high dose of 4 Gy, no difference in the cell survival was observed when cells were irradiated with low- or higher-energy X rays (Fig. 1). Again at 4 Gy, the frequency of transformed foci observed after irradiation with 15.2-keV X rays was about 20% higher compared to the frequency observed with high-energy X-ray irradiation (Fig 2).

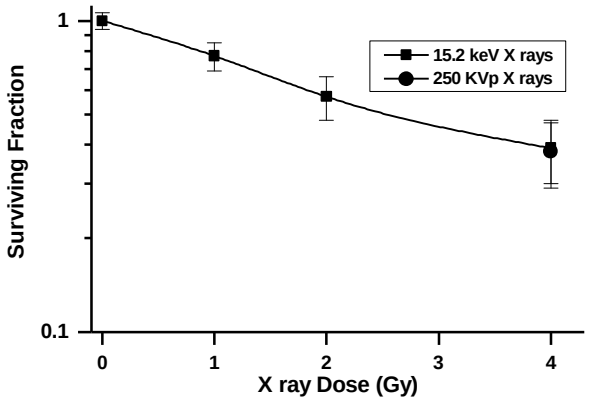

FIG. 1. Cell survival with 15.2-keV X rays. *Squares* refer to exposure of cells to 15.2-keV X rays. *Circle* refers to exposure of cells to 4 Gy of 250-kVp X rays. No difference is seen in clonogenic cell survival between cells exposed to low- and high-energy X rays.

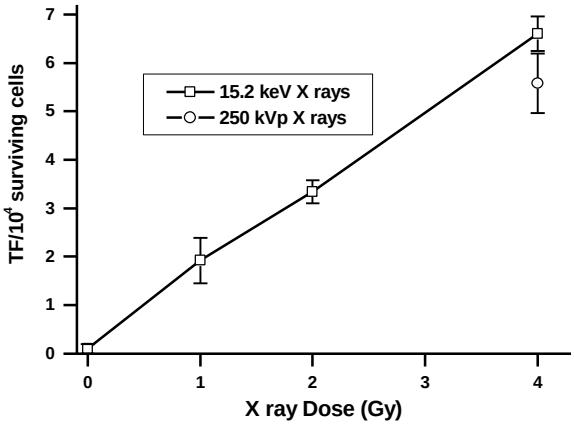

FIG 2. Yield, per surviving C3H10T½ cell, of oncogenically transformed cells produced by 15.2-keV and 250-kVp X rays. *Open Squares* refer to exposure of cells to 15.2-keV X rays. *Open Circle* refers to exposure of cells to 4 Gy of 250-kVp X rays. A higher transformation frequency (by 20%) is seen in cells treated with soft X rays compared to high-energy X-ray exposure.

Malignant Transformation of Human Bronchial Epithelial Cells with Tobacco-Specific Nitrosamine, 4-Methynitrosamine-1-3-Pyridyl-1-Butanone (NNK)

Hongning Zhou and Tom K. Hei

The role of tobacco and tobacco smoke as causative agents for various types of human cancer has been well established (*1*). Epidemiological evidence indicates that nearly 90% of lung cancers are attributable to cigarette smoking (U.S. Surgeon General Report, 1986). Although tobacco smoke contains more than 2,500 chemical and physical agents, it has been suggested that the tobacco-associated nitrosamines are the most potent carcinogenic component (*2*). Tobacco-specific nitrosamines are formed from nicotine and related tobacco alkaloids. Two of these, NNK, 4-Methynitrosamine-1-3-Pyridyl-1-Butanone and NNN, N-nitroso-nornicotine, are strong carcinogens in laboratory animals. They can induce tumors both locally and systematically. It has been shown that the amount of NNK in tobacco smoke is high enough that the total estimated doses to smokers and long term snuff-dippers are similar in magnitude to the total doses required to produce cancer in laboratory animals. These exposures thus represent an unacceptable risk both to cigarette smokers and to non-smokers exposed for years to environmental tobacco smoke.

The cellular and molecular mechanisms for human bronchial carcinogenesis by tobacco-specific nitrosamines are not clear. It is ideal to use a human bronchial cell line that has been exposed to these carcinogenic agents to assess the various transformation stages leading to malignancies. In the present study, we use human papillomavirous-immortalized bronchial epithelial cells (BEP2D) to study the various stages of neoplastic transformation induced by NNK. BEP2D cells were treated with graded doses of NNK for periods up to 7 days. Following treatment, cells were assayed for changes in growth kinetics, saturation density, resistance to serum-induced terminal differentiation, and anchorage-independent growth as described (*3*). Over a period of 10 months, NNK-treated cells acquired resistance to serum-induced terminal differentiation phenotype, and anchorage-independent growth ability (Table 1). Comparing NNK-treated and control cells, the number of cells per colony were significantly different, which showed the doubling time was different (Table 1). Upon inoculation into nude mice, the NNK-treated cells produced tumors in three out of four animals. Four months post-injection, one of the tumors that had attained a size of ~10 mm in diameter was excised, and a cell line was successfully established. Using an immunofluorescence technique, keratin expression confirmed its epithelial origin. These data suggest that NNK can induce malignant transformation of human bronchial epithelial cells, and the tumor cell line established is a useful model to investigate the molecular mechanism(s) of NNK-induced carcinogenesis.

Table 1. Characteristics of NNK-treated human bronchial epithelial cells.

Group	Plating efficiency		Formation of colonies in soft agar	Doubling time (hr)	Tumori-genicity*	Tumor cell line esta-blished
	0% FBS	8% FBS				
Control	0.34 ± 0.02	0.02 ± 0.02	0.04 ± 0.01	26.2 ± 1.4	0/30	0
NNK100	0.39 ± 0.08	0.23 ± 0.05	0.33 ± 0.13	20.9 ± 0.9	2/4	1
NNK400	0.44 ± 0.13	0.22 ± 0.05	0.36 ± 0.11	20.6 ± 0.2	2/4	NF**

*Number of animals with tumor/Number of animals injected
**Not finished.

References

1. Hecht SS, Abbaspour A, Hoffman D. A study of tobacco carcinogenesis. XLII. Bioassay in A/J mice of somestructural analogues of tobacco-specific nitrosamines. Cancer Lett. 42: 141-5,1988.
2. Hecht, S.S., Carmella, S.G., Foiles, P.G., and Murphy, S.E. Biomarks for human uptake and metabolic activation of tobacco-specific nitrosamines. Cancer Res. 54: 1912s-1917s, 1994.
3. Hei TK, Piao CQ, Willey JC, Thomas S, Hall EJ. Malignant transformation of human bronchial epithelial cells byradon-simulated alpha-particles. Carcinogenesis 15: 431-7, 1994.

Induction and Mutant Spectrum Analysis of *CD59* Mutations in Human-Hamster Hybrid Cells by Crocidolite Asbestos and Hydrogen Peroxide: Implications for Mechanisms of Fiber Mutagenesis

An Xu and Tom K. Hei

Asbestos fibers are a group of fibrous mineral silicates associated with the development of pulmonary fibrosis, bronchogenic carcinomas, and malignant mesotheliomas in both humans and experimental animals (*1*). Although asbestos has been shown to induce growth factors and cytokines, oncogene expression, DNA and chromosomal damage, and apoptosis, the underlying mechanisms remain elusive (*2-3*). Crocidolite, which is the most carcinogenic type of asbestos, has been shown to catalyze the formation of hydroxyl radicals by either the Fenton or Haber-Weiss reaction, and induces lipid peroxidation, DNA strand breaks, sister chromatid exchanges, and clastogenicity (*4-5*). The array of DNA and chromosomal damage induced by reactive oxygen species (ROS) may lead to a broad spectrum of mutations in mammalian cells (*6-7*). However, earlier studies on the mutagenicity of asbestos at either *hprt* or *oua* loci in a variety of mammalian cells have resulted in mostly negative findings (*8*). Subsequent studies have suggested that this could be a result of multilocus deletions induced predominantly by asbestos which are not compatible with the survival of the mutants (*9*). In recent years, several other mutagenic assays, which allow the recovery of large chromosomal mutations, have convincingly demonstrated that asbestos is indeed a potent mutagen of genes and chromosomes (*10-11*).

Human-hamster hybrid (A_L) cells, which contain a full set of hamster chromosomes and a single copy of human chromosome 11, are sensitive in detecting mutagens that induce mostly large, multilocus deletions such as those occurring from ionizing radiation and certain heavy metals (*12-13*). Since hydrogen peroxide can react with intracellular metals to produce ROS via the Fenton reaction (*14*), we speculated that asbestos fibers might induce similar types of mutations as that of chemically generated ROS at equitoxic doses.

Exposure of A_L cells to either graded doses of crocidolite fibers for 24 hr or to hydrogen peroxide in serum-free medium for 15 min resulted in a dose-dependent increase in toxicity of A_L cells (Fig. 1). Both crocidolite fibers and hydrogen peroxide induced a dose-dependent *CD59* mutagenesis in A_L cells. Mutation fraction increased with dose of fibers and reached a level that was ~4-fold higher than background at 4 $\mu m/cm^2$ dose of fibers in A_L cells. As shown in Figure 1, the mutant frequency was slightly higher for the hydrogen-peroxide-treated A_L cells than that for A_L cells exposed to crocidolite fibers at equal toxic doses, which indicates that the *CD59* gene of A_L cells is sensitive to detect mutations induced by ROS. Consistent with previous studies, the majority of spontaneous *CD59*$^-$ mutants (73%) showed no detectable changes in any of the marker genes examined (Fig. 2). Only 33% of mutants derived from cells exposed to a 2-$\mu g/cm^2$ dose of fibers retained all the marker genes examined, and 26% lost the proximal APO-A1 located on the long arm of the chromosome. The proportion of

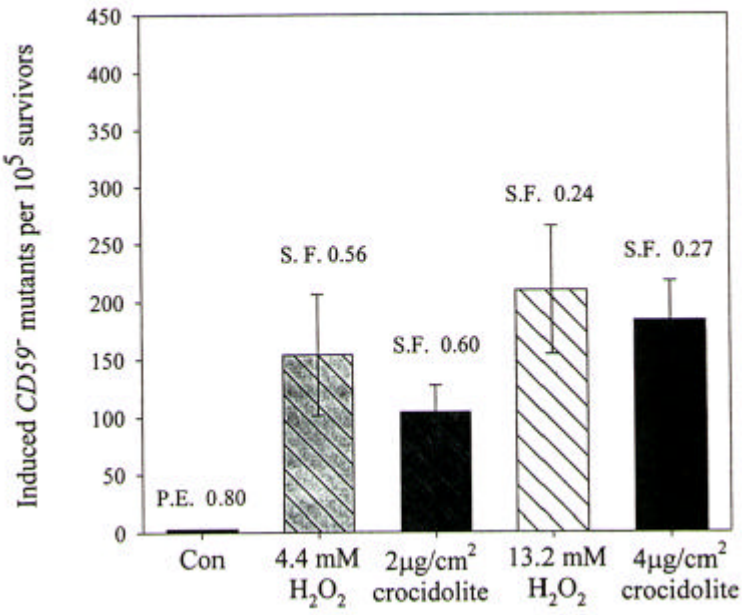

FIG. 1. Induction of *CD59*⁻ *m*utant fractions per 10^5 survivors in A_L cells exposed to either crocidolite fibers or H_2O_2. Error bars indicate ± SEM.

mutants suffering loss of additional chromosomal markers increased with increasing concentration of fibers, such that none of the 29 mutants induced by a 4-μg/cm^2 dose of fibers retained all five of the marker genes, and 66% of them lost the long-arm marker. Similarly, 39% of the mutants induced by a 4.4-mM dose of hydrogen peroxide retained all five primers, compared to none among those induced by the higher dose of 13.2 mM. In addition, loss of the long-arm marker was observed in more than 70% of the *CD59*⁻ mutants induced by 13.2 mM hydrogen peroxide. These results indicate that equitoxic doses of crocidolite fibers and hydrogen peroxide induced a similar spectrum of *CD59*⁻. Furthermore, the proportion of mutants suffering multilocus deletions increased in a dose-dependent manner. These results provide strong evidence that the mutagenicity of asbestos fibers is mediated by ROS in a way similar to those of hydrogen peroxide.

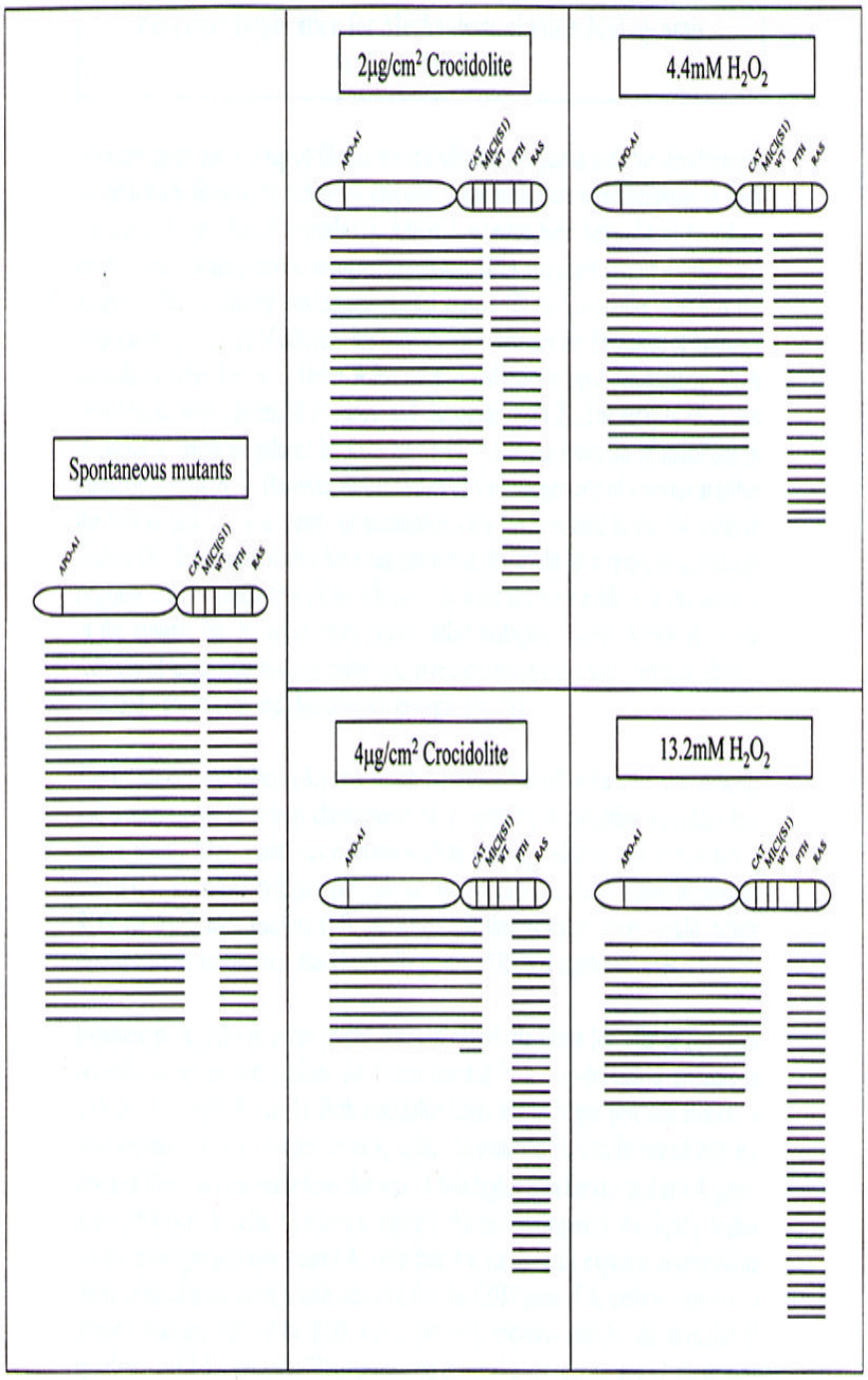

FIG. 2. Mutational spectra of *CD59*$^-$ mutants either of spontaneous origin or from A_L cells exposed to graded doses of crocidolite fibers or H_2O_2.

References

1. Mossman BT, Bignon J, Corn M, Seaton A, and Gee JBL. Asbestos: Scientific developments and implications for public policy. *Science* (Washington DC) 247:294-301, 1990.
2. Driscoll KE, Carter JM, Howard BW, Hassenbein D, Janssen YM, and Mossman BT. Crocidolite activates NF-kappa B and MIP-2 gene expression in rat alveolar epithelial cells. Role of mitochondiral-derived oxidants. *Environ Health Perspect* 106:1171-1174, 1998.
3. Timblin CR, Guthrie GD, Janssen YW, Walsh ES, Vacek P, and Mossman BT. Patterns of c-*fos* and c-*jun* proto-oncogene expression, apoptosis, and proliferation in rat pleural mesothelial cells exposed to erionite or asbestos fibers. *Toxicol Appl Pharmacol* 151:88-97, 1998.
4. Gulumian M and Kilroe-Smith T. Crocidolite-induced lipid peroxidation in rat lung microsomes. I. Role of different ions. *Environ Res* 43:267-273, 1987.
5. Adachi S, Yoshida S, Kawamura K, Takahashi M, Uchida H, Odagiri Y, and Takemoto K. Induction of oxidative DNA damage and mesothelioma by crocidolite, with special reference to the presence of iron inside and outside of asbestos fibers. *Carcinogenesis* 15:753-758, 1994.
6. Newcomb TG and Loeb LA. Oxidative DNA damage and mutagenesis. In: DNA Damage and Repair, Vol. 1: DNA Repair in Prokaryotes and Lower Eukaryotes. JA Nicholoff, MF Hoekstra (eds.), Humana Press: Totowa, NJ, pp.65-84, 1998.
7. Jaurand MC, Yeagles M, Dong HY, Renier A, and St. Etienne L. In vitro DNA and chromosomal damage produced by some minerals and man-made particles on rat pleural mesothelial cells. In: Cellular and Molecular Effects of Mineral and Synthetic Dusts and Fibers. JMG David and M Jaurand (eds.) Springer-Verlag: Heidelberg, pp. 183-192, 1994.
8. Jaurand MC. Mechanisms of fiber-induced genotoxicity. *Environ Health Perspect* 105:1073-1084, 1987.
9. Hei TK, Piao CQ, He ZY, Vanneis D, and Waldren CA. Chrysotile fiber is a strong mutagen in mammalian cells. *Cancer Res* 52:6305-6309, 1992.
10. Both K, Henderson DW, and Turner DR. Asbestos and erionite fibers can induce mutations in human lymphocytes that resulted in loss of heterozygosity. *Int J Cancer* 59:538-542, 1994.
11. Park SH and Aust AE. Participation of iron and nitric oxide in the mutagenicity of asbestos in *hgprt*$^-$, *gpt*$^+$ Chinese hamster V79 cells. *Cancer Res* 58:1144-1148, 1998.
12. Waldren CA, Correll L, Sognier MA, and Puck TT. Measurement of low levels of X-ray mutagenesis in relation to human disease. *Proc Natl Acad Sci USA* 83:4839-4843, 1986.
13. Hei TK, Liu SX, and Waldren CA. Mutagenicity of arsenic in mammalian cells: Rose of oxygen reactive species. *Proc Natl Acad Sci USA* 95:8103-8107, 1998.
14. Zhu LY, Stansbury HKH, and Trush MA. Role of reactive oxygen species in multistage carcinogenesis. In: Oxygen Radicals and the Disease Process. CE Thomas and B Kalyanaram (eds.), pp 237-277, Harwood Academic Publishers: Amsterdam, 1997.

Effects of Irradiated Medium on Chromatid Aberrations and Mutagenesis in Mammalian Cells: Studies Using Double-Mylar Dishes

Masao Suzuki, Hongning Zhou, Charles R. Geard, and Tom K. Hei

Ionizing radiations can cause damage to biologically important molecules, such as DNA, by either direct or indirect effect. Radiation-induced radicals that are originated in water, such as $OH^{\bullet}$, $[O_2]^-$ and $H^{\bullet}$, have been well-accepted to play an important role in the indirect mechanisms of radiation biology, since the human body is composed of more than 80% water. Although the half-life of these radicals is very short (less than 200 ns), their reactivity with macromolecules is very high and they are known to produce DNA strand breaks (*1*). Electron spin resonance (ESR) studies by Miyazaki, *et al.* (*2*) have shown that stable organic radicals with long lifetime (T1/2 > 20 h) are induced in X-ray-irradiated mammalian cells (*2*). There is evidence that such kind of radicals play an important role in radiation-induced biological effects (*3, 4*). Recent studies from this laboratory have shown that α particles induced an increase in mutation induction on non-irradiated bystander cells (*5*). Although gap-junction-mediated cell-cell communication appears to play an important role in mediate this bystander effect, we can't rule out completely a possible medium effect. In this study, we examine the potential contribution of irradiated medium to the bystander effect using the double-mylar method.

The double-mylar technique is very useful to evaluate the roles of medium in bystander effects. We can plate cells in either side or both sides of double mylar dishes. Since α particles can only traverse a very limited distance, cells plated on the other side of a medium-filled mylar dish would have no chance of being hit by α particles. Since there is no cell-cell contact between the two sides, the only communication available is through the medium. It is, therefore, a great tool to investigate the roles of medium in the bystander effect. Human-hamster hybrid (A_L) cells were plated on one or both sides of double-mylar dishes 2 to 3 days before irradiation, depending on the density requirement for the experiments. One side (with or without cells) was irradiated by α particles (from 0 to 100 Gy). After irradiation, cells were kept in the dishes for either 1, 24 or 48 hr before the non-irradiated cells were collected for survival, cytogenetic, and mutation assays. When one side of cells was irradiated by graded doses of α particles (from 1 to 100 Gy) using the track-segment mode, the survival fraction of non-irradiated cells was significantly lower than that of control after 48 hr co-culture. Such a change was not found in 1 hr co-culture nor in the medium-irradiation group. However, co-cultivation with irradiated cells had no effect on the spontaneous mutagenic yield of the non-irradiated half of the double-mylar cultures. These results suggest that the irradiated cells release some cytotoxic factor(s) into the culture medium that kill the non-irradiated cells, but such factor(s) had little or no effect on mutagenesis. Our results further suggest that different cellular endpoints may involve different mechanisms. To examine this phenomenon on a different biological level, we detected chromatid aberrations in G_2 PCCs, according to the schedule as follows:

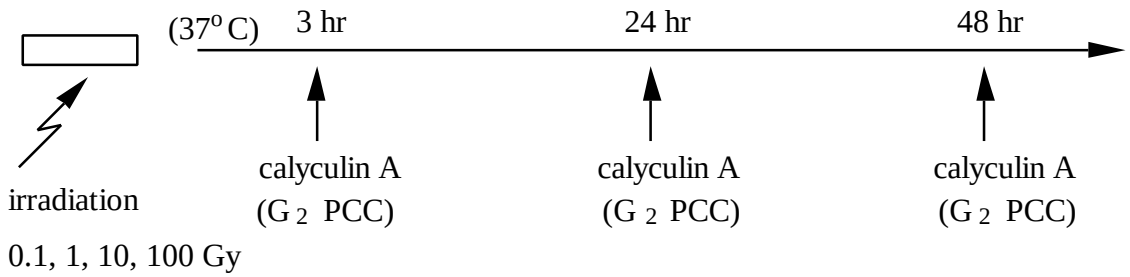

At the moment, our preliminary results are (Figure 1):

(1) There is no change in the number of both types of aberrations in the "medium irradiated" group with any treatment and dose.
(2) On the other hand, the number of aberrations in the "cell irradiated" group is slightly higher than those in both non-irradiated control and the "medium irradiated" group.
(3) In "cell irradiated" group, the frequencies depend on detection time.
(4) There is no clear dose-dependent response in chromatid breaks from 0.1 Gy to 100 Gy in the "cell irradiated" group.

We conclude that these results clearly show that some species-induced chromosomal damage exists in the medium of the "cell-irradiated" group.

References

1. R Roots, S Okada, Estimation of life times and diffusion distances of radicals involved in X-ray-induced DNA strand breaks or killing of mammalian cells. *Radiat.Res.* **64**, 306-320 (1975).
2. T Miyazaki, Y Hayakawa, K Suzuki, M Suzuki, M Watanabe, Radiprotective effects of dimethylsulfoxide in golden hamster embryo cells exposed to γ-rays at 77 K:Part I. Radical formation as studied by ESR. *Radiat.Res.* **124**, 66-72 (1990).
3. M Watanabe, M Suzuki, K Suzuki, Y Hayakawa, T Miyazaki, Radiprotective effects of dimethylsulfoxide in golden hamster embryo cells exposed to γ-rays at 77 K:Part II.Protection from lethal, chromosomal, and DNA damage. *Radiat.Res.* **124**, 73-78 (1990).
4. S Koyama, S Kodama, K Suzuki, T.Matsumoto, T.Miyazaki, M.Watanabe, Radiation-induced long-lived radicals which cause mutation and transformation. *Mutat.Res.* **421**, 45-54 (1998).
5. H Zhou, G Randers-Pehrson, C A Waldren, D Vannais, E J Hall, T K Hei, Induction of a bystander mutagenic effect of alpha particles in mammalian cells. *PNAS* **97**, 2099-2104 (2000).

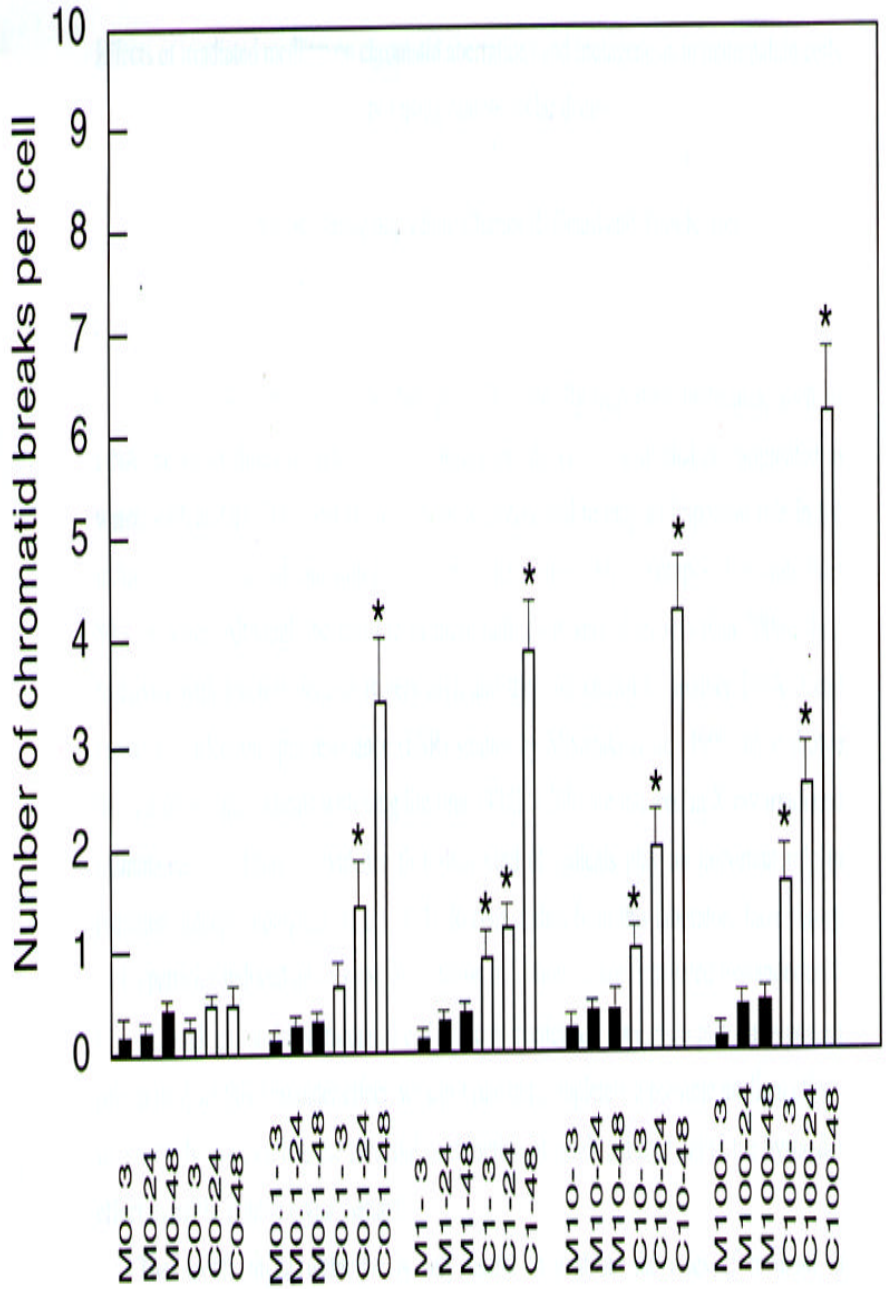

FIG. 1. Number of chromatid breaks per cell (0, 0.1, 1, 10, and 100 Gy) in G2 PCC 93, 24, and 48 hr after irradiation). The presented results are the mean and standard deviations of the two independent experiments. (*: $p<0.05$, compared to the data of M3-0); M: medium irradiation; C: cell irradiation)

Mutagenicity of Cadmium in Mammalian Cells

Fei Sung, Stephanie Stern (Intern), and Tom K. Hei

Cadmium, classified by the International Agency for Research on Cancer (IARC) as a human carcinogen in 1994, is commonly found in the environment. Cadmium has not been shown to be mutagenic in bacterial test systems and has generally been found to be non-mutagenic in most short-term mutagenicity tests. On the other hand, cadmium can induce DNA damage (*1*) and causes inhibition of DNA repair and replication of human cells (*2*) and V79 cells (*3*). However, the precise mechanism of its carcinogenic potential remains unclear. In the present study, we use the human-hamster hybrid (A_L) cell assay, which is highly sensitive in recovering large deletion mutations, to assess the genotoxic potential of cadmium in mammalian cells.

A_L hybrid cells, which contain a standard set of Chinese hamster chromosome and a single copy of human chromosome 11, were used. Cell surface markers encoded by chromosome 11 render A_L cells sensitive to killing by specific monoclonal antibodies in the presence of complement. Cells are maintained in Ham F12 medium supplemented with 8% heat-inactivated fetal bovine serum, 25 μg/ml gentamycin and 2×10^{-4} M glycine at 37°C in a humidified 5% CO_2 incubator. Cadmium cytotoxicity was determined by treating cells in logarithmic phase for 24 hours with different doses of cadmium chloride. After treatment, cells were replated into Petri dishes for colony formation. The quantification of mutations at *CD59* locus was determined as follows: Briefly, cells were plated into 60-mm dishes with 2-ml F12 medium. After 2 hours of incubation (to allow for cell attachment), 0.2% *CD59* antibody and 1.5% freshly thawed complement (vol/vol) were added to each dish. Cells were incubated for 7 days. Only mutants will form colonies.

Cadmium induced a dose-dependent toxicity in A_L cells, as shown in Figure 1, where surviving fractions are plotted against drug concentration. Figure 2 shows the induced *CD59*$^-$ mutants per10^5 survivors scored at 7 or 14 days after treatment. Although there is almost no difference in mutagenic yield between the 0.5-μM and 1.0-μM groups, cells exposed to doses of 1.25 μM and higher showed a significant increase in *CD59*$^-$ mutant inductions. These data provide clear evidence that cadmium is indeed a gene and chromosomal mutagen in mammalian cells. The cloning of *CD59*$^-$ mutants and analysis of the mutant spectrum are currently underway.

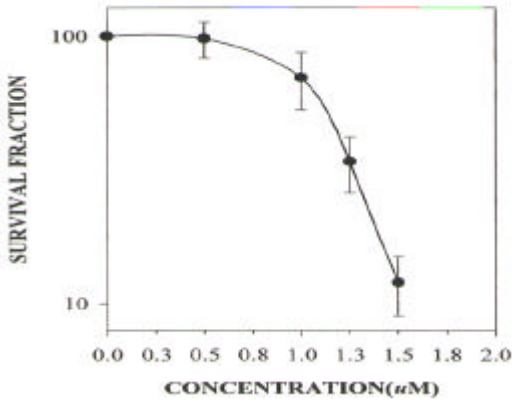

FIG. 1. Survival curve for A_L cells exposed to graded doses of cadmium chloride. Each point represents an average of five experiments. Bars represent ± SD.

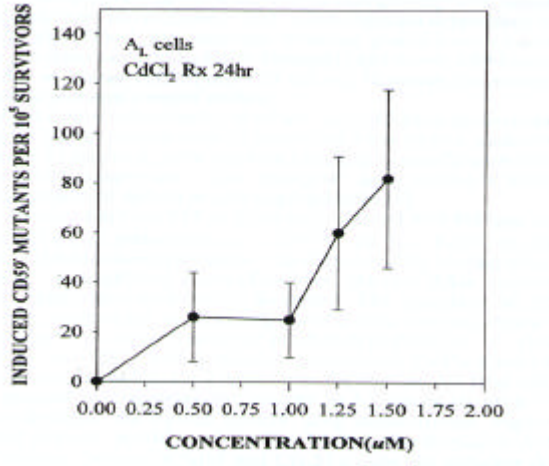

FIG. 2. Mutation induction in A_L cells by graded doses of cadmium chloride. Each point represents data of average 7 to 8 experiments 7 to 14 days after treatment. Bars represent ± SD.

References

1. Ochi T and Ohsawa M. (1983) Induction of 6-thioguanine-resistant mutants and single-strand scission of DNA by cadmium chloride in cultured Chinese hamster cells. Mutation Res 111:69-78.
2. Nocentini S. (1987) Inhibition of DNA replication and repair by cadmium in mammaliam cells: Protective interaction of zinc. Nucleic Acid Res 15(10).
3. Heike Dally, Hartwig A. (1997) Induction and repair inhibition of oxidative DNA damage by nickel and cadmium in mammalian cells. Carcinogenesis 18(5):1021-1026.

Quantitative Measurement of Superoxides and Hydroxyl Radicals Generated in Arsenite-Treated Cells Using ESR Spectroscopy

Su-Xian Liu, Istvan Lippai (Department of Physiology and Biophysics, Albert Einstein College of Medicine, Bronx, NY), Mohammad Athar (Department of Determatology, College of Physicians & Surgeons, Columba University), and Tom K. Hei

Although arsenic is a well-established human carcinogen, the mechanisms by which it induces cancer remain poorly understood. We previously showed arsenite to be a potent mutagen in human-hamster hybrid (A_L) cells (*1*). It has been suggested that an increase in superoxide-driven hydroxyl-radical production induced by arsenic mediates genotoxicity in mammalian cells. The detection of spin-trapped radical adducts by electron spin resonance (ESR) spectroscopy is a particularly powerful technique for the sensitive and specific detection, identification, and relative quantification of short-lived free radicals. Persistent nitroxide adducts resulting from the reaction of a spin trap with transient free-radical species have been used to detect, characterize, and quantify the production of free radicals in various *in-vitro* and *in-vivo* model systems. The spin-trap probe, TEMPOL-H, is a hydroxylamine, which reacts with free radicals to form the nitroxide TEMPOL that can be detected and quantified by ESR spectroscopy (*2*).

In this study, exponentially growing A_L cells (1×10^6) were plated in T25 cm^2 flasks 24 hr before the experiment. Cells were washed twice with phosphate-buffered saline. TEMPOL-H at a final concentration of 25 mM was added to the culture, along with graded doses of arsenite. The culture was incubated for 1 hr at 37^{o}C and ESR measurements were made at room temperature. In some experiments, superoxide at 400 U/ml or catalase at 5,000 U/ml was added to cultures containing the spin-trap probe and arsenic in order to ascertain the role superoxide anions or hydrogen peroxide has, respectively, in the reaction. ESR spectroscopy was conducted with an X-band Varian E-9 spectrometer equipped with Hewlett-Packard frequency counter WINCWEPR data acquisition software. The ESR spectra were recorded immediately after sample equilibration in the ESR cavity, usually within 5 min after loading the sample in the aqueous cell.

Figure 1(a) shows the ESR spectra of 25-mM TEMPOL-H in 2 ml of buffer in the presence of 3×10^6 A_L cells. The addition of sodium arsenite, 4 μm/ml, increased the ESR signal of TEMPOL by ~3 fold, based on the amplitude of the signals [Fig. 1(b)]. On the other hand, the addition of catalase to the reaction mixture reduced the signal by ~70% [Fig. 1(c)], indicating a contribution of hydrogen peroxide in the redox process. Likewise, the addition of superoxide dismutase to the reaction mixture resulted in a 50% reduction in the ESR intensity (data not shown). The doses of antioxidants used here have previously been shown to be non-toxic and effective as free-radical scavengers in a variety of *in-vitro* and *in-vivo* studies (*3-4*).

It has been proposed that in the spin-trap probe TEMPOL-H readily penetrates plasma membranes and detects free radicals, particularly hydroxyl radicals and

superoxide anions, with high sensitivity and specificity. In the presence of free radicals, TEMPOL-H is converted to TEMPOL (*5*), a nitroxide which is more stable than other nitrone-based spin traps such as DMPO (*6*). It is possible that arsenite is oxidized in cells into pentavalent arsenite with concomitant production of superoxide anions produced by a one-electron reduction of molecular oxygen. Alternatively, there is evidence that intracellular metabolism of arsenite into dimethylarsine is coupled with the production of superoxide anions and hydroxyl radicals (*7,8*). Our data with catalase, which reduced signals by more than 70%, implicated hydrogen peroxide as the likely intermediate in arsenite genotoxicity. Taken together, our data suggest the following sequence of events for arsenic-induced mutagenesis in mammalian cells:

Arsenic Ψ[Superoxide anions Ψ[Hydrogen peroxide Ψ[Hydroxyl radicals Ψ[Genotoxicity

The data are consistent with our previous results with the radical scavenger dimethyl sulfoxide, which reduced the mutagenicity of arsenic in these cells, and provide convincing evidence that reactive oxygen species, particularly hydroxyl radicals, play an important causal role in the genotoxicity of arsenic compounds in mammalian cells.

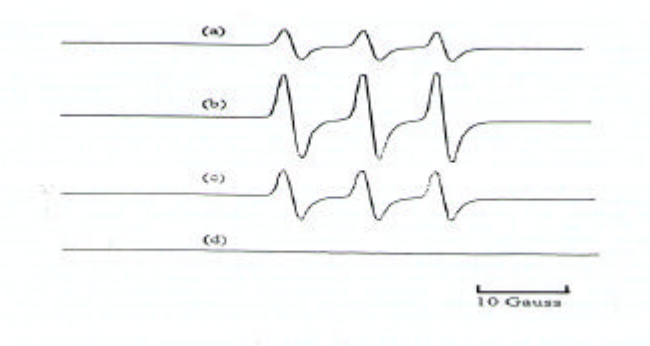

FIG. 1. ESR spectra of TEMPOL-H. (a) The ESR spectra of 25 mM TEMPOL-H in PBS measured in the presence of 3×10^6 A_L cells per ml; (b) the addition of sodium arsenite 4 μg/ml; (c) the addition of catalase to the reaction mixture; (d) ESR spectra in the presence of 3×10^6 A_L cells per ml.

References

1. Hei, et al. Proc Natl Acad Sci USA 95:8013-8017, 1998.
2. Krishna, et al. Proc Natl Acad Sci USA 89:5537-5541, 1992.
3. Shatos, et al. Environ Res 265:245-253, 1987.
4. Korkina, et al. Mut Res
5. Hahn, et al. Free Rad Biol & Med 28:953-958, 2000.
6. Dikalov, et al. Biochem & Biophys Res Comm 248:211-215, 1998.
7. Tezuka, et al. Biochem & Biophys Res Comm 191:1178-1181, 1993.
8. Chan, et al. Environ Carcinogen & Ecotox Rev C15:83-122, 1997.

Extension of Lifespan in Primary Human Bronchial Epithelial Cells by Expressing Telomerase

Chang Q. Piao, Yong L. Zhao, and Tom K. Hei

When normal human cells are cultured *in vitro*, they proliferate only a limited number of times and enter a state of growth-arrest termed "senescence". It has been proposed that telomere shortening may act as a molecular clock that determines the number of times that a cell has divided. When telomeres are shortened to a critical length, cellular senescence occurs. Introduction of the core catalytic subunit of telomerase (hTERT) into normal human cells without detectable telomerase results in restoration of telomerase activity. Recent studies indicate that the lifespan of normal human fibroblasts can be extended by stable expression of transfected telomerase (*1-2*). Since primary human epithelial cells are refractory to malignant transformation in vitro, it is of interest to immortalize normal human cells by telomerase expression for further studies of carcinogenesis and cellular aging. In this study, we introduce telomerase into normal human bronchial epithelial cells to observe its extension of lifespan or, finally, immortalization.

Primary cultures of normal human bronchial epithelial cells (NHBE) and small airway epithelial cells (SAEC) were purchased from Clonetics (Walkersville, MD). The cells were cultured in BEGM and SAGM medium (Clonetics) separately. In our laboratory, these cells can only be passaged for 20-25 population doublings in normal cultures. Introduction of telomerase into NHBE and SACE cells was achieved by retrovirus-mediated gene transfer. The construct of pBabest2, in which the cDNA-encoding hTERT was subcloned into the retroviral vector pBabe under the control of the promoter present in the Moloney murine leukemia virus long terminal repeat was kindly offered by Dr. Vaziri (*1*). The retroviral constructs, pBabest2 and pBabe, were packaged using the highly efficient and helper-free cell line Phoenix A (ATCC). Phoenix A cells were plated in 100-mm dishes and transfected, when reaching approximately 80% confluence, with 4-μg retroviral plasmid DNA in 10 ml medium by LipofectAMINE PLUS reagent (GibcoBRL), according to instructions of the manufacturer. At 48 h post transfection, the viral-containing medium was harvested, and the virus titre was determined using NIH3T3 cells. Titres of $>3\times10^6$ transducing units per ml were obtained. The NHBE and SAEC cells at passage 5 were infected with the viral supernatants in the presence of 4-μg/ml polybrene. The colonies were formed in both of the NHBE and SAEC cells transfected with pBabest2 after 3 weeks of transfection (Fig. 1). There was no colony formation in the cells transfected with pBabe. A total of 5 colonies were isolated and expanded in culture from NHBE cells and 7 from SAEC cells transfected with pBabest2. All of them are resistant to 400 μg/ml G418. Two single-clone cell lines and one mixed-clone cell line from each NHBE and SACE were continuously cultured, and when they reached 64 PDs, the cells were in exuberant proliferation (Fig 2). Relative telomerase activity (TRAP) was analyzed by telomerase PCR-ELISA kit, according to manufacturer's instructions (Roche Molecular Biochemica). The telomerase activity in parental NHBE and SAEC cells was at empty control (no PCR reaction sample was

added) level, however, all the transfected cell lines analyzed showed an increased telomerase activity that was 3- to 4-fold higher than parental cells (Fig. 3).

Studies are underway to analyze telomeric length, karyotype, and tumorigenicity in nude mice of the telomerase-transfected bronchial epithelial cells. This cell model will be useful for the studies of malignant transformation induced by radiation and chemical carcinogens.

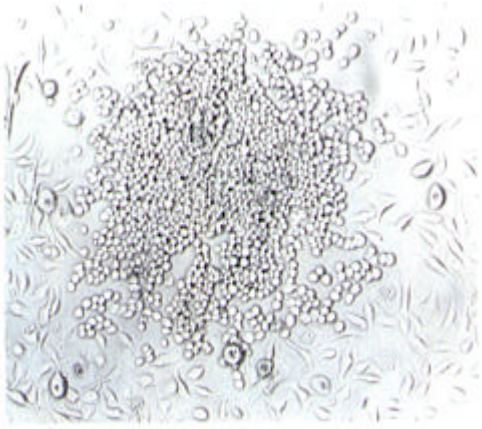

FIG. 1. Colony formed in NHBE cells transfected with pBabest2.

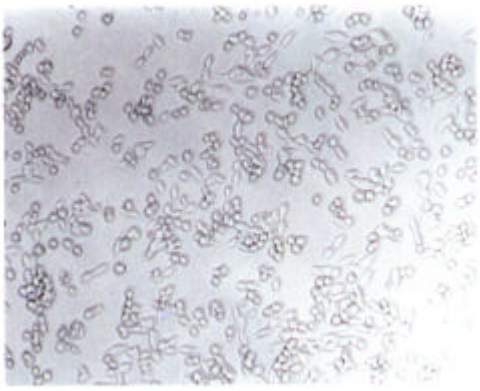

FIG. 2. Morphology and proliferation of the mixed-clone cell line from SAEC.

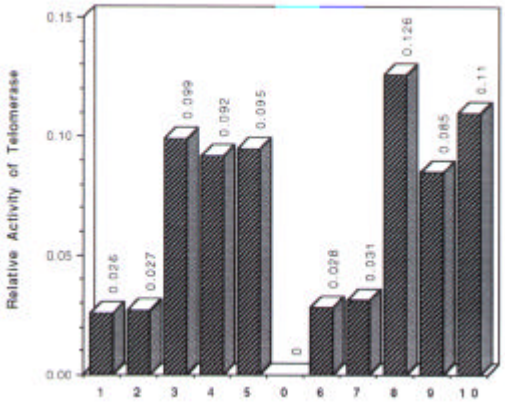

FIG. 3. Relative telomerase activity analyzed by PCR-ELISA. (1: Empty control; 2: Parental NHBE cells; 3: NHBE-hTERT-1; 4: NHBE-hTERT-2; 5: NHBE-hTERT-M; 6: SAEC-hTERT-1; 7: SAEC-hTERT-2)

References

1. Vaziri H, Benchimol S; *Brief Communication*; 1998; 8:297-282.
2. Bodnar AG, Ouellette M, Frolkis M, Holt SE, Chiu CP, Morin GB, Harley CB, Shay JW, Lichtsteiner S, and Wright WE; *Science*; 1998; 279:349-352.

Markers in Progression of Human Breast Epithelial Cells Transformed by Estrogen and High-LET Radiation

Gloria M. Calaf and Tom K. Hei

Breast cancer is a complex disease in which numerous genetic aberrations occur as a result of exposure to environmental carcinogens. *In vitro* model systems have been extensively used in the study of radiation-induced transformation. Identification of factors involved in cell transformation has been facilitated by studies using breast cancer cell lines representative of different tumor phenotypes. Since there is little or no information available on the mechanism(s) of radiation-induced breast cancer, an *in vitro* breast transformation model utilizing epithelial cells at different stages of the neoplastic process provides a unique opportunity for studying radiation carcinogenesis.

We have established an experimental breast cancer model to examine the neoplastic transformation of human breast epithelial cells induced by high-LET radiation in the presence of 17β estradiol (*1-4*). Immortalized human breast (MCF-10F) cells were exposed to low doses of high-LET α particles (150 keV/μm) and subsequently cultured either in the presence or absence of estrogen for periods up to 10 months post-irradiation. MCF-10F cells, irradiated with 60 cGy or 60/60 cGy doses of α particles, showed gradual phenotypic changes including altered morphology, increase in cell proliferation relative to control, anchorage-independent growth, and invasive capabilities, but no tumorigenicity in nude mice. However, MCF-10F cells irradiated with two doses of α particles in the presence of estrogens (60E/60E) showed tumorigenicity both in the SCID and nude mice (Table 1).

Since the identification of the genes involved in breast cancer is of critical importance in understanding the progression of this disease, it is important to define which oncoproteins are expressed in radiation-induced transformed human breast epithelial cells. To correlate alterations in gene expression level with the corresponding protein expression in transformed and tumorigenic MCF-10F cells, immunohistochemical staining coupled with confocal microscopy were used. Briefly, exponentially growing cells at similar passage numbers were plated on chamber slides until they were 70% confluent. After staining with the primary and then with Rhodamine-conjugated secondary antibodies, the cultures were visualized using a laser scanning confocal microscope. The fluorescent images were quantified using an analysis software image. Results indicated changes in expression levels of various cell cycle regulators and oncogenes as a function of the phenotypic progression in irradiated MCF-10F cells (Figs. 1-4). Thus, an increase in protein expression of the proliferating cell nuclear antigen (PCNA) (Fig. 1), and down regulation of p27 (Fig. 2) was observed in both non-tumorigenic and tumorigenic cells. However, an increase in Cyclin D1 was observed only in those cells treated with double doses of α particles in the presence of estrogen, regardless of tumorigenicity (not shown). The expressions of ERα (Fig. 3), c-erbB2 (Fig. 4) were only increased in the tumorigenic 60E/60E cell line. However, the ERα was

down regulated in the tumor cell line derived from such cells (Tumor 2). It is likely that the concerted action of many genes is critical for the tumorigenic phenotype.

Here we report that over-expression of several oncoproteins is important in the transformation of human breast epithelial cells. This study will allow us to examine the various aspects of regulation in gene expression and will provide us the basis for understanding the process of radiation-induced breast carcinogenesis. This *in vitro* system of induction of neoplastic transformation of human breast epithelial cells with radiation and estrogens will be helpful to answer specific questions on the mechanisms of cancer initiation and progression of breast cancer.

Table 1. Biological properties of α-particle-irradiated and estradiol 17β(E)-transformed human breast epithelial cells.

Cell line[1]	Passage[2]	Anchorage Independency[3]	Invasion Assay[4]	Tumorigenicity[5]
MCF10F	+86	-	-	-
MCF10F+E	+74	-	-	-
60cGy	+63	-	+	-
60cGy+E	+70	+	+	-
60cGy/60cGy	+85	+	+	-
60cGy/60cGy+E	+95	+	+	-
60cGy+E/60cGy+E	+99	++++	+++	+
Tumor 2	+30	+++++	++++	+

[1]Dose in cGy; number of exposures: E: 17β-estradiol treatment (10^{-8}M).
[2]Number of passages in culture after radiation treatment when tests were performed.
[3]Colony-forming efficiency in agar fluctuated from 1-3%.
[4]Invasive characteristics of control and treated MCF-10F cells.
[5]Average of 6 animals/group.

References

1. Calaf G. and Hei T.K. (2000) Establishment of a radiation-and estrogen-induced breast cancer model. Carcinogenesis 21 (4): 769-776.
2. Hei T.K., Roy D., Piao CQ. and Calaf G. (2000) Genomic instability in human epithelial cells transformed by high LET radiation Proc. 11th Intern Congress of Radiation Res. In: M. Moriarte, C. Mothersill, C. Seymour, M. Edington, J.F. Ward and R.J.M. Fry (eds): 560-563, Lawrence, KS, Allen.
3. Calaf G. and Hei T.K. (2000) Oncoprotein expressions in human breast epithelial cells transformed by high LET radiation" Intern. Journal of Radiation Biol. In press.
4. Hei T.K., Roy D. Piao CQ., Calaf G., Hall E.J. (2001) Molecular alterations in tumorigenic human bronchial and breast epithelial cells induced by high LET radiation. Adv. in Space Res. In press.

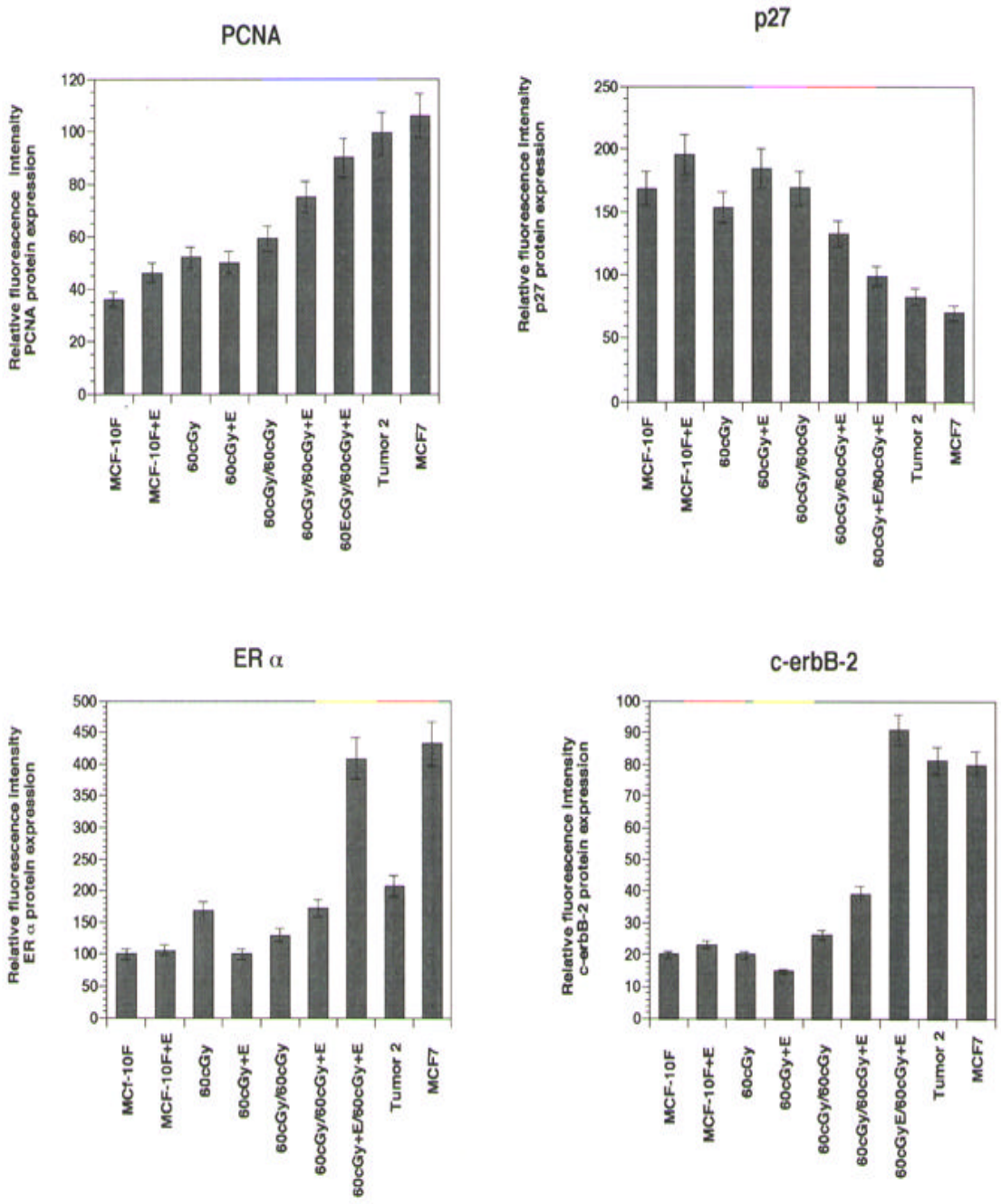

FIGS. 1-4. Represent the quantification of immunofluorescent imaging of PCNA (Fig. 1), p27 (Fig. 2), ER α (Fig. 3), and C-erbB2 (Fig. 4) protein expression expressed by α-particle-irradiated and estradiol 17β-transformed human breast epithelial cell lines. Protein expression was determined by immunofluorescent staining, visualized by using confocal microscopy, and quantified by a computer program that gives the area and the intensity of the staining.

Neoplastic Progression of Benzo(a)pyrene-Treated Breast Epithelial Cells

Gloria M. Calaf and Tom K. Hei

Neoplastic progression is a prolonged and stepwise process, and tumor growth occurs after a series of molecular alterations that culminate in tumorigenesis (*1*). Several non-malignant breast lesions have been associated with increased risk of cancer development. Women with carcinoma *in situ* have high risk (eight to ten times) and women with atypical hyperplasia have moderate risk (five times) of developing breast cancer (*2*). The correlation of particular lesions with cancer development suggests that specific genetic alterations in the early lesion may dictate tumorigenesis. Identification of such molecular changes provide tools for the diagnosis, prognosis, and treatment of breast cancer. A handful of molecular changes have been previously associated with breast cancer, including amplification of c-*erbB2*, which is a transmembrane tyrosine kinase and a member of the epidermal growth factor receptor family (*3*). Molecular events critical to breast cancer progression besides c-*erbB2* amplification are still poorly understood. Conversion of a normal cell to a malignant one is a multi-stage process that occurs after a series of phenotypic and molecular alterations. Several chemical and physical agents can alter morphology and induce genetic instability. Activated oncogenes have been detected in a variety of malignant tumors, and the altered expression of certain genes seems to play a role in the cancer process. In the present study, we examine the expression of several oncoproteins that are frequently shown to be associated with breast cancer in the progression of a malignant phenotype in an experimental cancer model.

MCF-10F, a spontaneously immortalized human breast epithelial cell line (4), was treated with benzo(a)pyrene (BP) (*5*) and then transfected with the c-*Ha-ras* oncogene (*6*). Carcinogen-treated and transfected cells showed progressive changes in morphology, anchorage-independent growth, invasiveness, and capability of tumor formation in SCID mice, and also in altered expressions of various oncoproteins (Table 1). The high proliferative activity and over-expression of the c-*erbB-2* oncoprotein has been

Table 1. Biological properties of benzo(a)pyrene-treated human breast epithelial cells transfected with the c-*Ha-ras* oncogene.

Cell Lines	Origin
MCF-10F	MCF-10F parental cells
BP1	Clone derived from parental BP
BP1-E	Sub-clone derived from BP1
c-*Ha-ras*	MCF-10F transfected with c-*Ha-ras* oncogene
BP1T*ras*	Clone BP1 transfected with c-*Ha-ras* oncogene
Tumor 1	Cell line derived from mammary tumors formed in SCID mice after injection of BP1T*ras* cells
MCF-7	Breast carcinoma cell line

considered as a marker for malignancy of the breast (*7*). The progression of breast cancer seems to depend on c-*erbB-2* gene expression. The correlation between c-*erbB-2* gene amplification and other protein markers has not been well documented. Results with immunofluorescence staining and protein quantification by confocal microscopy indicated increased PCNA (Fig. 1), c-*erbB-2* (Fig. 2) protein expression in non-tumorigenic BP1 and tumorigenic c-*Ha-ras*, BP1-E, BP1T*ras*, T1, and MCF-7 cells. A significant increase ($p<0.05$) in Cytokeratin 18 expression (Fig. 3) was observed in those cells altered by the c-*Ha-ras* oncogene. However, expression of β catenin was only significantly ($p<0.05$ increased in the tumorigenic BP1T*ras*, Tumor 1, and MCF7 cells (Fig. 4).

In summary, the chemical carcinogen BP and the insertion of c-*Ha-ras* did induce characteristics of transformed phenotypes in a suitable human breast epithelial cell line. We detected increased protein expression in breast epithelial cells transformed with a chemical carcinogen and/or transfected oncogene that was not present in its normal counterpart. These studies corroborated the morphological changes observed throughout the process of evolution. We can conclude from these studies that malignant progression is a stepwise process and that tumor growth occurs after a series of molecular events which parallel morphological changes indicative of cell transformation. The sequence of events known as malignant progression of breast cancer involves progressive changes of the normal mechanisms of cell-cycle progression until metastasis is reached.

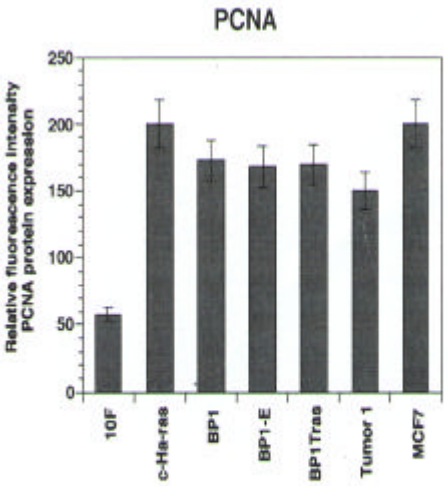

Figure 1

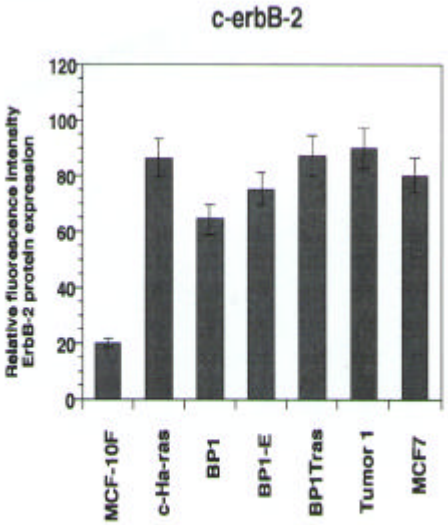

Figure 2

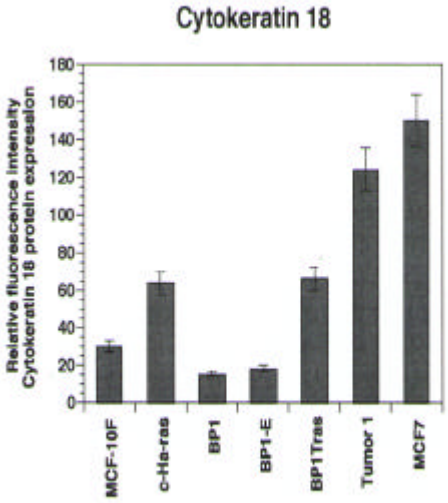

Figure 3

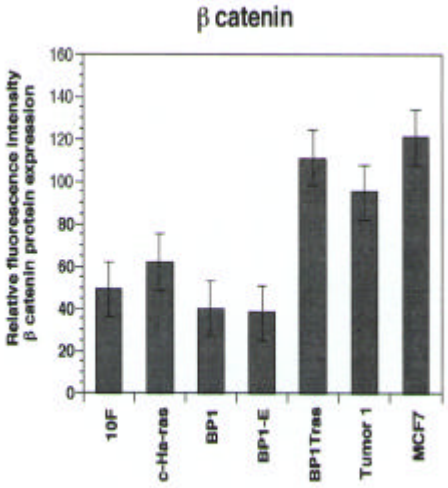

Figure 4

FIGS. 1-4. Quantification of immunofluorescent imaging of PCNA (Fig. 1), c-*erbB-2* (Fig. 2), Cytokeratin 18 (Fig. 3) and β catenin (Fig. 4) protein expression expressed by MCF-10F, in carcinogen-treated and transfected cell lines. Protein expression was determined by immunofluorescent staining, visualized by using confocal microscopy, and quantified by a computer program that gives the area and the intensity of the staining.

References

1. Foulds L. Neoplastic Development, Vols. I and II. Academic Press, 1975.
2. Page DL and Dupont WD. Anatomic markers of human premalignancy and risk of breast cancer. Cancer 66:1326-1335, 1990.
3. Bargman CI, Hung MC, and Weinberg. The *neu* oncogene encodes an epidermal growth factor receptor-related protein. Nature 319:226, 1986.
4. Soule H, Maloney TM, Wolman SR, Peterson WD, Brenz R, McGrath CM, Russo J, Pauley R, and Brooks SC. Isolation and characterization of a spontaneously immortalized human breast epithelial cell line, MCF-10. Cancer Res 50: 6075-6086, 1990.
5. Calaf G and Russo J. Transformation of human breast epithelial cells by chemical carcinogens. Carcinogenesis 14:483-492, 1993.
6. Calaf G, Zhang PL, Alvarado MV, Estrada S, Russo J. c-*Ha-ras* enhances the neoplastic transformation of human breast epithelial cells treated with chemical carcinogens. Int J Oncol 6:5-11, 1994.
7. Slamon DJ, Clark GM, Wong SG, Levin WJ, Ullrich A, McGuire WL. Human breast cancer: Correlation of relapse and survival with amplification of the HER-2*neu* oncogene. Science 235:177-182, 1987.

Karyotype Analysis in Tumorigenic Human Bronchial Epithelial Cells Transformed by Chrysolite Asbestos Using Chemically Induced PCC Technique

Masao Suzuki, Chang-Qing Piao, and Tom K. Hei

Asbestos fibers induce predominantly two types of cancer, mesothelioma and bronchogenic carcinoma. In cellular and cytogenetic studies, asbestos has been shown to induce drastic cytogenetic changes. In fact, some studies reported that enchanced effects of sister chromatid exchanges and chromosomal abnormalities were detected in human lymphocytes of asbestos workers (*1*). Using either normal human mesothelial cells or malignant mesotheliomas, which are known to be associated with asbestos exposure, there are many reports available regarding chromosome abnormalities (*2*). However, it is unclear whether specific chromosome(s) are involved. One of the difficulties of using malignant mesotheliomas for identifying primary chromosomal karyotypic change in response to asbestos exposure is that the karyotype of the cell line are largely abnormal. As such, it is very important to use a cell system with both a parental and a tumorigenic cell line, having the same gene background, for karyotype analysis. In the present study, we used a trypsin / Giemsa banding (G-banding) in conjunction with a Calyclin-A induced prematurely condensed G_2 chromosomes (G_2 PCC) to overcome the low incidence of well-stretched metaphase chromosomes. We examined the numerical change of specific chromosomes responsible for asbestos-induced tumorigenic conversion using the immortalized and five tumorigenic human bronchial epithelial cell lines having the same genetic background.

Immortalized human bronchial epithelial cell line (BEP2D) at passage 60, which was established from primary normal human bronchial epithelial (NHBE) cells by human papillomavirus 18, was used as parental cells in this study. Five asbestos-induced tumorigenic cell lines were used at passage 50~60. Cells, which reached late log phase in a T75 flask, were treated with Calyculin A (Wako Pure Chemical Industry, Ltd.) at a final concentration of 50 nM for 30 min in a CO_2 incubator at 37^oC. PCC samples were prepared according to a conventional cytogenetic procedure. To measure ploidy distribution, the number of condensed chromosomes with at least 100 G_2 PCCs was scored in each cell line. To analyze the karyotype with the G-banding method, 20 G_2 PCCs in each cell line were photographed and analyzed according to the International System for Human Cytogenetic Nomenclature (1978).

The distribution of modal chromosome number is shown in Figure 1. The number of parental BEP2D cells varied from 46 to 49, indicating hyper-anuploidy. Conversely, the modal number of each tumorigenic cell line showed 43 to 44, suggesting hypo-anuploidy. All cell lines had up to 10% of polyploidy population. These results suggest that the numerical changes of chromosomes play an important role in tumorigenic conversion.

To determine whether asbestos induces a specific pattern of chromosomal alterations in tumorigenic bronchial cells, we examined the karyotypes of their cells using G-banding technique. The results of karyotype analysis in six cell lines are summarized in

Tables 1 and 2. In the parental BEP2D cell, either monosomy of the autosomal chromosome or the loss of the sex chromosome was observed in chromosome 3 (40%), 10 (45%), 12 (75%), 13 (20%), 15 (35%), and Y chromosome (15%). Trisomies also were observed in chromosome 5 (85%), 8 (45%), 14 (65%), 15 (20%), and 20 (20%). In tumorigenic cell lines, the loss of one copy of chromosomes, which were commonly observed in a parental BEP2D cell, was in chromosome 3, 12, 13. The trisomies of chromosomes 5, 14, 15 and 20, which were observed in BEP2D cells, were slightly decreased. The remarkable changes between BEP2D and tumorigenic cell lines were the loss of one or two copies of chromosome 5, the monosomy of chromosome 19 (75-95%) and the increased trisomy of chromosome 8 mentioned above. It is well known that alterations at 19q are common in central nervous system tumors. Moreover, allelic loss of 19q regions is associated with malignant progression in astrocytic gliomas (*3*). Furthermore, the presence of tumor suppressor genes in 19q regions has been suggested (*4*). Also, loss of heterozygosity (LOH) of the long arm of chromosome 5 or complete loss of chromosome 5 has been reported in several malignant disorders, such as myeloid disorders and lung cancer. Moreover, there is evidence that candidate tumor suppressor genes are present on the long arm of chromosome 5 in several types of tumors (*5*-*7*). We showed in this report that the drastic karyotypic change of chromosome 5, 8, and 19 could be play an important role in asbestos-induced tumorigenic conversion in immortalized human bronchial epithelial cells. Although we have no information concerning expression and/or correlation of tumorigenicity-related genes located on chromosome 5, 8, and 19, our results suggest that it could be important that the change of several genes, such as known tumor suppressor genes or unknown genes on above chromosomes, collaborate with each other for changing the phenotype from immortalization to tumorigenicity induced by asbestos.

References

1. N Fatma, A K Jain, Q Rahman, Frequency of sister chromatid exchanges and chromosomal aberrations in asbestos cement workers. *Br J Ind Med* **48**, 103-105 (1991).
2. S S Murthy, J R Testa, Asbestos, chromosomal deletions, and tumor suppressor gene alterations in human malignant mesothelioma *J Cell Physiol* **180**, 150-157 (1999).
3. M J Bello, P E Leone, J Vaquero, J M deCampos, M E Kusak, J L Sarasa, A Pestana, J A Rey, Allelic loss at 1p and 19q frequently occurs in association and may represent early oncogenic events in oligodendroglial tumors *Int J Cancer* **22**, 207-210 (1995).
4. S K Horrigan, Z H Arbieva, H Y Xie, J Kravarusic, N C Fulton, H Naik, T T Le, C A Westbrook, Delineation of a minimal interval and identification of 9 candidates for a tumor suppressor gene in malignant myeloid disorders on 5q31 *Blood* **9**5, 2372-2377 (2000).
5. X Wu, G Ivanova, M Merup, M Jansson, B Stellan, D Grander, E Zabarovsky, G Gahrton, S Einhorn, Molecular analysis of the human chromosome 5q13.3 region in patients with hairy cell leukemia and identification of tumor suppressor gene candidsates *Genomics* **60**, 161-171 (1999).
6. K M Fong, P V Zimmerman, P J Smith, Tumor progression and loss of heterozygosity at 5q and 18q in non-small cell lung cancer *Cancer Res* **55**, 220-223 (1995).
7. J Sanz-Ortega, B Bryant, J Sanz-Esponera, J A Asenjo, M C Saez, A Torres, J L Balibrea, M E Sobel, M J Merino, LOH at the APC/MCC gene (5Q21) is frequent in early stages of non-samll cell lung cancer *Pathol Res Pract* **195**:677-680 (1999).

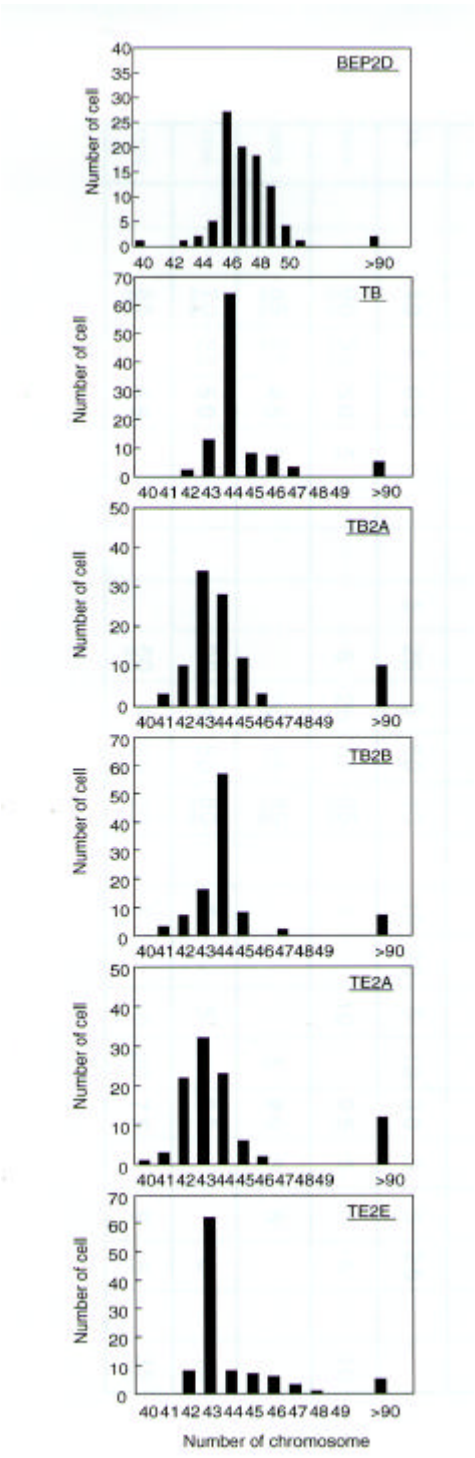

FIG. 1. Distributions of modal chromosome number in each cell line.

TABLE 1. Panel of comparison for chromosome karyotypes (monosomy of the autosomal chromosome the sex chromosome) between parental BEP2D and 5 tumorigenic cell lines. Represented data show perc in each cell line analyzed. Bold numbers show the change which is not observed in BEP2D. Number shows the increasing percentage in change, when comparing to BEP2D.

Ch.# /Cell	#1	#2	#3	#4	#5	#6	#7	#8	#9	#10	#11	#12	#13	#14	#15	#16	#17	#18	#19	#20	#21	#22	X	Y
BEP2D			40	5				5	5	45	5	75	20		35			5						15
TB			40	5	**60**				5	25	5	80	10		10	20	5	10	**80**	5	5	**25**		
TB2A			90	50	**50**	5				5	25	55	65		5		10		**95**	5		5		10
TB2B			65	35	**45**	5					30	65	85					5	**90**	5	5			
TE2A			70	20	**50**					35	30	50	60		5		5		**90**			5		10
TE2E			85		**45**					60	5	50	20		5		10	20	**75**		5	5		35

TABLE 2. Panel of comparison for chromosome karyotypes (trisomy) between parental BEP2D and 5 Represented data show percentage of 20 G2-PCCs in each cell line analyzed. Bold numbers show the observed in BEP2D.

Ch.# /Cell	#1	#2	#3	#4	#5	#6	#7	#8	#9	#10	#11	#12	#13	#14	#15	#16	#17	#18	#19	#20	#21	#22	X	Y
BEP2D					85			45			5			65	20				10	20				
TB					5			**85**	5		5		5	25	10						5			
TB2A					5			**75**		5				15	5						5			
TB2B					10	10	5	**75**							5					15		10		
TE2A					10			**85**		5				15										
TE2E				10		5		**65**						5										

High-Energy Ions and Genomic Instability

Chang-Qing Piao, Tom K. Hei, and Eric J. Hall

We have shown that exposure of immortalized cells of human origin to accelerator-produced high-energy ^{56}Fe ions, simulating those found in space, causes genomic instability that renders progeny of the cells many generations later to be susceptible to carcinogenesis by other more common types of radiation.

We used a papilloma-virus-immortalized bronchial epithelial cell line (BEP2D). Although immortal, this cell line is anchorage–dependent and does not form tumors in immune-suppressed host animals. We have previously shown that after exposure to a large dose of ^{56}Fe ions, transformed cells arise through a series of sequential stages, including altered growth pattern, resistance to serum-induced terminal transformation, and agar-positive growth before becoming tumorigenic in nude mice.

The experiments reported here involved exposure to a 30c-Gy dose of ^{56}Fe ions, which corresponds to rather less than one particle per cell. This resulted in no tumors in immune-suppressed animals, whether the cells were transplanted immediately after irradiation or 6 months later. However, if the cells that had received the 30 cGy of ^{56}Fe ions were subsequently given a 100-cGy dose of X-rays, 6 months later, 3/7 of the animals implanted developed tumors. This dose of X-rays alone did not produce any tumors, in agreement with previous experience.

While there is a large body of data concerning human cancer risks for low-LET radiation, such as X or γ rays, there are no data for radiations comparable to high-energy ^{56}Fe ions. Concern about these particles is based on two factors. First, the passage of a high heavy ion through tissue causes extensive damage to cells traversed. Second, and possibly more important, a large number of adjacent, spatially correlated, cells are affected along and around the track of a particle. Here we show that the exposure of cells of human origin to ions, mimicking those found in space, causes a genomic instability that is maintained and 'remembered' for many cell generations and renders them sensitive to malignant transformation by low-LET radiations, that are abundant in space, at doses that would otherwise be ineffective.

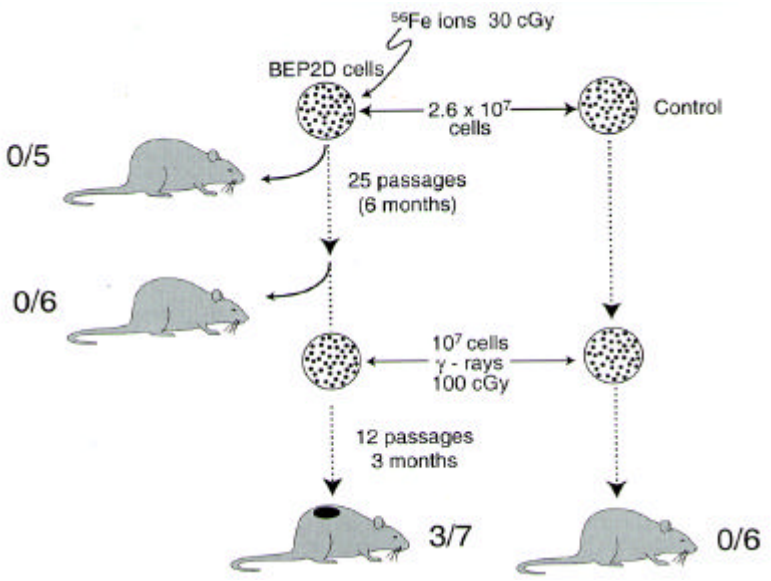

FIG. 1. Schematic diagram illustrating the induction of genomic instability by a non-tumorigenic dose of heavy ions. Exposure of BEP2D cells to a 30-cGy dose of heavy ^{56}Fe ions plus a subsequent dose of 100-cGy γ-rays resulted in tumors.

CYTOGENETIC STUDIES

Induction and Recovery of Cytotoxic and Chromatid Damage in Primary Human Bronchial Epithelial Cells Irradiated with ^{56}Fe Ions

Masao Suzuki, Chang-Qing Piao, and Tom K. Hei

At a time when manned space exploration is more a reality than a myth with the planned international space station well underway, the biological effects of low-flux galactic cosmic rays (GCR) to astronauts or crews of a spacecraft have become one of the major concerns of space agencies. One useful approach in risk assessment of high-energy and charged (HZE) particles is to investigate cellular responses using normal human cells. Many such studies have reported that high-LET charged particles are more effective per unit absorbed dose in the induction of lethality, chromosomal damage, and mutations than low-LET radiation. However, almost all of these studies have used normal human fibroblasts, and it is important for a realistic risk assessment of the carcinogenic potential of HZE particles to examine biological effects using normal human epithelial cells since the majority of human cancers are of epithelial-cell origin. In this study, we examined the effects of both cell killing and chromatid damage in primary human bronchial epithelial (NHBE) cells irradiated with high-energy ^{56}Fe ions.

Primary normal human bronchial epithelial (NHBE) cells were obtained from Clonetics Corporation (San Diego, CA). The NHBE cells were cultured in serum-free BEBM medium in a 5% CO_2 incubator at 37^{o}C. The expanded stock culture was frozen in liquid nitrogen until use (passage 3), and freshly thawed cells at passage 4 were utilized in the studies.

NHBE cells were irradiated with graded doses of ^{137}Cs γ rays or ^{56}Fe ions. ^{56}Fe-ion beams were accelerated with the Alternating Gradient Synchrotron (AGS) at the Brookhaven National Laboratory (BNL). The energy of the ^{56}Fe ions was 1 GeV/n and the dose-averaged LET value of the beam was estimated to be ~140 keV/μm at the sample position (*1*). The dose rate of ^{56}Fe-ion irradiation was 0.4 to 0.8 Gy/min. All of the irradiations were carried out at room temperature.

One hour after irradiation, a sufficient number of cells was plated onto 60- mm-diameter plastic dishes at a density such that 50 to 60 cells would form viable colonies to assess immediate plating (IP) effect. Another set of irradiated cells was incubated in a 5% CO_2 incubator at 37^{o}C for 24 hr for delayed plating (DP).

Cells were treated with Calyculin A at a final concentration of 50 nM for 30 min in a CO_2 incubator at 37^{o}C. Calyculin A was added 1 hr after irradiation for immediate assay (IA) or 24 hr after irradiation for delayed assay (DA). Cells for DA were kept in a CO_2 incubator at 37^{o}C until Calyculin A was added. PCC samples were prepared according to a conventional cytogenetic procedure. PCC samples of 50 G_2 phases were scored under a light microscope.

Figure 1 shows cell survival curves for IP and DP by ^{137}Cs γ rays and ^{56}Fe ions. The

curves for ^{137}Cs γ rays had larger shoulders than those for ^{56}Fe ions. Similarly, the curves for DP showed larger shoulders than those of IP in both radiation types. RBE values for ^{56}Fe ions, calculated using D_{10} , which was defined as the dose (Gy) required to reduce the surviving fraction to 10%, were 1.99 for IP and 2.73 for DP. RBE for IP (1.99) is smaller than those of the results using lighter ions (LET~150 keV/μm) reported previously (*2-5*). One possibility for the discrepancy is that the maximum peak for RBE-LET relationship changed to higher-LET regions. According to the previous reports (*3-7*), RBE maximum peak shifted to higher-LET regions for heavier ions. The RBE values obtained in this study, therefore, are smaller than those for lighter ions. Conversely, inactivation cross section of IP is 0.0314 μm^2 for γ rays and 31.2 μm^2 for ^{56}Fe ions. These values are similar to other *in vitro* and *in vivo* studies previously reported (*5, 8*). The results suggest that the target of radiation-induced reproductive cell death for primary human bronchial epithelial cells is the same as that for other human or rodent cells. Furthermore, based on the repair ratio (D_{10}[DP] / D_{10}[IP]) of 1.67 for γ rays and 1.22 for ^{56}Fe ions, these results indicate that HZE-ion beams are more effective in cell killing than low-LET γ rays.

The dose-response curves for both IA and DA in G_2 PCC were mostly linear over the range of dose examined (Figure 2). The results indicated that the induced frequency for initially measured fragments by ^{56}Fe ions were the same as that for γ rays. The number of chromatid fragments per Gy per cell was 5.56 for γ rays and 5.33 for ^{56}Fe ions. On the other hand, the frequency of residual fragments in NHBE cells irradiated with ^{56}Fe ions was ~4.2 fold higher than those of γ rays. The number of residual fragments per Gy cell was 0.80 for γ rays and 3.37 for ^{56}Fe ions. Around 85% of the fragments induced by γ rays rejoined after 24 hr of post-irradiation incubation, while only 37% of the fragments induced by ^{56}Fe ions did. These results suggested that damage induced by γ rays and ^{56}Fe ions were qualitatively different. Figure 4 shows the dose-response curves of chromatid exchanges. Curves for DA were curvilinear in both radiation types. The frequency for DA by γ rays was higher than that of ^{56}Fe ions, but there was no difference in IA between γ rays and ^{56}Fe ions. A low number of exchanges was observed in IA for both radiation types. This result suggested that some rejoining occurred during the 1.5 hr incubation and treatment with Calyculin A post-irradiation. The frequency induced by γ rays was 1.6 times higher than that by ^{56}Fe ions at the 0.15 exchange induction level. These results suggest that HZE particles induce complicated unrejoinable damage at the chromosomal level in NHBE cells.

In this study, we examined the biological effects at both the cellular and chromosomal levels induced by high-energy ^{56}Fe ions using primary human bronchial epithelial cells. Our data suggest that the HZE particles can induce more damage at both the cellular and chromosomal levels, when compared with lighter ions with a similar LET or with low-LET γ rays. Differences in track structure of energy deposition with different ion sources may play an important role in the biological effects of HZE particles. We further show the usefulness in applying the Calyculin-A-mediated PCC technique to primary human bronchial epithelial cells for detecting chromosomal damage induced by different radiation types.

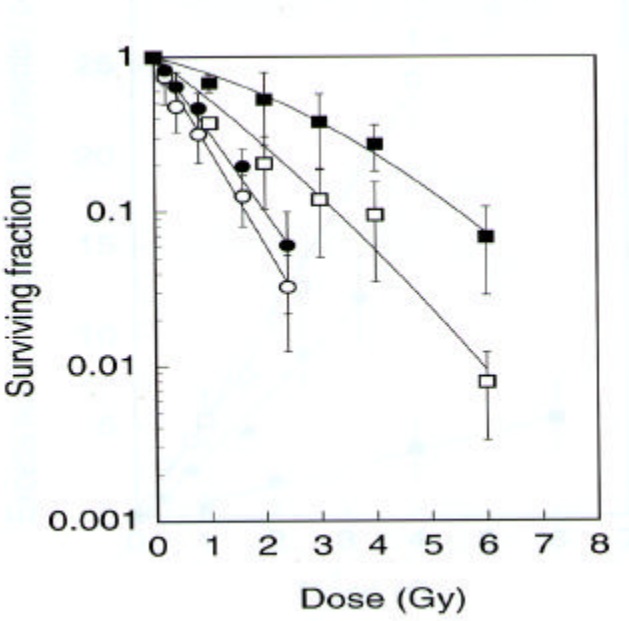

FIG. 1. Cell survival curves in NHBE cells irradiated with ^{137}Cs γ rays (ψ: immediate plating (IP) 1 hr after irradiation; η : delayed plating (DA) 24 hr after irradiation) and ^{56}Fe ions (: IP; { : DP). The presented results are mean and 95% confidence intervals of the two independent experiments. The curves were fitted by the least square method to a linear quadratic equation.

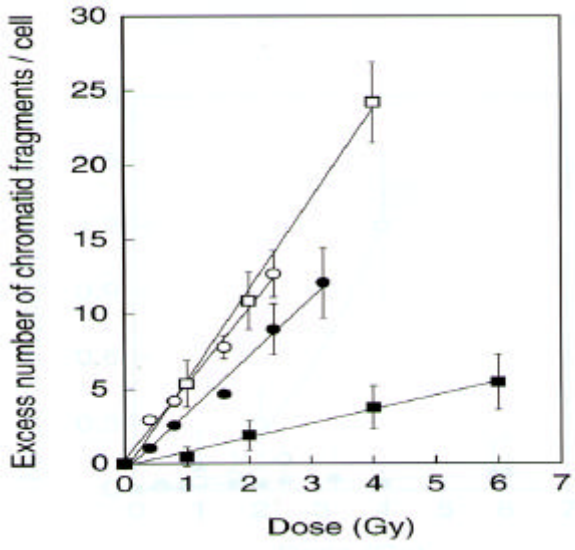

FIG. 2. Dose-response curves for chromatid aberrations (chromatid breaks, isochromatid deletions, and acentric fragments) irradiated with ^{137}Cs γ rays ({ : immediate assay (IA) 1 hr after irradiation; η : delayed assay (DA) 24 hr after irradiation) and ^{56}Fe ions (: IA; μ : DA). The presented results were mean and 95% confidence intervals of the two independent experiments. The curves were fitted by the least square method.

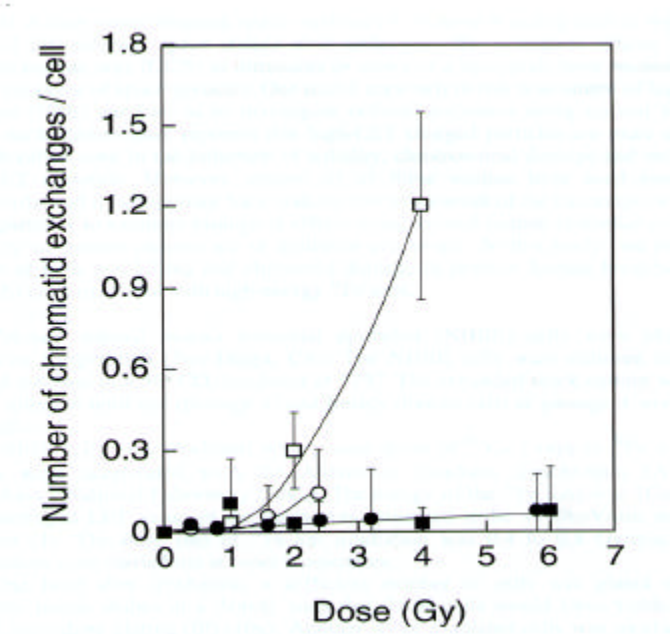

FIG. 3. Dose-response curves for chromatid exchanges (intrachanges and interchanges). The symbols are the same as in Figure 2. The presented results were mean and 95% confidence intervals of the two independent experiments. Curves were fitted by the least square method.

References

1. H Wu, K George and T C Yang, Estimate of the frequency of true incomplete exchanges in human lymphocytes exposed to 1 GeV/u Fe ions *in vitro*. *Int J Radiat Biol* **75**, 593-599 (1999).
2. K Tsuboi, T C Yang and D.J.Chen, Charged-particle mutagenesis. I.Cytotoxic and utagenic effects of high-LET charged iron particles on human skin fibroblasts. *Radiat Res* **129**, 171-176 (1992).
3. M Folkard, K M Prise, B Vojnovic, H C Newman, M J Roper and B D Michael, Inactivation of V79 cells by low-energy protons, deuterons and helium-3 ions. *Int J Radiat Biol* **69**, 729-738 (1996).
4. M Suzuki, Y Kase, T Kanai, F Yatagai and M Watanabe, LET dependence of cell death and chromatin-break induction in normal human cells irradiated by neon-ion beams. *Int J Radiat Biol* **72**, 497-503 (1997).
5. W K Weyrather, S Ritter, M Scholz and G Kraft, RBE for carbon track-segment irradiation in cell lines of differing repair capacity. *Int. J. Radiat. Biol*. **75**, 1357-1364 (1999).
6. G Kraft, Radiobiological effects of very heavy ions: inactivation, induction of chromosome aberrations and strand breaks. *Nuclear Science Applications* **3**, 1-28 (1987).
7. M Belli, R Cherubini, S Finotto, G Moschini, O Sapora, G Simone and M A Tabocchini, RBE-LET relationship for the survival of V79 cells irradiated with low energy protons. *Int J Radiat Biol* **55**, 93-104 (1989).
8. A Rodriguez, E L Alpen and P Powers-Risius, The RBE-LET relationship for rodent intestinal crypt cell survival, testes weight loss, and multicellular spheroid cell survival after heavy-ion irradiation. *Radiat. Res.* **132**, 184-192 (1992).

Conservation of Chromosome-Specific Telomere Length in Mammalian Cells

Andrei Tchirkov and Elizabeth Chavez (Terry Fox Laboratory for Hematology/Oncology, BC Cancer Research Centre, Vancouver, BC Canada), M. Prakash Hande, and Peter Lansdorp (TFL, BC Canada)

Telomeres constitute the ends of eukaryotic chromosomes and are essential for maintaining normal chromosomal structure and function. This nucleoprotein complex is organized as a t-loop structure that protects the natural ends of chromosomes from fusion events, degradation, and inappropriate recombination. The telomere sequences are gradually lost in normal somatic cells with each round of DNA replication until chromosomes become unstable, causing age-associated cell cycle arrest or replicative senescence (*1*). Although the telomere length is heterogeneous in a given population of somatic cells, specific chromosomes display a similar telomere length in different tissues of an individual organism (*2*). In human cells, significant and conserved differences in the telomere length of specific chromosomes were identified using quantitative fluorescence *in situ* hybridization (Q-FISH) (*3,4*). Thus, the telomere length of specific chromosomes may be inherited and maintained during normal embryonic, fetal, and postnatal somatic cell development. In particular, telomeres on human chromosome 17p were found to be significantly shorter than the median overall telomere length of all pooled autosomal and sex chromosomes.

To address the question if chromosome-specific telomere length is somewhat involved in the function of specific chromosomes, we investigated the relative telomere length on the chromosome that is homologous to human chromosome 17 in different species. A combination of Q-FISH and hybridization with chromosome-specific probes was used to analyze the telomere length on these particular chromosomes. We found that chromosome arms corresponding to 17p in a chimpanzee, an owl monkey, and several mouse strains also had significantly fewer than the average number of telomere repeats. This observation provides evidence of evolutionary conservation of relative chromosome-specific telomere length. It also suggests that the length of telomere "repeats" at individual chromosome ends may be functionally relevant, e.g., in the epigenetic control of gene expression or in the induction of telomere-mediated genomic rearrangements.

In both the chimpanzee and the owl monkey, chromosome 19 is homologous to human chromosome 17. A similarity in centromeric alpha satellite DNA sequences between human and non-human primates allowed the use of a centromere-specific peptide nucleic acid (PNA) probe for human chromosome 17 for a precise identification of corresponding chromosomes in chimpanzee and owl monkey metaphase preparations (hybridizes on chromosome 19) (Fig. 1a). The results of the telomere length analysis, which was carried out in 12-15 metaphases, are presented in Figure 2. In the two species, we observed significantly lower fluorescence intensities on chromosome 19p telomeres compared to the fluorescence values from either pooled p-arm telomeres or all chromosome (p & q) arms

combined, indicating that the 19p telomeres were relatively short in both species. There are extended homologies between human chromosome 17 and mouse chromosome 11. It should be noted that the mouse chromosome 11 is truly telocentric because of the apparent lack of non-satellite DNA between the minor satellite and the terminal repeat arrays on the p-arm (*5,6*). As indicated by comparative mapping experiments, the mouse coding gene homologues of human chromosome 17p are located on the long arm of chromosome 11 (*7*). Thus, mouse chromosome 11q may be considered a homologue to human chromo some 17p. To visualize chromosome 11 in mouse metaphase preparations, we used FISH with a specific paint probe following telomere hybridization (Figure 1c-d). In total, between 21 and 31 metaphases were analyzed for each mouse strain. A comparison of the fluorescence intensity of chromosome 11 telomeres to the p- and q-arm telomere fluorescence values from all chromosomes showed that both 11p and 11q had lower telomere signal intensities in most cases. In particular, the chromosome 11q telomeres were significantly shorter than the all q-arm telomeres in all but one mouse strain (Figure 3). Overall, the median telomere length in different *M. musculus* strains varied between 26.4 and 37.6 kb and was significantly longer than the values obtained in *M. spretus* (3.6 kb, median), consistent with previous reports (*8,9*).

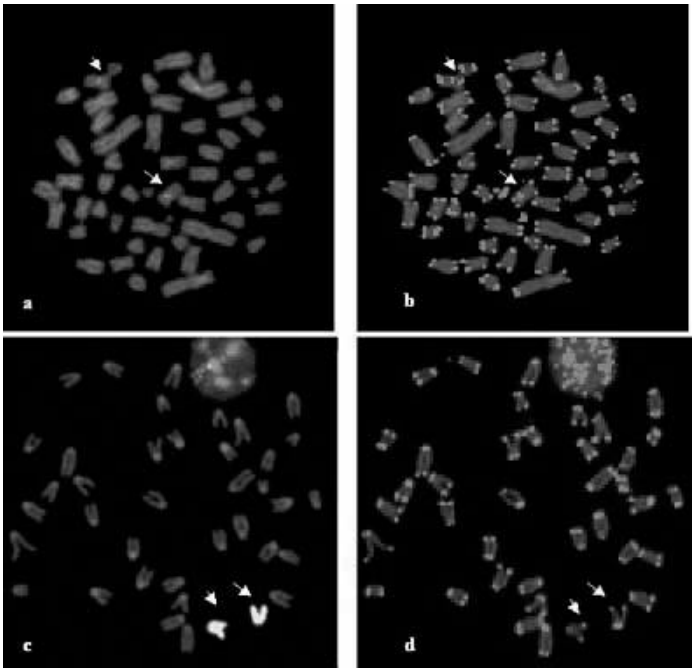

FIG. 1. Telomere labeling and detection of specific chromosomes on metaphase preparations obtained from the owl monkey (**a, b**) and the C57BL/6 mouse (**c, d**). Chromosomes are counterstained with DAPI (**a, b, d**) and PI (**c**). (**a**) Hybridization of the human chromosome 17 centromere-specific probe to chromosomes 19 (arrows) of the owl monkey; (**b**) Simultaneous visualization of individual telomeres and chromosomes 19 (arrows) on the same metaphase from the owl monkey; (**c**) Identification of the mouse chromosome 11 using a specific paint probe; (**d**) Telomere hybridization on the same metaphase from the C57BL/6 mouse.

Fig.2

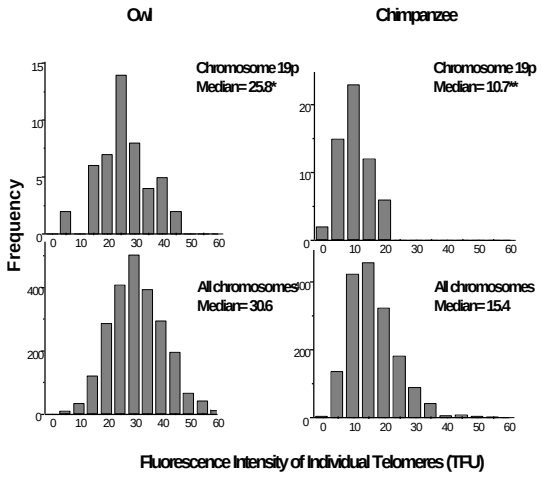

FIG. 2. Telomere fluorescence intensities from the chromosome 19p and all chromosomes in the chimpanzee and the owl monkey. The differences in median fluorescence intensity between 19p and all telomeres were significant (*P=0.002, **P<0.001, Wilcoxon rank sum test) in both species. Histograms express the fluorescence intensity distribution of individual telomeres from 12 to 15 metaphases. One telomere fluorescence unit (T.F.U.) corresponds to 1 kb of $(TTAGGG)_n$ sequence.

Fig.3

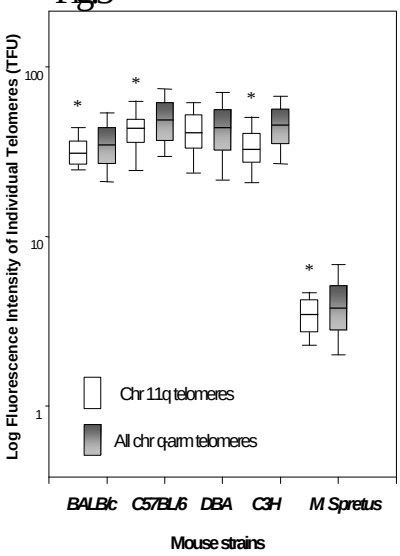

FIG. 3. Short telomeres are present on 11q chromosomes in all mouse strains with exception of the DBA mouse. The hatched box plots represent only the telomeres of the chromosome 11q. The open box plots represent all q-arm telomeres. In each box plot, the horizontal lines express the median, 10^{th}, 25^{th}, 75^{th}, and 90^{th} percentiles of the distribution of the fluorescence values. Asterisks (*) indicate statistically significant differences (Wilcoxon rank sum test).

References

1. de Lange T, DePinho RA (1999) Unlimited mileage from telomerase? *Science* 283, 947–949.
2. Zijlmans JM, Martens UM, Poon SS *et al.* (1997) Telomeres in the mouse have large inter-chromosomal variations in the number of T_2AG_3 repeats. *Proc Natl Acad Sci U S A* 94: 7423-7428.
3. Martens UM, Zijlmans JM, Poon SS *et al.* (1998) Short telomeres on human chromosome 17p. *Nat Genet* 18:76-80.
4. Hande MP, Samper E, Lansdorp P, Blasco MA, 1999, Telomere length dynamics and chromosomal instability in cells derived from telomerase null mice. J Cell Biol 144: 589-601.
5. Lee JJ, Warburton D, Robertson EJ (1990) Cytogenetic methods for the mouse: preparation of chromosomes, karyotyping, and in situ hybridization. *Anal Biochem* 189: 1-17.
6. Kipling D, Ackford HE, Mitchell AR, Taylor BA, Cooke HJ (1991) Mouse minor satellite DNA genetically maps to the centromere and is physically linked to the proximal telomere. *Genomics* 11: 235-241.
7. Copeland NG, Jenkins NA, Gilbert DJ, et al (1993) A genetic linkage map of the mouse: current applications and future prospects. *Science* 262:57-66.
8. Kipling D, Cooke HJ (1990) Hypervariable ultra-long telomeres in mice. *Nature* 347: 400-402.
9. Zhu L, Hathcock KS, Hande P, Lansdorp PM, Seldin MF, Hodes RJ (1998) Telomere length regulation in mice is linked to a novel chromosome locus. *Proc Natl Acad Sci U S A* 95: 8648-8653.

Chromosome Aberrations Induced by a Particles and Soft X-Rays in Human Primary Fibroblasts

M. Prakash Hande, Satin G Sawant, Brian Ponnaiya, Sonu Dhar, Stephen A. Marino, Adayabalam S. Balajee , Charles R. Geard, and David J. Brenner

Radiation-induced chromosome aberrations can be LET dependent. To study chromosome aberrations induced by high-LET radiation, human fibroblasts were exposed to different doses of alpha particles. Human primary fibroblasts were plated on 35-mm dishes made of specially constructed stainless steel rings with a Mylar bottom. Plateau-phase cells were irradiated with graded doses (0, 0.2, 0.4, 0.8 and 1.6 Gy) of alpha particles (90 keV/µm) in a track-segment mode (van de Graaff accelerator, RARAF, Columbia University). Cells were trypsinized and subsequently cultured for 40 to 45 hours for preparing metaphase chromosomes.

In order to measure the effects of low-energy X-rays relative to gamma rays, human primary fibroblasts (WI38) were irradiated at ~15 keV with monoenergetic X-rays produced by the National Synchrotoron Light Source (NSLS) of Brookhaven National Laboratory (BNL). The irradiation fixture and procedures used for this experiment are essentially the same as those used for charged-particle irradiations using the RARAF track segment facility and are performed using a personal computer. Special Kynar/Mylar dishes were constructed and cells were plated onto such dishes three to four days prior to irradiation. Plateau phase cells were irradiated with different doses of soft X-rays (0, 1, 2, and 4.0 Gy). The dosimetry and the irradiation were performed as described previously (*1*). Because the X-ray beam is horizontal, the cell dishes are vertical, and the side of each dish opposite the Mylar/Kynar surface is sealed with a layer of 6-µm thick Mylar film held in place with a metal ring. The dishes are filled with medium through the ports on the edge of the dish in order to prevent the cells from drying out during the irradiation. Up to 20 cell dishes can be placed on the irradiation wheel. Dose measurements are made using an ionization chamber made of the same material as the cell dishes.

Following irradiation, cells were trypsinized and replated into 100-mm cell culture dishes. Cells were harvested at 40 hours after irradiation to score only the first-division metaphase chromosomes for induced aberrations. Both stable and unstable aberrations were analyzed for the selected dose groups by using fluorescence in situ hybridization techniques. Asymmetrical exchanges such as dicentrics, rings, fragments were scored and compiled based on the DAPI staining in FISH. Telomeric and centromeric probes were combined in FISH to unequivocally differentiate dicentrics, interstitial deletions, fragments, and terminal deletions.

The dose-response curve for dicentric frequency obtained following irradiation with α particles is given in Figure 1. Dicentric frequency was detected based on the DAPI staining in a FISH painted slide. The dicentric yield per cell was fitted with a linear-quadratic equation: $-0.17x^2+0.59x-0.0077$; $r^2 = 0.9971$. The linear-quadratic model was the best fit for the dicentric frequency as was the case in earlier classical experiments, though

there exists a controversy on this aspect recently. Based on the aberrations, dicentrics, rings and fragments, detected, total aberrations induced followed a linear-quadratic function as well:

$$y_{total} = -0.38x^2+1.36x-0.004;\ r^2 = 0.9917.$$

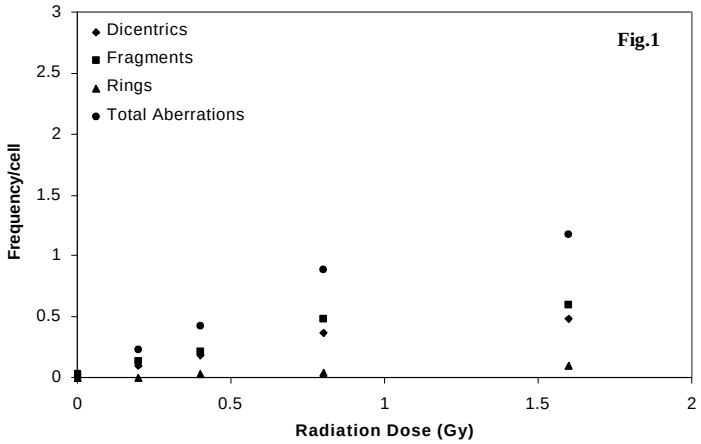

FIG. 1. Dose-response curve for chromosome aberrations induced by α particles in human fibroblasts. Aberrations were detected in the DAPI stained metaphase chromosomes.

As shown in Figure 2, aberrations detected after exposure to soft X-rays fitted with the following equations:

$$y_{total} = 0.025x^2 + 0.333x+0.0313;\ r^2 = 0.9957$$
$$y_{dic} = 0.0257x^2+0.123x+0.0173;\ r^2 = 0.9921$$

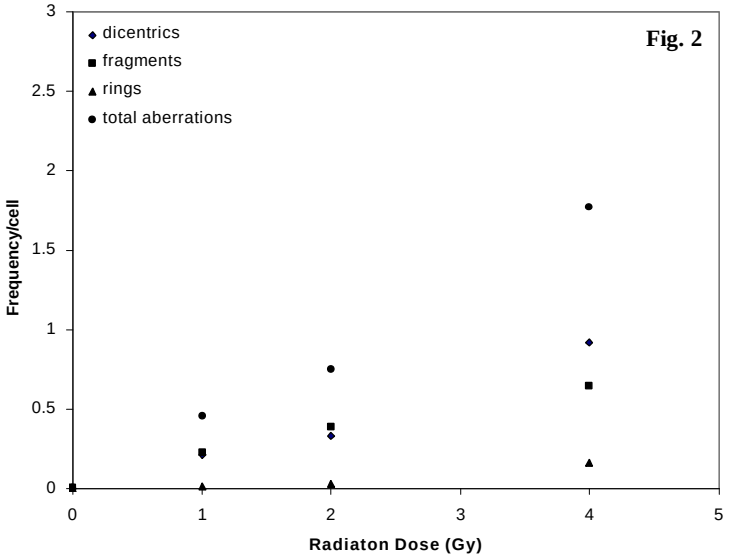

FIG. 2. Chromosome aberrations induced in human primary fibroblasts following exposure to soft X-rays.

Further, the metaphase spreads from the above experiments will be subjected to multicolor fluorescence in situ hybridization in order to detect the aberration spectrum using 24-color chromosome probes (mFISH; *ref 2*). Simultaneously, mBAND FISH will be performed to detect the induction of inter/intra-arm exchanges on a particular chromosome (*3*,*4*). The data obtained from different radiation qualities (gamma radiation, α particles and soft X-rays) will be compared for their effectiveness in inducing chromosome aberrations in human fibroblasts.

References

1. Marino, S, Srdoc D, Sawant S, Geard C, Brenner D, 1999, RBE and Microdosimetry of Low-Energy X-rays. *CRR Annual Report*, pp 43-47.
2. Speicher MR, Ballard SG, Ward DC, 1996, Karyotyping human chromosomes by combinatorial multi- fluor FISH. *Nat. Genet*. 12, 368-375.
3. Johannes C, Chudoba I, Obe G, 1999, Analysis of X-ray-induced aberrations in human chromosome 5 using high-resolution multicolour banding FISH (mBAND) *Chromosome Res*. 7(8), 625-33.
4. Chudoba I, Plesch A, Lörch T, Lemke J, Claussen U, Senger G , 1999, High resolution multicolor-banding: A new technique for refined FISH analysis of human chromosomes, *Cytogen Cell Genet*, 84, 156-160.

Use of Chromosome-Arm-Specific Probes in the Detection of Radiation-Induced Inter-Arm Exchanges

M. Prakash Hande, Sonu Dhar, Adayabalam S. Balajee, Charles R. Geard, and David J. Brenner

Exposure to ionizing radiation produces a number of biological consequences, including gene mutations, chromosome aberrations, cellular transformation, and cell death. These effects have been attributed to radiation-induced DNA damage, producing irreversible changes during DNA replication or during the processing of the DNA damage by enzymatic repair processes. Presumably, most of these changes occur during the cell cycles immediately following radiation exposure. There is evidence for a delayed radiation response in the form of genomic instability. Structural changes induced by irradiation lead to acute or late cellular effects including cell death, chromosomal aberrations, and neoplastic transformation. Radiation-induced chromosomal aberrations are believed to be the result of mis- or non-repair of chromosome breaks. Breaks resulted from irradiation can be efficiently repaired and such a restitution of chromosomes cannot be detected under the light microscope at metaphase. Mis-repair or mis-joining of breaks leads to the formation of exchange aberrations between chromosomes (dicentrics and translocations) or within a particular chromosome (rings and inversions). Lack of repair or incomplete repair of chromosome breaks leads to terminal deletions (a truncated chromosome together with a terminal fragment derived from the same chromosome) or incomplete exchanges *(for review: 1,2)*. The primary motivations for aberration studies have been the association of chromosome structural changes with cancer, and the importance of aberrations to the three main applications of radiobiology: biodosimetry, carcinogenesis risk estimation, and radiotherapy.

Human primary fibroblasts derived from four individuals (WI38, MRC-5, IMR-90 and IMR-91) were procured from Coriell Cell Repository (Camden, NJ) and utilized in the study. Cells at early passages were grown in complete medium (E-MEM supplemented with 15% FBS, essential amino acids, non-essential amino acids, vitamins, and anti-biotics). Plateau-phase cells were exposed to different doses of gamma radiation (0, 1 Gy, 2 Gy, 3 Gy, 4 Gy). They were allowed to complete one cell cycle after irradiation and then harvested for metaphase preparations using routine procedures. Cells were harvested 40 to 48 h after irradiation following a 2-hour colcemid treatment. After hypotonic swelling (0.075 M KCl) for 15 minutes at 37°C, the cells were fixed in methanol:acetic acid (3:1). Cell suspension was dropped on to a wet, clean slide for use in FISH. For long-term storage, the fixed cells were kept at −20°C until use.

Based on the yield of metaphase chromosomes, two cell lines were selected for further experimental analysis (WI38 and MRC-5). Both stable and unstable aberrations are analyzed for the selected dose groups by using fluorescence in situ hybridization techniques. Asymmetrical exchanges such as dicentrics, rings, and fragments are scored and compiled based on the DAPI staining in FISH. Telomeric and centromeric probes are combined in FISH to unequivocally differentiate dicentrics, interstitial deletions,

fragments, and terminal deletions. The data is generated using this approach. The different doses we plan to use in the study are 0, 0.5, 1.0, 2.0, 3.0, 4.0, 6.0, 8.0 and 10.0 Gy. The lower dose range (up to 4.0 Gy) is used in single- or double-color chromosome painting using selected chromosomes to detect dicentrics and translocations involving different chromosomes. Our aim is to study the induction of peri- and para-centric inversions following irradiation. Since these type of aberrations are induced at a lower frequency at low doses, we decided to use higher doses for the analysis. Chromosome-arm-specific painting probes (American Laboratory Technologies, USA; *3*) were used in FISH to detect inter-arm exchanges. The technique has been optimized to stain the p and q arms of the selected chromosomes (e.g.. 2, 3 or 4) in different colors to detect exchanges occurring between the two arms of the chromosomes. In this analysis, any aberration involving a particular arm is identified (inter-arm exchanges, translocations with other chromosomes, color junctions, dicentrics, and rings) and scored for frequency following irradiation at doses ranging from 4 to 10 Gy. The use of mBAND FISH (color bar code on a particular chromosome; *4-5*) is tested to determine the inter- and intra-arm chromosome exchanges.

The dose-response curve for dicentric frequency obtained following irradiation is given in Figure 1. Dicentric frequency was detected based on DAPI staining in a FISH painted slide, dicentric yield per cell followed a linear-quadratic model:

$y_{dic} = 0.\ 0.07x^2+0.003x+0.01$ with an r^2 value of 0.9976.

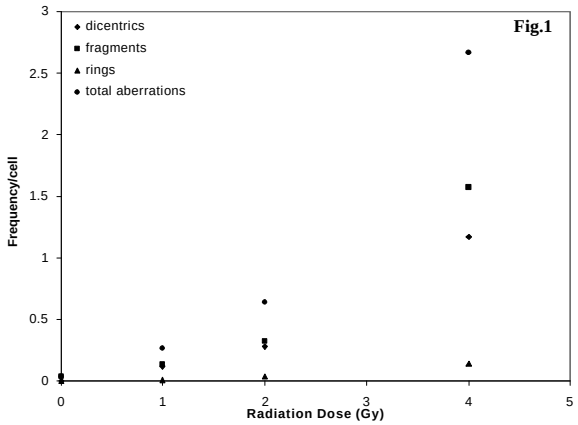

FIG. 1. Chromosome aberrations induced by gamma-radiation in human fibroblasts. Aberrations were detected in the DAPI stained metaphase chromosomes.

The linear-quadratic model was the best fit for the dicentric frequency, as was the case in earlier classical experiments, though there exists a controversy. Based on the aberrations, dicentrics, rings, and fragments detected, total aberrations induced followed a linear-quadratic function as well, being $y_{total} = 0.17x^2-0.02x+0.06$, with an r^2 value of 0.9986. As shown in Figure 2, the frequency of inter-arm exchanges is analyzed using the chromosome arm-specific probes and data compilation is still in progress.

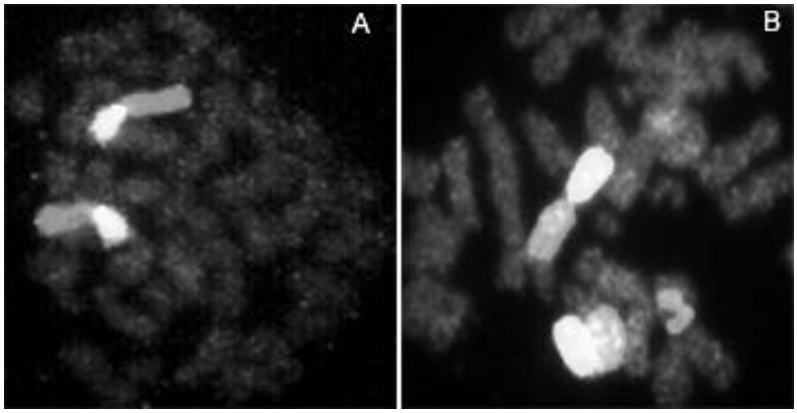

FIG. 2. A: Dual-color FISH using chromosome-arm-specific probes for 2p (green) and 2q (red) on human chromosomes. B: A metaphase showing chromosome exchange involving q-arm of chromosome 3 (red) and an unpainted chromosome in irradiated human fibroblasts. Chromosome arm 3p is painted in red color.

References

1. Savage JRK (1993) Update on target theory as applied to chromosomal aberrations. *Environ. Mol. Mutagen*. 22, 198-207.
2. Natarajan AT, Balajee AS, Boei JJWA, Darroudi F, Dominguez I, Hande MP, Meijers M, Slijepcevic P, Vermeulen S, Xiao Y (1996) Mechanisms of induction of chromosomal aberrations and their detection by fluorescence in situ hybridization. *Mutat Res* 372, 247-258.
3. Boei JJ, Vermeulen S, Natarajan AT (1998) Dose-response curves for X-ray induced interchanges and interarm intrachanges in human lymphocytes using arm-specific probes for chromosome 1. *Mutat Res* 404: 45-53.
4. Chudoba I, Plesch A, Lörch T, Lemke J, Claussen U, Senger G (1999) High resolution multicolor-banding :a new technique for refined FISH analysis of human chromosomes, *Cytogen Cell Genet*, 84, 156-160.
5. Johannes C, Chudoba I, Obe G (1999) Analysis of X-ray-induced aberrations in human chromosome 5 using high-resolution multicolour banding FISH (mBAND) *Chromosome Res*. 7(8): 625-633.

MOLECULAR STUDIES

S. pombe rad9 and Its Human Homologue Have a BH3-Like Domain and Can Promote Apoptosis in Human Cells

Howard B. Lieberman, Kevin M. Hopkins, and Haiying Hang, in collaboration with Hong-Gang Wang and Kiyoshi Komatsu (H. Lee Moffitt Cancer Center and Research Institute, University of South Florida

Analysis of the amino acid sequences of the fission yeast *S. pombe rad9* protein (*1*), as well as the human homologue (*2*), revealed that each has a region near its N-terminal, specifically, residues 16-30, highly similar to the BH3 (Bcl-2 Homology region 3) domain of pro-apoptotic proteins. Furthermore, we found that the yeast and human proteins can bind the anti-apoptotic proteins Bcl-2 and Bcl-x_L, and can cause apoptosis when overexpressed in human cells (*3-4*). In addition, we found these activities are completely dependent upon the BH3 domain within the RAD9 proteins. Interestingly, overexpression of either yeast *rad9* or human *RAD9* did not cause an apoptotic-like response in *S. pombe*, even though this fission yeast reportedly is a capable one (*5-6*).

These results suggest that *S. pombe* may contain a programmed cell death system that differs from the one inherent in mammalian cells. This is supported by the inability as of yet to find anti-apoptotic Bcl-2 family members or caspases in *S. pombe*. Furthermore, the loss of a pro-apoptotic function, such as by mutation in *S. pombe rad9*, would be expected to make cells resistant to DNA damaging agents. However, in contrast, *S. pombe rad9::ura4+* or *rad9-192* cells are sensitive to radiation and many types of chemicals that damage DNA. Nevertheless, these studies provide evidence that *S. pombe rad9* and human *RAD9* have a novel apoptotic function in addition to their more classical role in cell-cycle checkpoint control.

References

1. Lieberman, H.B., K.M. Hopkins, M. Laverty, and H.M. Chu. (1992) Molecular cloning and analysis of *Schizosaccharomyces pombe rad9*, a gene involved in DNA repair and mutagenesis. Mol. Gen. Genet. 232:367-376.
2. Lieberman, H.B., K.M. Hopkins, M. Nass, D. Demetrick, and S. Davey. (1996) A human homologue of the *Schizosaccharomyces pombe rad9+* checkpoint control gene. Proc. Natl. Acad. Sci. USA 93:13890-13895.
3. Komatsu, K., T. Miyashita, H. Hang, K.M. Hopkins, W. Zheng, S. Cuddeback, M. Yamada, H.B. Lieberman, and H.-G. Wang. (2000) Human homologue of *S. pombe* Rad9 interacts with Bcl-2/Bcl-xL and promotes apoptosis. Nat. Cell Biol. 2:1-6.
4. Komatsu, K., K.M. Hopkins, H.B. Lieberman, and H.G. Wang. (2000) *Schizosaccharomyces pombe* Rad9 contains a BH3-like region and interacts with the anti-apoptotic protein Bcl-2. FEBS Letters 481:122-126.
5. Ink, B., M. Zornig, B. Baum, N. Hajibagheri, C. James, T. Chittenden, and G. Evan. (1997) Human Bak induces cell death in *Schizosaccharomyces pombe* with morphological changes similar to those with apoptosis in mammalian cells. Mol. Cell. Biol. 17:2468-2474.
6. Jurgensmeier, J.M., S. Krajewski, R.C. Armstrong, G.M. Wilson, T. Oltersdorf, L.C. Fritz, J.C. Reed, and S. Ottilie. (1997) Bax- and Bak-induced cell death in the fission yeast *Schizosaccharmyces pombe*. Mol. Cell. Biol. 8:325-339.

Construction and Analyses of *Mrad9* Knockout Cells and Mice

Howard B. Lieberman, Kevin M. Hopkins, and Haiying Hang, in collaboration with Wojtek Auerbach and Alexandra L. Joyner (Skirball Institute, New York University)

The *rad9* gene from the fission yeast *S. pombe* is evolutionarily conserved and is critical for promoting resistance to gamma rays, UV light, and chemicals that damage DNA, as well as supporting the associated cell cycle checkpoints (*1-3*). In addition, recent studies indicate that the yeast gene and its human homologue (*4*) also bear pro-apoptotic function (*5,6*). In order to better understand the biological role of these multi-functional cognate proteins, especially in the context of an intact mammal, we isolated the mouse homologue of the gene (*Mrad9*; Ref. *7*), and initiated studies using established procedures (*8*) to construct knockout ES cells and mice.

We made a *Mrad9* targeting vector, such that loxP sites are located in the 5' untranslated region and in the first intron of the gene. The vector was introduced into ES cells derived from 129/Sv//Ev mice, and transformants with the modified *Mrad9* inserted at the corresponding inherent site were identified (Fig. 1). These cells were successfully used to make homozygous targeted ES cells as well as targeted mice. When a plasmid encoding Cre protein was added to the heterozygous and homozygous *Mrad9* targeted cells, heterozygous and homozygous *Mrad9* deleted cells were obtained. Furthermore, when targeted animals were mated to Cre-expressing mice, the first generation of progeny yielded heterozygous *Mrad9* knockout animals. However, thus far all initial heterozygous X heterozygous *Mrad9* knockout mouse crosses failed to produce homozygous knockout pups. These studies suggest that *Mrad9* is essential for embryonic viability. Studies are in progress to define the reasons for the lethality observed and to analyze the function of the gene at the cellular level.

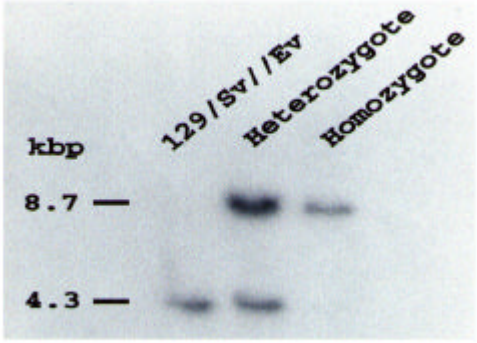

FIG. 1. ES cells heterozygous or homozygous targeted for the *Mrad9* knockout vector. The 5'-end of *Mrad9* was used as a probe for the Southern blot autoradiograph indicated.

References

1. Lieberman H.B., K.M. Hopkins, M. Nass, D. Demetrick, and S. Davey. (1996) A human homologue of the *Schizosaccharomyces pombe rad9+* checkpoint control gene. Proc. Natl. Acad. Sci. USA 93:13890-13895.
2. Al-Khodairy, F., and A.M. Carr. (1992) DNA repair mutants defining G2 checkpoint pathways in *S. pombe*. EMBO J. 15:1343-1350.
3. Rowley, R., S. Subramani, and P.G. Young. (1992) Checkpoint controls in *Schizosaccharomyces pombe*: *rad1*. EMBO J. 11:1335-1342.
4. Lieberman, H.B., K.M. Hopkins, M. Laverty, and H.M. Chu. (1992) Molecular cloning and analysis of *Schizosaccharomyces pombe rad9*, a gene involved in DNA repair and mutagenesis. Mol. Gen. Genet. 232:367-376.
5. Komatsu, K., K.M. Hopkins, H.B. Lieberman, and H.-G. Wang. (2000) *Schizosaccharomyces pombe* Rad9 contains a BH3-like region and interacts with the anti-apoptotic protein Bcl-2. FEBS Letters 481:122-126.
6. Komatsu, K., T. Miyashita, H. Hang, K.M. Hopkins, W. Zheng, S. Cuddeback, M. Yamada, H.B. Lieberman, and H.-G. Wang. (2000) Human homologue of *S. pombe Rad9* interacts with Bcl-2/Bcl-xL and promotes apoptosis. Nat. Cell Biol. 2:1-6.
7. Hang, H., S.J. Rauth, K.M. Hopkins, S.K. Davey, and H.B. Lieberman. (1998) Molecular cloning and tissue-specific expression of Mrad9, a murine orthologue of the *Schizosaccharomyces pombe rad9+* checkpoint control gene. J. Cell. Physiol. 177:241-247.
8. Joyner, A.L. (2000) Gene Targeting: A Practical Approach. 2nd Edition. IRL Press, New York, New York.

Effect of Human *HRAD9* Overexpression on Cell Survival, Growth, and Checkpoint Control

Haiying Hang and Howard B. Lieberman

Although the fission yeast *Schizosaccharomyces pombe* gene *rad9* plays essential roles in DNA repair, cell cycle checkpoint control, and radioresistance, so far the function of its human homologue *HRAD9* has not been shown in human cells. Effort has been made in our laboratory to characterize *HRAD9* function by overexpressing this gene in the human cell lines 293T and H1299. High-level expression of *HRAD9* after transfection kills more than 90% of recipient cells, compared with controls receiving an insertless vector or over-expressing *HRAD1*, *HHUS1* or *GFP*, probably through induction of apoptosis (*1*). Randomly selected *HRAD9*-expressing H1299 cell clones grow significantly more slowly than cells containing an insertless expression vector or expressing *HRAD1, HHUS1* or *GFP*. An investigation of the effects of high level *HRAD9* expression on the cell cycle is in progress.

Normally, cells arrest cycling in G1 or slow down passage from G1 to S phase after irradiation to allow extra time for repair of DNA damage, and this is termed G1 checkpoint control. Most immortalized cells, including H1299, have lost the ability to perform this checkpoint control. Over-expression of *HRAD9* in H1299 cells significantly slows down the G1/S transition following exposure to 10 Gy of gamma rays, while cells containing an insertless vector or expressing GFP do not demonstrate this slowdown (Fig. 1). These results suggest that high level *HRAD9* expression partially restores G1 checkpoint control in H1299 cells.

The proper regulation of cell survival, growth, and cell cycle checkpoint control is essential to ensure genome integrity under both normal and stress conditions. The involvement of *HRAD9* in all of these processes suggests that this gene is an important player in preserving the integrity of the human genome.

Reference

1. K.T. Komatsu, T. Miyashita, H. Hang, K.M. Hopkins, W. Zheng, S. Cuddeback, M. Yamada, H.B. Lieberman, and H.-G. Wang, Human homologue of *S. pombe* Rad9 interacts with BCL-2/BCL-xL and promotes apoptosis through a BH3-like domain. Nature Cell Biology, Vol. 2, pp. 1-6, 2000.

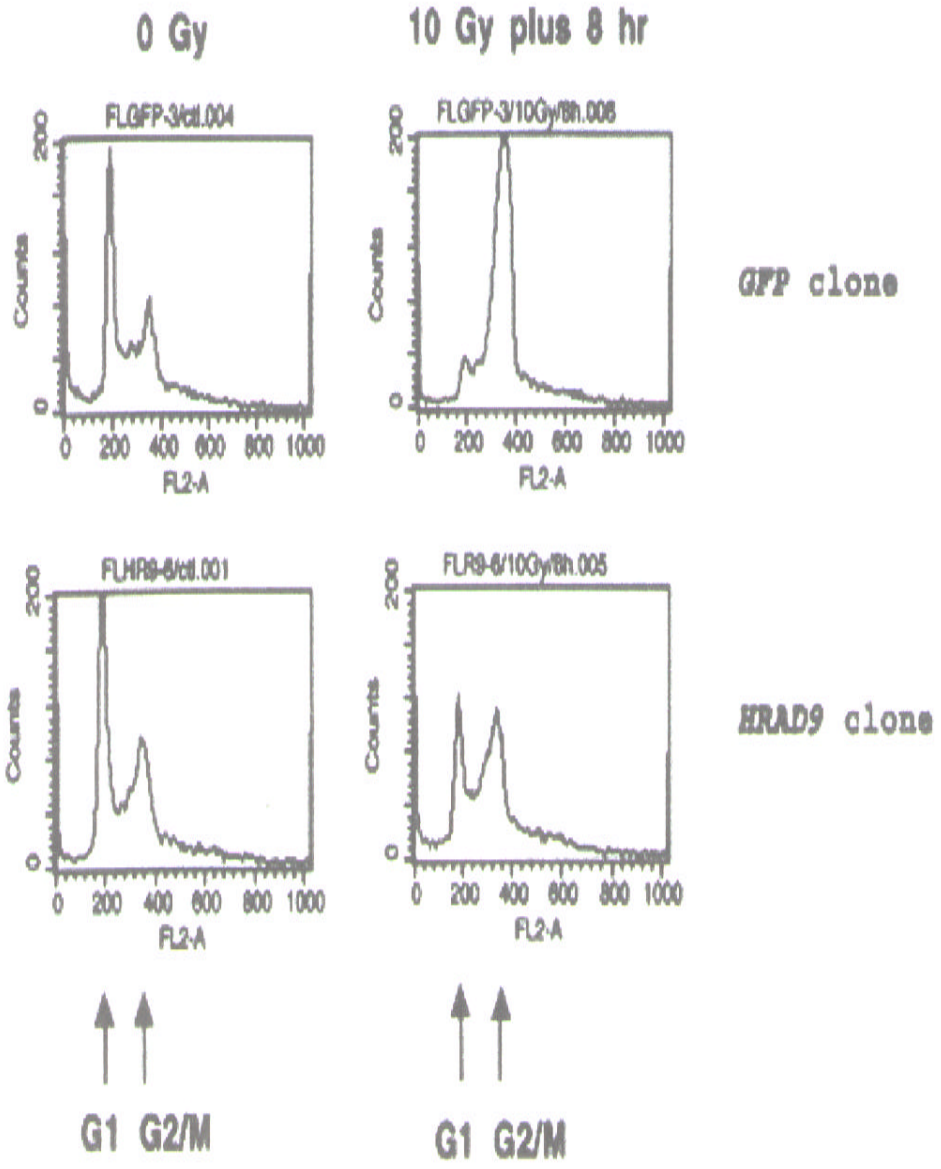

FIG. 1. *HRAD9* overexpression partially restores G1 phase checkpoint control. Cells producing GFP or HRAD9 protein were irradiated with 0 or 10 Gy gamma rays, and then incubated for 8 hr at 37^{O}C followed by fixation and flow cytometric analysis. (FL2-A = DNA content in each cell; Counts = cell number.)

ATM Gene Product is Not Required for DNA-Damage-Dependent Redistribution of PCNA Complex in Human Cells

Adayabalam S. Balajee, M. Prakash Hande, and Charles R. Geard

Proliferating cell nuclear antigen (PCNA) is a processivity factor for DNA polymerase δ and ε, and is an essential protein for replication of chromosomal DNA. PCNA forms a toroidal trimer with replication factor-C (RF-C) and DNA during replication in an ATP-dependent manner followed by loading of DNA polymerase δ and ε onto the complex. The close association of PCNA with kinase complexes involved in cell-cycle machinery indicates that PCNA has a regulatory role in cell-cycle progression. PCNA also participates in the processing of branched intermediates that arise during the lagging strand DNA synthesis. The amount of PCNA in eukaryotic cells is approximately ten fold more than that of polymerase δ and RF-C indicating the possibility that PCNA may have additional roles other than being a processivity factor. In support of this, PCNA has been demonstrated to be an integral component of diverse DNA repair pathways such as nucleotide excision repair (NER), base excision repair (BER) and mismatch repair (MMR). Reconstitution of NER reaction *in vitro* using the purified factors indicates a critical role for PCNA in the resynthesis step of NER. Although studies in yeast and Drosophila (*1*,*2*) have implicated a role for PCNA in transposase-induced strand break repair, its role in double strand break repair in mammalian cells is not known. We have set out to examine the involvement of PCNA complex in the repair of double strand breaks in normal and radiation-sensitive Ataxia telangiectasia (AT) cells synchronized in G1 phase by immunofluorescence and western blot techniques.

Two forms of PCNA exist in the cells: (i) a detergent insoluble trimeric form stably associated with the replicating forks during S-phase, and (ii) a soluble form in quiescent cells in G1 and G2 phases. However, treatment of quiescent cells with DNA-damaging agents like UV-C irradiation, alkylating agents, and hydrogen peroxide trigger the redistribution of PCNA from a soluble to an insoluble chromatin bound complex analogous to that found in S-phase cells. The transition of PCNA from a soluble form into an insoluble form in quiescent cells occurs rapidly after UV and hydrogen peroxide treatments (*3*-*5*), and is considered as a reliable marker for assessing the repair activity mediated by polymerase δ and ε. We have used this approach to determine the involvement of PCNA complex formation in DNA strand break repair in Normal and AT cells.

Normal (NHDF, WI38, MRC-5) and AT (GM5823C, GM2052C) cells were synchronized at G0/G1 phase by growth in low serum (0.5%) containing medium for 2-3 days prior to the treatment with DNA damaging agents. Alternatively, the cells were synchronized at G0/G1 by growing them to confluence, and then maintained in this state for a week. Flow cytometry analysis revealed that more than 95% of the cells were in G1 phase of the cell cycle. Gamma irradiation was done using a ^{137}Cs source delivering a dose rate of 0.98 Gy/min (Gamma Cell 40, Atomic Energy of Canada, Canada). The cells were irradiated either with 5 Gy (immunohistochemistry) or 10 Gy (western blotting)

and incubated for different post-incubation times. For BLM treatment, G1 cells were washed twice with phosphate buffered saline (PBS) containing 1 mM $CaCl_2$ and permeabilized with 40 µg/ml of L- α-Lysophosphatidylcholine (Sigma) in PBS-$CaCl_2$ for 2 min on ice. The solution was carefully removed and the cells were treated with BLM (Calbiochem; 10mU/ml) in serum-free medium for 30 min at 37°C. After treatment, the medium was removed and the cells were washed once with PBS. The cells were incubated in complete medium for different recovery times.

In quiescent cells, DNA damage triggers the transition of PCNA from a soluble into an insoluble chromatin-bound form, and this complex formation is considered to be a reliable marker for the PCNA-mediated repair activity of polymerase δ and ε. In the untreated cells, the major proportion of PCNA was in the soluble form and the PCNA was hardly detectable in them. In cells irradiated with 5 Gy gamma rays, intense PCNA staining was observed in the nuclei of all the cells after 30 min of irradiation. The PCNA complex appeared to form fairly rapidly during irradiation, as the cells fixed immediately after irradiation (irradiation time 5 min; no recovery time) also showed intense chromatin-bound PCNA. Microscopic examination of irradiated cells under high magnification (60×) revealed a nice speckled pattern of PCNA foci throughout the nucleus. The analysis of PCNA in irradiated cells at different post-incubation times revealed that the maximal induction of PCNA complex occurred immediately after irradiation and reached the basal level of unirradiated cells by 6 hr. The PCNA complex formed after irradiation was resistant to high salt extraction (0.5 M NaCl), indicating a very tight binding of PCNA to DNA. The chromatin association of PCNA was lost by DNase I treatment, evidenced by greatly diminished staining of PCNA. The chromatin-bound PCNA gradually declined with increasing post-irradiation times and almost reached the basal level to that of unirradiated cells by 6 hr, reflecting the completion of repair events.

AT cells are extremely radiosensitive and exhibit defects in the regulation of different cell-cycle phases after damage. The gene mutated in AT patients (ATM) is considered to play an important role in the radiation-induced damage-signaling pathway in mammalian cells. We therefore wished to determine whether or not ATM plays a role in regulating the efficiency of PCNA complex formation in response to DNA damage. PCNA complex formation after gamma irradiation was studied in two AT cell lines that carry homozygous mutations. Interestingly, two radiosensitive primary fibroblast cell lines derived from AT patients harboring homozygous mutations in the ATM gene, displayed efficient PCNA complex formation after gamma irradiation. The time-course kinetics of the PCNA complex was examined in Normal and AT cell lines by western blotting. The PCNA complex was readily detectable immediately after irradiation (irradiation time 10 min; no recovery time), and the intensity of PCNA gradually declined with increasing post incubation times (Fig.1). The enrichment of PCNA was maximal during the first 30 minutes after irradiation and reached the basal level by 6 hr. In order to verify the equal loading of proteins, the same membranes were stripped and probed with actin antibody (Fig.1).

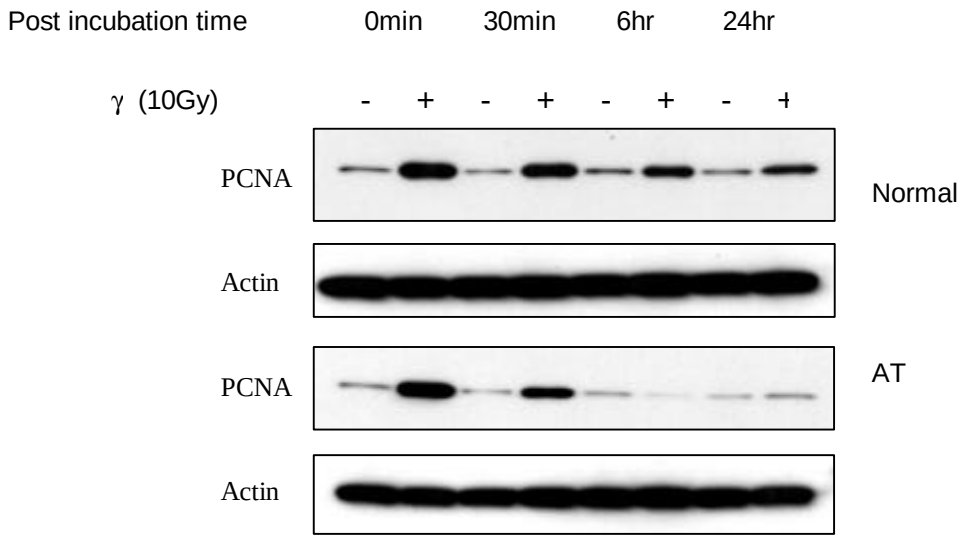

FIG. 1. Time-course kinetics of PCNA complex formation induced by γ radiation in normal and AT cell lines. The normal and AT cells in G1 phase were exposed to 10 Gy of γ radiation and post-incubated for the indicated duration of time. The insoluble proteins were extracted, size fractionated, and transferred to PVDF membrane. The membranes were immunoreacted with PCNA antibody and the signal was detected by enhanced chemiluminescence method. In order to verify equal loading of proteins, the same membranes were stripped off and immunoreacted with actin antibody.

This time-dependent association of PCNA with chromatin appears to coincide with the fast kinetics of DSB repair reported in earlier studies. We have also analyzed the PCNA complex induced by radiomimetic agent, Bleomycin (BLM), which induces predominantly single and double strand DNA breaks. The efficiency and the time course of PCNA complex induced by BLM were found to be identical in both normal and AT cells. Like gamma irradiation, BLM rapidly induced PCNA complex formation in both Normal and AT cells and the complex gradually declined to the basal level seen in control cells by 3 hr after treatment.

A recent study has suggested that the expression level of PCNA is regulated by p53 in rat-embryo fibroblast cells upon exposure to ionizing radiation. In order to examine this possibility, PCNA complex formation was compared with the time-course induction of p53 in both normal and AT cells. In gamma-irradiated normal cells, p53 induction was detectable 30 min after damage and the maximal induction was observed between 2 and 6 hr. On the contrary, PCNA level reached to that of unirradiated cells by 6 h in both normal and AT cells. Our study demonstrates for the first time that the ATM gene product is not required for the PCNA complex formation in response to DNA damage. In AT cells, the p53 induction was greatly attenuated, and the induction of p53 was only moderately detectable at 8 and 24 hr after irradiation. In spite of the abnormal p53 induction, AT cells showed efficient PCNA complex formation immediately after irradiation in a similar manner to that observed in normal cells. Likewise, p53 induction reached the peak at 3 hr after BLM treatment while PCNA at this time point reached the

basal level of control and AT cells failed to show p53 induction. This indicates that the p53-dependent pathway is not critical for DNA-damage-induced PCNA response. It is worthwhile to note that the p53 protein both in the unirradiated and irradiated cells was predominantly found only in the fraction of insoluble proteins.

Evidence for the role of PCNA in DSB repair has been obtained from yeast and *Drosophila*. In this study, we have demonstrated efficient PCNA complex formation in a dose- and time-dependent manner following IR and BLM treatments in normal and AT cells. The precise mechanism of PCNA participation in DSB repair is still unclear. One possibility is that the PCNA may scan the damage in the genomic DNA and effectively mediate repair by recruiting the repair factors involved in both NHEJ and homologous recombination repair pathways. In support of this, we have found that the interaction of PCNA with Ku 70 and 80 heterodimer increases after damage suggesting a role for PCNA in non-homologous end-joining repair pathway of double strand breaks. Consistent with this, PCNA has recently been shown to participate in a damage-signaling pathway. The recruitment of chromatin assembly factor (CAF-1) to single strand breaks and gaps is mediated by PCNA (*6*). This suggests a potential role for PCNA not only during the repair synthesis but also in nucleosome assembly following DNA repair. As PCNA complex formation constitutes an effective damage response to ionizing-radiation-induced DNA strand breaks, we are planning to use PCNA as a marker for our future studies aimed at understanding the biological significance of "bystander effects" by microbeam α-particle irradiation.

References

1. Holmes, A.M. and Haber, J.E. (1999) Cell 96, 415-424.
2. Henderson, D.S. and D.M. Glover (1998) Mutagenesis, 13, 57-60.
3. Balajee, A.S. et al. (1998) Mutat. Res. (DNA Repair) 409, 135-146.
4. Balajee, A.S. et al. (1998) Mutat. Res. 404, 3-11.
5. Balajee, A.S. et al. (1999) Nucleic Acids Res.27, 4776-4782.
6. Moggs J.G. et al. (2000) Mol.Cell Biol. 20, 1206-1218.

A Common Target Gene for p53 and Rb Functions in Apoptosis

Yuxin Yin, Yan Jin (Department of Biochemistry and Molecular Biophysics, College of Physicians & Surgeons, Columbia University), Jianfen Guo, and Eric J. Hall

p53 mediates cell cycle arrest or apoptosis in response to genotoxic stress. The type of p53-mediated cellular responses depends, in part, on the nature of the damage: for example, cell cycle arrest in response to DNA damage by irradiation versus apoptosis following oxidative stress by hydrogen peroxide (H_2O_2). However, the mechanism whereby p53 distinguishes damage signals and directs oxidative cell death is largely unknown. Through cDNA subtraction, we have identified ECK, an epithelial cell receptor protein-tyrosine kinase, as a p53-regulated gene. ECK is a trans-membrane receptor kinase implicated in normal growth and development. In p53 inducible systems, ECK is greatly upregulated upon activation of p53. We found that the expression of ECK mRNA and protein is greatly induced by H_2O_2, which causes apoptosis. In contrast, ECK is not induced following gamma irradiation, which causes G1 arrest. The response of ECK to oxidative stress is p53-dependent because there is no induction of ECK in mouse embryo fibroblasts null for p53 ($p53^{-/-}$MEF) after H_2O_2 treatment. Although ECK expression can be upregulated by p53, the levels of ECK mRNA and protein are not decreased in $p53^{-/-}$ MEFs, suggesting that ECK expression is also controlled by other mechanisms. We observed that the levels of ECK transcript and protein are significantly decreased in Rb-deficient mouse embryo fibroblasts ($Rb^{-/-}$MEF), indicating that Rb is the primary regulator of ECK. This is the first evidence that p53 and Rb share a common target gene. Our observations suggest that ECK is positively regulated by Rb to keep a basal level under normal conditions and that ECK is upregulated by p53 in response to oxidative damage.

To determine whether p53 is a direct regulator of ECK through its binding to consensus sites in the promoter of ECK gene, we have cloned a 2.5-kb regulatory region of the human ECK and our sequencing data revealed two consensus p53 binding sites within a 900-bp region upstream of the transcription start site. We have started functional analysis of this region for p53 binding activity by making reporters for luciferase activity. The luciferase reporters were created by ligating potential binding sequences upstream of the luciferase gene, resulting in luciferase reporters in a pGL3 vector that can be activated by protein-promoter interaction. Our results show that wild-type p53 can activate the promoter segment tested in luciferase assays. We have made a series of deletions of this region to narrow down the region for p53 binding. We observed that p53 can physically bind to one of these two sites, which was determined by gel shift assays. We further demonstrated that p53 activates the luciferase activity of the luciferase reporter in which this p53-binding site was used as the promoter of the luciferase gene.

Since ECK is controlled by these important tumor suppressors and ECK is responsive to genotoxic stress, we hypothesize that ECK plays an important role in signaling apoptosis. To test this possibility, we constructed a mammalian vector expressing human ECK. This plasmid was introduced into a breast cell line MDAMB435 where the ECK is undetectable through Northern analysis. We found that the clones with

high levels of ectopic ECK are highly susceptible to oxidative cell death by apoptosis. Our data demonstrate that ECK is a mediator of apoptosis in the p53 pathway. Identification and characterization of ECK as a foremost receptor for oxidative damage signals may lead to the development of a unique target in gene therapy or more effective chemotherapy for cancer treatment.

The Catalytic Subunit of Telomerase is Expressed in Developing Brain Neurons and Serves a Cell Survival-Promoting Function

Weiming Fu, Michael Killen, and Carten Culmsee (University of Kentucky), Sonu Dhar, Tej K. Pandita, and Mark P. Mattson (Univ. of Kentucky, and the National Institute of Aging, Baltimore, MD)

During adult life, telomeres (nucleoprotein structures that serve a critical function in protecting the ends of chromosomes) progressively shorten in somatic cells. Suppression of such shortening is accomplished by telomerase, which adds a six-base DNA repeat sequence TTAGGG to the ends of chromosomes. Telomerase activity decreases dramatically in association with growth arrest and cell differentiation, and increases in many tumors, suggesting a role for telomerase in preventing cellular senescence. Overexpression of telomerase in cultured fibroblasts extends their lifespan without changing G1 checkpoint (*1*), consistent with a pivotal role for telomerase in preventing cellular senescence. Telomerase consists of several proteins including a 120 kDA catalytic subunit called "TERT" (*2*). TERT is expressed in many tissues during embryonic and early postnatal development, but is greatly decreased thereafter. In tumor cells and non-neuronal cells, TERT is primarily located in the nucleus; the cellular localization and possible functions of TERT in the brain are unknown.

Apoptosis is a form of cell death that involves a stereotyped sequence of biochemical and morphological changes that include mitochondrial membrane depolarization and release of cytochrome C, activation of one or more cystein proteases of the caspase family, and cell shrinkage and nuclear DNA condensation and fragmentation. In the nervous system, apoptosis of neurons occurs naturally during development, and may also occur in several different neurodegenerative disorders, including Alzheimers's disease and Parkinson's disease. Cancer cells that have high levels of telomerase activity exhibit increased resistance to apoptosis, and very recent findings suggest that telomerase and telomere-associated proteins can prevent apoptosis in several types of tumor cells, including those of neural origin. However, the role of TERT in such resistance to apoptosis is unclear, and the possible roles of TERT in neuronal death in the nervous system are unknown.

Telomerase linked to cell immortalization and cancer, has been thought not to be expressed in postmitotic cells. We now report that telomerase activity, and its essential catalytic subunit telomerase reverse transcriptase (TERT) are expressed in neurons in the brains of rodents during embryonic and early postnatal development and are subsequently downregulated. Suppression of TERT expression in embryonic hippocampal and cortical neurons in culture increases their vulnerability to apoptosis and excitotoxicity. Overexpression of TERT in PC12 cells suppresses apoptosis induced by trophic factor withdrawal. TERT exerts its anti-apoptotic action at an early stage of the cell death process prior to mitochondrial dysfunction and caspase activation. TERT may serve a neuron survival-promoting function in the developing brain, and downregulation of TERT

in the adult brain may contribute to increased neuronal vulnerability in various age-related neurodegerative disorders.

References

1. Vaziri H., Squire J.A., Pandita T.K., Bradley G., Kuba R.M., Nolan G.P., Zhang H., Gulyas S., Hill R.P. and Benchimol S. (1999) Mol. Cell. Biol. **19**: 2373-2379.
2. Linger J., Hughes T.R., Shevchenko A., Mann M., Lundbald V. and Cech T.R. (1997). Science **276**: 561-567.

Regulation of the hTERT Telomerase Catalytic Subunit by c-*Abl* Tyrosine Kinase

S. Kharbanda and V. Kumar (Harvard Medical School, Boston, MA), Sonu Dhar, P. Pandy, C. Chen, P. Majumder, and Z-M. Yuan (HMS), Y. Whang (University of North Carolina), W. Strauss (HMS), Tej K. Pandita, and D. Weaver and D. Kufe (HMS)

Telomerase is a ribonucleoprotein complex that elongates telomeres. Telomeres consist of repetitive (TTAGGG) sequences that are maintained by the multi-subunit telomerase ribonucleoprotein. Telomerase consists of an RNA, which serves as template for the sequence tracts, and a catalytic subunit that functions in reverse transcription of the RNA template. Cells deficient in telomerase have short telomeres as a consequence of failure to synthesize telomeric DNA ends. Cloning and characterization of the human catalytic subunit of telomerase (hTERT) has supported a role in cell transformation. The demonstration that expression of telomerase activity can extend the lifespan of normal human cells has suggested that decreases in telomere length contributes to senescence. Studies in mice lacking telomerase RNA have also shown that telomeres function in maintaining genomic stability. Because telomerase activity is low in most somatic cells, telomeres shorten as cells progress through replicative cycles. Telomere shortening in cells continues until crisis and the escape of immortal cells that have reactivated telomerase. Other studies have shown that telomerase activity is detectable in human tumors. Moreover, recent work has shown that ectopoic expression of hTERT in combination with two oncogenes results in tumorigenesis of normal human epithelial and fibroblast cells. How telomerase activity is regulated, however, is largely unknown.

The ubiquitously expressed c-*Abl* protein tyrosine kinase is tightly regulated in cells. c-*Abl*, associated with the product of the gene mutated in Ataxia telangiectasia (ATM), which is a member of phosphotidylinositol (PI) 3-kinase-like enzymes involved in regulation of the cell cycle, recombination, telomere metabolism, and the DNA damage response. Because c-*Abl* is activated by DNA double-strand breaks and proteins involved in the repair of these lesions function in telomere control, we investigated whether c-*Abl* interacts with telomerase. We found hTERT associates directly with the c-*Abl* protein tyrosine kinase. We also found that c-*Abl* phosphorylates hTERT and inhibits hTERT activity. Moreover, our findings demonstrate that exposure of cells to ionizing radiation induces tyrosine phosphorylation of hTERT by a c-*Abl*-dependent mechanism. Thus c-*Abl* functions as a negative regulator of hTERT activity. The functional significance of the c-*Abl* -hTERT interactions is supported by the demonstration that cells deficient in c-Abl show telomere lengthening. The c-*Abl* null mice have pronounced defects in spermatogenesis at the pachytene stage. The c-*Abl* protein is localized at the ends of pachytene chromosomes, and therefore may also interact with telomerase in meiotic cells. Our finding of telomere lengthening in c-*Abl*-deficient cells and the functional interactions between c-*Abl* and hTERT support a role for c-*Abl* in the regulation of telomerase function.

Chronic Activation of Damage-Responsive Functions is Reduced by a-Lipoic Acid in Ataxia Telangiectasia Cells

Magtouf Gatei (Queensland Cancer Fund Research Laboratories, Australia), Dganit Shkedy (Tel Aviv University, Israel), Kum Kum Khanna (QCFRL), Tamar Uziel and Yosef Shiloh (TAU), Tej K. Pandita, Martin F. Lavin (QCFRL), and Galit Rotman (TAU)

The human genetic disorder Ataxia telangiectasia (A-T) is characterized by neurodegeneration, immunodeficiency, premature aging, telangiectases, genomic instability, cancer predisposition, and extreme sensitivity to ionizing radiation. A hallmark of A-T cells is hypersensitivity to agents that cause oxidative damage by generating reactive oxygen species (ROS), including ionizing radiation (IR) and various radiomimetic drugs. This hypersensitivity can be accounted for, at least in part, by failure to repair a significant fraction of DNA double strand breaks. In addition, these cells are impaired in their ability to activate radiation-induced signal transduction pathways, most notably those that control cell-cycle checkpoints. ATM, the gene responsible for A-T, seems to play a central role in sensing oxidative damage to DNA and in subsequent activation of a signaling network, leading to repair of the damage and cellular survival.

Constitutive activation of certain cellular functions has been reported occasionally in A-T cells. Singh and Lavin (*1*) described the constitutive presence in the nucleus of A-T cells of a DNA-binding protein that is present in the cytoplasm of normal cells, but migrates to the nucleus in response to treatment by agents that generate free radicals. Abnormal elevation of interferon-β (IFN-β) and IFN-β-inducible genes in A-T cells was also reported. The amount of p21 associated with cyclin A/cdk2 and cyclin B/cdc2 was higher in A-T cells than in controls. Basal levels of Gadd45 protein, another gene activated by p53, were also found elevated, and the phosphorylated form of cdc2 was more abundant in A-T fibroblasts. Hyperphosphorylation of Rb and constitutive activation of E2F-1 in A-T cells were also reported.

Based on the above-mentioned observations, we hypothesized that the chronic activation in ATM-deficient cells of pathways responsive to agents that generate ROS could indicate a tenuous state of oxidative stress in these cells. This prediction is supported by recent studies showing markers of oxidative stress in organs of ATM-deficient mice (*2*) and in cell lines derived from A-T patients (*3*).

Cells derived from A-T patients are hypersensitive to ionizing radiation and radiomimetic agents, both of which generate reactive oxygen species capable of causing oxidative damage to DNA and other macromolecules. We describe in A-T cells constitutive activation of pathways that normally respond to genotoxic stress. Basal levels of p53 and $p21^{WAF1/CIPI}$, phosphorylation on serine 15 of p53, and the Tyr15-phosphorylated form of cdc2 are chronically elevated in these cells. Treatment of A-T cells with the antioxidant α-lipoic acid significantly reduced the levels of these proteins, pointing to the involvement of reactive oxygen species in their chronic activation. These

findings suggest that the absence of functional ATM results in a mild but continuous state of oxidative stress.

Chronic oxidative stress could account for several features of the pleiotropic phenotype of A-T patients and ATM-/- mice. These include the preferential loss of particularly sensitive cells such as neurons and thymocytes, premature aging, and the occurrence of telangiectases in the eyes and sun-exposed areas of the skin of A-T patients. Thus, reducing this chronic stress could possibly alleviate some of the features of this disease.

References

1. Singh SP and Lavin MF. (1991) Mol. Cell. Biol., **10**: 5279-5285.
2. Barlow C, Dennery PA, Shigenaga MD, Smith MA, Morrow JD, Roberts LJ, Wynshaw-Boris A and Levine RL. (1999) Proc. Natl. Acad. Sci. USA, **96**: 9915-9919.
3. Watters D, Kedar P, Spring K, Bjorkman J, Chen P, Gatei M, Birrell G, Garrone B, Srinivasa P, Crane DI and Lavin MF. (1999). J. Biol. Chem., **274**: 34277-34282.

Meiotic Telomere Distribution and Sertoli Cell Nuclear Architecture is Altered in *Atm*- and *Atm*/*p53*-Deficient Mice

Harry Scherthan and Martin Jerratsch (University of Kaiserslautern, Germany), Sonu Dhar, Y. Alan Wang (Harvard Medical School, Boston, MA), Stephen P. Goff, and Tej K. Pandita

Ataxia telangiectasia (A-T) is a rare human recessive autosomal disorder with a pleiotropic phenotype, specifically including progressive neurological degeneration, telangiectasia, and is often associated with premature aging, reduced size, immuno-deficiency, sensitivity to ionizing radiation, cancer predisposition, and infertility. Individuals with Ataxia telangiectasia as well as *Atm*$^{-/-}$ mice are predisposed to cancer and are infertile due to spermatogenesis disruption during first meiotic prophase. Mice mutated in the homologue of ATM (ataxia telangiectasia mutated) gene (*Atm*) display similar pleiotropic defects (*1*). The ATM protein belongs to a growing family of phosphatidylinositol-3 (PI-3 K) related kinases and seems to play a role as an intrinsic part of the cell-cycle machinery that surveys genomic integrity, cell cycle progression, and processing of DNA damage. It shows similarity to several yeast and mammalian proteins involved in meiotic recombination and cell cycle progression, namely the products of *MEC1* in budding yeast and *rad*3^{+} of fission yeast (*2*), and the TOR proteins of yeast and mammals. Besides its role in the mitotic cell cycle and development, the ATM protein and its relative ATR (ATM and rad3 related) have been regarded as important components in the machinery monitoring progression of meiotic recombination, double-strand break (DSB) repair, and homologue pairing (60, 69), which is in agreement with the location of *Atm* throughout meiotic chromatin (*3*-*4*). Detection and signaling of DNA damage is possibly mediated through downstream targets of ATM like c-*Abl*, Chk1, Chk-2, and Rad51 proteins. Furthermore, MEC1, the yeast homologue of the ATM PI3 kinase, is known to exert checkpoint function in the mitotic and meiotic cell cycle and its absence mediates a defect in synapsis. MEC1 is required for phosphorylation of replication protein A (Rpa) as a response to radiation induced DNA damage. Rpa has been shown to interact with Rad51, which plays an important role in meiotic recombination and localizes to meiotic recombination complexes. Consistent with a role of ATM in meiosis, individuals with Ataxia telangiectasia display gonadal atrophy and spermatogenetic failure, a phenotype which is mirrored by *Atm*-deficient mice.

Spermatogenesis in male *Atm*$^{-/-}$ mice is disrupted during earliest prophase I leading to chromosome fragmentation and spermatocyte degeneration during zygotene (*5*). Aberrant zygotene-equivalent spermatocytes I of *Atm*-deficient mice frequently display a nuclear architecture of bouquet cells (*6*), which poses the question whether *Atm* inactivation stalls meiotic telomere movements at the cluster site. Here, we investigate telomere distribution in spermatocytes I of *Atm*/*p53* double-knockout mice which show a partial rescue of progression through first meiotic prophase (*7*). In this double mutant we observed a dramatic increase of the frequency of spermatocytes I with bouquet topology and show that a small number of mid-late pachytene and diplotene spermatocytes, as identified by the expression of the testis-specific histone H1 (H1t) and the synaptonemal complex protein SCP3, have telomeres dispersed over the nuclear periphery.

Atm$^{-/-}$ spermatocytes frequently display aberrant synapsis and clustered telomeres (bouquet topology). Here, we usedtelomere FISH and immunofluorescence (IF) staining of SCP3 and testes-specific histone H1 (H1t) to spermatocytes of *Atm* and *Atm*/*p53*-deficient mice and investigated whether gonadal atrophy in *Atm*-null mice is associated with stalling of telomere motility in meiotic prophase. SCP3/H1t IF revealed that most *Atm*$^{-/-}$/*p53*$^{-/-}$ spermatocytes degenerated during late zygotene, while a few progressed to pachytene and diplotene and some even beyond metaphase II, as indicated by the presence of a few round spermatids. In *Atm*$^{-/-}$/*p53*$^{-/-}$ meiosis the frequency of spermatocytes I with bouquet topology was elevated 72-fold. Bouquet spermatocytes with clustered telomeres were generally void of H1t signals, while mid-late pachytene and diplotene *Atm*$^{-/-}$/*p53*$^{-/-}$ spermatocytes displayed expression of H1t, and showed telomeres dispersed over the nuclear periphery. Thus, it appears that meiotic telomere movements occur independently of ATM signaling. *Atm* inactivation more likely leads to accumulation of spermatocytes I with bouquet topology by slowing progression through initial stages of first meiotic prophase and anensuing arrest and demise of spermatocytes I. Sertoli cells (SECs), which contribute to faithful spermatogenesis, in the *Atm*-mutants were found to frequently display numerous heterochromatin- and telomere clusters – a nuclear topology which resembles that of immature SECs. However, *Atm*$^{-/-}$ SECs exhibited a mature Vimentin and cytokeratin 8 intermediate filament expression signature. Upon IF with ATM Abs we observed ATM signals throughout the nuclei of human- and mouse SECs, spermatocytes I and haploid round spermatids. ATM, but not H1t, was absent from elongating spermatid nuclei. *Atm* disruption causes an immature nuclear architecture/heterochromatin distribution in Sertoli cells, the supportive somatic cell lineage of the seminiferous epithelium; they were found to display strong IF Atm signals in their chromatin. Atm was detected in the chromatin of human Sertoli cells, mouse and human spermatocytes I and developing spermatids. Thus, ATM appears to be removed from spermatid nuclei prior to the occurrence of DNA nicks which emanate as a consequence of nucleoprotamine formation.

References

1. Barlow, C., S. Hirotsune, R. Paylor, M. Liyanage, M. Eckhaus, F. Collins, Y. Shiloh, J. N. Crawley, T. Ried, D. Tagle, and A. Wynshaw-Boris. 1996. Atm-deficient mice: a paradigm of ataxia telangiectasia. Cell 86:159-171.
2. Bergmann, M., and S. Kliesch. 1994. The distribution pattern of cytokeratin and vimentin immunoreactivity in testicular biopsies of infertile men. Anat.Embryol .(Berl) 190:515-520.
3. Barlow, C., M. Liyanage, P. B. Moens, M. Tarsounas, K. Nagashima, K. Brown, S. Rottinghaus, S. P. Jackson, D. Tagle, T. Ried, and A. Wynshaw-Boris. 1998. Atm deficiency results in severe meiotic disruption as early as leptonema of prophase I. Development 125:4007-4017.
4. Gasior, S. L, A. K. Wong, Y. Kora, A. Shinohara, and D. K. Bishop. 1998. Rad52 associates with RPA and functions with rad55 and rad57 to assemble meiotic recombination complexes. Genes Dev. 12:2208-2221.
5. Xu, Y., and D. Baltimore. 1996. Dual roles of ATM in the cellular response to radiation and in cell growth control. Genes Dev. 10:2401-2410.
6. Pandita, T. K., C. H. Westphal, M. Anger, S. G. Sawant, C. R. Geard, R. K. Pandita, and H. Scherthan. 1999. Atm inactivation results in aberrant telomere clustering during meiotic prophase. Mol Cell Biol 19:5096-5105.
7. Barlow, C., M. Liyanage, P. B. Moens, C. X. Deng, T. Ried, and A. Wynshaw-Boris. 1997. Partial rescue of the prophase I defects of Atm-deficient mice by p53 and p21 null alleles. Nat Genet 17:462-466.

Characterization of Ataxia Telangiectasia Fibroblasts with Extended Lifespan through Telomerase Expression

Lauren D. Wood and Tanya L Halvorsen (University of California San Diego, La Jolla, CA), Sonu Dhar, Joseph A. Baur (University of Texas Southwestern Medical Center, Dallas, TX), Raj K. Pandita (Albert Einstein College of Medicine, Bronx, NY), Woodring E. Wright (UTSMC), M. Prakash Hande, Gloria M. Calaf, Tom K. Hei, Fred Levine (UCSD), Jerry W. Shay (UTSMC), Jean J. Y. Wang (UCSD) and Tej K. Pandita

Ataxia-telangiectasia (A-T) is an autosomal recessive disease characterized by progressive cerebellar degeneration, immunodeficiencies, genomic instability, and gonadal atrophy. A-T patients are hypersensitive to ionizing radiation and have an elevated cancer risk. Cells derived from A-T patients require higher levels of serum factors, exhibit cytoskeletal defects, and undergo premature senescence in culture. The premature senescence of primary cells from A-T patients makes it difficult to study the cellular and molecular basis of A-T defects in culture. Likewise, primary cells from the *Atm*-knockout mice have been difficult to culture in that they undergo arrest almost immediately upon explantation from the mouse. Previously, several lines of immortalized human A-T cells were created through the expression of SV40 T-antigen or infection with human EBV. However, the presence of the oncoproteins has complicated the interpretation of the data obtained. The ATM gene product has a role in cell-cycle progression following irradiation; however, the majority of the oncoproteins utilized to immortalize cell lines block the function of the p53 and Rb genes, both critical in the establishment of cell-cycle checkpoint. Furthermore, previous studies have implicated ATM in activating the transcription factor NF-κB following exposure to ionizing radiation. However, a recent report has shown that IR does not activate NF-κB in primary A-T cells, and attributed the previous finding to the effect of T-antigen (*1*). These controversies emphasize the importance of using primary A-T-deficient cells to study ATM-regulated pathways. Towards this end, we tested whether A-T patient cells can be immortalized through the expression of hTERT.

Expression of hTERT in human Ataxia telangiectasia fibroblasts expands lifespan

Primary fibroblasts derived from Ataxia telangiectasia individuals have a severely limited lifespan in cell culture as compared to fibroblasts from normal individuals. Ectopic expression of the human telomerase reverse transcriptase (hTERT), a subunit of telomerase, can immortalize normal human fibroblasts (*2*). We determined the effects of ectopic expression of hTERT in primary A-T fibroblast cell strains. Stable GM02052 and GM05823 cell populations (hTERT+) were generated by infection of GM02052 cells at 36 PD and GM05823 at 40 PD with hTERT-expressing retrovirus. GM02052 and GM05823 cells were also infected with control empty retroviral construct. These cells were selected and expanded as polyclonal populations. Expression of hTERT protein was assayed by immunostaining with a rabbit polyclonal antibody. No staining or telomerase activity was observed in the parental strain expressing the control construct while positive staining was seen in the hTERT infected cells. Telomerase activity measured by the

telomeric repeat amplification protocol --ELISA-- was absent in the uninfected or vector control infected cells but present following hTERT-infection both prior to and following drug selection (36 and 40 PD, respectively). GM02052 and GM05823 hTERT+ cells remained positive for telomerase activity after expansion, and these cells have exceeded 150 PD. The level of telomerase activity in A-T fibroblasts with ectopic expression of hTERT appeared three-fold higher that of normal fibroblasts with ectopically expressing hTERT.

Cells infected with control or hTERT-expressing viruses were passaged continuously following drug selection. Within 15 PD, uninfected and control-infected (hTERT-) GM02052 and GM05823 cells ceased proliferating. The cells increased in size and exhibited an altered morphology, consistent with changes associated with replicative senescence. Moreover, the majority of the control cells, (hTERT-) GM02052 clones (PD 42, PD 40), stained strongly positive for senescence-associated β-galactosidase activity. The level of SA-β-Gal staining was similar to that seen in senescent normal human fibroblasts. In contrast, hTERT-expressing A-T and normal cells that were at similar or greater population doublings proliferated to confluency, maintained their original morphology, and demonstrated much less SA-β-Gal activity.

To determine whether SA-β-Gal levels in the different cell populations correlated with cell growth, cells were labeled for 48 hours and the percentage of cells incorporating BrdU determined. Greater than 75% of both normal and A-T fibroblasts expressing hTERT incorporated BrdU at PD 60, indicating that the majority of the cultures were actively growing. In contrast, less than 20% of the control GM02052 at PD 50 and 26% of the control GM05823 cells incorporated BrdU, indicating cessation of growth. Similar to the hTERT negative parental A-T fibroblasts, we found that the hTERT+ GM02052 and GM05823 cell lines grew more slowly than the hTERT+ normal fibroblasts. This slower growth pattern is also reflected in the lower percentage of cells incorporating BrdU, and in the occasional appearance of SA-β-Gal cells. Nevertheless, the hTERT+ GM02052 cells were still proliferating after PD 150, whereas the control GM02052 cells had reached complete senescence by PD 54.

Telomere lengthening in A-T cells

The effect of exogenous hTERT on A-T cells was determined by measuring telomere lengths (TRF) in hTERT+GM02052 and hTERT+GM05823 cells, and compared to near senescence and senescent control cells. The TRF size of GM02052 and GM05823 at approximate PD 40 (time of infection) is 7.0 kb and 7.8 kb respectively, consistent with the previous reports (*3*). Telomeres progressively shortened in control cells, reaching an average TRF length of 5.0 to 6.0 kb at near senescence. However, expression of hTERT prevented most of this shortening, yielding the average TRF length of 6.7 and 5.9 Kb in two separate clones of GM02052 cell lines at PD 58 and PD 95. A similar phenomenon was observed in several clones of GM05823 expressing hTERT, yielding the average TRF length of 12.7 kb and 7.9 Kb in two separate clones of GM05823 cell line at PD 75. The telomere lengthening in hTERT+ A-T cells is similar to the increase observed in hTERT+ normal fibroblasts. These results demonstrate that ectopically expressed hTERT is able to

maintain or extend the endogenous telomeres in Ataxia telangiectasia fibroblasts and that telomeres are maintained at later passages.

Since accelerated loss of telomeres is reported in A-T cells, we were interested in determining whether expression of hTERT could compensate for this loss. By Southern blotting, we found differences in average TRF sizes when comparing DNA derived from cells with and without ectopic expression of hTERT in A-T cells. However, this analysis only yields an approximation of the population of TRFs generated, and does not monitor ends of individual chromosomes. We specifically examined this question by performing *in situ* hybridization, which allows us to determine the telomeres of individual chromosome ends. FISH for telomeric repeats in metaphase cells was done by using a telomere-specific Cy3-labeled $(CCCTAA)_3$ peptide nucleic acid probe. Fifty metaphase chromosome spreads from cells with (80 PD) and without (38 PD) hTERT were included and analyzed. A higher proportion of chromatid ends in A-T cells without hTERT (about 8% per metaphase) have less telomere specific fluorescent signals as compared to the A-T cells with hTERT.

Chromosome end-to-end associations

To determine whether the activation of telomerase by ectopic expression of hTERT influences the stability of telomeres, we examined the frequency of cells with telomere associations in A-T fibroblasts with and without hTERT. A-T fibroblasts (GM05823) with hTERT expression have 0.13 telomere associations per metaphase, compared to GM05823 without hTERT, which has 0.135 telomere associations per metaphase. Another A-T fibroblast cell line (GM02052) has 0.08 telomere associations per metaphase, compared to 0.075 telomere associations per metaphase in GM02052 without hTERT. These observations suggest the telomere end-association defect in A-T fibroblasts might not be a direct result of short telomeres since it was not corrected by hTERT.

Effect of hTERT expression on proliferation markers and tumorigenesis in A-T fibroblasts

Biochemical studies have established an association between telomere maintenance by hTERT and cellular immortalization. In most transformed cell populations, upregulation of telomerase is required for immortality, and telomerase activity is detected in most human tumors. Thus, we determined the influence of hTERT on the expression of seven different proteins that are linked with cell proliferation and oncogenesis in A-T and normal cells. We found that there are no significant differences in the expression of PCNA, an accessory factor of DNA polymerase that reflects the proliferative activity of the cells. However, there is a significant increase in protein levels for ER, PgR, HSP and ErbB-3, both in A-T and normal fibroblasts with ectopic expression of hTERT compared to fibroblasts without hTERT expression, suggesting upregulation of these genes might be required for immortalization, but not for the tumorigenic transformation. The levels of the tumor-suppressor genes like Tsg101 and ErbB-2 were similar in A-T and control cells with and without ectopic expression of hTERT gene.

We investigated the tumorigenic potential of both of the hTERT+ A-T fibroblast cell lines by injection of $2x10^6$ cells into the leg muscles of four Nu/Nu mice. No tumors were formed by hTERT+A-T cells after 120 days, where as RKO cells produced tumors.

Defective cell-cycle checkpoints in response to ionizing radiation are still present in hTERT+ A-T cells

A hallmark characteristic of A-T cells is the loss of DNA-damage-induced cell-cycle checkpoints. To determine whether telomerase activity affects the DNA-damage-induced cell-cycle response in A-T fibroblasts, hTERT+ GM02052 cells were exposed to 8 Gy of ionizing radiation. Fourteen hours following exposure, cell-cycle analysis was performed. Normal fibroblasts expressing hTERT showed a significant decrease in S-phase entry indicating G1 arrest, while there was not a significant decrease in S-phase entry in irradiated hTERT+ GM02052 cells. Similar results were observed in the hTERT+ GM05823 cells following a 2-Gy radiation dose. The loss of the G1 checkpoint seen is similar to the parental GM02052 and GM05823 cells, indicating that this phenotype is preserved in hTERT immortal A-T cells.

In addition to the G1 checkpoint, ionizing radiation (IR) causes a transient inhibition of DNA replication. Cells from A-T individuals and *Atm*-deficient mouse fibroblasts exhibit radioresistant DNA synthesis (RDS) (*4-5*). Normal fibroblasts expressing hTERT showed an inhibition in DNA synthesis similar to their parental cells following IR exposure. In contrast, both the parental and hTERT+A-T cells (GM02052 and GM05823) showed radioresistant DNA synthesis. These results indicate that hTERT expression extends the proliferative lifespan of A-T cells without altering the fundamental phenotype, as characterized by loss of IR-induced cell cycle checkpoints.

Chromosomal damage and radiation sensitivity in hTERT+GM02052 and hTERT +GM05823 fibroblasts

The effect of telomerase activity on ionizing-radiation-induced chromosome damage repair was examined in A-T fibroblasts with and without hTERT. G1 chromosome damage was examined after irradiating contact-inhibited cells with 1 Gy of gamma rays. A-T fibroblasts (GM02052 and GM05823) with and without hTERT showed chromatid- as well as chromosome-type aberrations; however, control cells showed only chromosome-type aberrations. No difference in the G1 type of aberrations was found between the A-T fibroblasts with or without hTERT. The levels of chromosome aberrations in the separate A-T cell lines were four-fold higher than the normal cells, indicating the defective G1 repair is not corrected in A-T cells by the ectopic expression of hTERT.

To determine the influence of hTERT on the G2 type of chromosome damage after ionizing-radiation treatment, the level of chromosomal damage was examined. The presence of telomerase had no effect on the numbers of chromosomal breaks or gaps. Normal fibroblasts repaired the initial damage rapidly, as shown by the reduction in chromosomal breaks and gaps by 90 minutes post irradiation. In contrast, A-T fibroblasts did not repair the damage, and the presence or absence of exogenous hTERT did not

affect the outcome. These results indicate that the chromosomal repair following IR is still defective in hTERT expressing A-T fibroblasts.

Cells derived from A-T patients are more sensitive to ionizing radiation as compared to cells from normal patients. Both parental and hTERT expressing A-T fibroblasts (GM02052 and GM05823) were exposed to various doses of ionizing radiation. The presence of hTERT slightly improved the survival of the GM02052 cells but not of GM05823. This probably reflects the fact that the GM02052 cells were assayed only 8 to 10 doublings prior to senescence, when clonogenicity in the absence of treatment is already compromised in the hTERT- control cells. The mild change in clonogenicity in the irradiated hTERT-expressing cells probably reflects the reduction of the signal from too-short telomeres rather than any fundamental change in the damage-response pathway. These results demonstrate that expression of telomerase does not significantly influence the radiosensitivity of A-T-patient fibroblasts.

We have demonstrated that expression of the catalytic subunit of telomerase (hTERT) in primary A-T-patient fibroblasts can rescue the premature senescence phenotype. Ectopic expression of hTERT does not rescue the radiosensitivity or the telomere fusions in A-T fibroblasts. The hTERT+AT cells also retain the characteristic defects in cell-cycle checkpoints, and show increased chromosome damage before and after ionizing radiation. Although A-T patients have an increased susceptibility to cancer, the expression of hTERT in A-T fibroblasts does not stimulate malignant transformation. These immortalized A-T cells provide a more stable cell system to investigate the molecular mechanisms underlying the cellular phenotypes of Ataxia telangiectasia.

References

1. Ashburner B.P., Shackelford R.E., Baldwin Jr A.S., and Paules R.S. (1999). *Cancer Res.*, **59**: 5456-5460.
2. Bodnar A.G., Ouellette M., Frolkis M., Holt S.E., Chiu C.P., Morin G.B., Harley C.B., Shay J.W., Lichtsteiner S., and Wright W.E. (1998). *Science*. **279**: 349-352**.**
3. Smilenov L. B., Dhar S., and Pandita T.K. (1999). *Mol Cell Biol*. **19**: 6963-6971
4. Barlow C., Hirotsune S., Paylor R., Liyanage M., Eckhaus M., Collins F., Shiloh Y., Crawley J.N., Ried T., Tagle D., and Wynshaw-Boris A. (1996). *Cell*. **86**:159-171.
5. Painter R. B., and Young B. R. (1980). *Proc Natl Acad Sci U S A*. **77**: 7315-7317.

Adenovirus-Mediated Antisense *ATM* Gene Transfer Sensitizes Prostate Cancer Cells to Ionizing Radiation

Zuoheng Fan and Prabir Chakravarty (Albert Einstein College of Medicine, Bronx, NY), Alan Alfieri (Beth Israel Medical Center, NY), Tej K. Pandita, Bhadrasain Vikram and Chandan Guha (AECOM)

Prostate cancer is the most common cancer in men and the second most common cause of death. Radiation therapy (RT) is frequently used in all stages of prostate cancer – from early, organ-confined, to advanced metastatic disease. High doses of RT (>70 Gy) are required to eradicate even early cancer, and can lead to acute and/or chronic side effects such as urethritis, proctitis, and erectile dysfunction, due to irradiation of the neighboring structures. Treatment failure after radiation therapy of prostate cancer (PC) could be a significant problem. Persistence of local disease following radiation is a significant issue in the management of this disease, as there remains a continuing potential for symptomatic local recurrence or metastatic seeding. A method of increasing the intrinsic radiosensitivity of the prostate cancer cells may allow eradication of the cancer with lower doses of RT, with resultant decrease in the side effects and improved quality of life.

Our objective is to design genetic radiosensitizing strategies for treatment of PC. Cells from individuals with the genetic disorder Ataxia telangiectasia (AT) are hypersensitive to ionizing radiation (IR). Ataxia telangiectasia is an autosomal recessive cancer-prone disorder that is characterized by pleiotropic phenotype including progressive cerebellar ataxia, neuronal degeneration, telangiectasia, hypogonadism, growth retardation, immune deficiency, defective telomere metabolism, and extreme hypersensitivity to ionizing radiation. The AT gene product, ATM, is a large 370-kDa protein that contains a COOH-terminal domain (~ 400 residues) homologous to the catalytic subunits of phosphatidylinositol 3-kinases and that encodes a protein kinase activity specific for serine and threonine residues. Disruption of the *Atm* gene in transgenic mice produced many features of the AT phenotype including exquisite sensitivity to low doses of IR. Inactivation of ATM function influences telomere metabolism (*1-3*). Recent studies have shown that ATM activates key regulators of multiple signal transduction pathways and mediates the efficient induction of the signaling network responsible for cell-cycle arrest and repair of IR-induced DNA damage, resulting in cellular recovery and survival following exposure to IR. We therefore examined whether attenuation of the AT gene product, ATM, in PC cells could result in an increased intrinsic radiosensitivity. A p53-mutant PC cell line, PC-3 was infected with adenoviral vectors, expressing antisense ATM RNA to various domains of the *ATM* gene. Immunoblot analyses of cellular extracts from antisense ATM-transfected PC-3 cells showed attenuated expression of the ATM protein within two days of viral infection. Compared to cells infected with an adeno-ß-galactosidase vector, antisense ATM-transfected PC-3 cells showed aberrant control of S-phase cell-cycle checkpoints after exposure to IR. Under these conditions, the

intrinsic radiosensitivity of the PC-3 cells was enhanced. Antisense *ATM* gene therapy could, therefore, serve as a paradigm for strategies that target the cellular survival mechanisms of an irradiated tumor cell and may provide therapeutic benefit to patients undergoing radiation therapy for prostate cancer.

References

1. Smilenov L.B., Morgan S.E., Mellado W., Sawant S.G., Kastan M.B. and PanditaT.K. (1997) Oncogene 15: 2659-2666.
2. Smilenov L.B., Dhar S., and Pandita T.K. (1999) Mol. Cell. Biol. 19:6963-6971.
3. Scherthan H., Jerratsch M., Dhar S., Wang Y.A., Goff S.P. and Pandita T.K. (2000) Mol. Cell. Biol.20:7773-7783.

Regulation of DNA-Dependent Protein Kinase Activity by Ionizing- Radiation-Activated *Abl* Kinase is an ATM-Dependent Process

Sanjeev Shangary (University of Pittsburgh Medical Center, Pittsburgh, PA), Kevin D. Brown and Aaron W. Adamson (Louisiana State University, LO), Scott Edmonson (Boston University, Boston, MA), Bobby Ng (UPMC), Tej K. Pandita, Jack Yalowich (UPMC), Guillermo E. Taccioli (BU), and R. Baskaran (UPMC)

Ionizing radiation (IR) exposure results in DNA damage, which activates a number of signaling pathways that serve, for example, to activate DNA repair mechanisms, halt cell cycle progression, and/or trigger advancement into apoptosis. Intensive efforts focused on elucidating the molecular nature of these pathways have identified many factors that participate in IR-induced DNA-damage response. Among those are the c-*Abl* protein-tyrosine kinase and two members of the phosphatidylinositol 3-kinase family, ATM (Ataxia telangiectasia mutated) and DNA-PK (DNA-dependent protein kinase).

The product of the proto-oncogene c-*Abl* is a non-receptor tyrosine kinase that is ubiquitously expressed and localized both in nucleus and cytoplasm. c-*Abl* protein is required for the normal growth and function of the organism because mice that are nullizygous for *Abl* die 14-15 days after birth for unknown reason. The c-*Abl* protein contains an unusually long C-terminus that is essential for *Abl*'s function because mice containing intact kinase domain but lacking in the C-terminus also exhibited neonatal lethality. In the C-terminus of c-*Abl*, the binding site for *Abl*'s nuclear substrate RNA polymerase II has been identified. In addition several other functional domains such as nuclear localization signal (NLS), DNA-binding domain (DBD) and actin-binding domain (ABD) have also been identified. Recently, a nuclear export signal (NES) has been identified in the extreme C-terminus of c-*Abl*.

The tyrosine kinase activity of c-*Abl* is normally tightly regulated during the cell cycle. This can be explained by binding partners of *Abl*. The kinase domain of *Abl* binds to the C-terminus of Rb (retinoblastoma protein). When Rb becomes hyperphosphorylated by Cdk4/6, *Abl* loses its association with Rb and gains its tyrosine kinase activity. Other members of *Abl* binding partner's include *Abl* interacting proteins Abi-1, Abi-2, and PAG, whose binding also leads to suppression of *Abl* kinase activity.

We have investigated the physiological relevance of both ATM and DNA-PK activity in the activation of *Abl* kinase following IR exposure. Ionizing-radiation treatment results in activation of the nonreceptor tyrosine kinase c-*Abl* because of phosphorylation of ATM. In-vitro evidence indicates that DNA-PK can also phosphorylate and thus potentially activate Abl kinase activity in response to IR exposure. To unravel the role of ATM and DNA-PK in the activation of *Abl*, we assayed *Abl*, ATM, and DNA-PK activity in ATM- and DNA-PKcs-deficeint cells after irradiation.

Phosphorylation at Serine 465 of c-*Abl* tyrosine kinase by ATM (Ataxia telangiectasia mutated) gene product is induced by ionizing radiation that results in activation of *Abl* kinase activity. In response to IR, the DNA-PK (DNA-dependent protein kinase) can also phosphorylate *Abl* and activate its kinase activity. To examine the physiological relevance of these two kinases in IR-induced *Abl* phosphorylation and activation, we assayed for *Abl*, ATM and DNA-PK activity in ATM and DNA-PK-deficient cells. Our results show that, despite the presence of a higher-than-normal level of DNA-PK kinase activity, c-*Abl* is not activated by IR in AT cells. On the other hand, activation of ATM and Abl kinase is observed in cells that are completely deficient for the catalytic subunit of DNA-PK. Furthermore, activation of *Abl* by IR correlates well with activation of ATM kinase activity by IR in G1 and S phase. Interestingly, the G2/M phase of the cell cycle exhibited enhanced *Abl* activity irrespective of exposure to IR. Together, these results indicate that ATM may regulate Abl kinase at every phase of the cell cycle in response to ionizing radiation. Furthermore, activation of *Abl* correlates well with activation of ATM at G1, S, and G2/M phase.

Our results show that despite the presence of higher-than-normal levels of DNA-PK kinase activity, c-*Abl* fails to become activated after IR exposure in ATM-deficient cells. Conversely, normal activation of both ATM and c-*Abl* occurs in DNA-PKcs-deficient cells, indicating that ATM but not DNA-PK is required for activation of *Abl* in response to IR treatment. Moreover, activation of *Abl* kinase activity by IR correlates well with activation of ATM activity in all phases of the cell cycle. These results indicate that ATM is primarily responsible for activation of *Abl* in response to IR exposure in a cell-cycle-dependent fashion. Examination of DNA-PK activity in response to IR treatment in *Abl*-deficient cells expressing mutant forms of *Abl* or in normal cells exposed to an inhibitor of *Abl* suggests an in vivo role for *Abl* in the down-regulation of DNA-PK activity. Collectively, these results suggest a convergence of the ATM and DNA-PK pathways in the cellular response to IR through c-*Abl* kinase.

High Frequency of Hypermethylation at the 14-3-3σ Locus to Gene Silencing in Breast Cancer

Anne T. Ferguson, Ella Evron, and Christopher Umbricht (Johns Hopkins Oncology Center, Baltimore, MD), Tej K. Pandita, Timothy A. Chan and Heiko Hermeking (JHOC), Jeffrey Marks, Aouk R. Lambers and P. Andrew Futreal (Duke University Medical Center, Durham, NC), Martha R. Stampfer (Berkeley National Labs, Berkeley, CA), and Saraswati Sukumar (JHOC)

Although many studies have identified critical genetic and epigenetic changes that mark the transformation of cells in tissues such as colon, pancreas, and lung, similar studies in breast cancer have met with limited success. We investigated the molecular mechanism underlying the low expression of σ in breast cancers.

14-3-3σ was originally identified as an epithelial-specific marker, HME1, which was down-regulated in a few breast cancer cell lines but not in cancer cell lines derived from other tissue types. Later studies showed that σ protein (also called stratifin) was abundant in differentiated squamous epithelial cells, but decreased by 95% in SV40-transformed epithelial cells and in primary bladder tumors.

Recent studies have shed light on the function of σ. It was identified as a p53-inducible gene that is responsive to DNA-damaging agents. σ apparently sequesters the mitotic initiation complex, cdc2-cyclin B1, in the cytoplasm after DNA damage. This prevents cdc2-cyclin B1 from entering the nucleus where the protein complex would normally initiate mitosis. In this manner, σ induces G2 arrest, and allows the repair of damaged DNA. Of note, we find that breast cancer cells that do not express σ accumulate significantly more G2-type chromosomal aberrations than cells that express σ. These results suggest that σ participates in a G2 checkpoint control in breast cells. We propose that loss of σ gene expression plays a significant role in breast cancer, as it may facilitate the accumulation of genetic damage conducive to malignant transformation. Furthermore, the absence of σ may also contribute to the radiosensitivity of breast neoplasms. Finally, methylation of the σ gene may prove to be a useful marker for early detection of breast cancer.

Expression of 14-3-3 sigma (σ) is induced in response to DNA damage, and causes cells to arrest in G2. By SAGE analysis, we identified σ as a gene whose expression is 7-fold lower in breast carcinoma cells than in normal breast epithelium. We verified this finding by Northern blot analysis. Remarkably, σ mRNA was undetectable in 45 of 48 primary breast carcinomas. Genetic alterations at σ such as loss of heterozygosity were rare (1/20 informative cases) and no mutations were detected (0/34). On the other hand, hypermethylation of CpG islands in the σ gene was detected in 91% (75/82) of breast tumors and was associated with lack of gene expression. Hypermethylation of σ is functionally important, since treatment of σ-nonexpressing

breast cancer cell lines with the drug 5-aza, 3'deoxycytidine resulted in demethylation of the gene and re-expression of σ mRNA. Breast cancer cells lacking σ expression showed increased accumulation of chromosomal breaks and gaps when exposed to gamma irradiation. Therefore, it is possible that loss of σ expression contributes to malignant transformation by impairing the G2 cell-cycle checkpoint, thus allowing an accumulation of genetic defects. Hypermethylation and loss of σ expression are the most consistent molecular alterations in breast cancer identified so far. Consequently, σ gene methylation may serve as a novel diagnostic marker and target for therapeutic strategies.

In summary, σ-CpG island methylation is an epigenetic change that is largely responsible for silencing of the gene and occurs in a majority of breast cancers. Loss of σ may play a role in the increased sensitivity of breast cancers to radiation therapy. Further evaluation of σ gene methylation in tissue samples, such as nipple aspirate cells, fine needle biopsies, microdissected premalignant lesions like DCIS, and pathologically negative sentinel lymph nodes, may provide the foundation for its development as a novel marker for early detection.

Inactivation of 14-3-3σ Influences Telomere Behavior and Ionizing-Radiation-Induced Chromosomal Instability

Sonu Dhar, Jeremy A. Squire (University of Toronto, Canada), M. Prakash Hande, Raymund J. Wellinger (Université de Sherbrooke, Canada), and Tej K. Pandita

The 14-3-3 proteins appear to modulate the activity of a large variety of functional proteins and enzymes, many of which are involved in control of cell cycle, cell death, and mitogenesis. The 14-3-3 proteins are thought to function as adaptor proteins that allow interaction between signaling proteins that do not associate directly with each other. The 14-3-3σ gene was originally identified as an epithelial-specific marker, HME1, which was downregulated in a few breast cancer cell lines but not in cancer cell lines derived from other tissue types. Our recent data indicate that the expression of 14-3-3σ is lost in 94% of breast tumors (*1*). At the functional level, the 14-3-3σ protein has been implicated in the G2 checkpoint (*2-3*). 14-3-3σ has been implicated in maintaining a post-DNA-damage G2-arrest, thereby allowing for DNA repair (*2*,*4*).

Genome stability is also maintained by the telomeres, as these chromosome terminal structures protect the chromosomes from fusions or degradation. Telomeres are complexes of repetitive DNA sequences and proteins constituting the ends of linear eukaryotic chromosomes. While these structures are thought to be associated with the nuclear matrix, they appear to be released from this matrix at the time when the cells exit from G2 and enter M-phase. Checkpoints maintain the order and fidelity of the eukaryotic cell cycle, and defects in checkpoints contribute to genetic instability and cancer. Here we demonstrate that inactivation of this gene influences genome integrity and cell survival.

We were interested to determine whether a normal G2 checkpoint is necessary for chromosome stability in mammalian cells. For this purpose, we studied the influence of the 14-3-3σ gene on chromosome behavior, as it relates to a gene involved in G2-checkpoint after DNA-damage. We used isogenic human colorectal cancer cells in which both 14-3-3σ alleles are inactivated and were generated by somatic-cell knockouts approach (*4*).

Inactivation of 14-3-3σ influences cell growth and survival after irradiation with gamma rays

14-3-3$\sigma^{+/+}$ and derivatives 14-3-4$\sigma^{+/-}$ and 14-3-3$\sigma^{-/-}$ are human colorectal cancer cells that were derived from cell line HCT116. Since the 14-3-3σ protein is involved in G2-checkpoint control, we examined whether inactivation of 14-3-3σ influences cell survival after irradiation with gamma rays using colony-forming experiments. Cells with both copies of 14-3-3σ nactivated exhibited a ~2-fold enhancement in ionizing-radiation sensitivity for reproductive cell death when compared to cells. No difference in ionizing radiation sensitivity for reproductive cell death was found in 14-3-3$\sigma^{+/-}$ and 14-3-3$\sigma^{+/+}$

cells, suggesting that cells with heterozygous status of the 14-3-3σ gene have a similar phenotype to that of parental cells.

Inactivation of 14-3-3 s leads to chromosome end-to-end associations and frequent losses of telomeric repeats.

Cells in which both alleles of 14-3-3σ were inactivated grow slowly and exhibit decreased cell survival after gamma-ray treatment. It is thus possible that damaged DNA is not repaired appropriately in these cells. To determine whether the inactivation of 14-3-3σ gene influences chromosome behavior, we compared 14-3-3$\sigma^{+/+}$, 14-3-3$\sigma^{+/-}$ and 14-3-3$\sigma^{-/-}$ cells for frequencies of chromosome end-to-end associations by analyzing colcemid-accumulated cells at metaphase. 14-3-3$\sigma^{-/-}$ cells had 1.9 chromosome end-to-end associations per metaphase, whereas their parental 14-3-3$\sigma^{+/+}$ cells had 0.12 chromosome end-to-end associations per metaphase. Since chromosome end-to-end associations may lead to anaphase bridge formation, cells without colcemid treatment were analyzed for anaphase bridges. 14-3-3$\sigma^{-/-}$ cells displayed an at least an 8-fold higher frequency of anaphase bridges as compared to 14-3-3$\sigma^{+/+}$ cells.

These data suggest that due to occasional losses of telomere function, chromosome-end associations are formed and these associations are not resolved in 14-3-3$\sigma^{-/-}$ cells. To further examine how inactivation of 14-3-3σ is linked with the loss of telomere function, we examined the sizes of terminal restriction fragments (TRFs). By Southern-blotting, we found no significant differences in TRF sizes when comparing DNA derived from 14-3-3$\sigma^{-/-}$ with that from 14-3-3$\sigma^{+/-}$ and 14-3-3$\sigma^{+/+}$ cells. However, this analysis only yields an appraisal of the population of TRFs generated, and does not monitor ends of individual chromosomes. We therefore performed FISH for telomeric repeats in metaphase cells by using a telomere-specific Cy3-labeled $(CCCTAA)_3$ peptide nucleic acid probe. A significantly higher proportion of chromatid ends in 14-3-3$\sigma^{-/-}$ cells (about 11% of telomeres per metaphase) have less telomere-specific fluorescent signals as compared to the 14-3-3$\sigma^{+/+}$ cells. These observations suggest that the chromosome end-to-end fusions observed in 14-3-3$\sigma^{-/-}$ cells correlated with losses of telomeric repeats. However, telomere signals were seen in about 18% of fusion sites, indicating total loss of telomeres is not required for telomere fusions.

Normally, mammalian telomeres end in a single-stranded G-tail overhang of about 100 to 200 bases. Recently, it was shown that these G-tails can invade the double-stranded portion of telomeric repeats, forming a D-loop (*5*). This telomeric DNA end-structure may be conserved among higher eukaryotes and is required for the association of terminus-specific proteins forming the cap. Clearly, if telomeres were fused by end-to-end associations or telomeric repeats were not present such as on broken chromosome ends, these G-tails would disappear. To assess whether the inactivation of 14-3-3σ also correlates with reduced signals for G-tails, we examined the signals for G-tails on TRFs of 14-3-3$\sigma^{-/-}$, 14-3-3$\sigma^{+/-}$, and 14-3-3$\sigma^{+/+}$ cells by a non-denaturing in-gel hybridization. The advantage of this method is that terminal fragments of any size can be analyzed by using an end-labeled $d(CCCTAA)_3$ probe. In DNA derived from 14-3-3$\sigma^{-/-}$ cells, the

signal for G-tails was significantly and reproducibly reduced by about 35% as compared to DNA from 14-3-3$\sigma^{+/+}$ cells.

A difference in the G-tails of telomeres might also be due to alterations in telomerase activity. We examined telomerase activity in extracts of 14-3-3$\sigma^{+/+}$ and 14-3-3$\sigma^{-/-}$ cells by a TRAP-ELISA assay, which detects the *in vitro* synthesis of telomeric repeats by telomerase (*6*). Using this method, no significant differences in telomerase activity between 14-3-3$\sigma^{-/-}$ and 14-3-3$\sigma^{+/+}$ cells was found, indicating that the overall activity of telomerase is not affected by the lack of the 14-3-3σ protein.

Enhanced chromosome-end fusions in cells with inactivated 14-3-3 s correlate with frequent terminal nonreciprocal translocations and ring formations

The above results indicate that inactivation of the 14-3-3σ gene enhances the frequency of observable chromosome end-to-end associations. We next determined whether such chromosome-end associations correlate with any other karyotypic changes. Chromosomal breaks were detected at 2.4 times higher levels in the 14-3-3$\sigma^{-/-}$ cells as compared to the parental 14-3-3$\sigma^{+/+}$ cells. Furthermore, in order to assess whether 14-3-3$\sigma^{-/-}$ cells show specific chromosome fragility, karyotypic changes were determined by spectral (SKY) karyotyping. This analysis uses colored fluorescent chromosome-specific paints that provide a complete analysis of possible interchromosomal changes. We found that 14-3-3$\sigma^{-/-}$ cells had about 3-fold higher levels of terminal non-reciprocal translocations. Further, we also found ring chromosomes in 4% of 14-3-3$\sigma^{-/-}$ cells, but not in 14-3-3-$\sigma^{+/+}$ cells. The presence of ring structures in 14-3-3$\sigma^{-/-}$ cells suggest that telomere functions can be simultaneously lost at both the ends of the same chromosome, allowing for fusion of the arms of the chromosome.

The higher frequency of chromosome end-fusions could be due to altered chromatin structure in cells with inactivated 14-3-3 s

To determine whether inactivation of 14-3-3σ gene influences the telomere nuclear matrix associations, exponentially growing cells were processed by the LIS procedure and the resulting nuclear matrix halos were cleaved with Sty1 (*7*). The nuclear remnant and associated DNA were separated by centrifugation and suspended in MWB-buffer. For genomic blotting analysis, equal volumes representing DNA from identical numbers of halos were fractionated side by side on 1.5% agarose gels. 14-3-3$\sigma^{+/+}$ cells have 56% of the telomeric DNA associated with the nuclear matrix (attached; P) fraction and 44% in the soluble (free; S) fraction. In contrast, 14-3-3$\sigma^{-/-}$ cells have 71% of the telomeric DNA associated with the nuclear matrix and 29% in the soluble fraction. In both instances summation of the P and S values is equal to total telomeric DNA (T), suggesting that no telomeric DNA was lost during the extraction procedure. These results suggest that inactivation of 14-3-3σ influences the association of telomeres with the nuclear matrix.

Observable chromosome aberrations in 14-3-3 $s^{-/-}$ ***cells correlate with a deficiency of G2-type, but not G1-type checkpoint***

In 14-3-3$\sigma^{-/-}$ cells, there is an increased frequency of chromosome end-fusions, nonreciprocal translocations, ring chromosome formations and losses of G-tails, indicating frequent loss of telomere functions in these cells. However, it remained unclear whether a defective G2-checkpoint contributes to these losses or whether other changes in these cells could induce general chromosome instability. One way to address this question is to compare cell-cycle stage-specific aberrations among 14-3-3$\sigma^{+/+}$ and 14-3-3$\sigma^{-/-}$ cells. Another way to address the same question is to compare the mitotic index of 14-3-3$\sigma^{-/-}$ cells with 14-3-3$\sigma^{+/+}$ cells after treatment with ionizing radiations. Therefore, we first set out to determine frequencies of chromosome aberrations induced in G1 or in G2 in 14-3-3$\sigma^{-/-}$ and 14-3-3$\sigma^{+/+}$ cells. G1-type chromosome damage was determined by the procedure described previously (*8*). We found no differences in residual G1-induced chromosomal aberrations seen at metaphase between 14-3-3$\sigma^{-/-}$ and 14-3-3$\sigma^{+/+}$ cells. These results confirm that cells with an inactivated 14-3-3σ gene have a normal G1 checkpoint, evidenced by similar chromosomal repair resulting in similar aberration frequencies. This suggests that the loss of telomere function with subsequent enhanced chromosome aberrations do not occur during the G1-to-S-phase transition in cells with an inactivated 14-3-3σ gene.

Since 14-3-3σ has been shown to be involved in a G2 checkpoint after DNA damage, we evaluated the influence of inactivation of 14-3-3σ gene on ionizing-radiation-induced G2-type chromosome aberrations. Cells in exponential phase were irradiated with 1 Gy, then metaphases were examined for chromatid-type breaks and gaps (*9*). Cells with both alleles of 14-3-3σ inactivated exhibited a 1.5-fold increased frequency of G2-type chromatid aberrations at 45 min post irradiation as compared to 14-3-3$\sigma^{+/+}$ cells, and this difference was increased to 2.8 fold at 90 min. In 14-3-3$\sigma^{+/+}$ cells, the frequency of G2-type aberrations decreased with longer incubations after irradiation, indicating a functional repair system in these cells. However, for 14-3-3$\sigma^{-/-}$ cells, no such decrease was found, reinforcing the idea that G2-type chromosomal aberrations are not repaired efficiently before onset of mitosis in these cells.

Further, when we examined the mitotic index of 14-3-3$\sigma^{-/-}$ and 14-3-3$\sigma^{+/+}$ cells after 90 minutes of post-treatment with 2 Gy of gamma rays, we found that cells with inactivated 14-3-3σ gene had only about 17% decrease in mitotic index, whereas cells with 14-3-3σ gene had about 61% decrease in mitotic index. These results suggest that defective G2 checkpoint contributes for mitotic catastrophe.

These results suggest that although the 14-3-3$\sigma^{-/-}$ cells have a functional G1 cell-cycle checkpoint, genetic damage accumulates in G2 following irradiation, which is consistent with a failure to arrest and repair in G2 in response to DNA damage. The frequency of observable spontaneous as well as ionizing-radiation-induced chromatid breaks was dramatically higher in 14-3-3$\sigma^{-/-}$ cells, suggesting that losses of telomere

function occurred by breakage near telomeres, rather than by a telomerase-based mechanism.

Since 14-3-3$\sigma^{-/-}$ cells are defective in maintaining G2 arrest, they enter M phase without repair of the aberrant chromosome structures and undergo cell death during mitosis. Thus, our studies demonstrate that a dysfunctional G2/M-checkpoint control correlates to genomic instability and loss of telomeres in mammalian cells.

References

1. Ferguson A.T., Evron E., Umbricht C., Pandita T.K., Hermeking H., Marks J., Futreal A., Stampfer M.R., and Sukumar S**.** 2000. High frequency of hypermethylation at the 14-3-3σ locus leads to gene silencing in breast cancer. PNAS USA **97**:6049-6054.
2. Hermeking H., Lengauer C., Polyak K., He T-C., Zhang L., Thiagalingam S., Kinzler K.W., and Vogelstein B. 1997. 14-3-3σ is a p53-regulated inhibitor of G2/M progresssion. Mol. Cell **1**: 3-11.
3. Peng C.-Y., Graves P.R., Thoma R.S., Wu Z., Shaw A.S., and Piwnica-Worms H. 1997. Mitotic and G2 checkpoint control; regulation of 14-3-3 protein binding by phosphorylation of Cdc25C on serine-216. Science **277**: 1501-1505.
4. Chan, T.A., Hermakin H., Lengauer C., Kinzler K.W., and Vogelstein B. 1999. 14-3-3σ is required to prevent mitotic catastrophe after DNA damage. Nature **401**: 616-620.
5. Griffith J.D., Comeau L., Rosenfield S., Stansel R.M., Bianchi A., Moss H. and de Lange T. 1999. Mammalian telomeres end in a large duplex loop. Cell **97**: 503-514.
6. Sawant S.G., Gregoire V., Dhar S., Umbricht C.B., Cvilic S., Sukumar S., and Pandita T.K. 1999. Telomerase activity as a measure for monitoring radiocurability of tumor cells. FASEB J **13**: 1047-1054.
7. Smilenov L.B., Dhar S., and Pandita T.K. 1999. Altered telomere nuclear matrix interactions and nucleosomal periodicity in cells derived from individuals with Ataxia telangiectasia before and after ionizing radiation treatment. Mol Cell Bio **19**: 6963-6971.
8. Pandita T.K. and Geard C.R. 1996. Chromosome aberrations in human fibroblasts induced by monoenergetic neutrons. I. Relative biological effectiveness. Radiat Res **145**: 730-739.
9. Morgan S.E., Lovly C., Pandita T.K., Shiloh Y. and Kastan M.B. 1997.Generation of dominant-negative and complementing fragments of ATM. Mol Cell Biol **17**: 2020-2029.

Telomerase-Associated Protein TEP1 is Not Essential for Telomerase Activity or Telomere-Length Maintenance *In Vivo*

Yie Liu and Bryan E. Snow (Ontario Cancer Institute/Amgen Institute, Toronto, Canada), M. Prakash Hande (Terry Fox Laboratory, British Columbia Cancer Research Center, Vancouver, Canada and CRR, NY), Gabriela Baerlocher (TFL), Valerie Kickhoefer (UCLA School of Medicine, Los Angeles, CA), David Yeung (OCII and Amgen, Inc., Thousand Oaks, CA), Drew Wakeham (OCII), Annick Itie (OCII), David Siderovski (University of North Carolina/Chapel Hill School of Medicine, Chapel Hill, NC), Peter Lansdorp (TFL), Murray O. Robinson (Amgen, Inc.), and Lea Harrington (OCII)

Most eukaryotic chromosome ends are maintained by a ribonucleoprotein complex, called telomerase. Telomerase is a reverse transcriptase that uses an integral RNA component to catalyze the addition of telomeric repeats to the 3' end of single-stranded telomeric DNA (*1*). In many organisms, the telomerase complex is a large (750 to 1000 kDa) RNP containing an integral RNA, a reverse transcriptase protein subunit, and several associated proteins. The telomerase RNA component provides a template for telomere DNA synthesis, and its essential role in telomerase activity, telomere length maintenance, and genome stability has been demonstrated in ciliates, yeast, and mice (*2*). Telomerase reverse transcriptase (TERT) was first identified in the yeasts *Saccharomyces cerevisiae* (*EST2*) and *Schizosaccharomyces pombe* (*trt1+*) and the ciliate *Euplotes aediculatus* (p123) (*3,4*), and subsequently in humans (*hTERT*) (*5,6*). In addition to the presumed "core" telomerase components consisting of the telomerase RNA and reverse transcriptase, several proteins associated with telomerase activity have also been identified. The mammalian homologue of p80, TEP1, is associated with telomerase activity in human, mouse, and rat immortalized cell extracts (*7,8*). Despite its association with telomerase components, the role of TEP1 in telomerase function is completely unclear. The genetic characterization of these proteins is critical to our understanding of the complexity, composition, and regulation of telomerase *in vivo*. We utilized homologous recombination to disrupt the first mammalian telomerase-associated protein identified, *mTep1*, in mice and embryonic stem cells, and analyzed the effect upon telomerase activity and telomere-length maintenance.

mTEP1 is not essential for telomerase catalysis in vivo

To determine the role of mTep1 in telomerase catalysis, we examined *mTep1*-deficient ES cells, MEF cultures derived from G1 $mTep1^{-/-}$ embryos, and several mouse tissues from $mTep1^{-/-}$ mice (up to G3) for telomerase activity. Using both the conventional telomerase elongation assay and the PCR-based telomerase assay (TRAP), all three independently derived $mTep1^{-/-}$ ES cell clones possessed similar levels of telomerase activity compared to the $mTep^{+/-}$ clone and the parental line. We also tested whether telomerase activity was altered in tissues from $mTep1^{-/-}$ mice. Telomerase activity was not significantly altered in testes, liver, kidney, lung, or thymus from the $mTep1^{-/-}$ mice compared to wild-type mouse tissues. Subsequent analysis of several tissues that normally lack telomerase activity including brain, skin, heart, and spleen (*2*) revealed no reactivation of telomerase activity in the same tissues from $mTep1^{-/-}$ mice. In

MEFs derived from G1 *mTep1*$^{-/-}$ embryos, there was also no significant change in telomerase activity compared to the *mTep1*$^{+/-}$ and wild-type MEFs. Using the conventional telomerase assay, we also did not detect any changes in telomerase activity levels in liver and testis extracts from *mTep1*$^{-/-}$ mice.

The role of mTEP1 in telomere length regulation in vivo

Mice and ES cells disrupted for the telomerase RNA component lack telomerase activity and undergo telomere shortening *in vivo* (*2*,*9*,*10*). To determine whether loss of *mTep1* could be essential for telomere-length maintenance, we analyzed telomere length in mice tissues and ES cells in successive generations of mTEP1 deficient mice. We used a quantitative method to examine telomere length in a total cell population, called fluorescence in situ hybridization (FISH) combined with flow cytometry (Flow-FISH) (*11*). We observed that none of the *mTep1*$^{+/-}$ and three independent *mTep1*$^{-/-}$ ES cell clones, regardless of increasing population doublings, showed significant changes in average telomere fluorescence intensity as compared to early or late passages of wild-type cells (Fig. 1A). Thymocytes and splenocytes derived from different generations of *mTep1*-deficient mice (G1 to G7) also yielded very similar measurements of relative telomere lengths, which were also comparable to the G1 *mTep1* heterozygote control (Figure 1B). The overall distribution of telomere signal fluorescence in the G1 and G7 samples was similar to the heterozygous *mTep1* control.

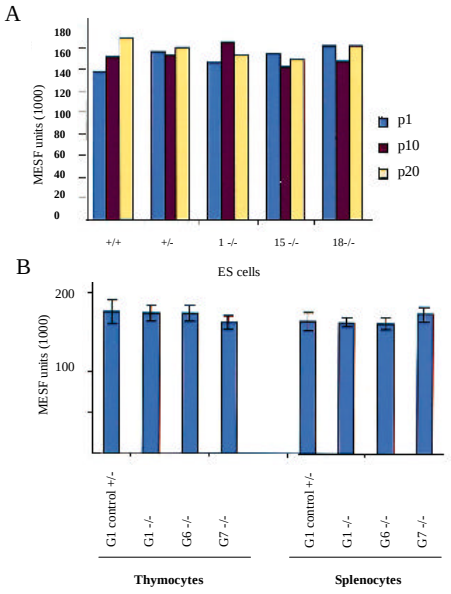

FIG. 1. Relative telomere lengths in ES cells and in spelnocytes and thymocytes derived from mouse tissues by Flow-FISH.

Similarly, FISH analysis of metaphase chromosome preparations from *mTep1*-deficient MEFs showed no significant change in telomere signal intensity or chromosomal aberrations compared to the wild-type MEFs. We therefore conclude that disruption of *mTep1* had no effect on either the distribution or mean length of telomeres.

References

1. Greider, C. W. 1996. Telomere length regulation. *Annu Rev Biochem* 65:337-65.
2. Blasco, M. A., H. W. Lee, M. P. Hande, E. Samper, P. M. Lansdorp, R. A. DePinho, and C. W. Greider. 1997. Telomere shortening and tumor formation by mouse cells lacking telomerase RNA. *Cell* 91:25-34.
3. Lingner, J., T. R. Hughes, A. Shevchenko, M. Mann, V. Lundblad, and T. R. Cech. 1997. Reverse transcriptase motifs in the catalytic subunit of telomerase. *Science* 276:561-7.
4. Nakamura, T. M., G. B. Morin, K. B. Chapman, S. L. Weinrich, W. H. Andrews, J. Lingner, C. B. Harley, and T. R. Cech. 1997. Telomerase catalytic subunit homologs from fission yeast and human. *Science* 277:955-9.
5. Meyerson, M., C. M. Counter, E. N. Eaton, L. W. Ellisen, P. Steiner, S. D. Caddle, L. Ziaugra, R. L. Beijersbergen, M. J. Davidoff, Q. Liu, S. Bacchetti, D. A. Haber, and R. A. Weinberg. 1997. hEST2, the putative human telomerase catalytic subunit gene, is up- regulated in tumor cells and during immortalization. *Cell* 90:785-95.
6. Harrington, L., W. Zhou, T. McPhail, R. Oulton, D. S. Yeung, V. Mar, M. B. Bass, and M. O. Robinson. 1997a. Human telomerase contains evolutionarily conserved catalytic and structural subunits. *Genes Dev* 11:3109-15.
7. Harrington, L., T. McPhail, V. Mar, W. Zhou, R. Oulton, M. B. Bass, I. Arruda, and M. O. Robinson. 1997b. A mammalian telomerase-associated protein. *Science* 275:973-7.
8. Nakayama, J., M. Saito, H. Nakamura, A. Matsuura, and F. Ishikawa. 1997. TLP1: a gene encoding a protein component of mammalian telomerase is a novel member of WD repeats family. *Cell* 88:875-84.
9. Niida, H., T. Matsumoto, H. Satoh, M. Shiwa, Y. Tokutake, Y. Furuichi, and Y. Shinkai. 1998. Severe growth defect in mouse cells lacking the telomerase RNA component. *Nat Genet* 19:203-6.
10. Hande MP, Samper E, Lansdorp P, Blasco MA, 1999, Telomere length dynamics and chromosomal instability in cells derived from telomerase null mice. *J Cell Biol* 144: 589-601.
11. Rufer, N., W. Dragowska, G. Thornbury, E. Roosnek, and P. M. Lansdorp. 1998. Telomere length dynamics in human lymphocyte subpopulations measured by flow cytometry. *Nat Biotechnol* 16:743-7.

A Few Percent of the Population May Be Genetically Predisposed to Radiation-Induced Cancer

Lubomir B. Smilenov, Eric J. Hall, and David J. Brenner

Human subpopulations that have a genetically based increased sensitivity to radiation-induced cancer could have significant consequences for mass radiological screening programs such as mammography, as well as in occupational radiation exposure settings. Individuals homozygous for the Ataxia telangiectasia gene (*ATM*) are indeed highly radiosensitive, but their numbers (~0.002%) are too small to be of societal importance. *ATM* heterozygotes constitute about 1 to 2% of the US population, and may well show an increased background rate for some cancers. With regard to radiation, although heterozygote *ATM* cells show some evidence of increased radiosensitivity, there are no data for cancer-related endpoints, and limited epidemiological studies have been equivocal.

Here we report a controlled comparison of radiation oncogenesis in *ATM* heterozygotes compared with the corresponding normal wild type, and present statistically significant evidence of a predisposition to cancer radiosensitivity in carriers of a heterozygous genetic mutation. Specifically, in direct intra-litter comparisons between *ATM* heterozygous and *ATM* wild-type mouse embryo fibroblasts, we show that the heterozygous cells are more sensitive to radiation oncogenesis than their normal, litter-matched counterparts. From these data it appears that AT heterozygotes could indeed represent a societally significant radiosensitive human subpopulation.

To directly compare the sensitivity to radiation oncogenesis in heterozygote vs. wild-type animals, pairs of *ATM* heterozygote mice were mated, and intra-litter comparisons made of the sensitivity to radiation-induced oncogenesis between freshly explanted MEF from *ATM*+/+ and *ATM*+/- embryos. The endpoint of interest here is the induction of radiation-induced morphologically transformed clones in the freshly-explanted MEF. Fresh explants of rodent embryo cells have been extensively used as a quantitative model of oncogenic transformation . The results of the radiation studies are shown in Table 1. As discussed below, mice with two different mutations in the *ATM* gene were used, one generated at Harvard Medical School, and the other at the National Institutes of Health. A total of 13 intra-litter comparisons were made between normal and AT heterozygote embryos. Yields of transformed clones were measured both for zero-dose exposure and for exposure to a gamma-ray dose of 2 Gy, and transformed clones were confirmed as neoplastic by their ability to produce tumors when injected into athymic nude mice.

We define the relative oncogenic radiosensitivity (ROR) as the yield of transformed clones per surviving *ATM* heterozygous MEF exposed to a dose of 2 Gy, relative to the yield of transformed clones per corresponding surviving wild-type MEF also exposed to 2 Gy.

To determine whether there was a common ROR (odds ratio) in intra-litter comparisons within the NIH mice, within the Harvard mice, and for all the mice, a Monte-Carlo simulation of Zelen's exact test was used. The results are shown in Table 2. Within neither strain of animals, nor for all the mice combined, could the hypothesis be rejected that a common ROR can describe the comparisons between the wild-type cells and the corresponding heterozygous cells.

The RORs for the heterozygote vs. wild type MEF were exactly estimated using maximum likelihood techniques , and the null hypothesis that the ROR was unity (no difference in sensitivity) subjected to two-sided test. The results are shown in Table 2: For the NIH mice, the *ROR* (heterozygote *vs.* wild type) was 1.48 [95% confidence interval: 0.65-3.51, p=0.35]; for the Harvard mice, the estimated ROR was1.89 [95% C.I.: 1.08-3.43, p=0.02], and for both animal strains combined, the ROR was 1.74 [95% C.I.: 1.11-2.80]. For the NIH mice, the null hypothesis could not be rejected that the wild-type and the heterozygous cells have the same sensitivity to radiation oncogenesis. However, for the Harvard mice, and for both strains of mice combined, the null hypothesis could be rejected (p=0.02), i.e., the *ATM* heterozygous mice were significantly more sensitive for radiation oncogenesis than were the corresponding wild-type animals, by a factor of almost 2.

By contrast, the ROR at 2 Gy for *ATM*-deficient homozygote mice (*ATM*-/-) compared to the normal wild type was 10.5 [95% C.I.: 4.4-26.2, p <0.001] (4 litter-matched comparisons made, data not shown), so the AT heterozygote mice are indeed intermediate in their radiation sensitivity between the normal and the *ATM* deficient homozygote mice.

The data reported here using a mouse model of *ATM* are strongly suggestive that the 1 to 2% of the human population who are heterozygous for the *ATM* gene may be genetically predisposed to radiation-induced cancer. It is quite likely, of course, that there are other genetically based radiosensitive subpopulations, though while possibly radiosensitive low-frequency subpopulations such as *BRCA1/2* (<0.2%) have been studied, there are currently no other obvious high-frequency candidates. The presence of comparatively large subpopulations who are genetically predisposed to radiation-induced cancer could be of broad societal relevance; for example, the risk (radiation-induced cancer) vs. benefit balance for mass screening mammography would be altered, of particular relevance to younger women, although the increased natural breast-cancer rate in AT heterozygotes could also be of relevance. More generally, application of the results of epidemiological studies of radiation-induced cancer risks, such as at Hiroshima or Chernobyl, are currently premised on an essentially unimodal distribution of radiation sensitivity across the population; if a significantly-sized identifiable subpopulation were hypersensitive to radiation-induced cancer, a single radiation protection standard across the whole population would be of questionable relevance.

Table 1. Irradiated and transformed clones from irradiated ATM wild-type and heterozygote embryo cells.

Mouse #	Embryo ID	Wild-type (W) / Heterozygous (H)	Number of surviving clones	Number of transformed clones	Frequency of transformed clones (%)
NIH mice					
N1	A	W	1,505	1	0.07
N1	B	W	2,600	4	0.15
N1	C	H	3,075	6	0.19
N2	A	W	2,832	2	0.07
N2	B	H	2,576	5	0.19
N2	C	H	1,600	1	0.06
N2	D	H	1,960	0	0.00
Harvard Mice					
H1	A	W	3,000	2	0.07
H1	B	W	2,250	2	0.09
H1	D	H	925	0	0.00
H1	E	H	1,617	6	0.37
H6	B	W	1,950	5	0.26
H6	E	W	2,050	1	0.05
H6	A	H	4,857	17	0.35
H6	G	H	3,737	4	0.11

Table 2. Litter-matched comparisons of radiation oncogenesis between heterozygous and normal wild-type MEF.

	NIH mice	Harvard mice	All mice
Zalen test for homogeneity of ROR*, [99% confidence limits of p value]	$p = 0.68$ [0.68, 0.68]	$p = 0.054$ [0.051, 0.058]	$p = 0.19$ [0.18, 0.19]
Estimated ROR [95% confidence interval] (two-sided p value)	1.48 [0.65, 3.51] ($p = 0.35$)	1.89 [1.08, 3.42] ($p = 0.024$)	1.74 [1.11, 2.80] ($p = 0.016$)

* ROR: Relative Oncogenic Radiosensitivity, *ATM* heterozygotes vs. wild type.

Differentially Expressed Genes in Asbestos-Induced Tumorigenic Human Bronchial Epithelial Cells

Yong L. Zhao, Chang Q. Piao, and Tom K. Hei

Although occupational exposure to asbestos fibers is associated with development of pulmonary fibrosis, bronchogenic carcinoma, and mesothelioma (*1*), the mechanism(s) of fiber carcinogenesis is not clear. There is evidence to suggest that asbestos-induced reactive oxygen species and/or growth factors may be involved in its genotoxic/carcinogenic process (*2*). The observation that antioxidant enzymes such as catalase and superoxide dismutase can protect cells against the cytotoxic and mutagenic effects of asbestos provides further evidence for the role of oxygen radicals in fiber toxicology (*3*). Asbestos has been shown to trigger many signaling events via activation of the nuclear factor-kB (NFkB) and other early-response proto-oncogenes, including c-*fos* and c-*jun* (*4*), which in turn increase the DNA binding activity of the activator protein-1 transcription factor (AP-1) and lead to increased cellular proliferation and morphological transformation of tracheal epithelial cells (*5*).

Previous studies from this laboratory have shown that asbestos is a potent genetic and chromosomal mutagen and induces predominately multilocus deletions (6). While chromosomal deletions in malignant mesotheliomas are relatively common events (*7*) no mutations in several common suppressor genes such as Rb, p53, and Wilm's tumor have been identified to play a causal role in asbestos-associated cancers (*8*). These findings suggest that loss and/or inactivation of multiple tumor suppressor genes are possible mechanism in fiber carcinogenesis (*9*).

Using human papillomavirus immortalized human bronchial epithelial (BEP2D) cells, our laboratory showed recently that a single, 7-day treatment with a 4-$\mu g/cm^2$ dose of chrysotile-induced neoplastic transformation of these cells in a step-wise fashion at a frequency of $\sim 10^{-7}$ (*10*). Transformed cells progress through a series of step-wise changes, including altered growth pattern, resistance to serum-induced terminal differentiation, and agar-positive growth, before becoming tumorigenic and producing subcutaneous tumors upon inoculation into athymic nude mice (*11*). However, control BEP2D cells are anchorage dependent and non-tumorigenic even in late passage (*10*). Since BEP2D cells express both E6 and E7 viral proteins, these data suggest that abnormal p53 and Rb functions by papillomavirus are insufficient to trigger tumorigenic cascade in BEP2D cells, and additional factors and cellular events are required. There are recent findings that Simian virus 40 (SV40), which also inactivates Rb and p53 functions in infected cells, was found in more than 60% of human malignant mesotheliomas (*12*). This data suggests that asbestos and SV40 could potentially act as co-carcinogens in asbestos-mediated malignancies, and it provides further support for the suitability of BEP2D cells in mechanistic study of fiber carcinogenesis.

Identification of alterations in gene expression profile in asbestos-induced transformed cells at various stages of the neoplastic process will lead to a better

understanding of the mechanism of fiber carcinogenesis. A recently developed technique, cDNA expression array, allows the large-scale comparison of multiple genes in a single hybridization. The assay has the advantage of providing rapid and immediate information on interested genes as well as the functions of their proteins. In this study, we used cDNA expression array to compare the expression of 588 known cellular genes in cell lines derived from control and tumorigenic BEP2D cells induced by asbestos fibers. The hybridization signals were further screened by Northern blotting using cell lines derived from different transformation stages (*10*). In addition, we generated fusion cell lines between fiber-induced tumorigenic and control BEP2D cells and showed that all fusion clones were no longer tumorigenic when subsequently inoculated into nude mice. The results are shown in Table 1. The total of 15 alterations in gene expression found in cDNA array were screened by Northern blot using mRNA obtained from cell lines, including serum-resistant transformed cells, early- and late-passage cells, five representative tumor cell lines, and four fusion cell lines. Eleven of 15 genes were confirmed to be differentially expressed in tumorigenic cells compared with control. Three genes, including DCC, Ku70, and HSP27, were lowered significantly in all five tumor cell lines, but there were no significant changes in serum-resistant transformed cells, early- and late-passage cells, compared with control. In fusion cells, the expression of these three genes was recovered to the expression levels of control cells. Eight genes, including insulin receptor (IR), *src* homolog 2 adaptor (SHB), Grb2, ERK2, c-*fos*, NFkB (p50/105), Ets-like gene and cdc2-related kinase (PISSLRE) were significantly overexpressed all all five tumor cells lines and suppressed in fusion cells. No significant changes of these genes were found in serum-

Table 1. Summary of differentially expressed genes in asbestos-induced transformed BEP2D cells.

Name of gene	cDNA* array	Northern Blot				
		Non-tumorigenic cells	Early passage	Late passage	Five tumor cell lines (average)	Fusion cells
Insulin receptor	1.81†	NC	1.48	1.61	2.20±0.25	NC
Shb adaptor	2.72	NC	NC	NC	3.64±0.37	NC
Grb2	1.71	NC	NC	NC	1.91±0.15	NC
Erk2	2.41	NC	NC	NC	2.24±0.15	NC
c-*fos*	3.89	5.82	NC	NC	4.80±1.45	NC
Ets-like gene	1.87	NC	NC	NC	2.41±0.32	NC
NFkB(p50)	2.48	NC	NC	1.70	3.00±0.45	NC
DCC	-1.91	NC	NC	NC	-2.98±0.67	NC
Ku70	-2.47	NC	NC	NC	-2.36±0.31	NC
PISSLRE	1.72	NC	NC	2.09	1.97±0.21	1.30
HSP27	-3.45	NC	NC	NC	-2.60±0.51	NC

*Using control and one tumorigenic BEP2D cell line to screen the differential gene expression by cDNA array

†The expression levels (fold) in transformed BEP2D cells compared with control cells quantified by ImageQuant version 3.22 (Molecular Dynamics). Positive and negative numbers represent upregulated and downregulated transformed cells.

NC: no significant changes.

resistant transformed cells, early- and late-passage cells except IR was about 1.5-fold higher in early- and late-passage cells, NFkB was 1.7-fold, and PISSLRE was 2-fold higher in late-passage cells than in control cells. The expression level of c-*fos* was also found to be 3.9-fold higher in non-tumorigenic serum-resistant cells.

Asbestos fibers have been shown to trigger a number of signaling cascades involving mitogen-activated protein kinases (MAPK), which may be initiated through receptor-mediated events (*13*). Insulin receptor is a member of a large family of receptor tyrosine kinase (RTK) possessing intrinsic cytoplasmic enzymatic activity, which is an essential component of signal transduction pathways that affect cell proliferation, differentiation, and migration (*14*). There is evidence that an activator of RTK, such as EGF receptor, can in turn activate numerous intracellular signal cascades by MAPK pathway, including extracellular signal-related kinases (ERK), which lead to activation of transcription factor c-*fos* and NH2-terminal kinases (JNK-SAPK), which activates c-*jun* (*4*). The proteins encoded by these stress genes could dimerize into the transcription factor AP-1 and promote G1$\rightarrow$ S phase transition (5,15). In the present study, expression of IR was upregulated by about 1.5 fold in both the early- and late-passage cells but by about 2.2 fold in all tumor cell lines examined. This significant increase in IR expression could, perhaps, account for the increased expression of other downstream genes such as SHB, Grb2, Erk2, Ets-like gene, and c-*fos* found in all tumor cell lines (*14*). Since no change in either the EGF receptor or c-*jun* expression was found among the tumor cells, these data clearly suggested that IR activation occurred at an early stage of asbestos-induced transformation which was linked to c-*fos* induction and in asbestos-induced cell proliferation via the ERK pathway. IR has been shown to be a potential oncogene for mammary epithelial cells (*16,17*), overexpression of which could enhance growth and transformed phenotypes in cultured cells. However, there is evidence that IR activation alone was insufficient to induce malignant transformation in epithelial cell lines (*17*). The reduced expressions of DCC and Ku70 might collaborate with IR activation in malignant progression by promoting genomic instability and increase susceptibility to oxidative damage. Evidence for this line of thought comes from the cell fusion studies which indicate that loss of tumorigenic potential is accompanied by a re-expression of these genes to the control levels. While our present findings provide some clues to the mechanism of fiber carcinogenesis, additional studies are needed to determine how these multiple pathways integrated in normal target epithelium.

References

1. Mossman BT, Bignon J, Corn M, Seaton A, Gee JB. (1990) Asbestos: scientific developments and implications for public policy. *Science*, 247(4940), 294-301.
2. Suzuki K, Hei TK. (1996) Induction of heme oxygenase in mammalian cells by mineral fibers: Distinctive effect of reactive oxygen species. *Carciongenesis*, 17(4), 661-667.
3. Hei TK, He ZY, Suzuki K. (1995) Effects of antioxidants on fiber mutagenesis. *Carcinogenesis*, 16, 1573-1578.
4. Heintz NH, Janssen YM, Mossman BT. (1993) Persistent induction of c-*fos* and c-*jun* expression by asbestos. *Proc. Natl. Acad. Sci. USA*, 90, 3299-3303.

5. Angel P, Karin M. (1991) The role of *jun, fos* and the AP-1 complex in cell proliferation and transformation. *Biochim. Biophys. Acta*, 1072, 129-157.
6. Hei TK, Piao CQ, He ZY, Vannais D, Waldren CA. (1992) Chrysotile fiber is a potent mutagen in mammalian cells. *Cancer Res.*, 52, 6305-6309.
7. Xu A, Wu LJ, Santella RM, Hei TK. (1999) Role of oxyradicals in mutagenicity and DNA damage induced by crocidolite asbestos in mammalian cells. *Cancer Res*., 59(23), 5922-5926.
8. Mayall FG, Jacobson G, Wilkins R. (1999) Mutations of p53 gene and SV40 sequences in asbestos associated and non-asbestos-associated mesothelioma. *J. Clin. Pathol.*, 52(4), 291-293.
9. Kane AB. (1996) Mechanisms of mineral fibre carciongenesis. In: Mechanism of fibre carciongenesis. *IARC Scientific Publication*, N0. 140, 11-34.
10. Hei TK, Wu LJ, Piao CQ. (1997) Malignant transformation of immortalized human bronchial epithelial cells by asbestos fibers. *Environ. Health Perspect*., 105 (suppl.5), 1085-1088.
11. Hei TK, Xu A, Louie D, Zhao YL. Genotoxicity versus carcinogenicity: Implications from fiber toxicity studies. (In press) *Inhal. Toxicol.*
12. Carbone M, Fisher S, Powers A, Pass HI, Rizzo P. (1999) New molecular and epidemiological issues in mesothelioma: role of SV40. *J. Cell Physiol*., 180(2), 167-172.
13. Mossman BT, Faux S, Jassen Y, Jimenz LA, Timblin C, Zanella C, Goldberg J, Walsh E, Barchowsky A, Driscoll K. (1997) Cell signaling pathways elicited by asbestos. *Environ. Health Perspect*., 105 (suppl.5), 1121-1125
14. Porter AC, Vaillancourt RR. (1998) Tyrosine kinase receptor-activated signal transduction pathways which lead to oncogenesis. *Oncogene*, 16, 1343-1352.
15. Ding M, Dong Z, Chen F, Pack D, Ma WY, Ye J, Shi X, Castranova V, Vallyathan V. (1999) Asbestos induces activatior protein-1 transactivation in transgenic mice. *Cancer Res*., 59(8), 1884-1889.
16. Papa,V. and Beliore,A. (1996) Insulin receptors in breast cancer: biological and clinical role. *J. Endocrinol. Invest*., 19, 324-333.
17. Frittitta,L., Vigneri,R., Stampfer,M.R. and Goldfine,I.D. (1995) Insulin receptor overexpression in 184B5 human mammary epithelial cells induces a ligand-dependent transformed phenotype. *J. Cell Biochem*., 57(4), 666-9.

Antisense ATM Gene Therapy: A Strategy to Increase the Radiosensitivity of Human Tumors

C. Guha, U. Guha, and S. Tribius (Albert Einstein College of Medicine, Bronx, NY), A. Alfieri (Beth Israel Medical Center, New York, NY), D. Casper and P. Chakravarty (AECOM), W. Mellado, T.K. Pandita, and B. Vikram (AECOM)

Ataxia telangiectasia (A-T) is a rare, pleiotropic, autosomal human recessive disorder characterized by progressive neurological degeneration, growth retardation, premature aging, oculocutaneous telangiectasia, specific immunodeficiencies, high sensitivity to ionizing radiation (IR), gonadal atrophy, genomic instability, defective telomere metabolism, and cancer predisposition. Cells derived from A-T individuals exhibit a variety of abnormalities in culture, such as a higher requirement for serum factors, hypersensitivity to ionizing radiation, and cytoskeletal defects. The gene that is mutated in A-T has been designated ATM (A-T, mutated) and its product shares the PI-3 kinase signature of a growing family of proteins involved in the control of cell-cycle progression, processing of DNA damage, and maintenance of genomic stability. ATM appears to be required for initiation of multiple DNA-damage-dependent signal transduction cascades that activate cell-cycle checkpoints.

In order to increase the intrinsic radiosensitivity of human glioblastoma cells, we attenuated ATM protein expression by expressing antisense RNA to a functional domain of the ATM gene. This was achieved by expressing antisense RNA, targeting the PI-3 kinase domain of the ATM. The expression of antisense ATM RNA was verified by RT-PCR. Further, protein expression was examined by using ATM-specific antibody. With the decrease in ATM expression, we found that a constitutive expression of p53 and p21 increased, demonstrating radioresistant DNA synthesis and enhanced cell killing by ionizing radiations.

The intrinsic radiosensitivity of human tumors has been shown to be an independent prognostic factor following radiotherapy. Our studies suggest that the SF2 can be reduced by 50% by attenuation of the ATM protein with antisense ATM gene therapy. We used retrovirus-based gene therapy vectors, which would target cycling tumor cells and spare the noncycling brain parenchyma.

Attempts to increase the radiosensitivity of human tumors have explored the use of suicide gene-therapy approaches, using the viral thymidine kinase gene, the cytosine deaminase/thymidine kinase fusion genes, or expressing tumor necrosis factor alpha under the control of a radiation-inducible promoter. Long-term effects of such suicide gene therapy approaches to the nervous system are not known. However, one recent report demonstrated that adenovirus gene therapy with HSVtk resulted in chronic brain inflammation because of generalized expression of the suicide gene and the presence of a diffusible toxic product. Thus, the absence of a diffusible product in our approach may improve the therapeutic ratio. Moreover, by targeting an intrinsic radioprotective signal

transduction pathway, we eliminated an important problem that is common in most suicide gene therapies, i.e., inadequate prodrug delivery. Thereby, antisense-ATM gene therapy could serve as a paradigm for strategies targeting the intrinsic survival mechanisms of cancer cells after irradiation.

Identification of a Defined Region with Allelic Loss in Chromosome 11 During Radiation Carcinogenesis

Debasish Roy, Gloria M. Calaf, and Tom K. Hei

Breast cancer is the most frequent malignancy in women, and a cumulative lifetime breast cancer risk in an unselected population has been estimated to be about 10 to 12%, whereas hereditary factors may account for about 5 to 10% of all cases (*1*). It is a genetically heterogeneous disease, and a variety of genetic lesions have been identified during its progression (*2*). One type of genetic alteration common to many tumor types is loss of heterozygosity (LOH)/microsatellite instability (MSI), which often seems to unmask recessive mutations in tumor suppressor loci.

Among the various human chromosomal regions that are frequently found to be altered in breast cancer, chromosome 11 is unique in that it commonly undergoes LOH. At least three separate regions of LOH have been consistently identified (11p15-15.5, 11q13, and 11q23), pointing to a potentially complicated role for this chromosome in breast tumorigenesis (*3-4*). Among them, chromosome 11p15 has attracted considerable attention, due to the biological importance of this region to human disease. Apart from being an important tumor suppressor locus showing LOH in different cancers, 11p15 has been shown by linkage analysis to harbor the gene(s) for the Beckwith-Wiedemann syndrome (*5*). Microcell-mediated chromosome transfer of an intact copy of chromosome 11 into tumor cell lines has provided additional evidence of tumor suppressor gene function in melanoma, breast cancer, and cervical cancer (*6*). The critical region of 11p15 in breast tumors lies between the genetic markers TH and HBB at 11p15.5, in a segment appearing to span a maximum of 3 to 4 MB of DNA. Other genetic markers such as D11S1318 (11p15), D11S1323 (11p15.4), D11S1338 (11p15.5), D11S4046 (11p15.5), D11S4088 (11p15.5), and HRAS1, etc., are also belonging to that region and showed alteration at different stages of breast cancer progression. Frequent LOH has previously been reported on chromosome 11p15 in 20 to 30% of breast carcinomas and correlated with poor prognosis and tumor progression in breast cancer (*7*).

The neoplastic transformation of HBEC (human breast epithelial cells) in vitro represents a successful model for obtaining knowledge on the molecular and biological alterations that may contribute to the tumorigenic mechanisms (*3*). Therefore, to study the effect of ionizing radiation, particularly of high-LET (linear energy transfer) radiation, on the progression of human breast carcinogenesis, we have developed a model system of irradiated, transformed, and tumorigenic MCF-10F cells with graded doses of high-LET radiation (*8*). Highly polymorphic $(CA)_n$ repeat microsatellite markers were utilized to determine the incidence of LOH/MSI to a more refined position. The MCF-7 cell line was used as a positive control. Eight microsatellite markers from the map position 11p15.4-15.5 are associated with various known oncogenes/tumor suppressor genes involved during breast cancer progression.

Results from PCR-SSCP analysis showed significant and consistent alterations of microsatellite markers in the form of MSI/LOH from early to late stage of progression, as shown in Figure 1. Frequent allelic imbalances were directly proportional to the doses of radiation and had more deleterious effects when given in combination with 17-β estradiol (E) (Table 2). Few markers (D11S4046, D11S1318, D11S1338, and HBB) appeared to be altered at the late stage in mammary tumorigenesis, whereas the markers HRAS1 and D11S4088 started to alter from early stage. Other markers TH and D11S1323 started to become affected by the initial radiation responses. As chromosome 11p15 is a subregion that is associated with poor prognosis and tumor progression in breast cancer, any genetic alteration including MSI/LOH could compromise the function of a mutative tumor suppressor gene in this region and lead to tumorigenesis in breast cancer.

Table 1. Map position of microsatellite markers and location of important genes residing in chromosome 11p15.

Markers	**Map position**	**Important genes in this marker**	**Size range**
D11S4046	11p15.5	LOH in breast cancer	183-203
HRAS1	11p15.5	H-ras-1 oncogene	244-261
TH	11p15/5	Tsg101 gene, LOH in breast	244-260
D11S1318	11p15.5	Tsg in breast, B-W syndrome	123-145
D11S1338	11p15.5	Tsg in breast	255-265
HBB	11p15.4	Tsg in breast, Gap junctn comm.	201-207
D11S1323	11p15.4	Tsg in breast, WT2 gene	201-206
D11S4088	11p15.5-15.4	Tsg in breast	204-252

Table 2. Chromosomal abnormality (MI/LOH) status of different irradiated and tumorigenic cells lines by using different microsatellite markers on chromosome 11.

Breast Cell Markers	Map Position	60α	60/60α (Early)	60/60α (Late)	60E/ 60E	Tumor-T	MCF-7
D11S4046	11p15.5						
HRAS1	11p15.5						
TH	11p15.5						
D11S1318	11p15.5						
D11S1338	11p15.5						
HBB	11p15.4						
D11S1323	11p15.4						
D11S4088	11p15.5-p15.4						

	= Retention of Heterozygosity
	= Loss of Heterozygosity
	= Microsatellite Instability
	= Inconclusive

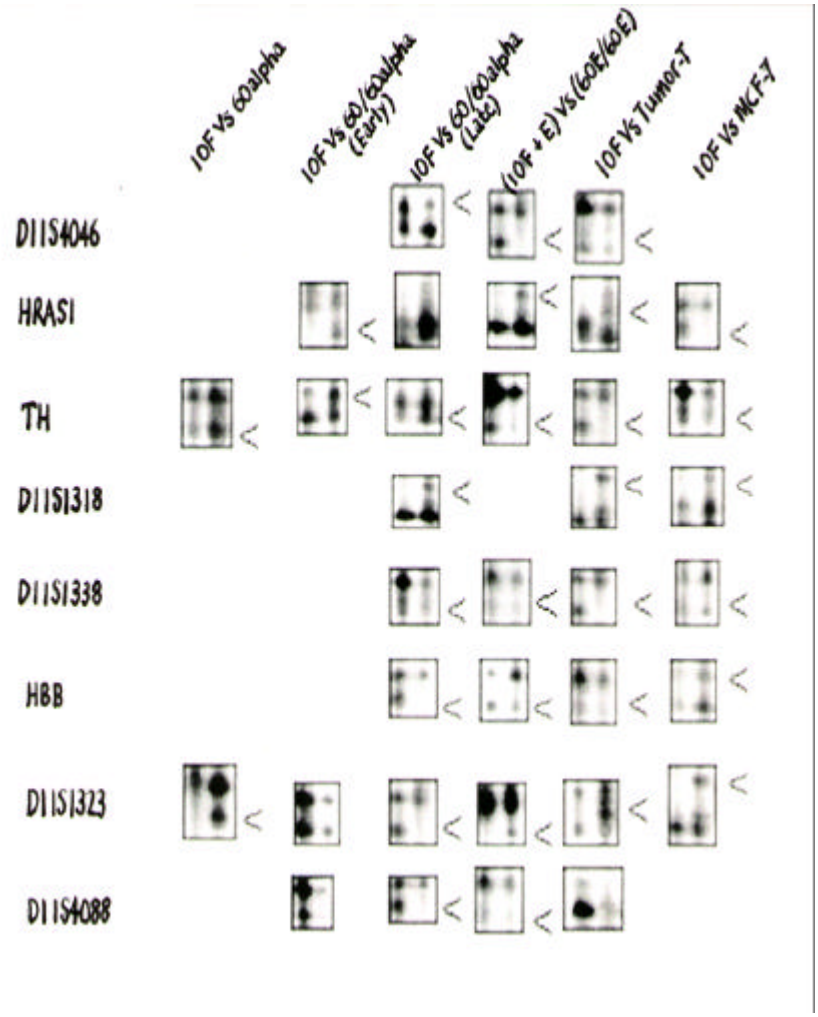

FIG. 1. Diagrammatic representation of frequent allelic imbalance at the chromosomal location 11p15.5 in various radiation- and estrogen-treated MCF-10F cells. "<" indicate prominent allelic alterations in the form of MSI/LOH.

References

1. Eeles RA, Stratton MR, Goldgar DE, and Easton DF. (1994) The genetics of familial breast cancer and their practical implications. Eur J Cancer 30:1383-1390.
2. Sato T, Tanigami A, Yamakawa K, Akiyama F, Kasumi F, Sakamoto G, and Nakamura Y. (1990) Allelotype of breast cancer: Cumulative allele losses promote tumor progression in primary breast cancer. Cancer Res 50:7814-7819.
3. Winqvist R, Mannermaa A, Alavaikko M, Blanco G, Kiviniemi H, Taskinen PH, Newsham I, and Cavenee W. (1993) Refinement of regional loss of heterozygosity for 11p15.5 in human breast tumors. Cancer Res 53:4486-4488.
4. Hampton G, Mannermaa A, Winqvist R, Alavaikko M, Blanco G, Taskinen PJ, Kiviniemi H, Newsham I, Cavenee W, and Evans G. (1994) Loss of heterozygosity in sporadic human breast carcinoma: A common region between 11q22 and 11q23.3. Cancer Res 54:4586-4589.
5. Karnik P, Paris M, Williams BR, Casey G, Crowe J, and Chen P. (1998) Two distinct tumor suppressor loci within chromosome 11p15 implicated in breast cancer progression and metastasis. Hum Mol Genet 7(5): 895-903.
6. Negrini M, Sabbioni S, Possiti L, Rattan S, Corallini A, Barbanti-Brodano G, and Croce CM. (1994) Suppression of tumorigenicity of breast cancer cells by micro-cell-mediated chromosome transfer: Studies on chromosome 6 and 11. Cancer Res 54:1331-1336.
7. Winqvist R, Hampton GM, Mannermaa A, Blanco G, Alavaikko M, Kiviniemi H, Taskinen PJ, Evans GA, Wright FA, Newsham I, and Cavenee WK. (1995) Loss of heterozygosity for chromosome 11 in primary human breast tumors is associated with poor survival after metastasis. Cancer Res 55:2660-2664.
8. Calaf G and Hei TK. (2000) Establishment of a radiation- and estrogen-induced breast cancer model. Carcinogenesis 21(4):769-776.

Vitamin D Receptor Gene in a High-LET-Radiation- and Estrogen-Treated Breast Cancer Model

Debasish Roy, Gloria M. Calaf, and Tom K. Hei

1,25-$(OH)_2$-Vitamin D_3, a physiologically active metabolite form of vitamin D, is a secosteroid hormone with a known differentiating activity and a regulatory function in bone metabolism and calcium homeostasis (*1*). It exerts its growth-regulatory effects through binding to the receptor (VDR), a member of the steroid/thyroid/retinoic acid receptor family, which function as a ligand-dependent transcription factor (*1*). VDRs mediate the action of their cognate ligand 1,25-dihydroxyvitamin D_3 by controlling the expression of hormone-sensitive genes (*2*). The VDR gene consists of nine exons and has several polymorphisms in intron 8 and exon 9, which are in linkage disequilibrium with each other (*3*).

This hormone promotes cellular differentiation and inhibits the proliferation and the invasive potential of a number of different cancer cells in vitro (*4-6*). Recently, $1,25(OH)_2D_3$ has been shown to induce apoptosis in human breast cancer cell lines (*7*) and can also inhibit tumor-induced angiogenesis (*8*). There is also accumulating evidence that vitamin D may be an important determinant of occurrence and progression of breast cancer too as the mortality rate increases significantly as the availability of UV-radiation exposure decreases, because the synthesis of vitamin D depends on UV radiation (*9*). VDR gene polymorphism might influence the outcome of women affected by breast cancer and may represent an important determinant in breast cancer evaluation, which might help to design targeted therapy. Due to the increase in different environmental radiation thresholds in recent times, accurate risk assessment of human exposure to these ionizing radiations, particularly high-LET radiations, becomes essential. Until recently, human-based models available for studying such interaction were limited. So, in order to study this interaction, we have developed a model system of human breast epithelial cells MCF-10F, where immortalized MCF-10F cells were irradiated with graded doses of high-LET radiation and treated with estrogen to achieve tumorigenic potential (*10*). The aim of this study was to analyze the expression and alteration of the VDR gene in this normal, irradiated, and tumorigenic breast model system, and to evaluate whether VDR can be used as a useful marker to study the progression of radiation- and estrogen-induced breast carcinogenesis.

A fragment of 195 bp from intron 8 and exon 9 of VDR gene was amplified by gene-specific PCR (Fig. 1A.). Expression of VDR gene in different cell lines were also determined by Northern blot analysis (Figure 1B.). The amplified fragments of 195bp from different cell lines were then directly sequenced in order to detect the mutational changes among different irradiated and tumorigenic cell lines with respect to control (Fig. 2.).

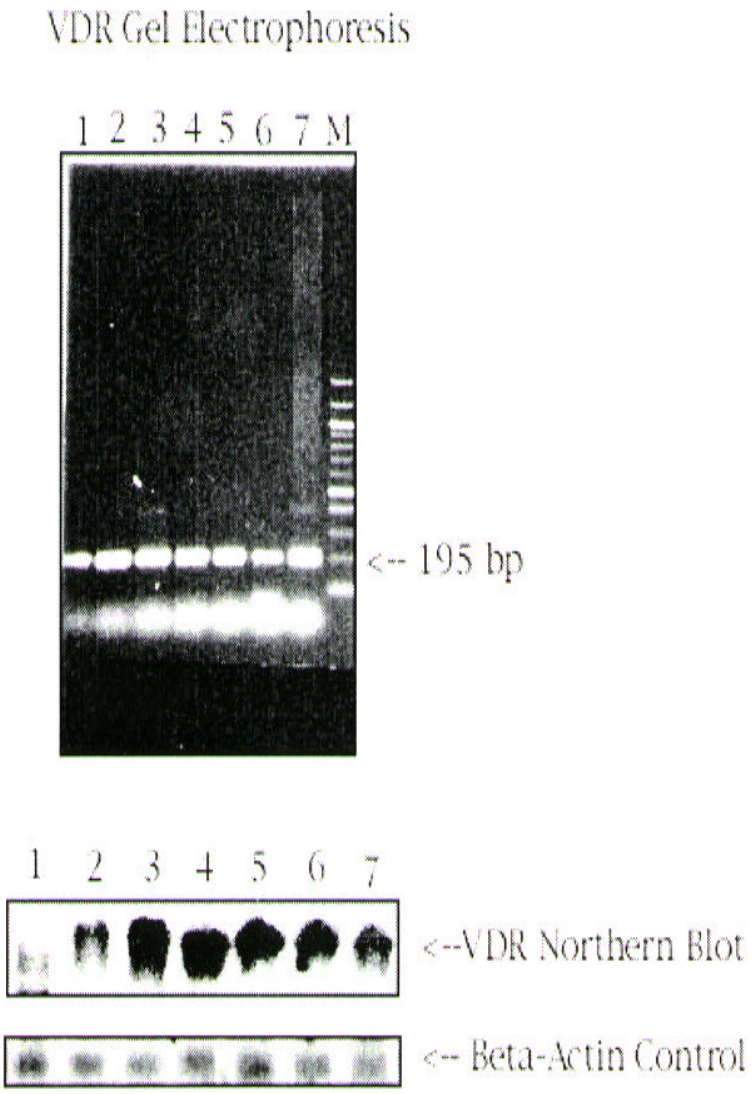

FIG. 1. A. VDR gel electrophoresis showing the 195 bp amplified fragment of VDR gene. M indicates 100 bp DNA ladder used as a marker. **B.** Northern blot analysis for VDR gene and β-actin used as a control. The different cell lines are: 1. MCF-10F; 2. 10F + Estrogen(E); 3. 10F + 60α; 4. 10F + 60α + E; 5. 10F + 60α/60α; 6. 10F + (60α +E)/ (60α + E); 7. Tumor-T [originate from 10F + (60α + E)/(60α + E)].

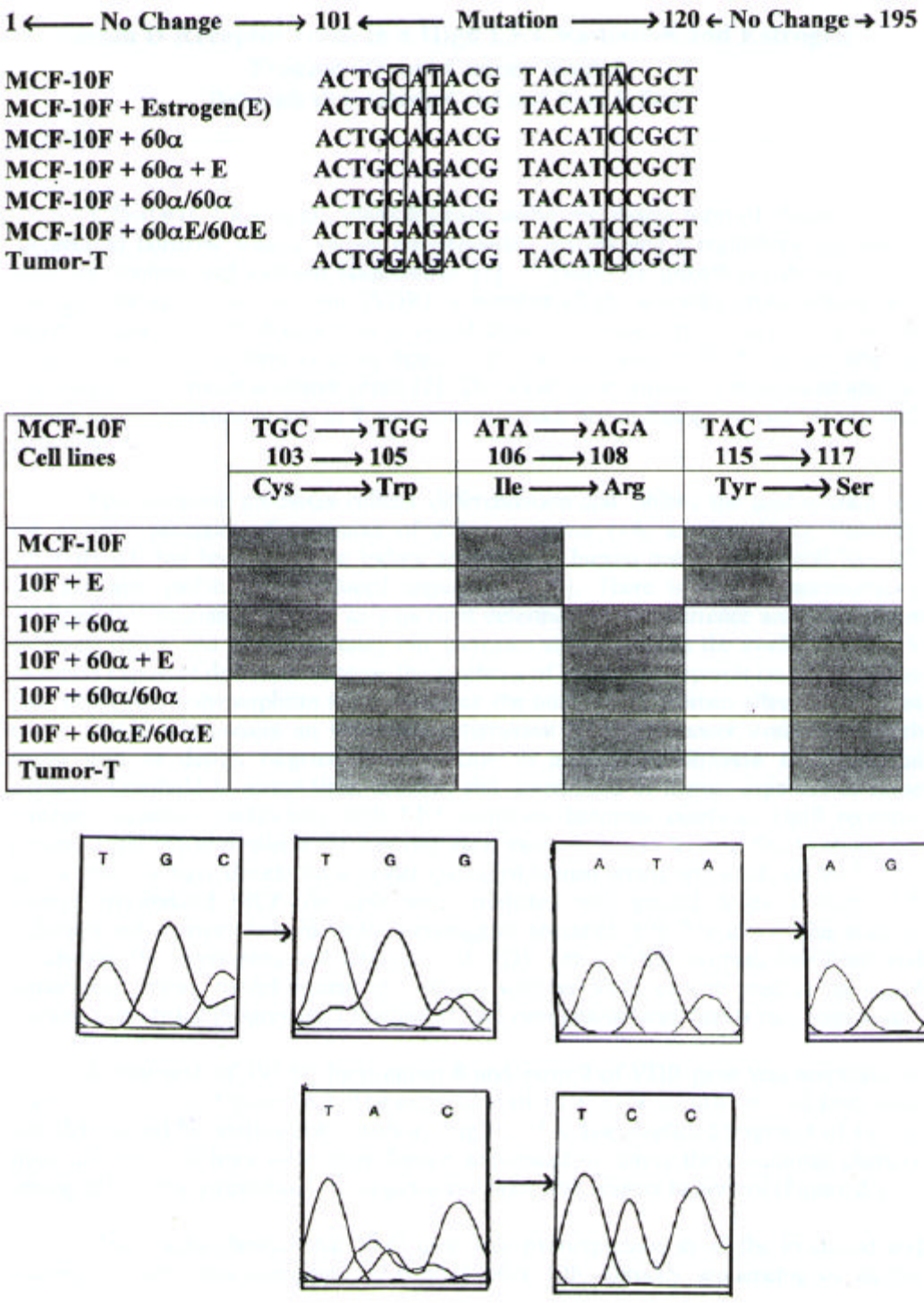

FIG. 2. Mutation spectrum of 195 bp amplified fragment of VDR gene from direct sequence analysis.

Results showed that VDR gene was overexpressed in all irradiated and tumorigenic cell lines compared to control MCF-10F. Direct sequencing of all the amplified fragments of the gene from different cell lines showed a C→G mutation at position 105, a T→G mutation at position 107, and a A→C mutation at position 116 in various irradiated and tumorigenic cell lines compared to control MCF-10F (Fig. 2). Considering all these observations, it becomes clear that the VDR gene is altered during breast tumor progression. So, the intact VDR gene may play a significant role in protecting against breast cancer and can be used as a marker to detect tumor progression.

References

1. Christakos, S., Raval-Pandya, M., Wernyj, R.P. and Yang W. (1996) Genomic mechanisms involved in the pleiotropic actions of 1,25-dihydroxyvitamin D_3. Biochem. J., **316** : 361 - 371.
2. McDonnell, D.P., Mangelsdorf, D.J., Pike, J.W., Haussler, M.R. and O'Malley, B.W. (1987) Molecular cloning of complementary DNA encoding the avian receptor for vitamin D. Science (Washington DC), **235** : 1214-1217.
3. Morrison, N.A., Qi, J.C., Tokita,A., Kelly, P.J., Nguyen, T.V., Sambrook, P.N. and Eisman, J.A. (1994) Prediction of bone density from vitamin D receptor alleles. Nature (Lond.), **367** : 284-287.
4. Peel, D.M., Skowronski, R.J., Leung, G.K., Wong, S.T., Stamey, T.A. and Feldman, D.(1994) Antiproliferative effects of 1,25-dihydroxyvitamin D_3 on primary cultures of human prostatic cells. Cancer Res., **54** : 805-810.
5. Mork Hansen, C., Frandsen, T.L., Brunner, N. and Binderup, L. (1994) 1(,25-Dihydroxyvitamin D_3 inhibits the invasive potential of human breast cancer cells in vitro. Clin. Exp. Metastasis, **12** : 195 – 202.
6. Feldman, D., Skowronski, R.J. and Peehl, D.M. (1995) Vitamin D and prostate cancer. Adv. Exp. Med. Biol., **375** : 53 – 63.
7. James, S.Y., Mackay, A.G. and Colston, K.W. (1996) Effects of 1,25-Dihydroxy vitamin D_3 and its analogues on induction of apoptosis in breast cancer cells. J. Steroid Biochem. Mol. Biol., **58** : 395-401.
8. Majewski, S., Szmurlo, A., Marczak, M., Jablonska, S. and Bollag, W. (1993) Inhibition of tumor cell-induced angiogenesis by retinoids, 1,25-dihydroxyvitamin D_3 and their combination. Cancer Lett., **75** : 35-39.
9. Habuchi, T., Suzuki, T., Sasaki, R., Wang, L., Sato, K., Satoh, S., Akao, T., Tsuchiya, N., Shimoda, N., Wada, Y., Koizumi, A., Chihara, J., Ogawa, O. and Kato, T. (2000) Association of vitamin D receptor gene polymorphism with prostate cancer and benign prostatic hyperplasia in a Japanese population, Cancer Res., **60** : 305-308.
10. Calaf, G. and Hei, T.K. (2000) Establishment of a radiation- and estrogen-induced breast cancer model. Carcinogenesis, **21**, (4) : 769-776.

STUDIES RELATED TO RADIATION THERAPY

Towards Optimal External-Beam Fractionation for Prostate Cancer

David J. Brenner

As an increasing number of men are undergoing radiotherapy for prostate cancer, and at younger ages it is becoming more and more important to define optimal radiotherapeutic (RT) regimens to treat the disease. A great deal of effort has rightly been put into improving dose distributions, through 3-D conformal RT and intensity-modulated RT, as well as through brachytherapy.

Less attention has, however, been paid to fraction size. By and large, most protocols for external-beam treatment of prostate cancer have adhered to 1.8- to 2-Gy fractions, although results with hyperfractionation and hypo-fractionation have recently been reported. In part, this lack of attention to fraction size can be attributed to the comparatively slow-growing nature of prostate tumors, implying that overall treatment time is unlikely to be a critical factor.

However, fractionation plays another key role in radiotherapy, typically providing a therapeutic advantage between tumor control and late sequelae. Generally speaking, this therapeutic advantage comes by fractionating as much as possible, in that fractionation spares late-responding normal tissues more than tumors, because tumors normally respond as early-responding tissue -- in the language of the LQ model, fractionation spares tissues with a low α/β ratio (late-responding tissues) more than it does tissues with a high α/β ratio (early-responding tissues typical of most tumors).

However, as we have known for many years, prostate tumors are highly atypical of most malignancies. Most prostate tumors consist of an extremely low proportion of cycling cells but with many dormant cells waiting to be recruited into cycle if stimulated. So, from the perspective of radiation sterilization, our major task is probably to sterilize non-cycling, as well as cycling, prostate cells. In such a situation, the prostate would be expected to respond to changes in fractionation as a late-responding tissue, in which case the rationale for increased fractionation would disappear.

These concepts have recently been quantified by estimating an average α/β value for prostate tumors directly from clinical data, and the value obtained was indeed typical of a late-responding tissue, about 1.5 Gy (*1-2*).

The same conclusion can be drawn from a recent report by Martinez *et al.* (*3*) on HDR brachytherapy boosts after external-beam treatment for unfavorable prostate cancers. HDR brachytherapy was given either as three 6-Gy treatments or two 9-Gy treatments. An α/β value of 10 Gy for the prostate tumors would result in essentially identical tumor control for these two treatments, whereas an α/β value of 1.5 Gy would result in significantly increased tumor control for the 2×9 Gy compared to the 3×6 Gy boost. In fact, a significantly increased tumor control was seen with the 2×9 Gy boost (96% *vs.* 70% at 3 years, p=0.002), consistent with a low α/β value.

What does this mean for external-beam radiotherapy of the prostate? Essentially what we have is a late-responding target tissue (the prostate tumor), adjacent to which are the bladder and rectum, both of which can exhibit early and late morbidity. Thus moving to a smaller number of larger fractions (hypo-fractionation) should affect tumor control and late morbidity in the same way, so, assuming the prescribed dose is decreased appropriately, no change in tumor control or late- sequelae rates would be expected. In other words, more convenient schedules, consisting of fewer larger fractions, should achieve equal tumor control with no increase in late effects.

As an added bonus, because early sequelae are less responsive to changes in fractionation, then for a given level of tumor control and late sequelae, one would expect less early morbidity from a hypo-fractionated regimen. While early sequelae are not generally dose limiting, a significant reduction in early GU and GI complications would certainly be welcome.

These notions are illustrated in Figure 1 for a "standard" prostate cancer external-beam regimen of 72 Gy in 36 2-Gy fractions. We assume typical α/β values for late-responding tissues (i.e., for the prostate, and for late morbidity) and a typical α/β value for early morbidity. Then 72 Gy in 2-Gy fractions would be equivalent, both in tumor control and late morbidity, to about 57 Gy given in 3-Gy fractions. However if we did give 57 Gy in 3-Gy fractions, this would be equivalent, in terms of early morbidity, to 62 Gy in 2-Gy fractions. So the net result of moving from 72 Gy in 2-Gy fractions to 54 Gy in 3-Gy fractions would be an unchanged level of tumor control and late sequelae, but a considerable reduction in early sequelae -- as well as a treatment regimen that is more convenient for the patient, and less resource-intensive for the clinic.

While a move to larger fractions may initially appear contrarian, in fact, highly hypo-fractionated schemes have been used in Britain and Canada for many years to treat prostate cancer, without excessive late sequelae.

In summary, while the advances made in the dose delivery of radiotherapy of prostate cancer have been very encouraging, improving treatments by tailoring site-specific fractionation patterns to the basic radiobiology also looks promising. Hypo-fractionation for prostate cancer appears to be 1) as efficacious as standard fractionation, 2) more convenient for the patient, both in terms of logistics and acute morbidity, as well as being 3) less resource-intensive than standard fractionation.

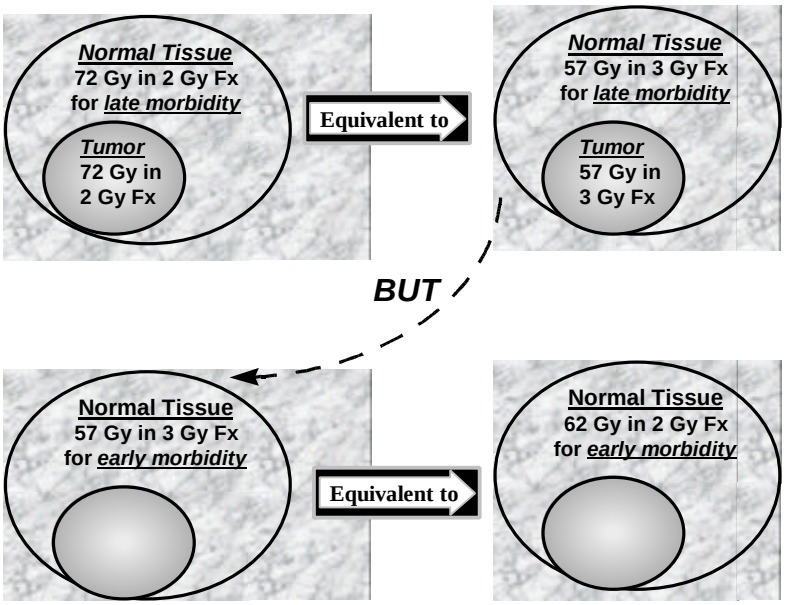

FIG. 1. Schematic of estimated equivalence between a "standard" 36 × 2-Gy (72 Gy) external-beam prostate cancer treatment, and a hypo-fractionated 19 × 3-Gy (57 Gy) treatment for a prostate tumor and adjacent normal tissue. Equivalency is expected both for tumor control and for late sequelae. However, for early sequelae the hypo-fractionated treatment is equivalent to 62 Gy in 2-Gy fractions which, compared to the original 72 Gy in 2-Gy fractions, means that the hypo-fractionated schedule should result in considerable sparing of early morbidity. Calculations were performed with α/β values of 1.5 Gy (prostate tumor), 1.5 Gy (late-responding normal tissue), and 10 Gy (early-responding normal tissue), though the principles would remain valid as long as the prostate tumor has an α/β value comparable to late-responding normal tissue.

References

1. Brenner DJ, Hall EJ. Fractionation and protraction for radiotherapy of prostate carcinoma. *Int J Radiat Oncol Biol Phys* 1999;43:1095-1101.
2. Brenner DJ, Hall EJ. Low ??? values for prostate appear to be independent of modeling details. *Int J Radiat Oncol Biol Phys* 2000;47:538-9.
3. Martinez AA, Kestin LL, Stromberg JS, *et al.* Interim report of image-guided conformal high-dose-rate brachytherapy for patients with unfavorable prostate cancer: the William Beaumont phase II dose-escalating trial. *Int J Radiat Oncol Biol Phys* 2000;47:343-352.

Adjuvant Radiotherapy for DCIS ? Pyrrhic or Low Risk?

David J Brenner, with Peter B Schiff and Lydia B Zablotska (Division of Epidemiology, Joseph L. Mailman School of Public Health, Columbia University)

A recent report (*1*) from EORTC on breast-conserving surgery with or without radiation for treatment of ductal carcinoma in situ (DCIS) showed a statistically significantly increased rate of cancers in the contralateral breast in the surgery + radiation arm, compared to surgery only (21/507 vs. 8/503, hazard ratio 2.6, p=0.01). The authors point out[1] that if this increase was truly radiation induced, it might well cancel out (and more) the clinical gains afforded by adjuvant radiotherapy for DCIS.

There is convincing evidence that this apparent increase i n contralateral breast cancer (*1*) is unlikely to be radiation induced. Specifically, we have used data in the SEER (Surveillance, Epidemiology and End Results) tumor registry for a cohort analysis of 32,000 women with DCIS treated between 1973 and 1993, directly comparing second-cancer risks in women who did or did not receive radiotherapy. This large number allows the hypothesis that radiotherapy induces an increased rate of second cancer in DCIS patients to be tested with considerable statistical power.

Details of the SEER DCIS subcohorts are shown in the Table. For comparison, in the EORTC study (*1*), the mean age at DCIS diagnosis was 53 and the mean follow up was 4.3 years.

The techniques used to estimate the relative risk of second cancer in the radiation vs. the no-radiation SEER DCIS subcohorts are as described elsewhere (*2*). The relative risks for radiation vs. no radiation were estimated using Mantel- Haenszel Poisson models, adjusting for age at, and calendar year of, DCIS diagnosis, and follow-up time.

For second malignancies in the contralateral breast, the adjusted relative risk for radiation vs. no radiation was 0.98 [95% CI: 0.80, 1.19]; when only long term (>10 y) survivors are considered, the adjusted relative risk was 1.07 [0.54, 2.12]. For all second malignancies, the adjusted relative risk was 1.00 [0.85, 1.18]. None of the adjusted relative risks were statistically significant.

These null results are consistent with the corresponding US study (*3*) on DCIS treatment, where no increase in contralateral breast cancers was observed in the radiotherapy group. The mean radiation doses to the contralateral breast are probably comparable in the EORTC (*1*) and US (*3*) studies (*4*), in that the EORTC protocol utilized wedge compensators, and the US protocol utilized half-beam blocks and, optionally, wedges.

These null results are also consistent with estimates of radiation-induced breast cancer derived from studies of A-bomb survivors (*5*). For example, a fractionated radiation dose of 2 Gy [an upper-end estimate of the average contralateral breast dose (*4*)]

to the breast of a 55 year old Caucasian woman gives a predicted lifetime breast-cancer risk of 0.33% -- a relative risk of 1.03 compared to the background lifetime risk of about 11%.

We conclude that the increased cancer incidence in the contralateral breast reported in the radiation arm of the EORTC DCIS study (*1*) is unlikely to be a consequence of radiation exposure to the contralateral breast, and is more likely to be an artifact of confounding variables. Any gains afforded by adjuvant radiotherapy in treating DCIS are unlikely to be ameliorated by an increase in second cancers.

Table 1. Details of women in SEER tumor registry treated for DCIS.

	No radiotherapy	**Radiotherapy**
DCIS cases with known treatment and follow up	26,390	5,650
Mean follow up (y)	6.7	4.2
Mean age at DCIS diagnosis (y)	58	57
Mean calendar year of DCIS diagnosis	1989	1992
Second cancers (all malignancies diagnosed >2 months after DCIS diagnosis)	1,816	270
Second cancers in contralateral breast	868	129

References

1. Julien J-P, Bijker N, Fentiman IS, et al. Radiotherapy in breast-conserving treatment for ductal carcinoma in situ: first results of the EORTC randomised phase III trial 10853. *Lancet* 2000; **355**: 528-33.
2. Brenner DJ, Curtis RE, Hall EJ, Ron E. Second malignancies in prostate carcinoma patients after radiotherapy compared with surgery. *Cancer* 2000; **88**: 398-406.
3. Fisher B, Dignam J, Wolmark N, et al. Lumpectomy and radiation therapy for the treatment of intraductal breast cancer: findings from National Surgical Adjuvant Breast and Bowel Project B-17. *J Clin Oncol* 1998; **16**: 441-52.
4. Fraass BA, Roberson PL, Lichter AS. Dose to the contralateral breast due to primary breast irradiation. *Int J Radiat Oncol Biol Phys* 1985;**11**: 485-97.
5. Land CE. Radiation and breast cancer risk. *Prog Clin Biol Res* 1997; **396**: 115-24.

THE RADIOLOGICAL RESEARCH ACCELERATOR FACILITY

THE RADIOLOGICAL RESEARCH ACCELERATOR FACILTY

An NIH-Supported Resource Center
WWW.RARAF.ORG
Director: David J. Brenner, Ph.D., D.Sc.
Manager: Stephen A. Marino, M.S.
Chief Physicist: Gerhard Randers-Pehrson, Ph.D.

Research Using RARAF

We have reached something of a milestone this year– experiment number 100! The last experiment listed in this report is the 100 th experiment proposal since RARAF moved from Brookhaven National Laboratory to Nevis Laboratories.

There has been considerable interest this year in the "bystander" effect in which only some cells are irradiated and there is a response greater than would be expected for the fraction of cells irradiated. In some experiments, the unirradiated cells can be identified due to a different staining and scored directly. Several experiments with a variety of endpoints have been undertaken to determine the size of the effect and whether the observed effects are due to direct cell-to-cell communication through their membranes or indirect, longer-range communication through some release into the cell medium. Both the microbeam and the track-segment facilities have been utilized in various investigations.

Table 1 lists the experiments performed at RARAF during the period May 1, 1999 through April 30, 2000 and the number of days each was run in this period. Seventeen different experiments were run during this 12-month period, about 20% more than the last two years, but about average for 1992-99. Five experiments were undertaken by members of the CRR, supported by grants from the National Institutes of Health (NIH) and the Department of Energy (DOE), and twelve by outside users, supported by various grants and awards from NIH and NASA. Brief descriptions of these experiments are given here:

Jamie Milligan of the University of California at San Diego continued his experiment to determine the mean number of damages per cluster in DNA caused by high-LET radiation (Exp.61). Bare SV40 virus DNA is irradiated with ^{4}He ions using the track-segment facility. Samples are treated with graded doses of radical scavengers to observe changes in the cluster sizes of damaged DNA. Large numbers of samples are required because of the number of radiation dose/scavenger concentration combinations and to have macroscopic amounts of single- and double-strand breaks. Doses as high as 1600 Gy were given to individual samples.

Studies using the RARAF single-particle microbeam facility to irradiate cell nuclei with specific numbers of ^{4}He ions to observe micronucleus production, cell growth, and progression through the cell cycle in normal human fibroblasts (Exp. 71) were continued by Charles Geard and Brian Ponnaiya of the CRR. This effort involves the bystander effect. In some experiments only a fraction of the cell nuclei are irradiated (2-20%) and the cells are observed for a result greater than would be expected for the fraction of cells hit. In other experiments, only some of the cells are stained with the dye used for observing nuclei during irradiation; the others are stained with a different vital

dye and are not irradiated because they do not fluoresce with the wavelength of light used for the microbeam and are not visualized. Unirradiated cells can be observed for scoring by using a different excitation wavelength. No difference in result has been observed for the two methods. Cell densities have been varied from intimate contact between cells to large separations. In other experiments, only the cytoplasm of the cells or only the cell medium has been irradiated. While there have been some effects observed for cytoplasmic irradiation, irradiation of only the medium with as many as 100 particles/cell yielded no difference from the controls. Additional studies of the effect of the irradiation of the cell medium are being carried out using the track-segment facility, where larger numbers of cells can be used. Stainless steel rings have Mylar epoxied to both sides, cells are plated on both inner surfaces and the volume is filled with medium. Cells on one surface are irradiated with ^{4}He ions; cells on the opposite surface are unirradiated because the particle range is much too short. This eliminates all possibility of cell-to-cell contact.

Satin Sawant of the CRR continued investigations involving the oncogenic neoplastic transformation of mouse C3H 10T½ cells (Exp. 73). Cells were irradiated individually through the nucleus or the cytoplasm, or a fraction of the cells were irradiated through the nucleus to observe the bystander effect. Because of the low yield of transformation, a considerable number of replicate experiments must be performed to obtain reasonable statistics.

Mutations induced at the S1 locus of human-hamster hybrid (A_L) cells by an exact number of ^{4}He ion traversals using the microbeam facility (Exp. 76) continue to be investigated by Tom Hei, Hongning Zhou, and An Xu of the CRR. The primary focus this year has been on extra-nuclear and extra-cellular targets. To evaluate the role of nitric oxide (NO), an important bioregulatory molecule, in mediating the mutagenicity of cytoplasmic irradiation, cells were irradiated with 8 ^{4}He ions through the cytoplasm in the presence or absence of L-NMMA, which has been shown to competitively inhibit nitric oxide synthases (NOS). Pretreatment with L-NMMA suppressed mutation induction by ~3-fold to near background level. In contrast the treatment had no effect on the mutagenic yield in A_L cells irradiated by 2 alpha particles through the nucleus. In other experiments, irradiation through the nuclei of 5-20% of randomly selected cells with 1-2 alpha particles each results in mutant fractions that are significantly higher than expected assuming no bystander modulation effect. Analysis by multiplex PCR shows that the types of mutants induced are significantly different from those of spontaneous origin. Pre-treatment of cells with the radical scavengers DMSO or NAC only had limited effect on the mutagenic incidence, however, pretreatment with lindane or Octanol, which inhibit gap junction cell-cell communication, significantly decreased the mutant yield.

Development of specialized neutron proportional counters (Exp. 82) was resumed by Gerhard Randers-Pehrson and Haijun Song of the CRR. The first counter being investigated uses a gas mixture consisting primarily of nitrogen. Monoenergetic neutrons produced by the Li(p,n) reaction using a thin target are being used to detect a resonance in the nitrogen at around 430 keV. If this detector is successful, other gas fillings may be tried.

William Morgan of the University of Maryland, in collaboration with Charles Geard of the CRR, continued use of the microbeam facility to investigate normal human fibroblasts derived from people with Nijmejen breakage syndrome (Exp. 84). These cells are deficient in a component of the repair process and are observed for intra-nuclear localization of repair proteins following site-specific irradiation.

Calibration of a portable neutron spectrometry system to cover the energy range from 20 keV to 500 MeV for use on the space shuttle and the manned mission to Mars (Exp. 89) is being performed by Richard Maurer, David Roth, Raul Fainchtein and others at the Applied Physics Laboratory of Johns Hopkins University. The low-energy portion of the neutron spectra is measured using ^{3}He proportional counters and the higher energy section is measured using a 5-mm-thick lithium-drifted silicon detector. This year, measurements were conducted to refine the discrimination in the ^{3}He counters of the pulses produced by neutrons from those produced by gamma rays in order to reduce the low-energy limit of the detector.

David Boothman of the University of Wisconsin at Madison, in collaboration with Charles Geard of the CRR, is examining the expression of radiation-induced proteins associated with apoptosis in human breast cells (Exp. 90). Breast carcinoma MCF-7 cells with and without a p53 construct are irradiated through the nucleus with ^{4}He ions using the single-particle microbeam and assessed for cell cycle progression, the incidence of micronuclei, and apoptosis. Cells undergoing apoptosis are examined to determine protein expression that may be associated with this process.

An experiment employing cDNA microarray technology (Exp. 92) was begun by Sally Amundson of the National Institutes of Health (NIH). ML-1 cells were irradiated with 0.43 MeV neutrons to determine gene induction as a function time after irradiation. RNA was extracted from the cells for use in microarray hybridization. Software is being developed by collaborators in the Human Genome Research Institute to allow cluster analysis of the data to detect genes with coordinate regulation. If this approach is successful, additional experiments will be performed to determine gene induction as a function of neutron energy.

George Sgouros and Ase Ballungrud of the Memorial Sloan-Kettering Cancer Institue along with Edward Lin, a high-school student from New York City, used the track-segment facility to simulate dual-agent radioimmunotherapy treatment of cancer cells (Exp. 93). Alpha-particle emitters such as ^{213}Bi have been used in the treatment of cancer to label antibodies against tumor-cell associated antigens. It has been proposed to follow this treatment with one using antibodies labeled with a short-range (internal conversion) electron emitter, hopefully producing a synergistic effect. Human breast carcinoma MCF-7 cells were irradiated with X rays, 120 keV/ μm ^{4}He ions or alpha particles followed by X rays and observed for survival.

Brian Ponnaiya of the CRR is developing a protocol in which small numbers of cells, as little as a single cell, can be observed for gene expression using reverse transcription polymerase chain reaction (RT-PCR) (Exp. 94). Copies of DNA segments are created by reverse transcription from RNA produced by the cell(s). The DNA is then amplified by PCR until enough material is available for gel electropheresis. This method permits observation of individual responses to radiation instead of just the

average response of a large number of cells. Single cells are obtained using a micromanipulator on the off-line microscope system of the microbeam facility. An efficiency of 80% has been achieved, i.e., 80% of the time a product is obtained when starting with a single cell irradiated using the microbeam facility.

Stig Palm of Göteborg University in Sweden spent two months at RARAF using the microbeam facility to simulate ^{211}At irradiations (Exp. 95). Astatine-211 is an alpha-particle emitter being studied at Göteborg for use in radioimmunotherapy (RIT). The doses delivered to the cells are determined by a complex calculation, and it was desir able to try to obtain some independent data of cell response to small numbers of alpha particles as a test to determine the accuracy of the calculations.

Radiation damage to the enamel of human teeth, observed using electron spin resonance (ESR), does not fade with time, making it useful as a retrospective biological dosimeter. It is of particular interest with respect to exposures of Japanese atomic bomb survivors since there continues to be controversy over the dosimetry calculations. John Zimbrick and Jeanine Katanic of Purdue University are studying the response of tooth enamel to neutrons (Exp. 96), an area in which there has been little investigation and considerable uncertainty. Small samples of powdered enamel irradiated with 10 Gy of 1-MeV neutrons showed no significant differences from the controls. An additional irradiation using 14-MeV neutrons is planned.

John Petrini of the University of Wisconsin and William Morgan of the University of Maryland, in collaboration with Charles Geard and Brian Ponnaiya of the CRR, have begun experiments to investigate repair protein complex localization after irradiation by ^{4}He ions (Exp. 97). Human or mouse fibroblasts are irradiated with a specific number of particles through the cell nucleus using the microbeam facility and examined for localization at DNA damage sites of the Mre11 complex and complex-interacting proteins.

Robert Ullrich of the University of Texas Medical Branch (UTMB) has begun an investigation into chromosomal instability (Exp. 98) in collaboration with Brian Ponnaiya of the CRR. It has been observed that the number of chromosomal aberrations in some irradiated cells decreases to the background level after a few cell passages, but may increase again several passages later. Human breast epithelial cells (MCF-10A) were irradiated using the microbeam facility and observed for chromosomal aberrations during successive passages to determine the amount of instability produced by specific numbers of ^{4}He ions.

Charles Limoli of the University of California at San Francisco and William Morgan of the University of Maryland, in collaboration with Charles Geard of the CRR, initiated another chromosomal instability experiment (Exp. 99). Chinese hamster ovary (CHO) cells were irradiated with ^{4}He ions using the microbeam facility and the number of chromosomal aberrations was assessed at various passages afterward.

A study of the effects of ^{4}He ions on normal and Ataxia telangectasia human fibroblasts using the comet assay (Exp. 100) was begun by T. Kumaravel of the National Institutes of Health in collaboration with Brian Ponnaiya and Adayabalam Balajee of the CRR. This procedure, like the single-cell PCR assay, is a way to observe effects in individual cells. Because the cells are irradiated using the microbeam facility, the

number of ^{4}He ion traversals is known, so variability in response is solely due to individual variability in the cells and the stochastic nature of the radiation.

Table 1. Experiments Run at RARAF May 1, 1999 - April 30, 2000

Exp. No.	Experimenter	Institution	Exp. Type	Title of Experiment	No. Days Run
61	S. Milligan	Univ. of California San Diego	Chemistry	Yields of strand breakage produced in DNA by radiation associated with radon decay	4.5
71	C. R. Geard, B. Ponnaiya	CRR	Biology	Chromosome aberration and micronucleus production in human cells lines by specific numbers of α particles	21.5
73	S. Sawant	CRR	Biology	Neoplastic transformation of C3H 10T½ cells by specific numbers of α particles	28.0
76	T. K. Hei, H. Zhou, A. Xu	CRR	Biology	Mutation at the S1 locus of human-hamster hybrid (A_L) cells by specific numbers of α particles	29.5
82	G. Randers-Pehrson, H. Song	CRR	Physics	Neutron detector development	13.0
84	W. Morgan (Geard)	UCSF	Biology	Genomic instability using specific numbers of α particles	2.0
89	R. H. Mauer, et al.	Johns Hopkins Univ.	Physics	Calibration of a portable real-time neutron spectrometry system	4.0
90	D. Boothman (Geard)	Case Western Reserve Univ.	Biology	Expression of radiation-induced proteins associated with apoptosis	2.5
92	S. Amundson	NIH	Biology	Functional genomics of cellular response to high-LET radiation	1.0
93	G. Sgouros	Memorial Sloan-Kettering	Biology	Alpha particle induced radiosensitization: A strategy for targeted therapy of micrometastases.	1.0
94	B. Ponnaiya	CRR	Biology	Development of single cell RT-PCR	5.5
95	S. Palm	Göteborg University	Biology	Simulation of ^{211}At cell irradiation	2.0
96	J. Zimbrick, J. Katanic	Purdue University	Chemistry	Response of tooth enamel to neutrons	1.5
97	J. Petrini, W. Morgan (Geard, Ponnaiya)	Univ. of Wisconsin/ Univ. of Maryland	Biology	Repair protein complex localization after irradiation	0.5
98	R. Ullrich (Ponnaiya)	UTMB	Biology	Chromosomal instability in MCF-10A human mammary epithelial cells	4.5
99	C. Limoli, W. Morgan (Geard)	UCSF/ Univ. of Maryland	Biology	Chromosomal instability in Chinese hamster ovary (CHO) cells	1.0

Exp. No.	Experimenter	Institution	Exp. Type	Title of Experiment	No. Days Run
100	T. Kumaravel (Ponnaiya, Balajee)	NIH	Biology	Comet assay of normal and *Ataxia telengectasia* cells irradiated with specific numbers of α particles	1.0

Accelerator Utilization and Operation

Accelerator usage is summarized in Table 2. Use of the accelerator for radiobiology and associated dosimetry increased by about 20% over last year, and is ~30% higher than the average for 1992-98. As was the case last year, almost 90% of the accelerator use for radiobiology and 70% of the accelerator use for all experiments was for microbeam irradiations. These experiments require considerable beam time to obtain sufficient biological material, especially for low-probability events such as trans formation and mutation. In addition, there has been considerable interest in "bystander" experiments that produce low yields even for normally frequent responses.

Utilization of the accelerator by radiological physics and chemistry increased 50% over last year and was considerably higher than the average for the past 7 years. Two of the projects (Exps. 89 and 95) should continue through at least next year.

Time spent on radiation safety system inspections continues to be minimized by not inspecting those systems that are rarely, if ever, used, such as the ^{137}Cs source used only for ionization chamber calibrations or the 50-kV X-ray source. No inspection is performed if the accelerator will be unused during the month due to meetings or installation of modifications. Any target stations that have not been used for a while are also not inspected. Of course, any facility is inspected before it is put back into use.

Accelerator reliability was about normal this year. Maintenance and repair time was about the same as last year. No major repairs or modifications to the accelerator were performed. The Freon 113 that has been used in the past to cool the ion source in the Van de Graaff terminal is no longer manufactured because it is a chlorofluorocarbon and can damage the ozone layer. It has been replaced with DuPont Vertrel XF, a hydrofluorocarbon that is still manufactured because it is much less damaging.

Table 2. Accelerator Use, May 1999 - April 2000. Percent Usage of Available Days.

Radiobiology and associated dosimetry	38%
Radiological physics and chemistry	9%
On-line facility development and testing	17%
Off-line facility development	25%
Safety system	2%
Accelerator-related repairs / maintenance.	11%

Development of Facilities

The considerable development of the single-particle microbeam facility is described here briefly:

- The single electrostatic quadrupole quadruplet constructed last year to focus the particle beam to ~2-μm diameter has been installed in the existing facility. In testing, it reduced the beam size to 20-μm diameter for an object aperture with a diameter of 50 μm, a demagnification factor of 2.5. Further testing will be done to try to obtain the calculated demagnification factor of 4 and the object aperture size will be reduced to reduce the final beam-spot diameter.
- A magnetic quadrupole lens has been installed in the beam line between the last two bending magnets for the microbeam in order to focus the beam on the object aperture of the electrostatic quadrupole system. This should assist in increasing the demagnification factor of the quadruplet lens.
- A fixture has been designed and is being constructed to rotate the ceramic rods used for the quadrupole electrodes so that their surfaces can undergo ion implantation. This will reduce the resistance and hopefully eliminate occasional electrical breakdown in the electrodes.
- The test laser system obtained from the University of Arkansas has been used successfully to oblate aluminum from a solid target. Work will now begin on extracting the ions produced by the laser pulses.
- A specially designed prism has been obtained that will be used along with a light pipe to couple our fast wavelength switcher to the microscope on the microbeam facility so that wavelengths can be changed rapidly under computer control to excite different cell stains.
- Design has been completed of a 90º magnet to be placed between the exit of the Van de Graaff and the switching magnet in order to direct the charged-particle beam to the floor above. It is capable of bending the heavy ion beams that will be eventually produced by the laser ion source under development. The magnet is under construction and should be delivered in December 2000. Because there now will be less room in this region, several new beam-line components have been purchased to replace existing ones in order to minimize the space required. Whereas the older components used o-ring seals, the new components all use metal vacuum seals that should result in better vacuum.
- Construction of a new laboratory on the floor over the exit of the Van de Graaff should begin in early December. This will house the next generation microbeam facility with an ultimate beam diameter of <0.5 μm.
- A new 650-MHz Pentium III computer with a large number of available slots has been purchased to control the microbeam experiment. In addition to being considerably faster than the computer now in use, all the control boards can be mounted in the computer. Presently many of the boards are mounted in an expansion chassis, which slows the system down somewhat.
- A new version of the image-analysis software has been obtained. This should provide "watershed" capability, i.e., the ability to find the boundary between cell

nuclei that are in contact by observing reductions in fluorescence and "pinching" of the outer edge of the image where the nuclei touch.

- Design has begun of an imaging system to observe the size of the focused microbeam using secondary electrons created by the charged particles.

Personnel

The Director of RARAF is Dr. David Brenner. The Van de Graaff accelerator is operated by Mr. Stephen Marino and Dr. Gerhard Randers-Pehrson.

Dr. Haijun Song, a post-doctoral fellow, left in February of this year to pursue a career in medical physics at Thomas Jefferson University Hospital in Philadelphia.

For the first time in six years, RARAF has a physics technician. Mr. Mutian Zhang started as a part-time employee in March of this year and became a full-time employee in July.

Dr. Alexander Dymnikov, an expert on ion beam transport who joined the RARAF staff in February, 1999 as a Visiting Research Scientist to assist in the development of electrostatic lenses for the microbeam, left RARAF in April 2000.

Mr. Francois Lueg-Althoff, an undergraduate student from the University of Aachen in Jülich, Germany, arrived in October 1999 for a nine-month visit to do his Praxissemester (practical semester) and Diplomarbeit (undergraduate thesis). He returned home in July of this year. As his thesis project, he irradiated track- etchant plastic using the single-particle microbeam to determine the radial distribution of alpha particles at the location of the cells.

Dr. Alan Bigelow, a post-doctoral fellow, arrived in August of this year, having recently received his Ph.D. degree from University of North Texas. As part of his duties he is continuing the development of the laser ion source begun by Haijun Song.

Biologists from the Center for Radiological Research not supported by the RARAF grant spend various amounts of time at the facility in order to perform experiments:

- Dr. Charles Geard spends most of each working day at RARAF. In addition to his own research, he is collaborating with several outside users on experiments using the single-particle microbeam facility.
- Dr. Satin Sawant, an Assistant Research Scientist, spends all his time at RARAF, primarily doing experiments utilizing the microbeam facility.
- Dr. Brian Ponnaiya, a post-doctoral fellow, works at RARAF full-time performing microbeam experiments.
- There is one full-time biology technician, Ms. Gloria Jenkins. Another technician, Ms. Mei Wang, spent most of her time at RARAF until she transferred to another department in November 2000. A third technician, Ms. Sonu Dhar, worked at RARAF full time for several months before being reassigned to the CRR.

Microbeam Meeting

The 5th International Workshop on Microbeam Probes of Cellular Radiation Response will be held in Lago Maggiore, Italy May 26-27, 2000 and is being organized in part by RARAF. More than 70 participants from 13 countries attended the previous

meeting, which was jointly sponsored by RARAF and the Massachusetts Institute of Technology. Twenty-four presentations were made, ranging from descriptions of microbeam facilities and biological effects to theoretical predictions of biological results.

RECENT PUBLICATIONS OF WORK PERFORMED AT RARAF (1999-2000)

1. Brenner, D. J. Rutherford, the Curies, and radon. Med. Phys. **27**, 618 (2000).

2. Brenner, D. J. and Elliston, C. D. The potential impact of the bystander effect on radiation risks in a Mars mission. Radiat. Res. (In press, 2001).

3. Brenner, D. J., Little, J. B. and Sachs, R. K. The Bystander effect in radiation oncogenesis: II. A quantitative model. Radiat. Res. (Accepted for publication.)

4. Calaf, G. and Hei, T.K., Oncoprotein expression in human breast epithelial cells transformed by high LET radiation. Int. J. Radiat. Biol. **76** (12), 1273-1283 (2000).

5. Hei, T.K., Zhao, Y. L., Roy, D., Piao, C. Q., Calaf, C. and Hall, E. J. Molecular alterations in tumorigenic human bronchial and breast epithelial cells transformed by ionizing radiation. Adv. Space Res. (In press, 2001).

6. Hei, T.K., Zhou, H.N., Wu, L.X., Randers-Pehrson, G., Waldren, C. and Geard, C.R. Radiation induced genotoxic damage: from cytoplasm to nucleus and the bystander phenomenon. In: *Free Radicals in Chemistry, Biology and Medicine*, Yoshikawa, T., Toyokuni, S., Naito, Y. and Yamamoto, Y., Eds.), pp. 241-247, OICA International Press, London, 2000.

7. Miller, R. C., Marino, S. A., Martin, S. G., Komatsu, K., Geard, C. R., Brenner, D. J. and Hall, E. J. Neutron energy-dependent cell survival and oncogenic transformation. J. Radiat. Res. **40** Suppl., 53-59 (1999).

8. Piao, C. Q. and Hei, T. K., Gene amplification and microsatellite instability in tumorigenic human bronchial epithelial cells induced by alpha particles and heavy ions. Radiat. Res. (In press, 2001).

9. Ponomarev, A. L., Brenner, D. J., Hlatky, L. R. and Sachs, R. K. DNA Fragment-size distributions for large sizes after high let radiation, derived from a polymer, random walk chromatin model. Rad. Environ. Biophys. **39**, 111-120 (2000).

10. Ponomarev, A. L., Cucinotta, F. A., Sachs, R. K., Brenner, D. J. and Peterson, L. E. Extrapolation of the DNA fragment-size distributions in a high-dose PFGE assay to low doses. Radiat. Res. (In press, 2001).

11. Randers-Pehrson, G., Geard, C. R., Johnson, G. W. and Brenner, D. J. The Columbia University single-ion microbeam. (Submitted, Radiat. Res.)

12. Sawant, S. G., Randers-Pehrson, G., Geard, C. R., Brenner, D. J. and Hall, E. J. The bystander effect in radiation oncogenesis: I. Transformation in C3H10T½ cells *in vitro* can be initiated in the unirradiated neighbors of irradiated cells. Radiat. Res. (Accepted for publication).

13. Zhao, Y. L., Piao, C. Q., Hall, E. J. and Hei, T. K. Mechanism of radiation induced transformation of human bronchial epithelial cells. Radiat. Res. (In press).

14. Zhou, H. N., Zhu, L. X., Li, K. B. and Hei, T. K. Radon, tobacco specific nitrosamine and mutagenicity. Mutation Res. **430**, 145-153 (1999).

RADIATION SAFETY OFFICE

RADIATION SAFETY OFFICE STAFF

PHOTO CAPTION:

Standing, left to right: Roman Tarasyuk, Tom Juchnewicz, Salmen Loksen, Jacob Kamen, Clifford Jarvis, Alexander Dymnikov, Ilya Pitimashvili, Ahmad Hatami.

Seated, left to right: Yvette Acevedo, Karolin Khalili, Zugeiry DeLeon, Raquel Rodriguez, Hayeon Kim, Milvia Perez, Diana Morrison.

RADIATION SAFETY OFFICE STAFF

Professional Staff

Salmen Loksen, M.S., CHP, DABR; Director, Radiation Safety Officer
Ahmad Hatami, M.S., DABMP, Assistant Director
Thomas Juchnewicz, M.S., DABR, Assistant Radiation Safety Officer
Jacob Kamen, Ph.D., Assistant Radiation Safety Officer
Ilya Pitimashvili, Ph.D., Radiation Protection Supervisor

Technical Staff

Clifford Jarvis, B.S., Chief Technician
Karolin Khalili, B.S., Senior Technician
Hayeon Kim, M.S., Technician B
Kenyel Spaulding, Technician B
Roman Tarasyuk, Technician A

Secretarial Staff

Yvette Acevedo, Administrative Aide
Diana Morrison, Executive Secretary
Raquel Rodriguez, Clerk A
Milvia Perez, Clerk A
Zugiery DeLeon, Clerk A

Consulting Staff

Bruce Emmer, M.S., DABMP, DABR, Physicist
Alexander Dymnikov, Ph.D., Physicist

Radiation Safety Office
Fiscal Year 1999-2000

INTRODUCTION

On May 19, 1957, the President of Columbia University distributed a memo entitled "*Directive to All University Departments Having a Source of Ionizing Radiation*," advising all parties of the expanded function of the Radiation Safety Committee.

Later, a notice entitled "*Radiation Safety Guide for Columbia University*," dated February 10, 1959, named Philip M. Lorio as the Health Physics Officer for University Departments and Laboratories other than the College of Physician & Surgeons, where Dr. Edgar Watts was the named Health Physics Officer. The Chairman of the Radiation Safety Committee was Dr. Gioacchino Failla, who initiated the Radiological Research Laboratory in the Department of Radiology of Columbia-Presbyterian Medical Center (CPMC).

By agreement between The Presbyterian Hospital in the City of New York (PH) and Columbia University (CU), the Radiation Safety Office (RSO) was established as an autonomous unit in 1962 for the purpose of maintaining radiation safety. The Joint Radiation Safety Committee (JRSC), appointed by the Medical Board of CPMC and the Vice President for Health Sciences of Columbia University, is charged with the responsibility of defining and ensuring enforcement of proper safeguards in the use of sources of ionizing radiation.

Dr. Harald H. Rossi, Director of the Radiological Research Laboratories, was appointed Chairman of the JRSC. Under his direction, this committee developed a Radiation Safety Code and Guide, the administration of which is assigned to the Radiation Safety Officer. Dr. Eric J. Hall, the present Director of the Center for Radiological Research, now chairs the JRSC.

The present Radiation Safety Office came into existence through an agreement made on February 12, 1991 between New York State Psychiatric Institute (NYSPI), the College of Physicians and Surgeons of Columbia University (P&S), and The Presbyterian Hospital in the City of New York (PH). This agreement combined several overlapping clinical and educational programs, including all programs for ensuring radiation safety. On December 16, 1996, Mr. Salmen Loksen was appointed Director of the Radiation Safety Office and Radiation Safety Officer.

The Radiation Safety Office advises CPMC and NYSPI through the JRSC, and also participates in the review of research protocols for the Radioactive Drug Research Committee under the jurisdiction of the U.S. Food and Drug Administration. The

Radiation Safety Office is responsible for ensuring compliance with federal, state and city regulatory agencies. These regulatory agencies, which mandate rules, regulations, and guidelines, include:

- United States Food and Drug Administration
- United States Nuclear Regulatory Commission
- New York State Department of Environmental Conservation
- New York State Department of Health
- New York City Department of Health Bureau of Radiological Health.

The Radiation Safety Office also ensures compliance with the rules and regulations of the "*Radiation Code and Guide of Columbia-Presbyterian Medical Center and New York State Psychiatric Institute*."

The Radiation Safety Office provides the following primary services:

- Radiation safety services to Columbia University.
- Radiation safety services to College of Physicians & Surgeons of Columbia University.
- Radiation safety services to New York Presbyterian Hospital.
- Radiation safety services to New York State Psychiatric Institute.
- Radiation safety services to the Cyclotron Facility.
- Radiation safety services to Radioligand Laboratory.
- Radiation safety services to PET Net Pharmaceuticals, Inc.
- Radiation safety services to Audubon Biomedical Science and Technology Park (Audubon I).
- Radiation safety services to the Russ Berrie Medical Science Pavilion (Audubon II).
- Reviewing and evaluating Human and Non-Human Use Protocols for the Joint Radiation Safety Committee and the Radioactive Drug Research Committee for compliance with federal, state and local regulatory requirements.
- Evaluation of education, training and experience of Responsible Investigators seeking to obtain radioactive materials and/or operate radiation-producing equipment for laboratory or hospital use.
- Initial and annual refresher training to personnel involved in handling radioactive materials or operating radiation-producing equipment.
- Personnel radiation dose monitoring and investigating reports of overexposure.
- Bioassay testing, including personnel thyroid uptake and urinalysis.
- Routine and specialized laboratory inspections for Human and Non-Human Use.
- Leak testing and inventory of sealed sources.
- Calibration of radiation survey instruments.
- Consultation for radiation shielding requirements.
- Emergency response, including weekends and after hours, in event of radiation accidents.

- Supervision and assistance with cleanup of contaminated-areas.
- Review and approval of the purchase of non-radiology dental and medical X-ray equipment.
- Monitoring and quality assurance testing of non-radiology dental and medical X-ray equipment.
- Radiation Safety support for clinical procedures performed at New York Presbyterian Hospital-Columbia-Presbyterian Center.
- Pick-up, storage and disposal of radioactive and mixed waste from laboratories and hospital facilities.
- Receiving, shipping and tracking of radioactive material packages, and wipe testing of packages for radioactive contamination.
- Monitoring and evaluating radioisotope effluent discharges to the atmosphere and the sewer system.

As a health sciences campus, Columbia-Presbyterian Medical Center has extensive teaching, research and clinical facilities in which sources of ionizing radiation are used. The goal of the Radiation Safety Office at Columbia-Presbyterian Medical Center is to provide adequate protective measures against exposure to these sources for patients, visitors, students, faculty and staff on campus, and for the community at large to ensure that the dose received by employees, patients and the general public from ionizing radiation is As Low As Reasonably Achievable (ALARA). The Radiation Safety Office ensures compliance with all regulatory requirements and guidelines for the use of radioactive material and radiation producing machines by means of training, education, consultation and a program of audits and inspections of facilities. These measures are required pursuant to CPMC Radioactive Materials License requirements and conditions.

The Radiation Safety Office is responsible for maintaining and updating licenses authorizing the use of radioactive materials and registrations of radiation producing equipment. Licenses include the New York City Department of Health, Bureau of Radiological Health, Broad Scope Research and Broad Scope Human-use licenses and specific licenses for a number of facilities, including the Cyclotron, the Gamma-Knife and the Cobalt-60 Teletherapy unit. Registrations include New York City Department of Health, registrations for X-ray equipment and the operation of medical accelerators. In addition the Radiation Safety Office maintains the New York State Department of Environmental Conservation Radiation Control Permit for the controlled discharge of radioisotopes to the environment.

Both the New York City Department of Health and the New York State Department of Environmental Conservation conduct periodic inspections and audits of the facilities at Columbia-Presbyterian Medical Center and New York State Psychiatric Institute operating under their licenses or permits. The Radiation Safety Office works continuously to ensure that regulatory violations are prevented and to ensure those that do occur are swiftly corrected.

The Radiation Safety Office reports to the Columbia-Presbyterian Medical Center and New York State Psychiatric Institute Joint Radiation Safety Committee. The Joint Radiation Safety Committee meets on a quarterly basis. For administrative purposes, the RSO reports to Dr. Richard Sohn, Associate Dean for Research Administration and Director of Grants and Contracts.

Radiation Safety Office staff are Columbia University employees. New York Presbyterian Hospital, Columbia University College of Physicians and Surgeons, and New York State Psychiatric Institute fund the RSO budget, via a cost sharing payback arrangement.

A full-asset merger between The Presbyterian Hospital in the City of New York and New York Hospital on December 1, 1997, created a single entity known as New York Presbyterian Hospital with facilities in two major Manhattan locations: Columbia Presbyterian Center at West 168th Street in Washington Heights and New York Weill Cornell Center at East 68th Street on the Upper East Side.

SUMMARY OF SERVICES

The statistical data detailed below are for the fiscal year, July 1, 1999 through June 30, 2000. Instances of Radiation Safety Office support, activities, incidents and response, include those from the date of the last Annual Report, December 1999, to the present, December 2000:

1. Performed routine radiation safety inspections and audits of 414 Columbia University and New York State Psychiatric Institute research laboratories using radioactive materials. Results of the audits were communicated to Responsible Investigators and 262 deficiencies were followed up, resulting in the correction of the cited deficiencies.

2. Received and distributed 4,065 packages containing radioisotopes, with a total activity of approximately 43 Curies, excluding Nuclear Medicine and Radiation Oncology Shipments. For all shipments the RSO conducts package surveys, ensures correct distribution to Authorized Users, maintains inventory control and associated records.

3. Performed 69 thyroid bioassays on radiation workers using isotopes of iodine including I-125, I-123 and I-131.

4. The Radiation safety Office distributed approximately 8,000 personnel radiation dosimeters per quarter, including monthly and quarterly badges. A total of 32,000 dosimeters were distributed and collected annually. To maintain dosimetry records the RSO uses dedicated computers with direct modem access to the vendor.

5. The changeover from standard LiF (TLD) dosimeters to Luxel optically stimulated luminescence dosimeters was completed during fiscal year 1999-2000. The Luxel

dosimeter has a sensitivity of 1 mrem for photons compared to the standard LiF sensitivity of 10 mrem. The RSO conducted a number of informational-training sessions on the use of and transition to the new Luxel system. In addition, training on the Luxel system is available on the RSO website.

6. An officer of the RSO participates as an Ad Hoc Member of the Animal Care Protocol Review Committee, reviewing all procedures using radionuclides in animal research. Before an authorization is granted for use of radioisotopes in animals, the RSO will review procedures with the applicant. The applicant must provide assurance that adequate animal care facilities are available and must make provision for collection and storage of animal carcasses and all associated waste. 42 protocols involving the use of radioactive materials in animals were approved in the last year. In order to minimize contamination in animal facilities and cages, protect Animal Care staff, and ensure proper disposal of animal carcasses with radioactivity, the Radiation Safety Office staff performed 31 routine animal radiation surveys in the Institute of Comparative Medicine.

7. Provided calibration and maintenance services for 244 radiation survey instruments used throughout the Columbia-Presbyterian Medical Center and New York State Psychiatric Institute. The RSO maintains a supply of portable survey instruments available for loan to Responsible Investigators.

8. During the 1999-2000 fiscal year, the Radiation Safety Office provided radiation safety support for 82 brachytherapy patients and nine 131-I radiopharmaceutical therapy patients receiving treatment from the New York Presbyterian Hospital Departments of Nuclear Medicine and Radiation Oncology. This support includes room preparation, the distribution of personnel radiation dosimeters, the performance of patient and room surveys, posting instructions in patient rooms, entering instructions in patient charts, patient discharge surveys, room decontamination and the removal of patient generated wastes for decay-in-storage and disposal.

9. The Radiation Safety Office operates an extensive program at the Columbia-Presbyterian Medical Center and New York State Psychiatric Institute for the collection, inventory, storage and disposal of Low Level Radioactive Waste (LLRW) including mixed wastes. This program operates from a number of LLRW/Decay-In-Storage facilities maintained by the Radiation Safety Office in the Columbia University College of Physicians & Surgeons Building, the Russ Berrie Medical Science Pavilion, the Hammer Health Sciences Building and the New York State Psychiatric Institute building on Riverside Drive. As part of this program the Radiation Safety Office maintains a South Carolina Waste Transport Permit and a Chem-Nuclear Waste Disposal Permit. In the fiscal year 1999-2000, due to the high costs associated with disposing of Dry Active Waste (DAW) by landfill burial at the Chem-Nuclear operated facility in Barnwell, South Carolina, and the possibility of that disposal site closing, the Radiation Safety Office carefully evaluated the costs and environmental impact associated with landfill burial of DAW at other sites. The last shipment of DAW was therefore made to the Envirocare facility in Utah at a cost equivalent to 50% of the cost associated with sending that

shipment to South Carolina. The Radiation Safety Office continues to monitor changes in broker fees and site availability for the disposal of Low Level Radioactive Wastes. The RSO is investigating different types of packaging (fiber drum, steel drum, etc.) for the future shipments, in order to reduce costs.

10. In fiscal 1999-2000 the Radiation Safety Office shipped the following amounts of Low-Level-Radioactive-Waste: 98 drums of Dry Active Waste totaling 574 cubic feet and containing 892 milliCuries of activity for supercompaction and landfill burial by Envirocare of Utah; 60 drums of Liquid Scintillation Vial wastes totaling 240 cubic feet and containing 136 milliCuries of activity shipped as non-radioactive hazardous waste for disposal by Perma-Fix of Florida; 4 drums of over-pack animals totaling 19.5 cubic feet and containing 0.47 milliCuries of activity for disposal by Allied Technology of Richland, Washington.

11. Additional LLRW disposed of on-site by the Radiation Safety Office in fiscal year 1999-2000 totals: 287 drums containing 1,150 cubic feet of short half-life research wastes which were held for decay-in-storage and ultimately cleared for landfill disposal as regular trash; 4,350 liters of low-activity aqueous research wastes assayed and disposed of by controlled sewer disposal; 336 thirty-gallon “black-bags” containing waste removed from patient rooms, held for decay in storage, and ultimately disposed of as “red-bag” patient waste.

In order to optimize the radioactive waste disposal program the RSO purchased a new network-ready low level radioactive waste monitoring system that will not only alert workers on the waste area loading docks to contaminated patient waste, but will display the alert on a work station in the RSO, and maintain a 24 hour-a-day, 7 day-a-week record of waste alarm response. After the system is installed the RSO will be able to more effectively ensure that radioactive patient waste does not enter the regular waste stream.

12. The Radiation Safety Office submits an annual Low-Level Radioactive Waste Report Form to the New York State Energy Research and Development Authority.

13. As required by 6 NYCRR Part 380 and the conditions of our New York State Department of Environmental Conservation Radiation Control Permit, No. 2-6201-00005/00006, the Radiation Safety Office operates an extensive program to control, monitor and document atmospheric discharges of volatile radioisotopes from research laboratories, the Cyclotron Facility and the Radioligand Laboratory and the sewer disposal of aqueous radionuclides.

In order to accomplish this task the Radiation Safety Office maintains records as to the source and nature of all radionuclide discharges from the Columbia-Presbyterian Medical Center campus. Our office has identified fifteen radioisotope effluent discharge points and characterized them as to location; exhaust system equipment, the laboratories and hoods served and the isotopes emitted. The Radiation Safety Office maintains records of effluent flow rates, methods of discharge treatment and control and the quantities of

radionuclides discharged. The Radiation Safety Office evaluates radionuclide discharges as to concentration and radiation dose to members of the public and to radiation workers.

The New York State Department of Environmental Conservation requires the Radiation Safety Office to perform quarterly ALARA reviews of these environmental discharges and to immediately report those that exceed the Permit or Part 380 limits to the NYSDEC. On April 13, 2000, as required by our Permit, the Radiation Safety Office submitted to the NYSDEC Radiation Section an Annual Report of discharges from the Columbia-Presbyterian Medical Center to the environment. On June 22, 2000 the Radiation Safety Office received from the NYSDEC Radiation Section a communication that radioactive discharges for 1999 were in compliance with the effluent limits of our Permit and the requirements of Section 380-5.1(a).

14. The RSO makes semi-annual measurements of the average face velocity of approximately 49 fume hoods in which radioisotopes are used or stored. Researchers whose hoods do not meet safe flow rate standards are directed to have their hoods repaired. Ventilation was measured in all rooms where radioactive gases or aerosols are used, and spill gas clearance times are calculated and posted.

15. On March 23, 2000, representatives of the New York State Department of Environmental Conservation, Radiation Section, inspected facilities, audited records and interviewed personnel operating at Columbia-Presbyterian Medical Center under Radiation Control Permit, No. 2-6201-00005/00006. On May 1, 2000 the Radiation Safety Office received from the NYSDEC Radiation Section a communication that operations at CPMC were found to be in compliance with Part 380 and the conditions of our permit.

From November 15, 2000 through November 20, 2000, a representative of the New York State Department of Environmental Conservation, Division of Solid and Hazardous Materials, Region 2, inspected facilities, audited records and interviewed personnel operating Columbia University facilities, receiving, storing and disposing of hazardous wastes. This inspection included Radiation Safety Office facilities handling hazardous mixed wastes. No major deficiencies were found. Minor deficiencies were corrected within 30 days of the inspection.

16. On April 26, 2000, the Radiation Safety Office received from the New York State Department of Environmental Conservation a Notice Of Permit Modification for NYSDEC Permit No. 2-6201-00005/00006. This amended NYSDEC radiation control Permit replaces in its entirety the original Permit No. 2-6201-00005/00006 issued June 12, 1996. The new Permit is the result of a comprehensive revised Permit Application submitted to the New York State Department of Environmental Conservation, at their direction on February 29, 2000, and is valid until June 12, 2001. This new Permit application unifies in its body corrections and amendments made to the old Permit over a period of four years. The number of radioactive effluent discharge points has been increased from seven (7) to fifteen (15), all gaseous radioactive isotopes discharged are explicitly identified and the dose to the public calculated by a National Council On

Radiation Protection And Measurements screening model accepted by the New York State Department of Environmental Protection. The new Permitted Discharge Levels are in compliance with the U.S.N.R.C. “constraint limit” of 10 mrem per year to the general public.

17. The Radiation Safety Office provides, under a Memorandum of Understanding, Radiation Safety support to the Cyclotron Facility operated by PET Net Pharmaceuticals under contract with Columbia University. The Radiation Safety Office maintains the New York City Radioactive Materials License and the New York State Radiation Discharge Permit under which the Facility operates. The Radiation Safety Office is responsible for: distributing and collecting personnel dosimetry, providing dose reports and ALARA review; calibration of survey meters, area monitors and well counters; leak testing and inventory of sealed sources; receipt and surveys of returned radioactive material packages; radiation safety training and postings; maintaining area dosimeters for isocurve generation; the calibration and operation of an effluent monitoring system and the compilation and analysis of stack data. On January 22, 2000 the Radiation Safety Office performed the annual filter replacement for the Cyclotron stack system.

During 1999 remote manipulators were installed in a Cyclotron Facility hot cell at the recommendation of the Radiation Safety Office. Intensive in-services were given to PET Suite technologists, researchers and medical staff regarding the safe handling of high-energy positron emitting radiopharmaceuticals. The Radiation Safety Office maintains a liaison with the corporate Radiation Safety Officer of PET Net, Inc., the operator of the Cyclotron under the CPMC license.

18. A large part of the Radiation Safety support for the Cyclotron Facility is the real-time monitoring of airborne radioactive effluents from the Cyclotron Facility stack. As the present monitoring system requires constant manual input to maintain reliability of operation, the Radiation Safety Office is evaluating replacement effluent monitoring systems for PET/Cyclotron applications offered by different vendors. Sales engineers have made site visits to evaluate our needs and have provided proposals and demo software for evaluation by the Radiation Safety Office.

19. On May 1, 2000 the Radiation Safety Office received two recommendations from the New York State Department of Environmental Conservation regarding the expansion of the environmental monitoring program for the Cyclotron Facility. The NYSDEC recommended that, in addition to operating the Cyclotron effluent monitoring system, the Radiation Safety Office deploy a system of thermoluminescent dosimeters to monitor the sites of highest potential public dose from cyclotron emissions and that a simple meteorological station be installed on the Milstein Building roof to measure wind velocity and direction. As of August 1, 2000, Landauer X-9 environmental TLDs were installed on air intake vents that determine public dose and in a cardinal point pattern on the Milstein Building Roof. Dosimeters were also installed on the public dose locations of the nearest adjacent buildings. Several models of automated meteorological stations are being evaluated as to suitability for our program. Data obtained by this expanded environmental

radiation monitoring program will allow the Radiation Safety Office to more accurately calculate the annual public dose commitment from Cyclotron discharges.

20. The Radiation Safety Office provides radiation safety support for the new Columbia University Radioligand Laboratory Facility for the synthesis of PET imaging radiopharmaceuticals. During the construction phase of the facility the Radiation Safety Office provided assistance in the design and specification of the radioisotope exhaust and effluent monitoring systems.

In January 2000, at the completion of the construction of the Radioligand Laboratory, a comprehensive radiation safety survey was conducted by the RSO to ensure that the actual shielding conform to regulatory requirements and to conform to ALARA principles. The survey confirmed that all measured radiation levels were within regulatory requirements as anticipated by RSO calculations.

At present, the Radiation Safety Office is involved in the preliminary planning for the proposed second Cyclotron Facility. The Radiation Safety Office is providing professional health physics consultation with regard to all radiation safety aspects of the new facility. This includes shielding design and evaluation for the cyclotron and radiochemistry laboratories and design and specification of the radioisotope exhaust and effluent monitoring systems, including the design and specification of radioactive waste gas hold-up and treatment equipment.

21. The Radiation Safety Office is in the process of acceptance testing the effluent monitoring system serving the Radioligand Laboratory in order to insure that the system meets all specifications claimed by the manufacturer. Because of some problems identified by Radioligand Lab and Radiation Safety Office personnel with this new system, company service engineers have visited Columbia-Presbyterian to replace hardware and update software. Acceptance testing of the effluent monitoring system continues.

22. From January 23, 2000 through February 14, 2000 the Radiation Safety Office performed controlled releases of 11-CO2 and 15-OH2 in order to calibrate the Cyclotron Facility and Radioligand Laboratory stack monitoring systems. An accurate multi-point calibration and a new methodology for identifying and calculating discharges has allowed the Radiation Safety Office to prepare quarterly environmental discharge reports of greater utility for the Cyclotron Facility and Radioligand Lab personnel in controlling emissions.

23. In association with the Department of Radiology, the RSO maintains a radiation safety inspection and audit program for non-Radiology X-ray equipment at CPMC to assure compliance with regulatory requirements. The audit program includes evaluation of compliance with Quality Assurance requirements and procedures, attendance of employees at radiation safety training sessions, and compliance with regulatory requirements for use and timely return of personnel radiation dosimeters. Prior to the audit a form is sent to each non-Radiology X-ray facility requesting a list of individuals

responsible for performing QA/QC functions and an inventory list of all X-ray equipment and film processors.

24. The RSO performed quarterly inspections and audits of all CPMC clinical facilities using radioactive materials to ensure compliance with City of New York Radioactive Materials License conditions and with RCNY Article 175, Radiation Control. These audits include quarterly inventories of all sealed sources of radioactivity, and leak testing of sources and irradiators as required. The facilities audited include: New York Presbyterian Hospital Nuclear Cardiology, New York Presbyterian Hospital Neuroanesthesiology, Milstein Hospital Department of Nuclear Medicine, Milstein Hospital Cyclotron Facility, Milstein Hospital PET Suite, New York State Psychiatric Institute Brain Scan Department, Allen Pavilion Nuclear Medicine and Allen Pavilion Nuclear Cardiology.

25. In addition, the RSO investigates all major spills, inciden ts, misadministrations, anomalous exposures and reports of missing sources, and provides timely notice of reportable incidents to the City of New York Department of Health Bureau of Radiological Health.

26. The RSO maintained the City of New York Radioactive Materials Licenses: 75-2878-01 (Human Use), 92-2878-02 (Teletherapy), 74-2878-03 (Non-Human Use), 58-2878-04 (Cyclotron Facility) 93-2878-05 (Gamma Knife), and City of New York Therapeutic Radiation Linac Unit Certified Registration No. 77-0000018 (East 60th Street) and No. 77-0000019 (168th Street).

27. Additional interactions with the New York City Department of Health Bureau of Radiological Health included:

- On February 10, 2000 the RSO requested an amendment to the 75-2878-01 (Human Use) License to permit the use of Holimium-166 (10 Ci for possession limit, however it is anticipated that patients will only receive up to 4 Ci of the Ho-166) from NeoRx, for use in patients with metastatic breast cancer.

- On March 3, 2000 the RSO obtained an amendment to the 77-0000019 Linac Registrations, to add the newly installed Varian Associates Clinac-2100EX linear accelerator to the Permit.

- On March 8, 2000 the RSO obtained an amendment to Radioactive Materials License No. 75-2878-01 (Human Use) from the New York City Department of Health Bureau of Radiological Health, to modify the patient release criteria for Iodine-131 Radiopharmaceutical therapy. The amendment authorizes CPMC to release patients containing substantially higher activity of I-131, subject to compliance with the measured and documented patient-specific parameters in accordance with RCNY 175.103(c)(9).

- The RSO obtained amendments dated March 2000 to the 75-2878-01 (Human Use), 92-2878-02 (Teletherapy), 93-2878-05 (Gamma Knife) Licenses, and the 77-

0000018 and 77-0000019 Linac Registrations, to add four qualified radiation oncology physicians approved by the CPMC JRSC as authorized users.

- On October 16, 2000 the RSO requested an amendment to the 75-2878-01 (Human Use) License to permit the use of 850 mCi of 32-P in the form of sealed sources.

28. As a major function of the maintenance of the City of New York Radioactive Materials licenses, X-ray registrations and Linac Registrations, the RSO represents the CPMC and New York State Psychiatric Institute Joint Radiation Safety Committee during inspections and audits conducted by the City of New York Department of Health Bureau of Radiological Health. The RSO accompanies the inspectors, provides access to information and records, participates in the exit interviews and receives the written report of the City. Inspections performed in 2000 were:

- January 24, 2000 through February 2, 2000, inspection for compliance with the requirements of X-ray Permit No. H96 0076353 86 (Columbia-Presbyterian Medical Center's X-ray facilities).

- June 2, 2000 through September 15, 2000, inspection for compliance with the requirements of 52-2878-04 (Cyclotron) and 74-2878-01 (Human Use).

- On June 20, 2000, an inspection of New York State Psychiatric Institute NYC BRH Permit No. 91-0076342 (Dental) was completed.

- August 24, 2000, inspection for compliance with the requirements of 92-2878-02 (Teletherapy).

- September 15, 2000, inspection for compliance with the requirements of Linac Registration No. 77-0000019 (NYPH).

In all cases either no deficiencies were found or minor deficiencies discovered were corrected within thirty days of the inspection.

29. During the fiscal year 1999-2000, 86 ALARA Level 1 and 24 ALARA Level 2 Notification Reports provided by our personnel radiation dosimetry vendor were investigated and the radiation workers were informed of their exposures. Particular attention is paid to three occupational groups typically at or exceeding ALARA limits for whole body, extremity or eyes: workers and researchers in the Cyclotron Facility; technologists, researchers and physicians in the PET Suite; and physicians in the Angiography Suite.

30. During fiscal year 1999-2000, 25 employees of the Columbia-Presbyterian Medical Center completed a declaration of pregnancy form and received health physics counseling. These individuals were counseled concerning risk factors and provided with additional

monitoring of the fetus for the gestation period. The RSO continues to closely follow the personnel exposure reports of this group.

31. The RSO continues to maintain a program for emergency response. A system was established by the RSO with a list of names and beeper numbers, including a group pager number, and a procedure for Security to contact members of the RSO in an emergency.

32. The Radiation Safety Office provided 24 sessions of initial training. These were scheduled well in advance and were spaced to allow the new employees to satisfy mandatory training requirements. For employees who could not attend the regularly scheduled classes, the Radiation Safety Office designed and implemented a self-study program including the use of videotapes available at the Health Sciences Library. A passing grade on the quiz administered after viewing the video qualifies an employee working in non-human use applications to be issued a radiation monitor badge. If the individual's employment involves human use of radioactive material, a passing grade on the quiz results in obtaining a temporary badge until the next regularly scheduled training session. The Radiation Safety Office is continuing to study this procedure.

33. The staff of Radiation Safety Office provided fifteen sessions of required annual refresher training during the fiscal year, to all radiation workers, including employees from clinical departments, nursing, research laboratories, dental areas, security and facilities. These sessions are scheduled on different days of the week and at various times of the day, in order to enable radiation workers to fit these classes into their busy schedule. The Radiation Safety Office is in the process of revising the radiation safety training schedule and procedures in a manner that would provide each individual numerous opportunities during the year to comply with the annual refresher training requirement.

34. The following radiation safety courses and training sessions, pursuant to Article 175 of the New York City Health Code, were presented July, 1999 through June, 2000:

- 24 regular training seminars for a total of 718 individuals.
- 15 refresher seminars for a total of 779 individuals.
- 12 nursing seminars for a total of 195 individuals.
- 2 special dental seminars for a total of 122 individuals.
- 3 training sessions for CU Security Department for a total of 112 individuals.
- 3 training sessions for Presbyterian Hospital ancillary personnel and for the Cs-137 irradiator blood bank personnel, for a total of 84 and 11 individuals respectively.
- 2 training sessions for Radiology residents.

35. On November 17, 2000 the officers and technical staff of the RSO attended a training session on Hazardous Chemical Waste Management, which was given by a certified Hazardous Material specialist from the Columbia University Environmental Health & Safety Office. At the end of the session all the attendees were given a certificate of accomplishment.

36. The RSO is in the process of creating options for web-based radiation safety training. Proceeding toward this goal the RSO has obtained authorization from a number of vendors to use their video training on the RSO website. As a part of these steps, the RSO and Dr. Hall, Chairman of the JRSC, have been actively engaged in preparing material to be utilized in a web-based training program customized to the requirements of CPMC. The advantages of web-based training for radiation safety are: Web-based training can be done at any time, from any internet-connected computer; once the system is in operation, staff involvement is greatly reduced; on-line training sessions can consist of selected modules focused selectively for different groups of employees; record keeping is managed by the computer database; learning can be in small sections at the user's pace and convenience, can be reviewed as needed, is interactive, and uses a multimedia approach, all of which are conducive to effective learning and result in a much higher retention rate; and on-line material can be standardized and updated as needed with instant dissemination of new material.

37. The RSO reviewed applications submitted to the CPMC Radioactive Drug Research Committee (RDRC) and/or the CPMC Joint Radiation Safety Committee (JRSC) to administer radioactivity to human test subjects. A total of 24 applications were reviewed. Of these, 21 were JRSC applications and 3 were RDRC applications. All were approved, some with modifications. In addition, 18 new Responsible Investigator applications for non-human use of radioactivity were reviewed and approved.

38. The RSO participates as part of the Columbia University Health Science Division (CUHSD) Emergency Management Plan Task Force. The Emergency Management Plan is necessary in event that any significant occurrence disrupts the normal day-to-day operation at CUHSD, including University research activity and/or employee safety. The objective of the plan is to utilize University resources in an effective manner should interruption of an essential service occur. The plan provides written policies and procedures to be implemented in event of emergencies including radiation spills, chemical spills, transit disruption, utility shutdown, etc. A number of meetings were held in order to formulate policies, and an Emergency Management Plan document was completed in September 2000.

39. The RSO participates as part of the Columbia University Health Science Division (CUHSD) Institutional Health and Safety Council (IHSC). The IHSC has encouraged the utilization of the Web to provide information, education and training to personnel. The RSO continues development of its Webpage to improve dissemination of information and communication with Responsible Investigators and members of the CPMC community (http://cpmcnet.columbia.edu/dept/radsafety).

40. RSO officers continues to participate at joint meetings that included representatives of New York Presbyterian Hospital-Columbia Presbyterian Center, New York Presbyterian Hospital-Weill Cornell Center, and Memorial Sloan-Kettering Cancer Center, in order to set uniform policy, procedures and criteria for Radioimmunotherapy

Outpatient Release. The multi-institution discussion and generation of policy documents is helpful in reducing duplication of effort and ensuring a through review of policy issues.

41. Monthly inventories of all radioisotopes present at Columbia-Presbyterian Medical Center under New York City Department of Health Bureau of Radiological Health License No. 74-2878-03 were conducted. A computer program, "Health Physics Assistant," is used to track the inventory and compare it with licensed limits. Columbia-Presbyterian Medical Center had approximately 25 Curies of by-product material present under the broad license. Another 11,200 Curies were present under the Irradiator license.

42. The Radiation Safety Office updated its Health Physics Assistant software to include in its laboratory equipment module a section that maintains records on fume hoods installed in laboratories using radioactive materials. The database is useful for scheduling quality assurance procedures; including flow rate measurements for fume hoods.

43. The Radiation Safety Office assisted with the installation of a new 84.3 Tbq Blood Irradiator at the Harkness Pavilion of New York Presbyterian Hospital, under New York City Radioactive Materials License No. 75-2878-01 (Human-Use). The RSO provided support during the installation and held radiation safety training sessions for all the employees in the blood irradiator facility.

44. On November 15, 1999, the Radiation Safety Office filed a request to amend Radioactive Materials License No. 75-2878-01 (Human Use) with the New York City Department of Health Bureau of Radiological Health, to modify the patient release criteria for Iodine-131 Radiopharmaceutical therapy. On March 8, 2000, the requested amendment (Amendment 15) was approved, authorizing CPMC to release patients containing substantially higher activity of I-131, subject to compliance with the measured and documented patient-specific parameters in accordance with RCNY 175.103(c)(9). In addition, radiation safety instruction is required to be provided to the patient or patient's competent representative in compliance with RCNY 175.103(f)(3). Prior to receipt of the amendment the License restricted release of patients to those with less than 1.2 Gbq (32.4 mCi) of activity. Under certain conditions, based on NUREG 8.39, these new guidelines will result in release of patients with up to 8,103 Mbq (219 mCi) of I-131.

45. The Radiation Safety Office updated and modified the existing Human Use Authorization Form. The application form previously used was identical for RDRC, JRSC Radioactive Materials and JRSC X-ray submissions. The new forms are specifically geared to the requirements of RDRC, JRSC Radioactive Materials or JRSC X-ray study proposals. At the direction of the RDRC, the Radiation Safety Office created a new Health Physicist position. The position's responsibilities include auditing of worksites approved for use of radioactive agents in studies involving human subjects, and evaluation of compliance with all aspects of the approved protocol.

46. The Radiation Safety Office submitted a proposal to the Joint Radiation Safety Committee to amend the period of authorization for Non-Human use of radioactive

materials to a finite term. The proposed modification to the application form would be the insertion of a designated expiration date to the authorization. The committee approved amending the terms of the authorization to a period of seven years.

47. The RSO continues the dental quality assurance program for Columbia University Health Science Division and Morningside Campus, CPMC East 60 th Street, and New York State Psychiatric Institute dental facilities, to optimize the radiological safety and clinical quality of dental radiography. The quality assurance program is based on recommendations for quality assurance that have been promulgated by a number of professional organizations, including the National Council on Radiation Protection and Measurements (NCRP), the Bureau of Radiological Health of the FDA, the American College of Radiology (ACR), and the American Academy of Dental Radiology Quality Assurance Committee.

48. Quality Assurance testing was performed on dental X-ray units at the Columbia University School of Physicians and Surgeons Dental School, including:

- Morningside Dental Associates – 6 intraoral units, 1 panorex unit, and 1 cephalographic unit.
- Ambulatory Care Networked Corporation (ACNC) – 2 intraoral units.
- Babies Hospital OR – 1 portable intraoral unit.
- Vanderbilt Clinic Teaching & Research Area – 1 panorex unit, and 2 cephalographic units.
- Dentcare Clinic (Intermediate School 183) – 1 intraoral unit.
- New York State Psychiatric Institute – 1 intraoral unit.
- Columbia Eastside – 6 intraoral units, 1 manorex unit, and 1 cephalographic unit.

Acceptance testing and radiation safety surveys were performed for two new intraoral units on VC-7, and a new Panorex unit at ACNC.

The Radiation Safety Office is currently examining the need for additional test equipment to properly enable the Radiation Safety Office to perform quality assurance evaluation of the X-ray units assigned to its responsibility.

49. On January 5, 2000, representatives of the Radiation Safety Office met with the staff of the Environmental Health and Safety Office regarding coordination of emergency response and the prioritizing of biological, chemical and radiological hazards to insure appropriate response. A document specifying response priorities was agreed to, essentially providing that Environmental Health and Safety will give initial clearance, with the exception of several listed sites on the Health Sciences Campus where objective radiological hazards exist. In addition, Environmental Health and Safety and the Radiation Safety Office agreed to a combined standardized clearance form.

50. The Radiation Safety Office participated in planning discussions with personnel in Electronic Research Administration in order to facilitate the integration of the RSO computerized database with the RASCAL system.

CENTER FOR RADIOLOGICAL RESEARCH

PROFESSIONAL ACTIVITIES
COLUMBIA COLLOQUIUM AND LABORATORY SEMINARS
PUBLICATIONS

PROFESSIONAL ACTIVITIES

Dr. Adayabalam S. Balajee

Member

American Association for Cancer Research
Radiation Research Society

Reviewer

Mutation Research
Cancer Research
Advances in Space Research

Dr. David J. Brenner

Chairperson

Columbia University Radiation Safety Committee

Member

National Council on Radiation Protection and Measurements (NCRP)
Joint Task Force on Vascular Radiation Therapy
NCRP Committee 1-6 on Risk Linearity
ASTRO Refresher Course Program Committee
Radiation Research Society Policy Committee

Dr. Gloria M. Calaf

Member

Tissue Culture Association
The New York Academy of Sciences
International Association for Breast Cancer Research
Chilean Society of Citology, Chile
Chilean Cancer Society, Chile
Society of Biology of Chile
Society of Mastology of Chile
American Association for Cancer Research
Society for Experimental Biology and Medicine
Radiation Research Society

Reviewer

Mutation Research
Radiation Research
International Journal of Radiation Biology

Dr. Charles R. Geard

Member

American Society of Therapeutic Radiology and Oncology (ASTRO)
Environmental Mutagen Society
Radiation Research Society
Advisory Committee on Radiobiology, Brookhaven National Laboratory

(Dr. Charles R. Geard, continued)

Associate Member, Radiobiology Advisory Team (AMRAT) of the Armed Forces Radiobiology Research Institue (AFRRI)
Columbia University, Faculty Council (Voting Member)

Editorial Work

Editorial Board, *International Journal of Radiation Biology*
Radiotherapy and Oncology
British Journal of Cancer
Clinical Cancer Research, *Mutagenesis*
Mutation Research
Radiation Research

Ad Hoc Reviewer of Grant Proposals

American Cancer Society
National Institutes of Health
Ad Hoc Member of Program Project Review Committee

Dr. Eric J. Hall

Member

American Board of Radiology
Radiotherapeutic Written-Test Committee
National Academy of Sciences
American Society of Therapeutic Radiology and Oncology (ASTRO)
Radiation Research Society
Internationl Stereotactic Radiosurgery Society
Member of the Board
American Radium Society
Program Committee Chairman
International Association of Radiation Research
President
Columbia University, College of Physicians & Surgeons
Cancer Center, Internal Advisory Committee/Executive Committee
Columbia-Presbyterian Medical Center
Chairman, Joint Radiation Safety Committee
Chairman, Radioactive Drug Research Committee
National Council on Radiation Protection and Measurements
Member of Council
Member, Committee 1

Editorial Work

International Journal of Radiation Oncology, Biology, and Physics
International Journal of Brachytherapy

Dr. M. Prakash Hande

Member

Indian Association for Radiation Protection, India
Association of Medical Physicists of India
Indian Society for Radiation Biology

(Dr. M. Prakash Hande, continued)

Environmental Mutagen Society
Radiation Research Society
New York Academy of Sciences

Reviewer

International Journal of Radiation Biology
Advances in Space Research

Dr. Tom K. Hei

Adjunct Faculty

Adjunct Professor, Department of Radiological Health Sciences,
Colorado State University, Fort Collins, Colorado
Adjunct Professor, Department of Ion Beam Bioengineering,
Chinese Academy of Sciences, Hefei, China.

Member

Chemical Pathology Study Section, 1998- present
Ad hoc review panel, Metabolic Pathology Study Section, 1999, 2000
Ad hoc review panel, National Science Foundation, 2000
Ad hoc review panel, UICC Fellowship
Program Committee, International Microdosimetry Meeting
Radiation Research Society
American Association for Cancer Research
Environmental Mutagen Society
Oxygen Society

Student Mentoring

Master degree students of Environmental Heath Sciences, Columbia University
School of Public Health.
New York City high school science students for Intel Science project

Reviewer:

British Journal of Cancer
Cancer Research
Carcinogenesis
Occupational and Environmental Medicine
International Journal of Radiation Biology
Radiation Research
Environmental Health Perspective
Proceedings of the National Academy of Sciences

Editorial Work

Section editor, *Advances in Space Sciences*

Dr. Howard B. Lieberman

Member

Advisory Board, Summer Research Program for New York City Secondary School
Science Teachers, Columbia University
American Association for the Advancement of Science
American Society of Microbiology

(Dr. Howard B. Lieberman, continued)

Environmental Mutagen Society
Genetics Society of America
Radiation Research Society
Elected Biology Councilor
Chairman, Web-Site Committee
Sigma Xi
Theobald Smith Society

Reviewer

Grants

Chairman, NIH Radiation Study Section
Member, Israel Cancer Research Fund, Scientific Review Panel "A"

Manuscripts

BioTechniques
Gene
International Journal of Radiation Oncology, Biology, and Physics
Radiation Research

Stephen A. Marino

Member

Columbia University Radiation Safety Committee
Radiation Research Society

Guest Scientist

Brookhaven National Laboratories, Upton, NY

Dr. Tej K. Pandita

Member

American Association for the Advancement of Science.
American Association of Cancer Research.
Radiation Research Society
The American Society of Microbiology

Reviewer

Cancer Research
Carcinogenesis
Clinical Cancer Research
FASEB Journal
International Journal of Radiation Oncology, Biology and Physics
International Journal of Radiation Biology
Molecular and Cellular Biology
Mutation Research
Nature Genetics
Neoplasia
Oncology Reports
Oncogene
Proceedings of the National Academy of Sciences, USA
Radiation Research

THE COLUMBIA COLLOQUIUM AND LABORATORY SEMINARS

At intervals of approximately one month during the academic year, a regular colloquium has been held to discuss ongoing research. Dr. Howard Lieberman organized them and scheduled the speakers. These have been attended by the professional staff, graduate students, and senior technical staff of this Laboratory and RARAF, as well as by scientists from other departments of the College of Physicians & Surgeons interested in collaborative research. Attention has focused on recent findings and future plans, with special emphasis on the inter-disciplinary nature of our research effort.

During the year, we have been pleased to welcome a number of visitors who have presented formal seminars and/or spent time discussing ongoing research with various members of the Laboratory. These have included Drs. Prakash Hande, British Columbia Cancer Center, Jean Y.J. Wang, University of California at San Diego, Guy Garty, Weizmann Institute, Israel, Vicente Notario, Georgetown University, and Kum Kum Khanna, The Queensland Institute of Medical Research, Australia.

PUBLICATIONS

Ansari R and Hei TK. Effects of 60 Hz extremely low frequency magnetic fields on radiation and chemically induced mutagenicity in mammalian cells. *Carcinogenesis* 21(6): 769-776 (2000).

Balajee AS and Bohr VA. Genomic heterogeneity of nucleotide excision repair. *Gene* 250: 15-30 (2000).

Balajee AS, Desantis L, Brosh RM Jr., Selzer R, and Bohr, VA. Role of the ATPase domain of Cockayne syndrome group B gene in UV induced apoptosis. *Oncogene* 19, 477-489 (2000).

Brenner DJ. Towards optimal external-beam fractionation for prostate cancer. Int J *Radiat Oncol Biol Phys* 48, 315-6 (2000).

Brenner DJ. Rutherford, the Curies, and radon. *Med. Phys*. 27, 618 (2000).

Brenner DJ, Curtis RE, Hall EJ and Ron E. Second malignancies in prostate cancer patients after radiotherapy compared to surgery. *Cancer,* 88:398-406 (2000).

Brenner DJ, Schiff PB, Zablotska LB. Adjuvant radiotherapy for DCIS. *Lancet 355*:2071 (2000).

Calaf G and Hei TK. Establishment of a radiation- and estrogen-induced breast cancer model. *Carcinogenesis 21* (4): 769-776 (2000).

Calaf G and Hei TK. Oncoprotein expression in human breast epithelial cells transformed by high LET radiation. *Int. J. Radiation Biology 76* (12), 1273-1283 (2000).

DeSantis LP, Garci CL, Balajee AS, Brea Calvo GT, Bassi L, and Palitti F. Transcription coupled repair deficiency results in increased chromosomal aberrations and apoptotic death in the UV61 cell line, the Chinese hamster homologue of Cockayne's syndrome B. *Mutat Res* (DNA Repair) 400:1-12 (2000).

Dhar S, Squire JA, Hande MP, Wellinger RJ, and Pandita TK. Inactivation of 14-3-3σ gene influences telomere behavior and ionizing radiation induced chromosomal instability. *Mol Cell Biol 20*:7764-7772 (2000).

Dymnikov AD, Brenner DJ, Johnson G, Randers-Pehrson G. Theoretical study of short electrostatic lens for the Columbia ion microprobe. *Rev. Sci. Instr. 71:* 1646-1650 (2000).

Fan Z, Chakravarty P, Alfieri A, Pandita TK, Vikram B, and Guha C. Adenovirus-mediated antisense ATM gene transfer sensitizes prostate cancer cells to ionizing radiation. *Cancer Gene Therapy 7*:1307-1314 (2000).

Ferguson AT, Evron E, Umbricht CB, Pandita TK, Chan TA, Hermeking H, Marks JR, Lambers AR, Futreal PA, Stampfer MR, and Sukumar S. High frequency of hypermethylation at the 14-3-3σ locus leads to gene silencing in breast cancer. *PNAS USA 97*:6049-6054 (2000).

Fu W, Killen M, Culmsee C, Dhar S, Pandita TK, and Mattson MP. Expression of the catalytic subunit of telomerase in developing brain neurons: Evidence for a cell surviving-promoting function. *J Mol Neuroscience 14*:3-15 (2000).

Grigorova M, Balajee AS, and Natarajan AT. Spontaneous and X-ray-induced chromosomal aberrations in Werner syndrome cells detected by FISH using chromosome-specific painting probes. *Mutagenesis*, 15, 303-310 (2000).

Guha C, Guha U, Tribius S, Alfieri A, Casper D, Chakravarty P, Mellado W, Pandita TK, and Vikram B. Antisense *ATM* gene therapy: a strategy to increase the radiosensitivity of human tumors. *Gene Therapy 7*: 852-858 (2000).

Hall, EJ. Radiation Carcinogenesis; will "how" much tell us "how much"? *Radiation Research, Volume 2*; Proceedings of the Eleventh International Congress of Radiation Research, Dublin, Ireland, July 18-23, 1999, pp. 547-552, M. Moriarty, C. Mothersill, C. Seymour, M. Edington, J.F. Ward, R.J.M. Fry (eds.), 1999.

Hall, EJ. A radiation biologist looks to the future. (Editorial) *Int J Radiation Oncology Biol Phys 46*:1-2, 2000.

Hande MP. "Metaphase" (Cover photo). *Molecular and Cell Biology 20*:22 (2000).

Hang H and Lieberman, HB. Physical interactions among human checkpoint control proteins HUS1p, RAD1p and RAD9p, and implications for the regulation of cell cycle progression. *Genomics 65*:24-33 (2000).

Hang H, Rauth SJ, Hopkins KM, and Lieberman, HB. Mutant alleles of *Schizo-saccharomyces pombe rad9+* alter hydroxyurea resistance, radioresistance and checkpoint control. *Nucl Acids Res 28*:4340-4349 (2000).

Hei TK, Roy D, Piao CQ, and Calaf GM. Genomic instability in human bronchial epithelial cells transformed by high LET radiation. In: Proceedings of Radiation Research, M Moriarty, C Mothersill, C Seymour, M Edington, JF Ward, and RJM Fry (eds). Allen Press, Lawrence, KS, pp. 560-563 (2000).

Hei TK, Xu A, Louie D, Zhao YL. Genotoxicity versus carcinogenicity: Implications from fiber toxicity studies. *Inhalation Toxicology 12*: 141-147 (2000).

Kharbanda S, Kumar V, Dhar S, Pandey P, Chen C, Yuan Y, Whang Y, Saywers C, Strauss W, Pandita TK, Weaver D, and Kufe D. Regulation of the EST2 telomerase catalytic subunit by the c-Abl protein tyrosine kinase. *Current Biology 10*:568-575 (2000).

Komatsu K, Hopkins KM, Lieberman HB, and Wang HG. *Schizosaccharomyces pombe* Rad9 contains a BH3-like region and interacts with the anti-apoptotic protein Bcl-2. *FEBS Letters* *481*:122-126 (2000).

Komatsu KT, Miyashita T, Hang H, Hopkins KM, Zheng W, Cuddeback S, Yamada M, Lieberman HB, and Wang HG. Human homologue of *S. pombe* Rad9 interacts with Bcl-2/Bcl-xL and promotes apoptosis through a BH3-like domain. *Nat Cell Biol 2*:1-6 (2000).

Komatsu K, Wharton W, Hang H, Wu C, Singh S, Lieberman HB, Pledger WJ, and Wang HG. PCNA interacts with hHus1/hRad9 in response to DNA damage and replication inhibition. *Oncogene 19*:5291-5297 (2000).

Liu Y, Snow BE, Hande MP, Baerlocher G, Kickhoefer V, Yeung D, Wakeham D, Itie A, Siderovski DP, Lansdorp PM, Robinson MO, Harrington L. The telomerase-associated protein TEP1 is not essential for telomerase activity or telomere length maintenance in vivo. *Molecular and Cellular Biology 20*(21): 8178-8184 (2000).

Liu Y, Snow BE, Hande MP, Yeung D, Erdmann NJ, Wakeham A, Itie A, Siderovski DP, Lansdorp PM, Robinson MO, Harrington L. The telomerase reverse transcriptase is limiting and necessary for telomerase function in vivo. *Current Biology 10*:1459-1462 (2000).

Miller RC, Marino SA, Napoli J, Shah H, Hall EJ, Geard CR, Brenner DJ. Oncogenic transformation in C3H10T½ cells by low-energy neutrons. *Int J Radiat Biol 76*:327-334 (2000).

Niida H, Shinkai Y, Hande MP, Matsumoto T, Takahara S, Tachibana M, Oshimura M, Lansdorp PM, Furuichi Y. Telomere maintenance in telomerase deficient mouse embryonic stem cells: Characterization of an amplified telomeric DNA. *Molecular and Cellular Biology 20*(11): 4115-5127 (2000).

Pandita TK, Lieberman HB, Lim DS, Dhar S, Zheng W, Taya Y, and Kastan MB. Ionizing radiation activates the ATM kinase throughout the cell cycle. *Oncogene 19*:1386-1391 (2000).

Pandita TK and Dhar S. Influence of ATM function on telomere nuclear matrix interactions. *Radiation Research 154*:133-139 (2000).

Pichierri P, Franchitto A, Mosesso P, Proietti de Santis L, Balajee AS, and Palitti F. Werner's syndrome lymphoblastoid cells are hypersensitive to topoisomerase II

inhibitors in the G2 phase of the cell cycle. *Mutat Res* (DNA repair), 459:123-133 (2000).

Ponomarev AL, Brenner DJ, Hlatky LR, and Sachs RK. DNA fragment-size distributions for large sizes after high LET radiation, derived from a polymer, random walk chromatin model. *Rad Environ Biophys 39,* 111-120 (2000).

Scherthan H, Jerratsch M, Dhar S, Wang YA, Goff SP, and Pandita TK. Meiotic telomere distribution and Sertoli cell nuclear architecture is altered in *Atm* and *Atm*/p53 deficient mice. *Mol Cell Biol 20*: 7773-7783 (2000).

Shangry S, Adamson AW, Pandita TK, Yalowich J, Tacciolo GE, Kevin DB, and Baskaran R. Activation of Abl kinase following ionizing radiation requires ATM but not DNA-PK activity. *JBC 275*: 30163-30168 (2000).

Sunesan M, Sezer R, Brosh RM, Balajee AS, Stevnsner T, and Bohr VA. Molecular characterization of an acidic region deletion mutant of Cockayne syndrome group B protein. *Nucleic Acids Res 28,* 3151-3159 (2000).

Surralles J, Hande MP, Marcos R, Lansdorp PM. Accelerated telomere shortening in the human inactive X-chromosome. *American Journal of Human Genetics 65*:6, 1617-1622 (1999).

Waldren CA, Ueno A, Vannais DB, Kramer S, Lenarczek M, Zhang, Kronenberg A, Davies A, and Hei, TK. A brief look at some in vitro tests of genotoxic effects of ionizing radiation: Experience with the AL-CD59 assay. In: *Proceedings of Radiation Research*, M Moriarty, C Mothersill, C Seymour, M Edington, JF Ward, and RJM Fry (eds). Allen Press, Lawrence, KS, pp. 527-530 (2000).

Xu A, Wu LJ, Santella R, and Hei TK. Role of oxyradicals in mutagenicity and DNA damage induced by asbestos in mammalian cells. *Cancer Research 59*: 5615-5624 (1999).

Zhao YL, Piao CQ, Wu LJ, Suzuki M, and Hei TK. Differentially expressed genes in asbestos-induced tumorigenic human bronchial epithelial cells: implication for mechanism. *Carcinogenesis 21* (11): 2005-2010 (2000).

Zhou HN, Randers-Pehrson G, Waldren CA, Vannais D, Hall EJ, and Hei, TK. Induction of a bystander mutagenic effect of alpha particles in mammalian cells. *Proc National Academy Science USA 97*: 2099-2104 (2000).

Zhou HN, Zhu LX, Li KB, and Hei TK. Radon, tobacco specific nitrosamine and mutagenicity. *Mutation Research 430*: 145-153 (1999).

Published Twice Monthly
June 2000, Volume 20, Number 11

AMERICAN SOCIETY FOR MICROBIOLOGY

MCB

Molecular and Cellular Biology